THIRD SEMI-ANNUAL

radiation effects symposium

Sponsored by Air Research and Development Command
UNITED STATES AIR FORCE

LOCKHEED NUCLEAR PRODUCTS
Lockheed Aircraft Corporation, Georgia Division

VOLUME 2 OF 6

Dosimetry and Nuclear Measurements Papers

Third Semi-annual

radiation effects symposium

28-30 October 1958

Sponsored by
Air Research and Development Command
UNITED STATES AIR FORCE

LOCKHEED NUCLEAR PRODUCTS

LOCKHEED AIRCRAFT CORPORATION
GEORGIA DIVISION – MARIETTA, GEORGIA

FOREWORD

The proceedings of the Third Semi-Annual ANP Radiation Effects Symposium, held at the Dinkler-Plaza Hotel in Atlanta, Georgia, October 28 through 30, 1958, are in six volumes. Each of the first five volumes presents the unclassified papers from one of the five sessions; the sixth volume presents classified papers from all five sessions.

Each volume contains a complete table of contents and an index of authors. Volume One contains a list of the names of all who attended the Symposium.

VOLUME 1

GENERAL SESSION

1. APPLICATION OF RADIATION EFFECTS DATA TO NUCLEAR AIRCRAFT PROBLEMS by C. G. Collins, Aircraft Nuclear Propulsion Department, General Electric Company, Cincinnati, Ohio

2. RADIATION EFFECTS TESTING OF AIRCRAFT SUBSYSTEMS AND COMPONENTS AT AIR FORCE PLANT No. 67 FOR THE ANP PROGRAM by W. L. Bridges, Lockheed Nuclear Products, Lockheed Aircraft Corporation, Georgia Division, Marietta, Georgia

3. *MISSION AND TRAFFIC CONTROL REQUIREMENTS FOR THE WS/125A by James R. Burnett, Bendix Systems Division, Bendix Aviation Corporation, Ann Arbor, Michigan

4. NEW RADIATION TEST FACILITIES IN THE GENERAL ELECTRIC COMPANY by S. S. Jones, Vallecitos Atomic Laboratory, General Electric Company, San Jose, California,and W. R. Langdon and T. T. Naydan, General Electric Company, Schenectady, New York.

5. THE CONVAIR RADIATION EFFECTS TESTING SYSTEM by J. W. Allen, Convair, A Division of General Dynamics Corporation, Fort Worth, Texas

6. RADIATION EFFECTS REACTOR by W. T. Scarborough, Lockheed Nuclear Products, Lockheed Aircraft Corporation, Georgia Division, Marietta, Georgia

7. A DESCRIPTION OF A MULTI-KILOCURIE IRRADIATION FACILITY AND THE ASSOCIATED RADIATION DOSIMETRY by R. E. Simpson, Lockheed Nuclear Products, Lockheed Aircraft Corporation, Georgia Division, Marietta, Georgia,and M. Z. Fainman, M. E. Krasnow, E. R. Rathbun, C. R. Memhardt, Inland Testing Laboratories and Cook Research, Morton Grove, Illinois

8. START-UP OF THE CRITICAL EXPERIMENT REACTOR by M. A. Dewar, Lockheed Nuclear Products, Lockheed Aircraft Corporation, Georgia Division, Marietta, Georgia

9. REMOTE AREA MONITORING SYSTEM AT AIR FORCE PLANT No. 67 by E. N. Lide, Lockheed Nuclear Products, Lockheed Aircraft Corporation, Georgia Division, Marietta, Georgia

* This paper is classified and is bound in Volume Six.

10. AREA MONITORING FOR RADIOACTIVITY by Roy Shipp, Lockheed Nuclear Products, Lockheed Aircraft Corporation, Georgia Division, Marietta, Georgia

11. LOGARITHMIC CIRCUITS FOR RADIATION DOSIMETRY by L. A. Turner, Lockheed Nuclear Products, Lockheed Aircraft Corporation, Georgia Division, Marietta, Georgia

VOLUME 2

DOSIMETRY AND NUCLEAR MEASUREMENTS

12. INFLUENCE OF ENERGY SPECTRA ON RADIATION EFFECTS by F. C. Maienschein, Oak Ridge National Laboratory, Oak Ridge, Tennessee

13. CROSS SECTION AVERAGES FOR TYPICAL REACTOR SPECTRA by Walter R. Burrus and Russell P. Sullivan, Physics Department, Ohio State University, Columbus, Ohio

14. NUCLEAR UNITS AND MEASUREMENTS by R. S. Caswell and S. W. Smith, Atomic and Radiation Physics Division, National Bureau of Standards, Washington, District of Columbia

15. COMPARISON OF RADIATION EFFECTS IN DIFFERENT FACILITIES by W. T. Harper, Lockheed Aircraft Corporation, Lockheed Missile Systems Division, Palo Alto, California, and W. R. Burrus, Ohio State University, Columbus, Ohio

16. THE DETERMINATION OF NUCLEAR PARAMETERS FOR EXPERIMENTAL RADIATION EFFECTS by G. A. Wheeler, Convair, A Division of General Dynamics Corporation, Fort Worth, Texas

17. CALORIMETRIC DOSIMETRY PROGRAM AT LOCKHEED by Roger L. Gamble, Lockheed Nuclear Products, Lockheed Aircraft Corporation, Georgia Division, Marietta, Georgia

18. DOSIMETRY AND ENERGY DISTRIBUTION OF FAST NEUTRONS USING LI I by F. D. Schupp and S. L. Ruby, Radiation & Nucleonics Laboratory, Materials Engineering Department, Westinghouse Electric Corporation, East Pittsburgh, Pennsylvania

VOLUME 3

AIRCRAFT SYSTEMS AND MATERIALS

27. AIRCRAFT RADOME DESIGN PROBLEMS ASSOCIATED WITH A NUCLEAR ENVIRONMENT by Frank W. Thomas, Lockheed Nuclear Products, Lockheed Aircraft Corporation, Georgia Division, Marietta, Georgia

28. *EFFECTS OF HIGH ALTITUDE NUCLEAR DETONATIONS ON PROPAGATION OF ELECTROMAGNETIC WAVES by Samuel Horowitz and Lt. Richard Sugarman, U. S. Air Force Cambridge Research Center, Bedford, Massachusetts

29. *THE EFFECTS OF GAMMA RAY AND REACTOR IRRADIATIONS ON THE SENSITIVITY OF EXPLOSIVES by Paul W. Levy, Brookhaven National Laboratory, Upton, Long Island, New York,and J. V. R. Kaufman and James E. Abel, Explosives Research Section, Picatinny Arsenal, Dover, New Jersey

30. ON THE ENERGY LEVELS IN NEUTRON IRRADIATED SILICON by C. A. Klein and W. D. Straub, Research Division, Raytheon Manufacturing Company, Waltham, Massachusetts

31. EFFECT OF RADIATION ON THE CRITICAL SHEAR STRESS OF A METAL SINGLE CRYSTAL by C. E. Morgan, Convair, A Division of General Dynamics Corporation, Fort Worth, Texas

32. MEASUREMENT OF THE RANGE OF RECOIL ATOMS by R. A. Schmitt and R. A. Sharp, General Atomic, A Division of General Dynamics Corporation, San Diego, California

33. THE EFFECTS OF NUCLEAR ENVIRONMENT ON METALLIC AND NONMETALLIC MAGNETIC MATERIALS by E. I. Salkovitz and A. I. Schindler, U. S. Naval Research Laboratory, Washington, District of Columbia

34. *THE EFFECT OF NUCLEAR RADIATION ON COMMUNICATIONS SET AN/ARC-34 by D. L. Jacobs, Convair, A Division of General Dynamics, Fort Worth, Texas

35. RADIATION TESTING OF J-79 ORGANIC ENGINEERING MATERIALS AND COMPONENTS by D. E. Barnett, Aircraft Nuclear Propulsion Department, General Electric Company, Cincinnati, Ohio

36. *THE EFFECT OF NUCLEAR RADIATION DURING ESCAPE ON F-104 by F. L. Bouquet, Jr., Lockheed Aircraft Corporation, California Division, Burbank, California

* This paper is classified and is bound in Volume Six.

VOLUME 4

ELECTRONICS AND SEMI-CONDUCTORS

37. THE EFFECTS OF RADIATION ON VARIOUS RESISTOR TYPES by E. R. Pfaff and R. D. Shelton, Admiral Corporation, Chicago, Illinois

38. RADIATION EFFECTS IN COMPOUND SEMICONDUCTORS by L. W. Aukerman and R. K. Willardson, Battelle Memorial Institute, Columbus, Ohio

39. A CRITICAL SURVEY OF RADIATION DAMAGE TO CIRCUITS by W. W. Happ and S. R. Hawkins, Lockheed Aircraft Corporation, Lockheed Missile Systems Division, Palo Alto, California

40. RADIATION STABILIZATION OF TRANSISTOR CIRCUITS BY ACTIVE FEEDBACK by S. R. Hawkins and W. W. Happ, Lockheed Aircraft Corporation, Lockheed Missile Systems Division, Palo Alto, California

41. COMPARISON OF NEUTRON DAMAGE IN GERMANIUM AND SILICON TRANSISTORS by J. W. Easley, Bell Telephone Laboratories, Whippany, New Jersey

42. PULSED RADIATION EFFECTS IN SEMICONDUCTORS by J. M. Denney, C. W. Perkins, and J. R. Wieneke, Nuclear Electronics Department, Hughes Aircraft Company, Culver City, California

43. THE EFFECT OF VARIATION OF THE WIDTH OF THE BASE REGION ON THE RADIATION TOLERANCE OF SILICON DIODES by Gerald C. Huth, Aircraft Nuclear Propulsion Department, General Electric Company, Cincinnati, Ohio

44. THE EFFECT OF NUCLEAR RADIATION ON COMMERCIAL SILICON DIODES by John R. Crittenden, Aircraft Nuclear Propulsion Department, General Electric Company, Cincinnati, Ohio

45. EVALUATION OF SILICON DIODE IRRADIATION RESULTS IN TERMS OF MAGNETIC AMPLIFIER PERFORMANCE by J. A. Russell, Aircraft Nuclear Propulsion Department, General Electric Company, Cincinnati, Ohio

46. GAMMA RADIATION EFFECTS IN SILICON SOLAR CELLS by G. Enslow, F. Junga, and W. W. Happ, Lockheed Aircraft Corporation, Lockheed Missile Systems Division, Palo Alto, California

47. THE EFFECTS OF NUCLEAR RADIATION ON POWER TRANSISTORS by Frederick Gordon, Jr., U. S. Army Signal Corps, Research and Development Laboratories, Fort Monmouth, New Jersey

48. THE PERFORMANCE OF SOME ZENER REFERENCE ELEMENTS DURING EXPOSURE TO NUCLEAR RADIATION by M. A. Xavier, Cook Research Laboratory Division, Cook Electric Company, Morton Grove, Illinois

49. EFFECTS OF ELECTRON BOMBARDMENT ON CADMIUM SULFIDE WHISKERS by B. A. Kulp and D. C. Reynolds, Aeronautical Research Laboratory, Wright Air Development Center, Wright-Patterson Air Force Base, Ohio

VOLUME 5

LUBRICANTS AND PLASTICS

50. THE BEHAVIOR OF FUELS AND LUBRICANTS IN DYNAMIC TEST EQUIPMENT OPERATING IN THE PRESENCE OF GAMMA RADIATION by M. Z. Fainman, Inland Testing Laboratory, Morton Grove, Illinois

51. THE DEVELOPMENT OF NUCLEAR RADIATION RESISTANT SOLID FILM LUBRICANTS by William L. R. Rice and Lieutenant William L. Cox, Materials Laboratory, Wright Air Development Center, Wright-Patterson Air Force Base, Ohio

52. INTEREFFECTS BETWEEN REACTOR RADIATION AND MIL-L-7808C AIRCRAFT TURBINE OIL by F. A. Haley, Convair, A Division of General Dynamics Corporation, Fort Worth, Texas

53. DEVELOPMENT OF RADIATION-RESISTANT HIGH-TEMPERATURE LUBRICANTS by C. L. Mahoney, W. S. Saari, K. J. Sax, W. W. Kerlin, E. R. Barnum, P. H. Williams, Shell Development Company, Emeryville, California

54. ELECTRICAL EFFECTS OF HIGH-INTENSITY IONIZING RADIATION ON NONMETALS by V. A. J. Van Lint and P. H. Miller, Jr., General Atomic, A Division of General Dynamics Corporation, San Diego, California

55. STUDY OF RADIATION EFFECTS ON ELECTRICAL INSULATION by J. F. Hansen, Battelle Memorial Institute, Columbus, Ohio, and M. L. Shatzen, Lockheed Nuclear Products, Lockheed Aircraft Corporation, Georgia Division, Marietta, Georgia

56. A STUDY OF RADIATION EFFECTS ON FUEL TANK SEALANTS AND BLADDER CELL MATERIAL by M. L. Shatzen, Lockheed Nuclear Products, Lockheed Aircraft Corporation, Georgia Division, Marietta, Georgia, and R. S. Tope, C. W. Cooper, and R. G. Heiligmann, Sealants and Elastomers Division, Battelle Memorial Institute, Columbus, Ohio

57. THE EFFECT OF ELECTRON RADIATION ON THE COMPLEX DYNAMIC MODULUS OF POLYSTYRENE AND HIGH DENSITY POLYETHYLENE by R. H. Chambers, General Atomic, A Division of General Dynamics Corporation, San Diego, California

58. RADIATION RESISTANT SILICONES by E. L. Warrick, D. J. Fischer, and J. F. Zack, Dow Corning Corporation, Midland, Michigan

59. RADIATION EFFECTS ON ORGANO-SILICONS by T. W. Albrecht, Convair, A Division of General Dynamics Corporation, Fort Worth, Texas

60. EFFECTS OF GAMMA RADIATION ON FLUOROCARBON POLYMERS by Leo A. Wall, Roland E. Florin, and D. W. Brown, National Bureau of Standards, Washington, District of Columbia

61. *FAST NEUTRON ACTIVATION OF SEAPLANE MATERIALS by L. Brandeis Wehle, Jr., Michael D. D'Agostino, and Anthony J. Favale, Grumman Aircraft Engineering Corporation, Bethpage, Long Island, New York

62. EFFECTS OF NUCLEAR RADIATION ON CORK, LEATHER, AND ELASTOMERS by Chester J. De Zeih, Boeing Airplane Company, Seattle, Washington

63. THE "PLATE SHEAR METHOD" OF DETERMINING THE MODULUS OF RIGIDITY OF SANDWICH PANELS by R. R. Bauerlein, Convair, A Division of General Dynamics Corporation, Fort Worth, Texas

64. "O" RING TESTING IN A MIXED FIELD IRRADIATION by E. E. Kerlin, Convair, A Division of General Dynamics Corporation, Fort Worth, Texas

* This paper is classified and is bound in Volume Six.

65. RADIATION EFFECTS ON 23 SILICONE RUBBERS AT AMBIENT TEMPERATURE by D. M. Newell, Convair, A Division of General Dynamics Corporation, Fort Worth, Texas

66. *THE RADIATION ENVIRONMENT DUE TO ACTIVATION AND SCATTERING EFFECTS NEAR BASED SEAPLANES by F. L. Bouquet, Jr., Lockheed Aircraft Corporation, California Division, Burbank, California

* This paper is classified and is bound in Volume Six.

VOLUME 6

CLASSIFIED PAPERS

3. MISSION AND TRAFFIC CONTROL REQUIREMENTS FOR THE WS/125A by James R. Burnett, Bendix Systems Division, Bendix Aviation Corporation, Ann Arbor, Michigan

28. EFFECTS OF HIGH ALTITUDE NUCLEAR DETONATIONS ON PROPAGATION OF ELECTROMAGNETIC WAVES by Samuel Horowitz and Lt. Richard Sugarman, U. S. Air Force Cambridge Research Center, Bedford, Massachusetts

29. THE EFFECTS OF GAMMA RAY AND REACTOR IRRADIATIONS ON THE SENSITIVITY OF EXPLOSIVES by Paul W. Levy, Brookhaven National Laboratory, Upton, Long Island, New York,and J. V. R. Kaufman and James E. Abel, Explosives Research Section, Picatinny Arsenal, Dover, New Jersey

34. THE EFFECT OF NUCLEAR RADIATION ON COMMUNICATIONS SET AN/ARC-34 by D. L. Jacobs, Convair, A Division of General Dynamics, Fort Worth, Texas

36. THE EFFECT OF NUCLEAR RADIATION DURING ESCAPE ON F-104 by F. L. Bouquet, Jr., Lockheed Aircraft Corporation, California Division, Burbank, California

61. FAST NEUTRON ACTIVATION OF SEAPLANE MATERIALS by L. Brandeis Wehle, Jr., Michael D. D'Agostino, and Anthony J. Favale, Grumman Aircraft Engineering Corporation, Bethpage, Long Island, New York

66. THE RADIATION ENVIRONMENT DUE TO ACTIVATION AND SCATTERING EFFECTS NEAR BASED SEAPLANES by F. L. Bouquet, Jr., Lockheed Aircraft Corporation, California Division, Burbank, California

INDEX OF AUTHORS

INFLUENCE OF ENERGY SPECTRA ON RADIATION EFFECTS

by

F. C. Maienschein

Oak Ridge National Laboratory
Oak Ridge, Tennessee

ABSTRACT

The energy spectra of neutrons and gamma rays influence in an important way the production of displacements in crystal lattices. A lack of knowledge of the energy distributions in many past and current reactor irradiations for radiation "effect" studies has led to the accumulation of relatively meaningless data. Special problems arise in attempting to compare data taken at different types of reactors with unknown energy spectra. The available data for reactor spectra are listed and examples given. Methods of spectroscopy are considered briefly which may be useful for developing further spectral data. Finally, the merits are examined of several possible characterizations of a radiation field which are simplier to obtain than the energy spectrum. Comparison of these parameters with those commonly used now shows that the new parameters would constitute a marked improvement in understanding and correlating radiation effects.

I. INTRODUCTION

For the shield of a nuclear reactor, the distributions in energy and direction of the radiation within the shield may be as important as the magnitude. The strong dependence of radiation attenuation upon energy is easily understood by examining the energy dependence of the cross sections for the reactions responsible for attenuating the radiation.

It is the purpose of the present paper to determine whether the energy distribution or spectrum is as influential in determining the capabilities

of the radiation for producing "damage," or solid-state "effects." The answer to this question may be anticipated by stating that radiation effects depend on the radiation energies in complex and poorly-understood ways. Further, because the spectra in different reactors may vary widely, it is not possible to intelligently compare data developed in different facilities unless the pertinent spectral data are available.

In Section III, a summary is given of the spectra available for reactors that have been employed for radiation effects studies. Because of the paucity of such data it is necessary to consider in Section IV methods which might be employed to develop additional spectral data for irradiation effects facilities. Finally, because these spectroscopic techniques are difficult and expensive to employ, other, simplier methods of characterizing a radiation field are discussed in Section V. Agreement upon suitable choices of such methods has not yet been reached, but it can be shown that such agreement is urgently needed since the parameters used at present may introduce uncertainties of an order of magnitude.

II. DEPENDENCE UPON ENERGY OF RADIATION EFFECTS

In this discussion, consideration is limited to reactors which are used for the study of radiation-produced phenomena. Thus the radiations of primary interest are neutrons and gamma rays. For neutrons, displacement effects predominate, while for gamma rays ionization effects are the most important. The postulated mechanisms for these effects and their dependence upon energy are described below.

A. Neutrons

Neutrons produce elastic or inelastic recoils as well as nuclear transmutations. Appreciable energy may be transferred to a recoil which in turn may create atomic displacements. The removal of a bound atom from a lattice is assumed to require of the order of 25 ev, which is approximately twice the binding energy for an atom in the interior of a lattice.[1] This minimum neutron energy for displacement production, E_d, although called a threshold, does not represent a sharp discontinuity and surely must depend on the lattice structure as well as the relative orientation of crystal

and incident radiation. In order to transfer 25 ev to an atom of atomic weight, A, bound in a lattice, a neutron must have an energy at least as great as the minimum shown in Table I.

TABLE I. THRESHOLD FOR THE PRODUCTION OF DISPLACEMENTS[a]

A	1	10	50	100	200
Threshold Energy, E_d, for Neutrons (ev)	25	76	320	640	1260
Threshold Energy, E_d, for Gamma Rays (kev)[b]		100	410	680	1100

a. Taken from Ref. 2. E_d is assumed to be 25 ev.

b. Note change of units.

At energies appreciably above the threshold for displacement production, the neutron-produced recoils begin to lose energy by the production of ion pairs and at still higher energies this process predominates. The neutron energy at which ionization starts to become important, E_i, is very approximately given by:[5]

$$E_i \approx \frac{M}{2}\left(\frac{e^2}{\hbar}\right)^2 \times \frac{(M+1)^2}{4M} \qquad (1)$$

where

M = the mass of the atomic recoil, and

$\frac{e^2}{\hbar}$ = the velocity of an electron in the hydrogen orbit.

The second term accounts for the transfer of energy from the neutron to the atom. This estimate follows from the assumption that if the recoil atom is moving with a velocity greater than that of an electron in the target atom, excitation becomes probable.

For energies intermediate between the above limits, the dependence upon energy of displacement production may be estimated as follows: (assuming a thin sample and no annealing).

$$N_d = \int_{E_k} n_d(E_k)\ \nu(E_k)\ dE_k \qquad (2)$$

$$= \int_{E_n}\int_{E_k} n_o\ \phi(E_n)\ \sigma_d(E_n \rightarrow E_k)\ \nu(E_k)\ dE_n\ dE_k$$

where

N_d = the number of atoms displaced per unit volume per unit time,

$n_d(E_k)$ = the number of primary knock-ons produced per unit volume at energy E_k,

$\nu(E_k)$ = the number of secondary atomic displacements produced by one primary knock-on of energy E_k,

n_o = the total number of atoms in the crystal per unit volume,

$\phi(E_n)$ = the neutron flux,

$\sigma_d(E_n \rightarrow E_k)$ = the cross section per atom for neutrons of energy E_n to produce collisions which yield primary knock-ons of energy E_k.

The calculation of the number of primary knock-ons produced proceeds in a straight-forward manner if the necessary angular distributions for neutron scattering are available.[3] The calculations of the cascade process which would lead to a prediction of the value of $\nu(E)$, however, are quite difficult. Several rather crude models have been proposed[1,4,5] which give results for the energy dependence of ν. The general shape is shown in Fig. 1. For the energy region between $2E_d$ and E_i it is seen that the value of ν is proportional to E_k. The model of Kinchin and Pease[4] gives the following value for the constant of proportionality for this energy region.

$$\nu(E_k) = E_k/2E_d \quad (2E_d < E_k < E_i) \qquad (3)$$

Substituting this value of $\nu(E_k)$ into Eq. (2), it follows that the number of displacements is proportional to the energy absorbed in the material. This would be a very significant result if it were valid but it is only applicable for neutron irradiations of high-A materials. For materials of low atomic number many of the neutrons in a reactor spectrum will exceed E_i in energy and thus the number of displacements produced will drop more rapidly at high energy than the energy absorbed.

The determination of the number of displacements does not yet yield direct information about other radiation effects and the inverse of this uncertain correlation makes difficult the performance of experiments to determine the number of displacements produced. However, it is reasonable to assume that the effects of neutron irradiation will follow qualitatively the energy dependence of the displacement production rate.

For certain materials, the nuclear cross sections may become very large and the reaction products may be especially effective in producing displacements. For such reactions as $B^{10}(n,\alpha)$ and fission, the energy dependence of displacement production and other radiation effects will be drastically different from that for other materials, since these reactions have an approximate $E^{-1/2}$ energy dependence.

B. Gamma Rays

The effects on insulators due to gamma rays are primarily chemical, such as broken bonds, free radical production, etc. These effects follow largely from the production of ion pairs in the material. Since the energy required to form an ion pair is remarkably independent of the energy of the radiation,[6] the above chemical effects are proportional to the energy absorbed in the material, or dose. The dose D_γ, per unit time is given by:

$$D_\gamma = \int_{E_\gamma} \int_{E_e} n_o \phi_\gamma(E_\gamma)\, \sigma(E_\gamma \rightarrow E_e)\, E_e\, dE_\gamma\, dE_e \qquad (4)$$

where the symbols have the same meaning as in Eq. 2 except that the subscripts γ and e refer to the gamma ray and recoil electron, respectively.

For metals, on the other hand, the conduction electrons are so loosely bound that ionization effects are negligible. Therefore the displacement

effects which are possible with gamma rays may become important for metals. For displacement effects, the production of electron recoils by the photoelectric, Compton or pair processes may be calculated from the known cross sections. The number of displacements produced by such electron recoils has been calculated[1] on the basis of relativistic Coulomb scattering with a resulting complicated dependence on energy. Because of the small mass of the electron and the concomitant low efficiency of energy transfer from the electron to the displaced atom, the gamma-ray energy must be high to produce any displacements (see Table I for typical values). Thus it is clear that displacement production by gamma rays may not be related at all to the energy absorbed in the material being irradiated.

C. Summary

In many cases of irradiations by neutrons and gamma rays, not only the magnitude but even the type of effect may be determined by the energy distribution of the incident radiation. Ionization effects appear to have an energy dependence equivalent to that of the energy absorbed from the radiation. Displacements effects may also follow the absorption of energy for certain energy regions but may also deviate significantly from energy absorption for other energies. Thus, in order to perform radiation effects studies intelligently, either the energy spectra of the reactor facility must be available or another suitable characterization of the radiation field must be found. In the next two sections of this report, available data and techniques for obtaining spectral data will be considered. In the last section, other parameters for the characterization of radiation fields will be considered.

III. AVAILABLE DATA FOR REACTOR ENERGY SPECTRA

Presented herein are those spectra of neutrons and gamma rays for reactors which have been used for irradiation studies. It is hoped that this is an incomplete list and that other data is available but unknown to the author.

A. Neutron Spectra

1. Light-Water Moderated Reactors. Probably the largest amount of

spectral data has been generated for the pool-type research reactors because such reactors have been used extensively for shielding measurements. Much of the available data is therefore directed toward shielding applications and is not particularly suitable for radiation effects studies. However, even this type of data is much better than none at all.

a. BSR. For the Bulk Shielding Reactor at the Oak Ridge National Laboratory several data are available. The differential flux spectrum above ~ 1.5 Mev at the face of the reactor is shown in Fig. 2 as measured with a proton-recoil telescope.[7] Other measurements were made with this instrument for water thicknesses of 5 and 20 cm between the reactor face and the spectrometer.[7] The leakage spectrum was checked, within the large experimental errors, by nuclear plate measurements,[8] and also by a calculation based on the fission spectrum and a simple model of the reactor.[9] Further measurements were made using threshold and resonance detectors in a position at the edge of the reactor core but with a partial reflector of BeO.[10,11] The BSR normally does not use such a reflector. The data obtained with the resonance detectors is reproduced in Fig. 3 along with the proton-recoil data from Fig. 2 in order to illustrate the gap in energy between the data obtained by the two techniques.

b. LITR. The differential fast-neutron spectrum above 1.5 Mev has been measured in beam hole HB-2 of the Low Intensity Training Reactor at the Oak Ridge National Laboratory.[12] The data are shown in Fig. 2 together with those already described for the BSR. It may be seen that the spectral shapes agree within the experimental errors and in addition, are quite similar to the shape of the fission spectrum.[27] Calculated spectra (method unspecified) are presented for this same beam hole by Trice.[11,13]

c. GTR. Neutron spectral data are available for the Ground Test Reactor at Convair, Ft. Worth. Both nuclear plates[14] and radioactivants[15] were employed to determine the leakage spectrum at a point about 3 in. from the reactor face. Further data is available for much thicker shields surrounding the ASTR.[16] These data appear to show a spectral hardening with increasing water thickness.

d. MTR. In spite of the importance of the Materials Testing Reactor

for radiation effects studies, little data exists to describe the spectral characteristics of the radiations in this reactor. Only one series of measurements in Hole BH-3 using resonance and threshold detectors has been reported.[11,17]

2. Heavy-Water Moderated Reactors. The only available data would appear to be a calculation of the differential flux spectrum by Primak for Hole VT-4 of CP-3.[18]

3. Graphite-Moderated Reactors. Spectral data for Hole 19 of the Oak Ridge National Laboratory Graphite Reactor were obtained in an old threshold detector measurement.[19] A more recent attempt to determine the leakage neutron spectrum was not very successful.[20]

4. Unmoderated Reactors. Good nuclear plate measurements have been made by Rosen for Godiva, an unmoderated U^{235} critical assembly.[21] The neutron spectral results indicate a marked change from the fission spectrum. Threshold detectors have been exposed to numerous bomb detonations by Hurst and coworkers.[21a] The major objective of these measurements has been the determination of the fast-neutron dose but in the analysis of the data crude energy spectra are also obtained.

B. Gamma-Ray Spectra

For gamma rays the published spectral data for currently operating reactors is limited to that obtained for the leakage of the BSR.[22,23] This data, which was obtained with a three-crystal scintillation spectrometer, is shown in Fig. 4. Calculations of the gamma-ray spectrum to be expected from the BSR yield the same spectral shape as the measurements but a discrepancy in absolute magnitude of about a factor of 2.[24,25] Other data were obtained with the BSR for the spectra of gamma-rays transmitted through water in the forward direction for thicknesses up to 267 cm.[22] These spectra show a marked hardening with increased water thicknesses but for a non-directional detector the hardening would be much less.

Figure 4 also shows the spectral shape (not the absolute magnitude) observed by Motz for the Los Alamos Fast Reactor. This reactor has since been dismantled.

It is clear from the above summary that little spectral data is available for those reactors which have been most used in radiation-effects experiments. Surely this unfortunate situation will be somewhat alleviated when the USAF facilities at Dayton and Dawsonville are placed in operation.

All of the above data for either neutrons or gamma rays are valid only for samples thin with respect to a mean-free-path of the incident radiation. For thick samples such as are invaribly encountered in systems tests, perturbation of the radiation field by the sample must be taken into account. This perturbation may be calculated approximately if the incident spectra are known, although, in principle, the angular distribution of the radiation must also be known. Alternatively, spectral measurements may be made with the sample in place.

IV. METHODS FOR THE DETERMINATION OF UNKNOWN SPECTRA

A. Calculation

Calculations of the leakage spectra of reactors may be carried out since the sources of radiation are largely known.

1. Sources of Radiation. For neutrons the prompt fission spectrum is of predominant importance. The combination of several sets of measurements[27] gives results which may be fitted with an analytical expression of the form:

$$N_n(E) = 0.453\, e^{-E/0.965} \sinh(2.29E)^{1/2} \qquad (5)$$

where

$N_n(E)$ = the fraction of neutrons per unit energy per fission,

E = the neutron energy in Mev.

A simpler approximation to the fission spectrum, which is valid to within about $\pm 15\%$ for energies below 9 Mev, is the following:

$$N(E) = 0.77\, E^{1/2}\, e^{-0.776\, E}, \quad E \text{ in Mev} \qquad (6)$$

For reactor gamma rays the sources of radiation are much more complex but considerable effort has been expended in studying these sources because

of their importance for shielding. The recent data for the gamma rays emitted promptly in fission is shown in Fig. 5.[28] For the energy range between 1 and 7 Mev, this spectraldata may be approximated within ±40% by an expression of the form:

$$N_\gamma(E) = 8.0\, e^{-1.1\,E},\ \text{Mev}^{-1} \qquad (7)$$

where N(E) is the number of photons per Mev per fission.

The spectra from the other important fission-associated source, the fission products, varies as a function of the history of reactor operation. Data are available which allow predictions of these variations in great detail.[28,29,30] In Fig. 5 is reproduced a spectrum that corresponds approximately to that arising from a reactor in steady state equilibrium, i.e., after long operation.[28] It will be observed that this fission-product spectrum is not grossly dissimilar from that due to prompt fission. Thus for very crude calculations the total fission-associated source of gamma rays may be taken as:

$$N(E) = 14\, e^{-1.1\,E},\ \text{Mev}^{-1} \qquad (8)$$

The other important gamma-ray source is that due to the capture of the neutrons (mostly thermal) in the reactor. Data are available for the spectra of gamma rays due to thermal neutron capture in most materials to be encountered in reactors.[31,31a,32] The only outstanding exception is U^{235}. Because of the lack of any data for this isotope its contribution is often taken into account roughly by adding about 1.4 Mev to the constant, 14, which appears in the approximate expression for the fission-associated gamma-ray spectrum.

An excellent discussion of other, less important sourcesof radiation, as well as a much more detailed discussion of the sources mentioned above, is presented in Goldstein's book on Shielding.[33]

2. Calculation of Spectra. Once the sources of radiation are known, a determination of the flux impinging on a sample requires calculation of the transport and absorption probabilities for the radiations in the core. For neutrons, this calculation is one of the central tasks of reactor calculations. Thus the neutron spectrum for a particular reactor may be

available from the reactor calculations. However, the energy groups chosen for reactor calculations will seldom be suitable for radiation effects studies. Some reactor codes may be sufficiently flexible to permit changing to more suitable energy groups. However, only the more sophisticated codes, employing many energy groups, would yield useful data. A few codes permit consideration of the actual reactor geometry. If suitable machine codes are not available, an analytical treatment may be followed. The methods are outlined in Weinberg and Wigner.[34] Applications of such treatments to specific reactors have been described,[35] including application to the Convair GTR, a reactor which has been used for radiation damage studies.[14]

For gamma rays, calculations of the leakage flux for a pool-type reactor have been made using the known sources together with build-up factors to account for the absorption in the core.[24,25] For such considerations the pool-type reactor core may be considered to be homogeneous. It should be pointed out that the results of the above calculations, although agreeing approximately in spectral shape with the experimental measurements reported in Section II, do not agree in magnitude.

For a heterogeneous reactor, such as the graphite-moderated natural uranium reactors at ORNL and BNL, more careful consideration of the geometry must be made. Primak has considered this problem in detail for the calculation of the gamma-ray dose in heterogeneous reactors.[36] He gives examples for CP-3 and the ORNL Graphite Reactor.

B. Neutron Spectroscopy

Of the many possible methods for neutron spectroscopy, only those which have been demonstrated to be useful for reactor spectra will be considered here. Even these will not be described in detail since published reports are already available and references thereto are cited herein.

1. Proton-Recoil Techniques. The use of photographic emulsions is one of the oldest and best understood methods of fast neutron spectroscopy. In general the direction of travel of the neutrons must be known and the plates must be protected from very high gamma-ray exposures. These requirements may constitute insuperable problems for some reactor facilities. The lower-energy limit of about 0.5 Mev is as low as that for any of the neutron

spectrometers. The labor required for examining tracks on the photographic plates is very considerable but this should not become a major objection for the determination of a few important spectra.

Many general review articles on nuclear-emulsion techniques have appeared. Reports concerned specifically with neutron spectroscopy are less numerous[37,38] but include a how-to-do-it type handbook.[39] Applications to reactor spectra have already been mentioned.[8,16,21]

Proton-recoil counter telescopes have also been used for the determination of reactor spectra.[7,12] The instrument used in these measurements has been described[40] as well as a more recent instrument with higher sensitivity.[41] The limitations of the counter telescopes are similar to those for photographic plates except that the lower-energy limit tends to be higher (1.0 - 1.5 Mev). The sensitivities are very low (10^{-7} to 10^{-8}). The effect of gamma-ray background for the newer more sensitive telescope[41] has not been tested. The old spectrometer[40] was extremely resistant to gamma radiation.

2. Nuclear Reactions. Two nuclear reactions have properties which indicate their use as neutron spectrometers. The first of these, the He^3(n,p)T reaction, has been utilized by incorporating He^3 gas in a proportional counter.[42] The detection efficiency, energy resolution, and energy range are quite favorable for radiation-effects applications but unfortunately the production of He^3 elastic recoils by high-energy neutrons makes interpretation of the results obtained very difficult. The technique has been applied to a fast reactor at Harwell.

The second nuclear reaction, $Li^6(n,\alpha)T$, has been employed as a spectrometer with the Li^6 embodied in a scintillator of Li^6I.[44,45] This spectrometer has an efficiency which is very high ($\sim 10^{-3}$) and the apparatus is simple. However, the energy resolution is limited to about 1 Mev and thus the amount of data of interest for radiation effects that could be developed would be limited. The spectrometer has been used successfully to measure the fission neutron spectrum[44,45] but its use in reactors may give rise to problems with gamma-ray background.

3. Threshold Detectors. The above list of instruments completes the consideration of true energy spectrometers which might be useful for reactor

measurements. However, many nuclear reactions have energy thresholds (minimum energies at which the reactions occur). Thus by counting the reaction products, the magnitude of the integral neutron flux above the threshold may be determined. By combining measurements for several threshold detectors an integral, or even an approximate differential, neutron energy spectrum may be obtained. The various suitable reactions and the counting techniques are described in detail elsewhere.[46,10,11,13] For summary here, we may note that the method, in general, has produced only an approximate spectrum. To improve this situation more use should be made of the several theoretical analyses of threshold detector data.[47,48,49] In order to use threshold detectors materials are required which may be difficult to obtain, eg Np^{237}, and in only few cases are the energy dependences of the neutron cross sections known with adequate accuracy.

In spite of the above difficulties the threshold technique is probably the most applicable to radiation effects problems. For this reason a set of threshold measurements has been recommended as a minimum measurement for USAF-connected radiation effects studies by the ANP Advisory Committee for Nuclear Measurements and Standards.[50] The specific foils recommended, together with a set of "effective thresholds" and "effective cross sections" are shown in Table II.

TABLE II. "EFFECTIVE THRESHOLDS" AND "EFFECTIVE CROSS SECTIONS"[50]

Reaction	"Effective Threshold"	"Effective Cross Section"	Reference
$S^{32}(n,p)P^{32}$	2.9 Mev	300 mb	48
$U^{238}(n,f)$	1.45 Mev	540 mb	48
$Np^{237}(n,f)$	.75 Mev	1.5 b	48
$Pu^{239}(n,f)$[a]	~ 1 Kev	1.9 b	46

a. Covered with 1 cm of B^{10} with a density of 1.11 g cm^{-3}.

Two limitations in the use of the above foils should be noted. First, none of the thresholds except the Pu^{239} fall at as low an energy as would

be desirable, and the Pu^{239} is too low. Second, counting of fission products with their complex decay may be difficult for foil activations in radiation-effects facilities where access is limited and reactor operation is not held at a constant power level. Little can be done to alleviate the first limitation but the second can be eliminated by counting the fission fragments in a chamber during the irradiation.[62] Difficulties may be encountered in making the fission chamber sufficiently insensitive, but such measurements have been made in the MTR.[17]

C. Methods of Gamma-Ray Spectroscopy

For gamma-ray spectroscopy requiring moderate energy resolutions and high detection efficiency, the sodium-iodide (Tl) scintillator has become of dominant importance. For measurements of continuous spectra such as are encountered in reactors (Section III), however, problems arise. The use of a simple single crystal spectrometer[51,52] requires an "unscrambling" process which may become very difficult or even impossible for reactor applications.[52,53,54,55] Methods of attacking the unscrambling problem were discussed in detail at the ANP Spectroscopy Information Meeting held August 1957 at WADC.[56] The use of more complicated coincidence or anti-coincidence spectrometers, which tend to reduce the unscrambling problem to a tractable level, requires quite complex instrumentation.[57] The use of large-crystal, total absorption gamma-ray spectrometers has not yet developed to a useful state.[58]

For only a few cases could the gamma-ray spectrum become of sufficient importance for the production of displacement effects to justify measurements. Such measurements should utilize the largest-obtainable sodium-iodide scintillator which afforded at least moderate energy resolution and did not give rise to spurious peaks in the response function.[58] A 3 in. dia. x 3 in. high cylindrical crystal should be readily available at the present time. A catalog of response functions for this size crystal is available[59] but these would be of only very limited value for a reactor measurement. Thus a major proportion of the effort expended for any reactor gamma-ray spectral measurement would probably be required for the determination of spectrometer response functions.

V. OTHER CHARACTERIZATIONS OF A RADIATION FIELD

The difficulties encountered in attempting to determine spectra in reactor facilities make clear the desirability of finding alternative methods of characterizing the radiation field. Such alternative methods cannot be regarded as a complete substitute for a spectral determination, however.

In order to be useful, any alternative characterization of the radiation field should satisfy several requirements. These are: (1) that the energy dependence of the characterization must be as closely as possible the same as that of the radiation-induced effect, (2) the characterization must be readily related to a physically measurable quantity, and (3) the characterization should be derivable without the expenditure of an inordinate amount of effort. It is apparent that requirement (1) can only be met by a single characterization if the energy dependences of all radiation-induced effects are similar.

A. For Neutrons

In order to examine the energy dependence of neutron-induced effects in more detail than was presented in Section II, the formulation of Snyder and Neufeld[5] will be used. For this approach (S-N), which is one of the most detailed available, it is assumed that all interactions are binary, thermal motion and lattice positions of the struck atoms are ignored, a reasonable shape (i.e. non-step function) for the threshold, E_d, is assumed and finally some elastic collisions are considered to occur above the ionization energy, E_i. It should be noted that the values of E_i used by S-N are significantly larger than those given by Seitz.[1] This affects the subsequent data very greatly. In Fig. 7 are shown values of the S-N G(E) function, which is the number of displacements produced by a single neutron collision. G(E) is almost the same as $\nu(E)$ in Eq. 2. For the determination of G(E), the recoil threshold energy was taken as 25 ev. Shown in Fig. 6 are curves of the total number of displacements per cc per unit time, produced by neutrons of energy E, $N_d(E)$:

$$N_d(E) = n_o \phi(E)\, \sigma(E)\, G(E) \qquad (9)$$

The neutron spectrum, $\phi(E)$, was taken from Fig. 3, which required bold interpolation of the data available. The cross sections, $\sigma(E)$, were taken as the total neutron cross sections from BNL-325 as suggested in S-N. In Fig. 6 are shown curves A = 12 and A = 56. Another curve is indicated for A $\approx$ 1 even though the S-N formulation is not valid for A so low. It is obvious from the considerable variation in the shapes of the curves for different A that no single energy dependence function could match all. However, the data in Fig. 6 does indicate that the energy region of most importance for the production of neutron effects in solids increases with A from a few hundred kilovolts to a few Mev. For high A materials, the contribution of the neutrons in the fission spectrum is quite important and the assumption of a 1/E spectrum for a pool-type reactor would introduce considerable error.

1. Poor Characterizations. The following characterizations are those which have been used most widely in the past for radiation-effects measurements. The thermal-neutron flux, as such, has no unique correlation with the neutrons which produce damage. If the correlation is known for a particular reactor, then the flux which produces damage, not the thermal flux, should be reported. The "total" or epithermal neutron fluxes have no meaning until defined further. While such fluxes might be defined to be useful for radiation effects, other names and concepts (see below) would be more suitable. The use of megawatt days per adjacent ton would appear to be unjustified for any future use. (Megawatt days per ton is a very suitable unit for fuel damage studies, however.) All of the above characterizations may be considered as meaningless to within a factor of 10.

2. Damage Functions. The use of a neutron-induced solid-state effect has been suggested as a method of characterizing a neutron field for radiation-effects measurements. This concept has been pursued in considerable detail by Primak who has suggested that the change in the electrical resistivity of graphite might be a suitable property.[60] The energy dependence of this property would obviously be suitable for radiation effects in materials of A close to carbon and in principle, the property is directly measurable. In practice, however, annealing of the radiation

effect takes place giving rise to a non-linear dependence upon the time of exposure. Primak has made suggestions for overcoming this difficulty but some complications are necessarily introduced. Other physical property changes have been suggested for use in characterizing a neutron field but all probably exhibit some annealing. Irradiation at sufficiently low temperatures to arrest annealing would be very difficult in high-flux reactors.

3. Absorbed Energy. The energy absorbed in a specified material might be considered as a method of characterizing a neutron field. This parameter has been used almost exclusively in radiobiology and in early shielding investigations. The energy dependence of the energy absorbed in hydrogen or water (as suggested by Burrus[61]) is shown in Fig. 7. In the same figure are shown the G(E) functions used in predicting the energy dependence of displacement production. The similarities of the curves for energy absorbed in hydrogen and that for G(E) for A = 12 are striking. Burrus[61] has made calculations for different assumed reactor neutron energy spectra which showed that the energy absorbed in hydrogen corresponded to displacement production in aluminum, copper, and gold (according to the theory of Kinchin and Pease[4]) to within about ±40%.

The energy absorbed from neutron fields of sufficient intensity to produce solid-state effects may be readily observed directly by calorimetric methods. However, the concomitant gamma-ray heating makes such measurements virtually impossible. Therefore, indirect methods of determining the energy absorbed have to be utilized. The threshold detectors discussed in Section IV would be the most likely choice for high radiation level facilities. Hurst[46] has emphasized the methods of determining dose from threshold detector measurements. The Hurst proton-recoil or other counter-type dosimeters might be used if the radiation levels were not too high.

4. A Nuclear Reaction. If the threshold detectors are to be used for experimental measurements to characterize the neutron field, the question logically arises as to whether any one of them could be used as a single parameter. In order to examine the energy dependence of the threshold reactions, the pertinent cross sections for the most likely possibilities

are plotted in Fig. 7. Here, the dependence on energy may be compared with that for a calculated displacement production. The use of sulfur as a single parameter would appear to be undesirable since its "threshold" is so high. Neptunium ^{237} is much more suitable.

B. For Gamma-Rays

For gamma rays the predominate effects in insulators are due to ionization, which in turn follows the absorption of energy since the energy required to form an ion pair is virtually independent of energy. Thus absorbed dose is the logical parameter for studies of gamma-ray effects in insulators. The ANP Advisory Committee for Nuclear Measurements and Standards has suggested that carbon or graphite be adopted as a standard material[50] for reporting gamma-ray energy absorption. The measurements might be made using graphite directly in an ionization chamber or calorimeter. If other measurement methods are used, it is suggested that the results be converted to "carbon dose". The conversion could follow from either an experimentally or theoretically determined conversion factor.

For studies of insulating materials other than graphite, it would be optimum to measure the energy absorbed in the material under investigation. The suggestion of the single material, carbon, was made because it may not be practical to employ measuring devices containing many different materials. The use of a single reference medium is made possible by the natu re of the energy absorption due to gamma rays. The most important contribution to the energy absorption, that due to Compton interactions, is independent of A. Therefore a conversion of absorbed doses between materials of differing A may be made with only the very approximate knowledge of the gamma-ray spectrum which is needed in order to determine the photoelectronic contribution to the absorbed-dose. Burrus has given explicit examples of such calculations.[50]

For the few reactors for which the gamma-ray spectra are known, the energy absorbed in any material, D_γ, may be calculated directly: (assuming a small sample).

$$D_\gamma = \int \phi_\gamma(E)\, E\, \Sigma(E)\, dE$$

where the cross section, $\Sigma(E)$, is the true energy absorption coefficient.[33]

The effects of gamma rays upon metals do not follow from ionization but rather from displacement production. For this phenomena the correlation between the radiation effect and the gamma-ray energy would appear to be even less understood than for displacement production by neutrons. Gamma-ray spectral determinations or studies with monoenergetic electrons will surely be required for increased understanding. In the interim, the use of absorbed dose would appear to be the best procedure.

C. Summary

Radiation effects studies (especially for neutrons) would appear to be producing a vast amount of meaningless data because of a lack of sufficient characterization of the radiation field. (Meaningless may be considered as without meaning within a factor of 10.) Lack of such a characterization not only limits the physical understanding of the processes involved but also prohibits meaningful comparisons of data obtained from different facilities. Effort must be diverted from the radiation-effects studies and expended in determining a better characterization of the radiation field. The optimum characterization would consist of a knowledge of the energy spectra (and perhaps angular distributions) of the radiations in a reactor or other irradiation facility. The few available spectra have been examined and the difficulties encountered in making spectral determinations considered. Because of these difficulties, simplier characterizations have been proposed elsewhere which would constitute a vast improvement over the "poor" characterizations most often used at present. Three such characterizations for neutrons are (1) a solid-state effect such as the change of electrical resistivity of graphite, (2) absorbed energy in a reference material such as hydrogen, and (3) a nuclear reaction such as $Np^{237}(n,f)$. Annealing phenomena may create serious difficulties for the first method. The energy dependence of the last two characterizations is not identical to that of any radiation-induced effect but the theoretically determined energy dependence of displacement production varies greatly for materials of different A.

For gamma rays, a simplier radiation characterization is readily available. The dose absorbed in an insulator may be correlated with the ionization effects produced by gamma rays. A reference material, carbon, has already been selected for reporting the energy absorption from a gamma-ray field.

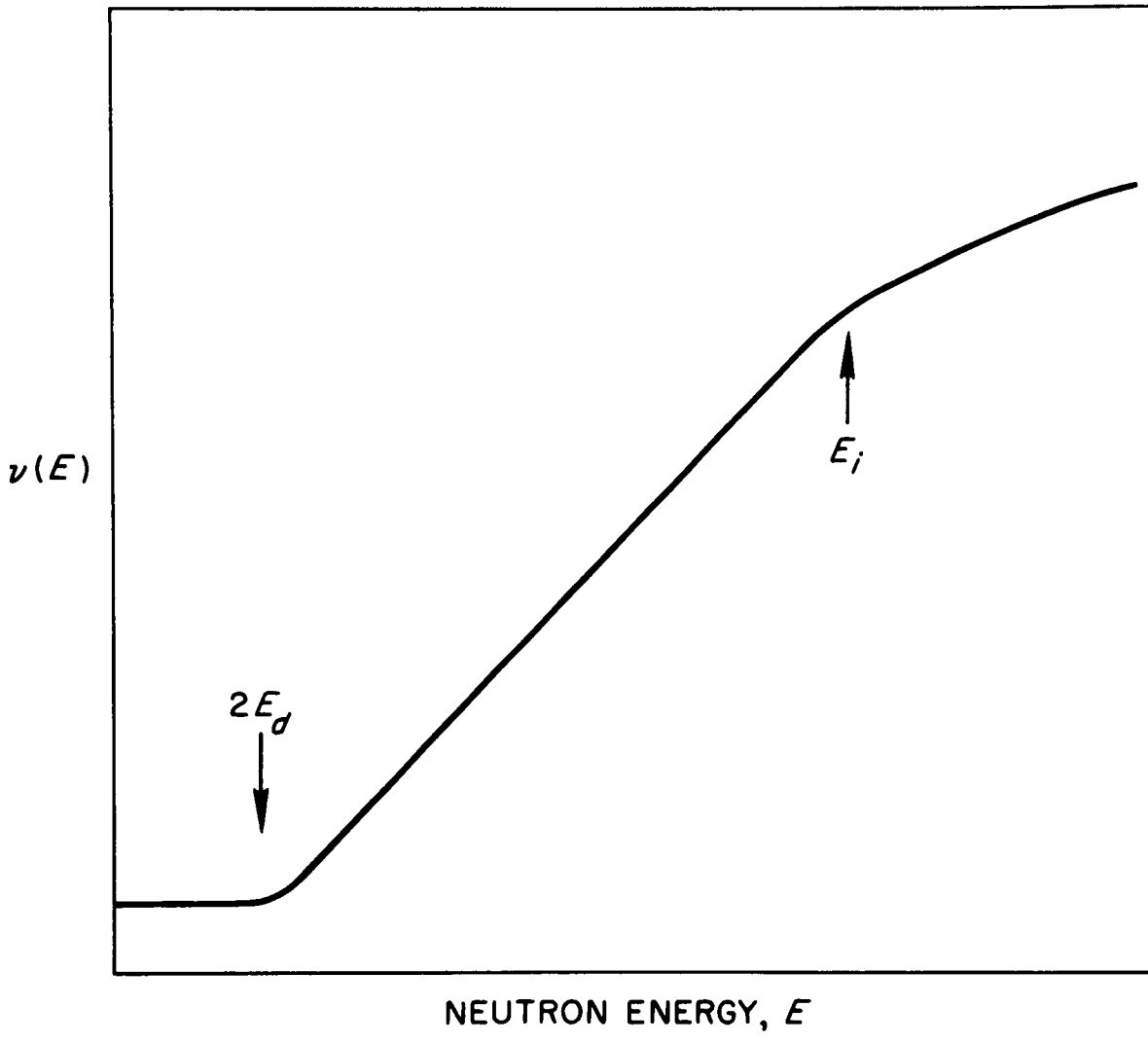

Fig. 1. Dependence upon energy of the number of atomic displacements produced per neutron, $\nu(E)$, in a material of medium or high atomic weight. E_d and E_i are displacement and ionization thresholds as defined in the text.

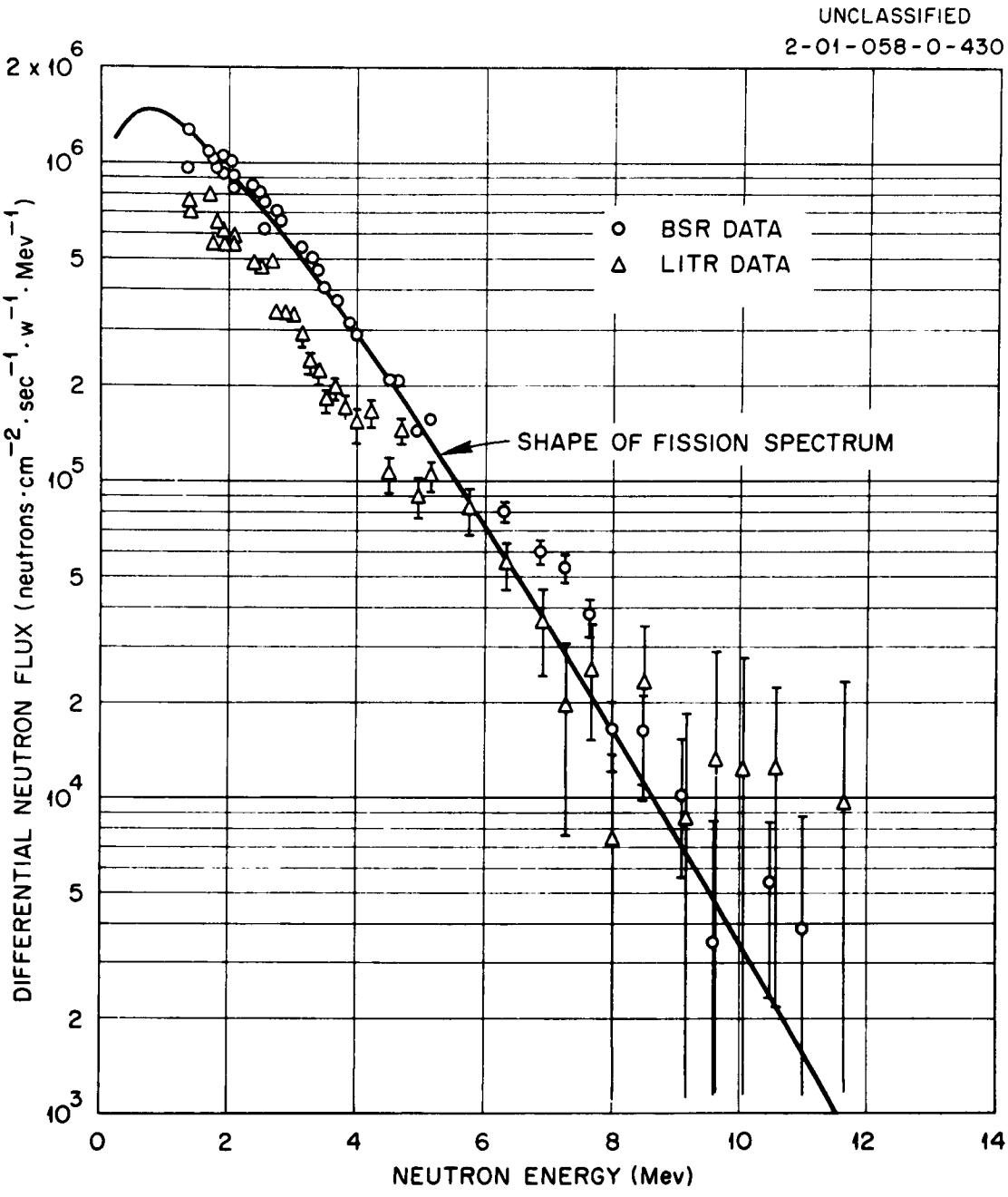

Fig. 2. Differential fast-neutron energy spectra as measured for the BSR and the LITR with the proton-recoil spectrometer. The data for the BSR[7] represent the leakage from the reactor face while the LITR measurements[11] were made in beam hole HB-1. The solid line represents the shape of the fission spectrum[27] as normalized by eye to the BSR spectral data.

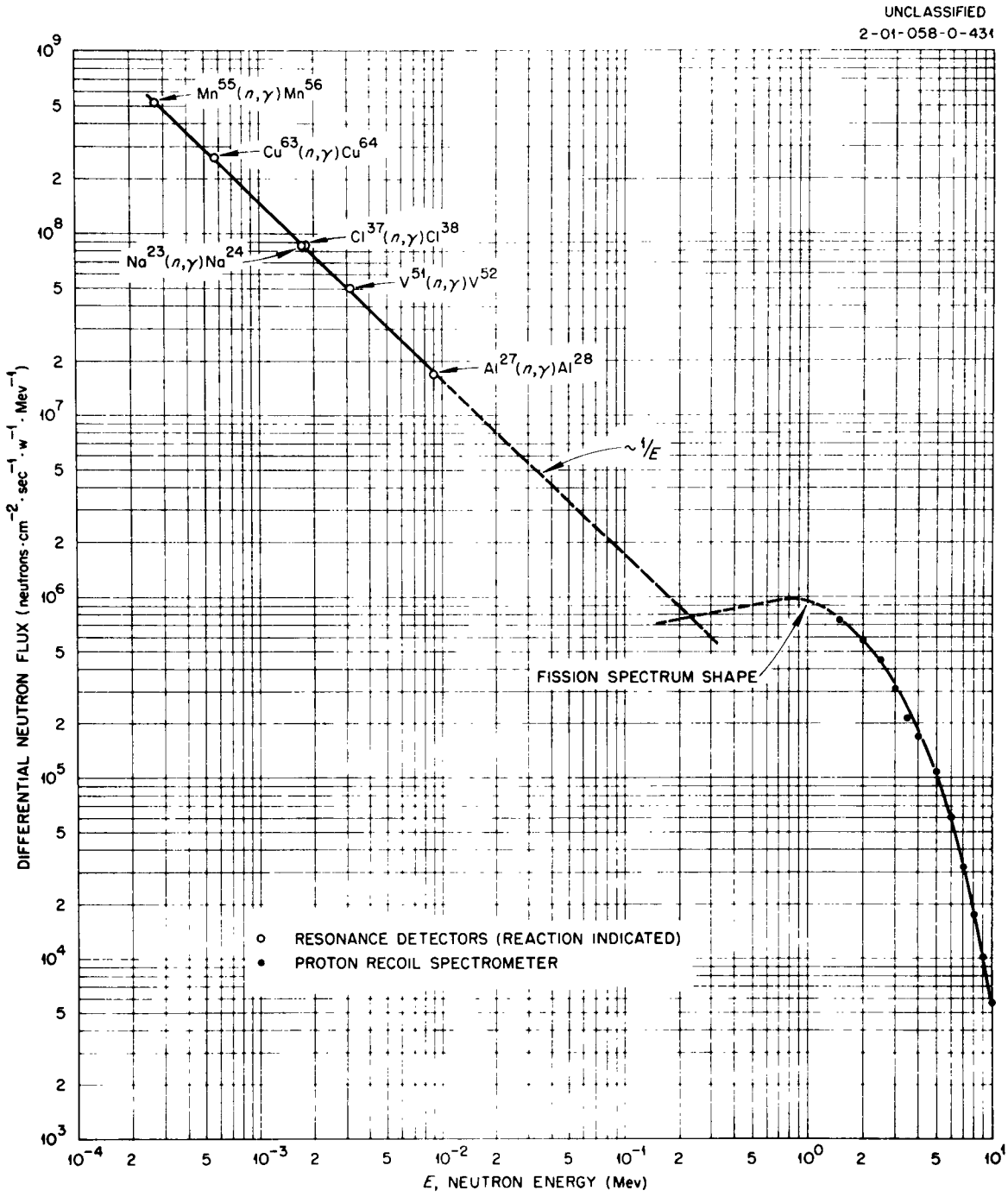

Fig. 3. Differential fast-neutron leakage spectrum for the BSR. The high-energy data are taken from Fig. 2. The low-energy data were obtained with resonance detectors with reactions as shown on the graph.[10] The physical positions for the two measurements were not identical. The figure shows the gap in energy which covers over two logarithmetic decades in the region of maximum radiation effectiveness.

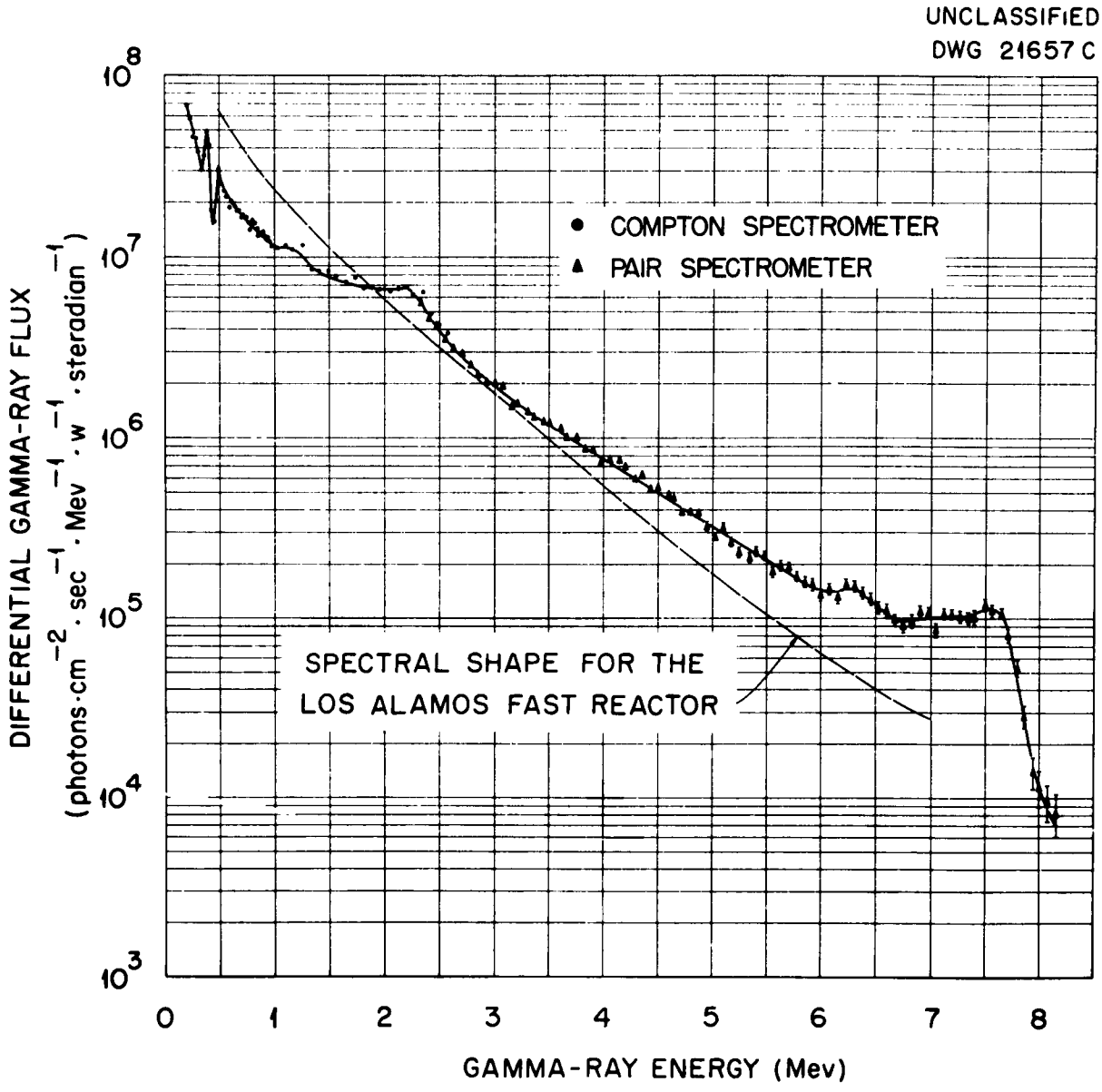

Fig. 4. Gamma-Ray spectrum of the Bulk Shielding Reactor. The compton and pair spectrometer notations refer to different configurations of the three-crystal scintillation spectrometer.[22,23] The data for the Los Alamos Fast Reactor represents the shape (not the magnitude, which was not determined) of the spectrum observed from that reactor.

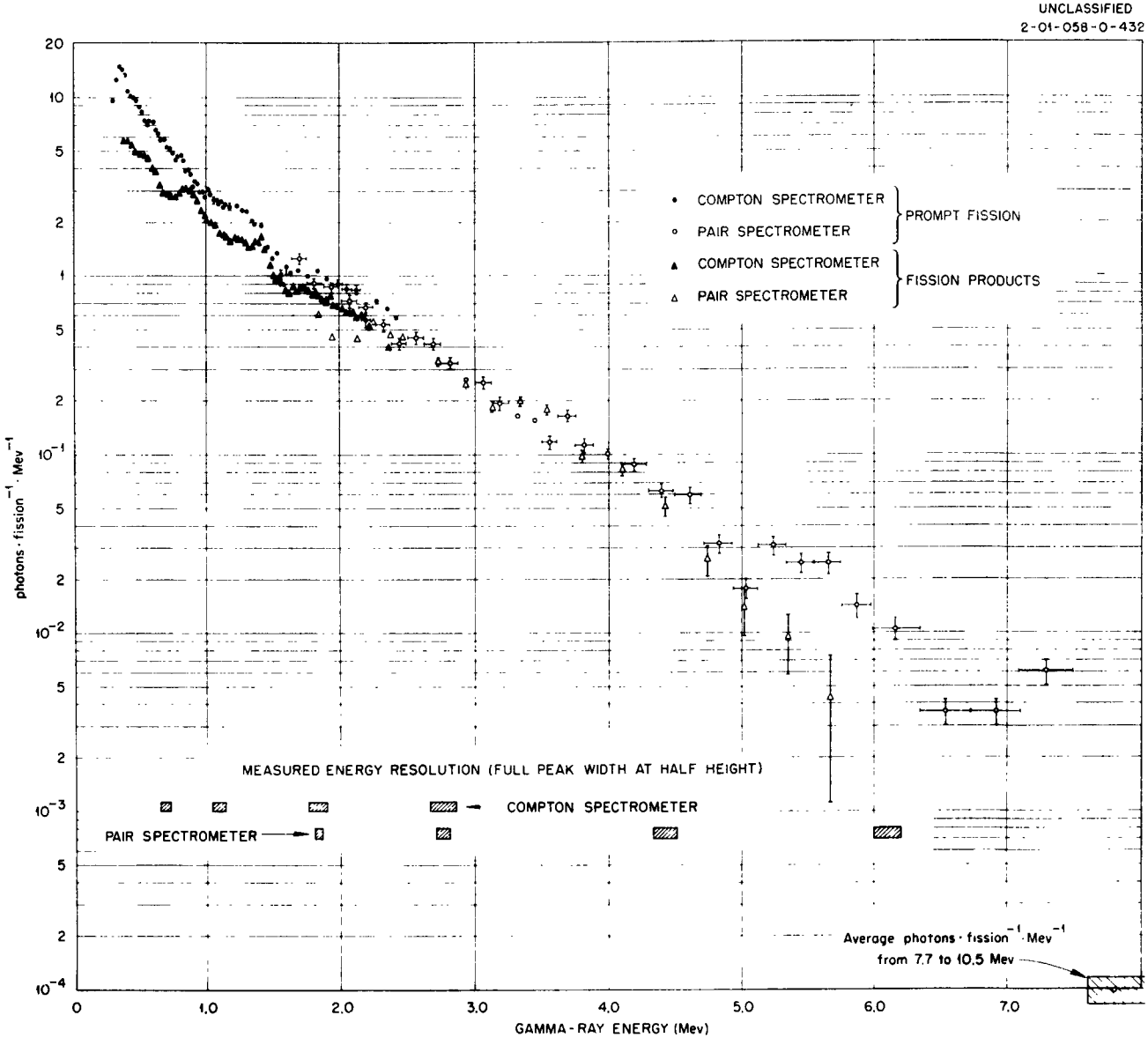

Fig. 5. The spectra of fission-associated gamma rays. All of the data are the result of a preliminary analysis of experiments and are thus subject to further corrections (of the order of 20%) and possible systematic errors. The prompt fission spectrum was that observed within 10^{-7} sec after the fission of U-235 by thermal neutrons. The fission-product spectrum was obtained with a source of U-235 circulating between reactor and spectrometer so that gamma-rays emitted in the time interval from about 1 sec to 10^{4} sec were included.

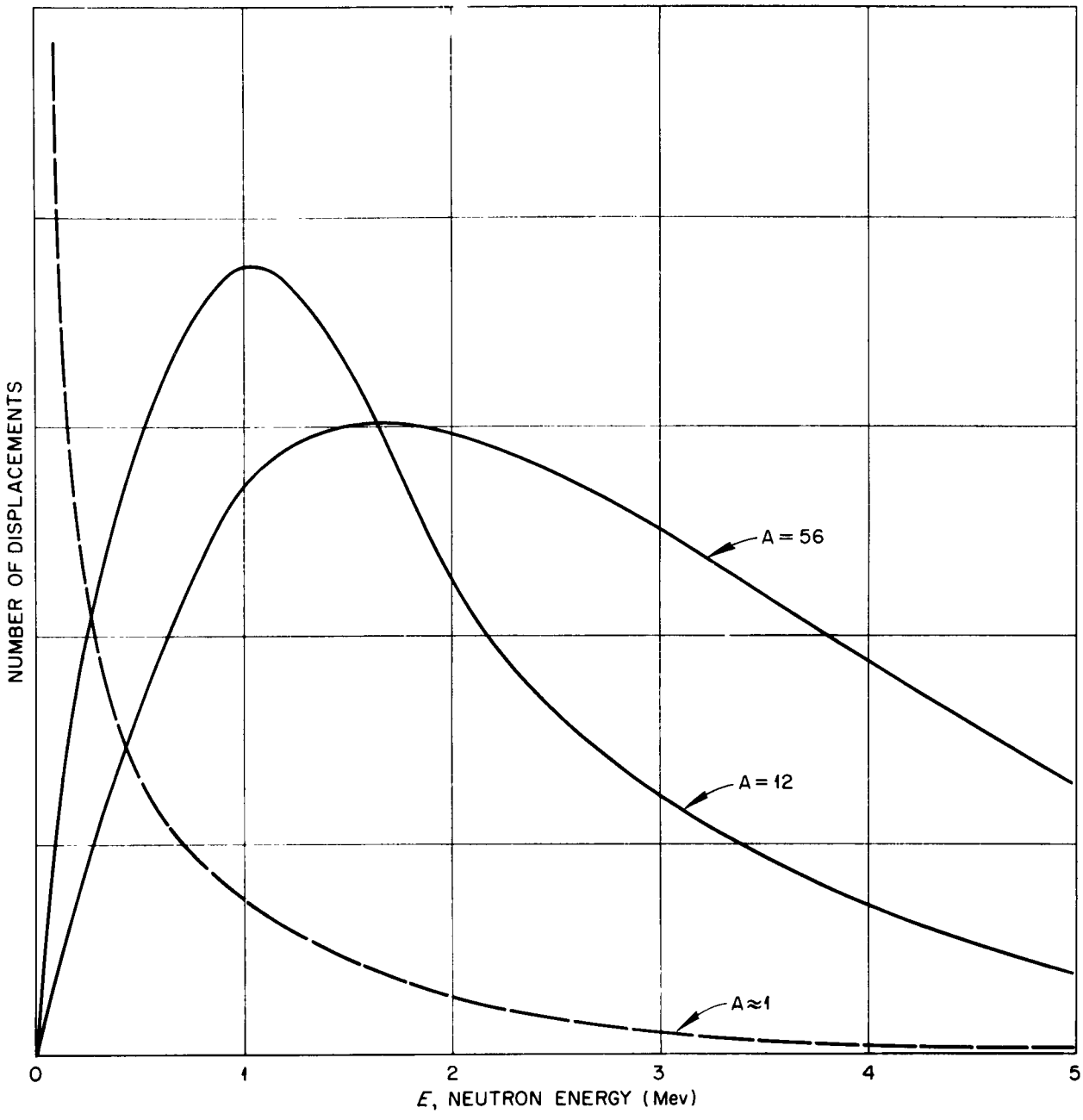

Fig. 6. Displacement production by neutrons. Three curves are shown for the number of displacements, N_d, produced in materials of different A per cc per unit time by neutrons of energy, E. The number of displacements produced by a single neutron, G(E), was determined from the formulation of Snyder and Neufeld (See text 1). The neutron spectrum was taken from Fig. 3. The curve for A = 1 was calculated assuming G(E) = const. The scale for the number of displacements is arbitrary and is not the same for all the curves.

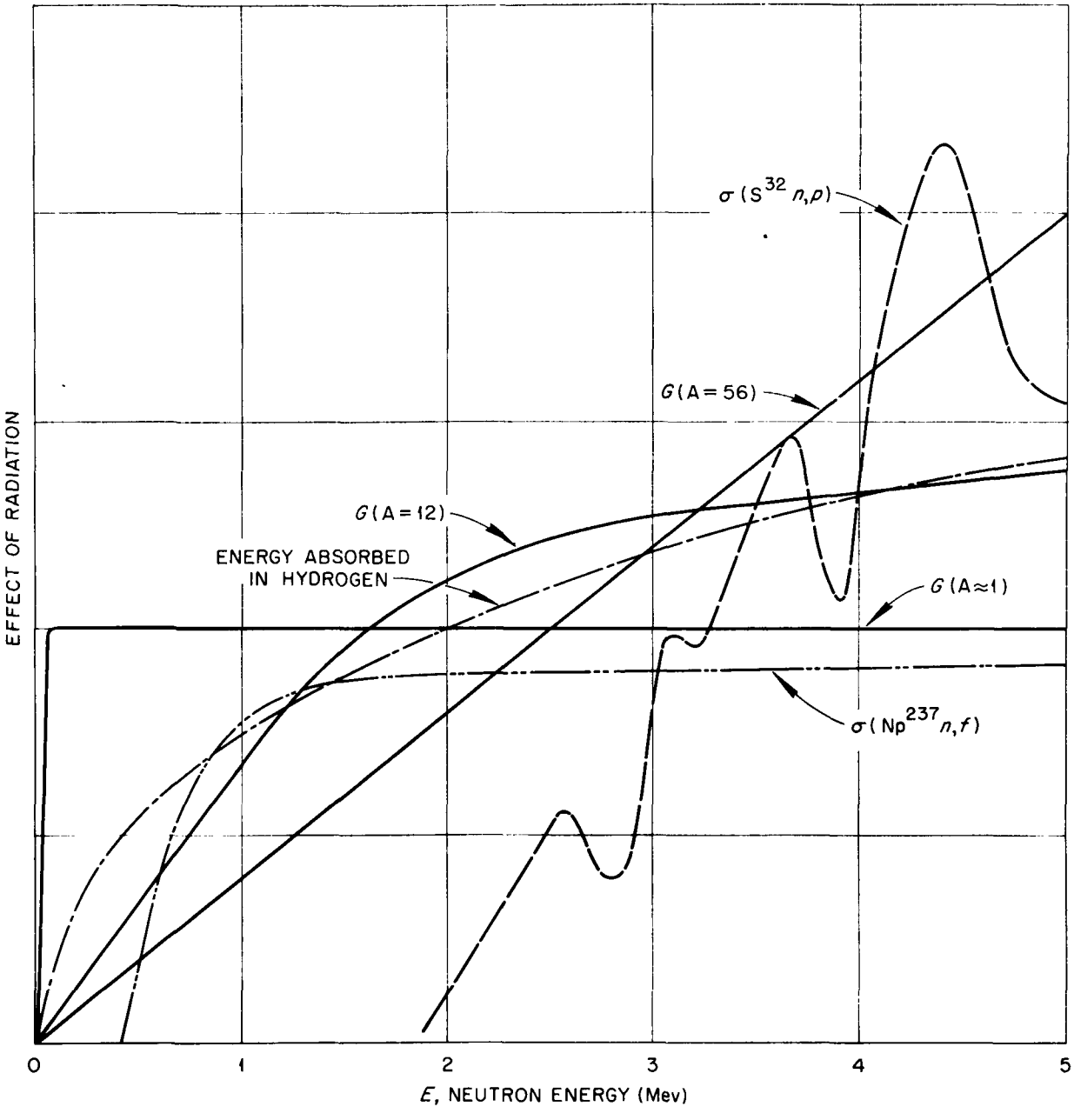

Fig. 7. Radiation characterizations. Values of the Snyder-Neufeld G(E) function, the number of displacements produced by a single neutron collision are shown for A = 12 and A = 56. (Fluctuations in cross sections have been smoothed out.) A constant G(E) curve is also shown to represent the behavior of the G function for A small. Also shown are curves for the energy absorbed in hydrogen and the neutron cross sections for the $N^{237}(n,f)$ and $S^{32}(n,p)$ reactions. All of the values are given in arbitrary units.

REFERENCES

1. Seitz and Koehler, "The Theory of Lattice Displacements Produced During Irradiation," Proc. of Int. Conf. on Peaceful Uses of Atomic Energy, UN P/749 (1955).

2. Dienes and Vineyard, Radiation Effects in Solids, Interscience Publishers, p. 58 (1957).

3. Hughes and Carty, Neutron Cross Sections-Angular Distributions, BNL-400 (1956).

4. Kinchin and Pease, "The Displacement of Atoms in Solids by Radiation," Progress in Physics 18, 1-51 (1955).

5. Snyder and Neufeld, "Diordering of Solids by Neutron Irradiation," Phys. Rev. 97, 1636 (1955), 99, 1326 (1955) and 103, 862 (1956).

6. Bethe and Askin, "Passage of Radiations through Matter," Experimental Nuclear Physics, Wiley, p. 232 (1953).

7. Cochran and Henry, "Fast Neutron Spectra of the Bulk Shielding Facility Reactor," ORNL-CF-53-5-105 (1953).

8. Haydon, Johnson and Meem, "Measurement of the Fast-Neutron Spectrum of the Bulk Shielding Reactor using Nuclear Plates," ORNL-CF-53-8-146 (1953).

9. Faulkner, "Neutron Leakage Spectrum of the Bulk Shielding Reactor," ORNL-CF-54-8-101 (1954).

10. Trice, Muckenthaler, Smith and Johnson, "Two Neutron Energy Measurements in the Bulk Shielding Facility using Radioactivants," ORNL-CF-53-5-139 (1953).

11. Trice, "Measuring Reactor Spectra with Thresholds and Resonances," Nucleonics, 16, No. 7, 81 (1958).

12. Cochran and Henry, "Fast-Neutron Spectrum of the LITR," ORNL-CF-53-12-51 (1953).

13. Trice, "Spectroscopy Requirements for ANP Radiation Damage Program," Proc. of ANP Spect. Info. Meeting Held Aug. 6-7 at WADC, p. 15 (1958).

14. Romanko, "The Neutron Flux Spectrum of the GTR," NARF-57-2T (1957).

15. Eggen, French and Rotz, "Calculation of Fast Neutron Spectra and Dose Rates," FZM-1130 (1958).

16. Schaeffer and Stokes, "ASTR Fast Neutron Spectra," FZM-1047A (1958).

17. Trice, et al, "A Series of Thermal, Epithermal, and Fast Neutron Measurements in the MTR," ORNL-CF-55-10-140 (1955).

18. Primak, "Fast Neutron Damaging in Nuclear Reactors II," NSE 2, 119 (1957)

19. Bopp and Sisman, "The Neutron Flux Spectrum and Fast and Epithermal Flux in Hole 19 of the ORNL Reactor," ORNL-525 (1950).

20. Blosser, et al, "Fast-Neutron Flux Measurements in the ORNL Graphite Reactor Shield," ORNL-CF-58-8-1 (1958).

21. Rosen, "Techniques for Measurements of Neutron Cross Sections and Energy Spectra for Sources which are Continuous in Energy and Time," Proc. of the Inst. Conf. on the Peaceful Uses of Atomic Energy, Vol. 4, U.N. p. 100 (1956).

21a. Hurst, et al, to be published in Health Physics.

22. Maienschein and Love, "Gamma-Ray Spectrum of the BSR," Nucleonics, 12, No. 5, 6-8 (1958).

23. Maienschein and Love, "Spectrum of Gamma Rays Emitted by the BSR," ORNL-CF-53-10-16 (1953).

24. deSaussure, "A Calculation of the Gamma-Ray Spectrum of the BSR," ORNL-CF-57-7-105.

25. Bowman, Dunn, Lessig and Trubey, "A Calculation of the Energy Spectrum and Angular Distribution of Gamma Rays at the Surface of the BSR," ORNL-2609, p. 11 (1958).

26. Motz, "Gamma-Ray Spectra of the Los Alamos Reactor," Phys. Rev. 86, 753 (1952).

27. Cranberg, et al, "Fission Neutron Spectrum of U^{235}," Phys. Rev. 103, 662 (1956).

28. Maienschein, Peelle, Zobel and Love, "Gamma Rays Assoicated with Fission," Proc. Second Int. Conf. on the Peaceful Uses of Atomic Energy, Paper No. 659 (1958).

29. Perkins and King "Energy Release from the Decay of Fission Products," NSE, 3, 726 (1958).

30. Scoles, "Calculated Gamma-Ray Spectra from U^{235} Fission Products," NARF-58-37T (1958).

31. Mittleman and Liedtke, Nucleonics, 13, No. 5, 50 (1955).

31a. Deloume, "Gamma-Ray Energy Spectra from Thermal Neutron Capture," APEX-407 (1958).

32. A new compilation is being prepared by NDA. It will probably appear in the next edition of the Reactor Handbook.

33. Goldstein, The Attenuation of Gamma Rays and Neutrons in Reactor Shields, Second Edition (1958).

34. Weinberg and Wigner, The Physical Theory of Neutron Chain Reactors, Chapt. X, University of Chicago Press (1958).

35. Brooks and Glick, "The Fast-Neutron Flux Spectrum of a Proton-Moderated Thermal Reactor," WAPD-45 (1951).

36. Primak, "Gamma-Ray Dosage in Inhomogeneous Nuclear Reactors," Jour. App. Physics, 27, 54-62 (1956).

37. Rosen, "Nuclear Emulsion Techniques for the Measurement of Neutron Energy Spectra," Nucleonics 11, No. 7, 32 (1953).

38. Cranberg and Rosen, "Measurement of Fast Neutron Spectra," Chapt. in the book Nuclear Spectroscopy to be published by Academic Press.

39. Allred and Armstrong, "Laboratory Handbook of Nuclear Microscopy," LA-510 (1953).

40. Gossick, Cochran, and Henry, "Proton Recoil Fast-Neutron Spectrometer," Rev. Sci. Inst. 26, 754-762 (1955).

41. Johnson and Trail, "Proton-Recoil Neutron Spectrometer," Rev. Sci. Inst. 27, 468 (1956).

42. Batchlor, Aves, and Skyrme, "Helium-3 Filled Proportional Counter for Neutron Spectroscopy," Rev. Sci. Inst. 26, 1037 (1955).

44. Murray, "Use of $Li^6I(E_u)$ as a Scintillation Detector and Spectrometer for Fast Neutrons," Nuclear Instruments 2, 237 (1958).

45. Murray, "Methods of Fast Neutron Spectroscopy," Proc. of ANP Spect. Info. Meet. Held Aug. 6-7 at WADC, WADC-57-298, p. 151 (1958).

46. Hurst, et al, "Techniques of Measuring Neutron Spectra with Threshold Detectors - Tissue Dose Determination," Rev. Sci. Inst. 27, 153 (1956).

47. Hartman, "A Method for Determining Neutron Flux Spectra from Activation Measurements," WADC-TR-57-375 (1957).

48. Uthe, "Attainment of Neutron Flux Spectra from Foil Activation,"

49. Fullwood and Anderson, "An Improved Technique for Deriving Spectral and Dose Data for Threshold Detectors," Proc. Shielding Symposium at NRDL, Vol I, p. 235 (1956).

50. Burrus, "Standard Instrumentation Techniques for Nuclear Environmental Testing," WADC-TR-57-207 (1957).

51. Bell, "The Scintillation Method," in Beta and Gamma-Ray Spectroscopy, Interscience, p. 133 (1955).

52. Lazar, "Analysis of Gamma-Ray Scintillation Spectra for Quantitative Photo Intensities," presented at the Sixth Scintillation Counter Symposium, Washington, Feb. 27-28, 1958.

53. Hubbel and Scofield, "Unscrambling of Gamma-Ray Scintillation Spectrometer Pulse-Height Distributions," presented at the Sixth Scintillation Counter Symposium, Washington, Feb. 27-28, 1958.

54. Beach, Thesis and Faust, "Analysis of Scintillation Spectrometer Observations of the Penetration of Cs^{137} Gamma Radiation through Water," NRL-4277 (1953).

55. W. R. Burrus, private communication.

56. In Proceedings of ANP Spectroscopy Info. Meeting held Aug. 6-7 at WADC (1958) see papers by Beach, Cook, Scofield, and Zobel.

57. Love, et al, "Electronic Instrumentation for a Multiple-Crystal Gamma-Ray Scintillation Spectrometer," ORNL-1929 (1955).

58. Chapman and Lazar, "Total Absorption Gamma-Ray Spectroscopy," Proc. of the ANP Spectroscopy Info. Meeting Held Aug. 6-7, 1958 at WADC, p. 97 (1958).

59. Heath, "Scintillation Spectrometer Gamma-Ray Spectrum Catalog," IDO-16408 (1957).

60. Primak, "Fast Neutron Damaging in Nuclear Reactors - The Radiation Damage Dose," NSE, 2, 320 (1957).

61. Burrus, "How to Systematize the Correlation of Radiation Damage Data," Proc. of the Second Semi-Annual Radiation Effects Symposium, Oct. 22-23, 1957.

62. Trice, "Miniature Fission Chamber," Nucleonics 16, No. 7, p. 84 (1958).

AVERAGE NEUTRON CROSS SECTIONS FOR TYPICAL REACTOR SPECTRA

by

Walter R. Burrus[+]
and
Russell P. Sullivan

Ohio State University
Physics Department

Average neutron cross sections are calculated for fifteen common elements. Elastic scattering, inelastic scattering, and charged particle reactions are considered. From these average cross sections, one may calculate a dose in one material from a measured dose in another or one may calculate a dose from an activation, an activation from a dose, or an activation from an activation. The spectra used for calculating the averages are for fission neutrons which have penetrated various thicknesses of water and graphite[1] (calculated by NDA by use of the "moments method" [1]). The relationship of the calculated averages to other types of averages is discussed and conversion factors are given. Cross section averages are also given for several fission foils. Finally, the fraction of the absorbed dose which is transferred to recoil nuclei which does not result in ionization is calculated for five elements. This fraction is useful in comparing radiation effects which are caused by atomic displacements.

+ Mershon Fellow and formerly with Lockheed Aircraft Corporation, Georgia Division.

INTRODUCTION

In the interpretation of radiation damage experiments performed in different facilities, the dose which is deposited by neutrons (or the number of transmutations) will depend upon the spectrum of the neutrons as well as upon a dosimetric quantity (tissue dose, flux, aut. cet.) unless the dosimetric device has the same relative response as a funtion of energy as the sample. This paper consist of a compilation of average cross sections for dose deposition and transmutations by charged particle reactions which allow the effects of different spectra to be taken into account. These average cross sections are discussed in greater length in a previous paper [2]. The primary difference in the calculated average cross sections appearing in the two reports is that the spectra calculated by the "moments method" [1] and a more rigorous treatment of non-isotropic scattering and inelastic scattering are used here.

The primary use of these average cross sections is to allow the dose or number of transmutations in one material to be computed from a measured dose or number of transmutations in another material (which might be a dosimetric standard). This comparison is done as follows:

Eq. 1 $$P_s = P_o \, \sigma_s/\sigma_o \, (N_s/N_o) \; ;$$ N_s = no. atoms/gm. in sample; N_o = no. atoms/gm. in reference material

where:

P_s = deposited dose (kev g^{-1}) or number of transmutations (atoms g^{-1}) in the sample

P_o = deposited dose (kev g^{-1}) or number of transmutations (atoms g^{-1}) in some reference material

σ_s = dose deposition cross section (millibarns) or transmutation cross section (millibarns/kev) of sample

σ_o = dose deposition cross section (millibarns) or transmutation cross section (millibarns/kev) of reference material

Eq. 1 may be used to find a deposited dose from either another deposited dose or from a transmutation determination, or it may be used to find the number of transmuted atoms from another transmutation determination or from a deposited dose measurment. In order to obtain this flexibility, it is necessary to use consistent units for dose and for the transmutation cross section. The dose in kev g^{-1} can be converted to erg g^{-1} by multiplying by the conversion factor of 1.602×10^{-9} erg/kev or to rads by multiplying by 1.602×10^{-11} rad-g/kev.

A secondary purpose of this paper is to provide a method for calculating a dose or transmutation rate from the "number flux" ϕ or the "energy flux" I. Using this method, one may convert a variety of radiation damage data to a common basis even though the original data may have been reported in terms of flux or in terms of a dose or a number of transmutations. In general, these calculations can not be done with as great an accuracy as the direct comparison expressed by Eq. 1. Moreover, the use of "number flux" introduces considerable difficulty. This is due to a predominance of moderated low energy neutrons (less than 1 kev) which do not contribute to dose deposition or production of transmutations by charged particle reactions. The extrapolation from higher significant energies to lower energies is very difficult because thermal neutrons, which make up the greater part of the low energy neutrons, are greatly perturbed by absorbing materials in or near the sample or by boundries near the sample. Seperate measurements to account for the thermal neutron effects are generally preferable. (Sometimes the effect of the thermal neutrons can be included in a gamma radiation measurement if the primary result is the production of capture radiation.)

The "energy flux" I and the "number flux" ϕ are related by the simple relation:

Eq. 2. $$I = \int_0^\infty E\phi' \, dE = \bar{E}\phi$$

where: $\bar{E}$ = the average neutron energy

ϕ = the total "number flux"

It is fairly common practice to calculate the product of average energy and the average cross section so that absorbed dose is given by flux × (tabulated product). In this report, the average energy is tabulated seperately. An advantage of this proceedure is that $\bar{E}$ may be considered as a conversion factor from "number flux" to "energy flux" and its definition may be extended to convert from "integral number flux" (i.e. the flux above a certain energy, E_L) to "energy flux".

CALCULATIONS

Seven spectra have been chosen for the calculation of the cross section averages. These spectra were calculated by NDA using the "moments method" [1] and apply to a point isotropic fission source which has penetrated a specified distance through the moderator. It was intended that these spectra be typical of radiation damage facilities. In actual multi-region shield, the spectra may be much more complicated, but the results given here should indicate qualitatively the effects of varying spectral conditions. In subsequent discussions and tables, the spectra are designated by their symbols given below.

Moderator	Penetration	Symbol
Carbon	10 g cm^{-2}	C-10
Carbon	30 g cm^{-2}	C-30
Carbon	90 g cm^{-2}	C-90
Water	10 g cm^{-2}	W-10
Water	30 g cm^{-2}	W-30
Water	90 g cm^{-2}	W-90
Unmoderated	- - - - - -	UN-MOD

TABLE I. SPECTRA AND THEIR SYMBOLS

The numerical calculations required were performed with an IBM-650 computer at the Ohio State University Numerical Computation Laboratory. The energy range was divided into five proportionally spaced intervals per decade from 1 kev to 4 mev and into 6 equally spaced 2 mev intervals from 4 mev to 16 mev. The contribution from neutrons below 1 kev and above 16 mev was negligible except where specifically mentioned.

All cross sections and angular distributions required were obtained from references (3), (4), and (5). Liberal extrapolation and interpolation of the data was necessary to cover the entire energy range. The Coulomb barrier penetration curves given by Hughes [6] were used as a guide in estimating the (n, p) and (n, α) cross sections which had not been measured.

The (n, 2n) and (n, γ) interactions were not considered here. The (n, 2n) reaction is entirely negligible in dose deposition compared to the elastic scattering contribution, but the (n, 2n) interaction may cause significant transmutations. The (n, γ) interaction is generally not negligible for dose deposition, but it depends very strongly upon the thermal neutron spectrum because of the 1/v dependence of most (n, γ) cross sections. In addition, the (n, γ) interaction is often the most significant contribution to transmutations (and associated activation). A knowledge of the thermal (n, γ) cross section, the decay chain of the isotope produced, and a measurement of the thermal neutron "flux", (nv_o), is usually sufficient to calculate the dose deposition and transmutations due to all the neutrons below 1 kev.

"NUMBER FLUX" TO "ENERGY FLUX" CONVERSION

As has been suggested earlier, Eq. 2 can be generalized to give the "energy flux" I in terms of the integral flux $\underline{\underline{\phi}}(E_L)$. This generalized "average energy" is denoted by $\bar{\bar{E}}$ (with a double bar) and is given by:

Eq. 3 $$\bar{\bar{E}} = \int_o^\infty E\phi' \, dE \Big/ \int_{E_L}^\infty \phi' \, dE = I / \underline{\underline{\phi}}(E_L)$$

where: $\bar{\bar{E}}$ = generalized "average energy" (kev) -- conversion factor from integral flux to "energy flux"

$\underline{\underline{\phi}}(E_L)$ = integral flux -- the "number flux" of neutrons with energy above E_L

Table II gives values of $\bar{\bar{E}}$ for all seven spectra for different values of E_L from 0 to 4 mev. The values of $\bar{\bar{E}}$ for $E_L = 0$ are sensitive to perturbations of the thermal flux. For this reason, a perturbed value of $\bar{\bar{E}}$ is also listed for $E_L = 0$ to indicate qualitatively how much change might be expected.

The NDA "moments method" calculation is extended down to thermal energies by assuming a 1/E dependence of the "number flux" ϕ' except for SPECTRUM C-10 where "Fermi Age" theory was used. The relation between thermal neutrons and epi-thermal neutrons was estimated from experimental measurments in graphite and water moderated experimental facilities. The flux perturbation estimates include only the purturbation at the surface of the samples and do not include "self shielding" effects within the sample. A sample which is opaque to thermal neutrons and several diffusion lengths in extend is assumed for the perturbation estimation.

E_L (kev)	SPECTRUM C-10	SPECTRUM C-30	SPECTRUM C-90	SPECTRUM W-10	SPECTRUM W-30	SPECTRUM W-90	SPECTRUM UN-MOD
4 (3)	8.00 (3)	1.06 (4)	1.00 (4)	6.80 (3)	6.53 (3)	6.37 (3)	6.76 (3)
1 (3)	2.74 (3)	2.78 (3)	3.02 (3)	3.09 (3)	3.41 (3)	4.67 (3)	2.85 (3)
4 (2)	1.79 (3)	1.56 (3)	1.65 (3)	2.17 (3)	2.62 (3)	4.00 (3)	2.18 (3)
1 (2)	1.43 (3)	1.15 (3)	1.19 (3)	1.68 (3)	2.16 (3)	3.54 (3)	2.03 (3)
1 (1)	1.14 (3)	8.26 (2)	8.00 (2)	1.35 (3)	1.82 (3)	3.16 (3)	2.00 (3)
1 (0)	1.10 (3)	6.37 (2)	5.35 (2)	1.16 (3)	1.61 (3)	2.90 (3)	2.00 (3)
1 (-1)	1.08 (3)	5.18 (2)	3.92 (2)	1.01 (3)	1.44 (3)	2.67 (3)	2.00 (3)
1 (-2)	1.07 (3)	4.36 (2)	3.10 (2)	9.00 (2)	1.31 (3)	2.48 (3)	2.00 (3)
1 (-3)	1.06 (3)	3.77 (2)	2.56 (2)	8.10 (2)	1.19 (3)	2.32 (3)	2.00 (3)
4 (-4)	1.05 (3)	3.58 (2)	2.39 (2)	7.78 (2)	1.15 (3)	2.25 (3)	2.00 (3)
0 *	1.0 (3)	1.5 (2)	2.7 (1)	3.5 (2)	5.0 (2)	1.4 (3)	2.00 (3)
0	6.0 (2)	1.1 (1)	2.0 (0)	1.1 (2)	1.5 (2)	5.6 (2)	2.00 (3)

* PETURBED THERMAL FLUX (SEE TEXT)

TABLE II. "NUMBER FLUX" TO "ENERGY FLUX" CONVERSION $\bar{\bar{E}}(E_L)$ (kev)

	SPECTRUM C-10	SPECTRUM C-30	SPECTRUM C-90	SPECTRUM W-10	SPECTRUM W-30	SPECTRUM W-90	SPECTRUM UN-MOD
U-234	6.98 (-1)	7.56 (-1)	7.15 (-1)	6.07 (-1)	5.36 (-1)	4.11 (-1)	6.20 (-1)
U-236	3.05 (-1)	2.98 (-1)	2.80 (-1)	2.84 (-1)	2.70 (-1)	2.32 (-1)	3.03 (-1)
U-238	1.54 (-1)	1.44 (-1)	1.37 (-1)	1.52 (-1)	1.49 (-1)	1.33 (-1)	1.60 (-1)
Np-237	6.70 (-1)	7.22 (-1)	6.81 (-1)	5.79 (-1)	5.11 (-1)	3.92 (-1)	5.98 (-1)
Pu-239 *	1.70 (0)	3.02 (0)	3.67 (0)	1.66 (0)	1.22 (0)	7.37 (-1)	9.87 (-1)
Pu-239 +	1.28 (0)	1.74 (0)	1.79 (0)	1.12 (0)	8.77 (-1)	5.81 (-1)	8.58 (-1)

* SHIELDED BY 1 CM OF B^{10}_{10} (LINEAR DENSITY 1.11 G CM^{-2})
\+ SHIELDED BY 4 CM OF B^{10} (LINEAR DENSITY 1.11 G CM^{-2})

TABLE III. FISSION FOIL CROSS SECTIONS (MILLIBARNS/KEV)

DOSE DEPOSITION CROSS SECTION

The dose deposition cross section $\bar{\sigma}_d$ is defined by:

Eq. 4 $$D = N \int_0^\infty \phi' E \sigma(E) f \, dE = N I \bar{\sigma}_d$$

where: D = deposited dose rate (kev g^{-1} sec^{-1})

N = number of sample atoms per gram (atom g^{-1})

$\phi' dE$ = number of neutrons crossing surface of a unit flux flux detector with energy between E and E+dE (neutrons cm^{-2} sec^{-1} kev^{-1})

E = neutron energy (kev)

I = "energy flux" = $\int_0^\infty E \phi' dE$ (kev cm^{-2} sec^{-1})

$\sigma(E)$ = interaction cross section per sample atom (cm^2)

f = average fraction of neutron energy which is deposited in sample

$= [2A/(A+1)^2](1 - \overline{\cos \phi})$ for elastic scattering

$= [2A/(A+1)^2][1 - \frac{1}{2} \frac{A}{A+1}](E\gamma/E)$ for inelastic scattering

$= [E + Q]/E$ for (n, p) and (n, α) reactions

A = atomic weight of sample

$\overline{\cos \phi}$ = average scattering angle in center of mass system

Q = total energy relase per reaction

$E\gamma$ = total gamma energy emitted per inelastic collision

The dose deposition cross sections $\bar{\sigma}_d$ are tabulated inTable IV for fifteen common elements. The cross sections are listed seperately for each type of interaction. The interactions are identified by a number in the first column of the tables as follows:

1 elastic scattering contribution
2 inelastic scattering contribution
5 (n, p) reaction contribution
8 (n, α) reaction contribution

	SPECTRUM C-10	SPECTRUM C-30	SPECTRUM C-90	SPECTRUM W-10	SPECTRUM W-30	SPECTRUM W-90	SPECTRUM UN-MOD
			HYDROGEN				
1	1.62 (+3)	1.87 (+3)	1.83 (+3)	1.44 (+3)	1.23 (+3)	9.00 (+2)	1.34 (+3)
			DEUTERIUM				
1	1.20 (+3)	1.26 (+3)	1.22 (+3)	1.12 (+3)	1.02 (+3)	8.12 (+2)	1.12 (+3)
			BORON				
1	2.57 (+2)	2.86 (+2)	2.76 (+2)	2.30 (+2)	2.01 (+2)	1.50 (+2)	2.23 (+2)
2	1.05 (+1)	8.22 (+0)	1.04 (+1)	1.46 (+1)	1.91 (+1)	2.87 (+1)	1.43 (+1)
8 *	7.40 (+2)	2.98 (+3)	4.71 (+3)	1.18 (+3)	7.25 (+2)	3.27 (+2)	1.69 (+2)
			CARBON				
1	2.53 (+2)	2.79 (+2)	2.70 (+2)	2.27 (+2)	1.96 (+2)	1.44 (+2)	2.18 (+2)
2	1.14 (+0)	8.12 (-1)	1.43 (+0)	2.43 (+0)	4.67 (+0)	1.05 (+1)	2.14 (+0)
8	3.85 (-1)	2.49 (-1)	4.22 (-1)	8.38 (-1)	1.90 (+0)	5.28 (+0)	7.10 (-1)
			NITROGEN				
1	1.73 (+2)	1.93 (+2)	1.88 (+2)	1.56 (+2)	1.37 (+2)	1.04 (+2)	1.49 (+2)
2	1.60 (+1)	1.25 (+1)	1.39 (+1)	1.97 (+1)	2.26 (+1)	2.81 (+1)	1.97 (+1)
5 *	3.61 (+1)	4.27 (+1)	4.00 (+1)	2.78 (+1)	2.26 (+1)	1.58 (+1)	2.86 (+1)
8	4.14 (+1)	3.60 (+1)	3.77 (+1)	4.71 (+1)	5.30 (+1)	6.32 (+1)	4.85 (+1)
			OXYGEN				
1	2.39 (+2)	2.69 (+2)	2.58 (+2)	2.07 (+2)	1.75 (+2)	1.23 (+2)	2.00 (+2)
2	1.23 (+0)	8.63 (-1)	1.58 (+0)	2.84 (+0)	5.73 (+0)	1.33 (+1)	2.41 (+0)
5	1.58 (-1)	1.00 (-1)	1.50 (-1)	3.34 (-1)	7.92 (-1)	1.98 (+0)	2.89 (-1)
8	1.33 (+1)	1.02 (+1)	1.46 (+1)	1.92 (+1)	2.27 (+1)	2.54 (+1)	1.97 (+1)
			FLOURINE				
1	1.31 (+2)	1.52 (+2)	1.46 (+2)	1.15 (+2)	9.64 (+1)	6.64 (+1)	1.06 (+2)
2	8.47 (+1)	9.34 (+1)	9.09 (+1)	7.72 (+1)	6.85 (+1)	5.41 (+1)	7.45 (+1)
5	4.04 (+0)	3.00 (+0)	5.27 (+0)	8.33 (+0)	1.45 (+1)	2.83 (+1)	7.52 (+0)
8	3.87 (+1)	2.95 (+1)	4.50 (+1)	6.30 (+1)	8.75 (+1)	1.33 (+2)	6.18 (+1)
			ALUMINUM				
1	9.30 (+1)	9.10 (+1)	8.35 (+1)	8.44 (+1)	7.69 (+1)	5.52 (+1)	9.21 (+1)
2	1.77 (+1)	1.45 (+1)	1.60 (+1)	2.13 (+1)	2.41 (+1)	2.86 (+1)	2.16 (+1)
5	9.70 (+0)	7.17 (+0)	1.10 (+1)	1.70 (+1)	2.74 (+1)	5.25 (+1)	1.59 (+1)
8	1.44 (+0)	9.77 (-1)	1.72 (+0)	3.24 (+0)	6.88 (+0)	1.72 (+1)	2.75 (+0)

* (SEE TEXT FOR ADDITIONAL CONTRIBUTION FROM NEUTRONS LESS THAN 1 KEV)

TABLE IV. DOSE DEPOSITION CROSS SECTIONS (MILLIBARNS)

	SPECTRUM C-10	SPECTRUM C-30	SPECTRUM C-90	SPECTRUM W-10	SPECTRUM W-30	SPECTRUM W-90	SPECTRUM UN-MOD
			SILICON				
1	1.53 (+2)	1.86 (+2)	1.79 (+2)	1.30 (+2)	1.04 (+2)	6.48 (+1)	1.17 (+2)
2	1.15 (+1)	8.94 (+0)	1.07 (+1)	1.48 (+1)	1.72 (+1)	2.03 (+1)	1.50 (+1)
5	5.82 (+0)	3.80 (+0)	6.56 (+0)	1.27 (+1)	2.84 (+1)	7.88 (+1)	1.08 (+1)
8	3.61 (+0)	2.45 (+0)	4.11 (+0)	7.65 (+0)	1.61 (+1)	4.11 (+1)	6.64 (+0)
			SULPHUR				
1	6.90 (+1)	7.57 (+1)	7.23 (+1)	6.13 (+1)	5.31 (+1)	3.88 (+1)	6.00 (+1)
2	1.85 (+1)	1.46 (+1)	1.65 (+1)	2.28 (+1)	2.57 (+1)	2.98 (+1)	2.31 (+1)
5	1.21 (+2)	9.38 (+1)	1.13 (+2)	1.61 (+2)	1.99 (+2)	2.74 (+2)	1.60 (+2)
8	8.47 (+1)	6.77 (+1)	7.44 (+1)	1.03 (+2)	1.18 (+2)	1.43 (+2)	1.04 (+2)
			CHLORINE				
1	7.37 (+1)	7.75 (+1)	7.38 (+1)	6.71 (+1)	6.00 (+1)	4.56 (+1)	6.75 (+1)
2	1.22 (+1)	9.20 (+0)	1.19 (+1)	1.70 (+1)	2.13 (+1)	2.88 (+1)	1.69 (+1)
5	1.40 (-3)	9.71 (-4)	1.19 (-3)	3.01 (-3)	7.22 (-3)	1.01 (-2)	2.50 (-3)
8	2.54 (+1)	1.92 (+1)	2.78 (+1)	4.01 (+1)	5.69 (+1)	9.21 (+1)	3.89 (+1)
			IRON				
1	4.93 (+1)	5.54 (+1)	5.42 (+1)	4.48 (+1)	3.94 (+1)	3.05 (+1)	4.25 (+1)
2	2.14 (+1)	1.90 (+1)	1.95 (+1)	2.32 (+1)	2.47 (+1)	2.66 (+1)	2.40 (+1)
5	2.62 (+0)	1.84 (+0)	3.22 (+0)	5.62 (+0)	1.11 (+1)	2.58 (+1)	4.91 (+0)
8	8.35 (-1)	5.39 (-1)	8.34 (-1)	1.83 (+0)	4.17 (+0)	1.08 (+1)	1.56 (+0)
			COPPER				
1	6.01 (+1)	6.91 (+1)	6.73 (+1)	5.32 (+1)	4.58 (+1)	3.51 (+1)	4.99 (+1)
2	1.70 (+1)	1.43 (+1)	1.56 (+1)	2.02 (+1)	2.27 (+1)	2.67 (+1)	2.06 (+1)
5	1.32 (+1)	1.00 (+1)	1.52 (+1)	2.25 (+1)	3.42 (+1)	5.98 (+1)	2.13 (+1)
8	1.56 (+0)	1.07 (+0)	1.82 (+0)	3.31 (+0)	6.76 (+0)	1.65 (+1)	2.89 (+0)
			GERMANIUM				
1	5.36 (+1)	6.41 (+1)	6.20 (+1)	4.56 (+1)	3.75 (+1)	2.60 (+1)	4.21 (+1)
2	1.87 (+1)	1.54 (+1)	1.66 (+1)	2.18 (+1)	2.39 (+1)	2.68 (+1)	2.22 (+1)
5	3.65 (+0)	2.61 (+0)	4.24 (+0)	7.06 (+0)	1.30 (+1)	2.93 (+1)	6.36 (+0)
8	5.04 (-2)	3.19 (-2)	4.93 (-2)	1.07 (-1)	2.52 (-1)	6.80 (-1)	9.20 (-2)
			GOLD				
1	2.15 (+1)	2.46 (+1)	2.37 (+1)	1.90 (+1)	1.59 (+1)	1.06 (+1)	1.77 (+1)
2	1.64 (+1)	1.55 (+1)	1.54 (+1)	1.68 (+1)	1.69 (+1)	1.67 (+1)	1.73 (+1)
5	5.42 (-2)	3.45 (-2)	5.08 (-2)	1.16 (-1)	2.71 (-1)	6.79 (-1)	1.00 (-1)
8	1.41 (-4)	1.05 (-4)	1.24 (-4)	3.25 (-4)	7.69 (-4)	8.29 (-4)	2.36 (-4)

TABLE IV. DOSE DEPOSITION CROSS SECTIONS (MILLIBARNS)

The total dose deposition cross section is the sum of these four contributions. The dose deposition cross section per molecule for a sample consisting of a number of different elements may be found by adding together the cross sections of the atoms in a molecule.

It has been assumed that the average scattering angle in the center of mass system is zero for inelastic scattering. The uncertainty in the inelastic contribution introduced by this approximation is estimated to be less than $\pm$ 30 %. The energy release per reaction, Q, has been adjusted to include all the short half life disintegration energies. $E\gamma$ was estimated from the known energy levels of the nuclei. Above 6 mev, $E\gamma$ was taken as (E - 1.5 mev). This last approximation is not serious. The basic "Q values" were obtained from published isotopic masses [8].

TRANSMUTATION CROSS SECTION

The transmutation cross section is defined by:

Eq. 5 $$T = N \int_0^\infty \phi' \sigma_t \, dE = N \int_0^\infty E \phi' [\sigma_t/E] \, dE = N \, I \, \overline{[\sigma_t/E]}$$

where: T = number of transmutations produced (atoms g^{-1} sec^{-1})

N = number of atoms per gram (atoms g^{-1})

σ_t = transmutation cross section (n, p), (n, α), or (n, f) (cm^2)

$\overline{[\sigma_t/E]}$ = average transmutation cross section (millibarns kev^{-1})

Table III list the cross sections for several fission foils. Table V list (n, p) and (n, α) cross sections for all fifteen elements unless the cross section is insignificant. The interactions are identified by a number in the first column of Table V.

7 (n, p) reaction
6 (n, α) reaction

ATOMIC DISPLACEMENT PRODUCTION

Part of the energy deposited by neutron radiation produces ionization. The rest either displaces atoms from their original location or excites thermal vibrations in the structure of the sample. Instead of calculating the number of atomic displacements which are produced, it is possible to calculate the fraction of the absorbed dose which produces ionization much more accurately. The remaining fraction is closely related to the number of atomic displacments by the relation:

	SPECTRUM C-10	SPECTRUM C-30	SPECTRUM C-90	SPECTRUM W-10	SPECTRUM W-30	SPECTRUM W-90	SPECTRUM UN-MOD
			BORON				
6 *	2.41 (-1)	1.04 (+0)	1.66 (+0)	4.00 (-1)	2.39 (-1)	9.98 (-2)	4.13 (-2)
			CARBON				
6	4.32 (-5)	2.82 (-5)	4.86 (-5)	9.45 (-5)	2.10 (-4)	5.83 (-4)	8.00 (-5)
			NITROGEN				
7 *	1.81 (-2)	2.27 (-2)	2.12 (-2)	1.29 (-2)	9.50 (-3)	4.79 (-3)	1.30 (-2)
6	1.58 (-2)	1.48 (-2)	1.39 (-2)	1.54 (-2)	1.48 (-2)	1.23 (-2)	1.65 (-2)
			OXYGEN				
7	1.37 (-5)	8.74 (-6)	1.33 (-5)	2.90 (-5)	6.88 (-5)	1.79 (-4)	2.50 (-5)
6	3.06 (-3)	2.35 (-3)	3.22 (-3)	4.25 (-3)	4.85 (-3)	5.07 (-3)	4.38 (-3)
			FLOURINE				
7	5.81 (-4)	4.36 (-4)	7.58 (-4)	1.15 (-3)	1.93 (-3)	3.59 (-3)	1.06 (-3)
6	8.13 (-3)	6.22 (-3)	9.04 (-3)	1.23 (-2)	1.60 (-2)	2.16 (-2)	1.23 (-2)
			ALUMINUM				
7	1.62 (-3)	1.21 (-3)	1.75 (-3)	2.61 (-3)	3.82 (-3)	6.55 (-3)	2.50 (-3)
6	1.74 (-4)	1.19 (-4)	2.15 (-4)	3.96 (-4)	8.27 (-4)	2.02 (-3)	3.37 (-4)
			SILICON				
7	6.16 (-4)	4.05 (-4)	7.09 (-4)	1.34 (-3)	2.98 (-3)	8.17 (-3)	1.14 (-3)
6	4.59 (-4)	3.18 (-4)	5.41 (-4)	9.53 (-4)	1.90 (-3)	4.68 (-3)	8.40 (-4)
			SULPHUR				
7	2.72 (-2)	2.15 (-2)	2.36 (-2)	3.28 (-2)	3.63 (-2)	4.09 (-2)	3.32 (-2)
6	2.65 (-2)	2.20 (-2)	2.19 (-2)	2.89 (-2)	2.92 (-2)	2.69 (-2)	2.99 (-2)
			CHLORINE				
7	9.61 (-8)	6.56 (-8)	8.14 (-8)	2.03 (-7)	4.89 (-7)	6.99 (-7)	1.70 (-7)
6	5.68 (-3)	4.36 (-3)	5.79 (-3)	8.14 (-3)	1.03 (-2)	1.43 (-2)	8.07 (-3)
			IRON				
7	3.26 (-4)	2.34 (-4)	4.10 (-4)	6.90 (-4)	1.30 (-3)	2.90 (-3)	6.10 (-4)
6	8.21 (-5)	5.33 (-5)	8.43 (-5)	1.80 (-4)	4.07 (-4)	1.06 (-3)	1.53 (-4)
			COPPER				
7	2.36 (-3)	1.81 (-3)	2.55 (-3)	3.67 (-3)	5.12 (-3)	8.00 (-3)	3.56 (-3)
6	2.05 (-4)	1.45 (-4)	2.48 (-4)	4.27 (-4)	8.30 (-4)	1.93 (-3)	3.78 (-4)
			GERMANIUM				
7	5.32 (-4)	3.88 (-4)	6.03 (-4)	9.57 (-4)	1.61 (-3)	3.35 (-3)	8.82 (-4)
6	4.89 (-6)	3.09 (-6)	4.85 (-6)	1.04 (-5)	2.45 (-5)	6.80 (-5)	8.90 (-6)
			GOLD				
7	4.60 (-6)	2.92 (-6)	4.37 (-6)	9.92 (-6)	2.30 (-5)	5.94 (-5)	8.51 (-6)
6	9.50 (-9)	7.09 (-9)	8.36 (-9)	2.17 (-8)	5.15 (-8)	5.55 (-8)	1.58 (-8)

* (SEE TEXT FOR ADDITIONAL CONTRIBUTION FROM NEUTRONS LESS THAN 1 KEV)

TABLE V. TRANSMUTATION CROSS SECTIONS (MILLIBARNS/KEV)

Eq. 6 $N_d = D [R]_{av} k / s_d$

where: N_d = rate of atomic displacement production (dis. g^{-1} sec^{-1})

D = total deposited dose from neutrons (kev g^{-1} sec^{-1})

$[R]_{av}$ = average fraction of deposited dose which does not produce ionization

k = a numerical constant which lies between about 0.3 and 0.8 in various theories [7]
0.5 is a commonly used value

s_d = energy required to displace atom - - - - values lie in the range 0.010 to 0.030 kev for most materials - - - - 0.025 kev is a commpnly used value [7]

The fraction of the deposited dose which does not produce ionization is given by:

Eq. 7 $$R(E) = 1 - \int_o^\infty s N_r' [1 - R(s)] ds \; / \; \int_o^\infty s N_r' ds$$

where: $R(E)$ = the fraction of deposited dose which does not produce ionization for incident neutrons of energy, E

s = energy of recoil nuclei (kev)

$N_r' ds$ = number of recoil nuclei produced which have energies between s and s + ds

$R(s)$ = fraction of energy of recoil atom of energy s which does not produce ionization

Except for the lightest elements, one may consider that $R(s) = 1$ up to a critical threshold energy s_c at which the velocity of the recoil nuclei begins to be comparable with the slowest atomic electrons of the sample. At energies above s_c, almost all of the recoil energy is expended in producing ionization so that $R(s) = [s_c/s]$. In this case, Eq. 7 becomes:

Eq. 8 $$R(E) = 1 - \int_o^\infty (s - s_c) N_r' ds \; / \; \int s N_r' ds \quad \text{if} \quad s > s_c$$

$$= 1 \quad \text{if} \quad s < s_c$$

For incident neutrons of energy E, the energy of the recoil atoms is related to the cosign of the scattering angle by the relation:

Eq. 9 $\mu = \cos \phi = 1 - (s/2A)(A + 1)^2 \frac{1}{E}$

Using this, Eq. 8 may be written in terms of μ instead of E as follows:

Eq. 10 $R(E) = 1 - \int_{-1}^{\mu_c} \sigma(\mu)\ (\mu_c - \mu)\ d\mu \ / \ \int_{-1}^{+1} \sigma(\mu)\ (1 - \mu)\ d\mu$ if $\mu_c > -1$

where: $\sigma(\mu)$ = differential angular scattering cro s section (cm^2 $steradian^{-1}$) - - center of mass system - -

μ = cos of the scattering angle in the center of mass system

μ_c = critical scattering angle for ionization

$= 1 - (s_c/2A)(A + 1)^2$

For elastic scattering, R(E) was calculated using measured angular distributions. For inelastic scattering, the scattering was assumed to be isotropic since very little data was available. The threshold energies that were used in the calculation are 17 kev, 34 kev, 50 kev, 76 kev, and 120 kev for Al, Si, Cu, Ge, and Au respectively.

Finally, the average value of R(E) averaged over each of the seven spectra is obtained from:

Eq. 11 $[R]_{av} = \int_o^\infty E \phi' \sigma_d f R(E)\ dE \ / \ \int_o^\infty E \phi' \sigma_d f\ dE$

Table VI list the values so obtained are tabulated seperately for tne elastic and inelastic scattering contribution identified by the numbers 3 and 4 in the first column of the table respectively.

ERRORS

The overall accuracy is difficult to estimate since the input data has variable accuracy in different energy regions and the computations introduce unknown uncertainties. It would have been desirable to have included a numerical computation of the error in the basic calculational program so that the errors could be tabulated with the average cross sections.

~~The following~~ Table VII gives a semi-subjective estimate of the 2:1 confidence limits of the errors (i.e. there is a two to one chance that the tabulated value is within the stated limits).

	SPECTRUM C-10	SPECTRUM C-30	SPECTRUM C-90	SPECTRUM W-10	SPECTRUM W-30	SPECTRUM W-90	SPECTRUM UN-MOD
			ALUMINUM				
3	1.68 (-1)	1.77 (-1)	1.72 (-1)	1.54 (-1)	1.44 (-1)	1.16 (-1)	1.58 (-1)
4	1.07 (-1)	1.14 (-1)	1.04 (-1)	9.62 (-2)	8.66 (-2)	6.93 (-2)	9.89 (-2)
			SILICON				
3	4.57 (-1)	3.27 (-1)	3.27 (-1)	3.09 (-1)	2.95 (-1)	2.49 (-1)	3.07 (-1)
4	1.96 (-1)	2.01 (-1)	1.83 (-1)	1.78 (-1)	1.64 (-1)	1.39 (-1)	1.81 (-1)
			COPPER				
3	7.86 (-1)	8.36 (-1)	8.27 (-1)	7.34 (-1)	6.68 (-1)	5.24 (-1)	7.07 (-1)
4	6.03 (-1)	6.26 (-1)	5.78 (-1)	5.49 (-1)	5.00 (-1)	4.09 (-1)	5.62 (-1)
			GERMANIUM				
3	9.16 (-1)	9.42 (-1)	9.34 (-1)	8.79 (-1)	8.31 (-1)	7.00 (-1)	8.67 (-1)
4	5.69 (-1)	5.17 (-1)	5.37 (-1)	5.93 (-1)	5.83 (-1)	5.67 (-1)	5.83 (-1)
			GOLD				
3	9.99 (-1)	9.99 (-1)	9.99 (-1)	9.98 (-1)	9.96 (-1)	9.89 (-1)	9.98 (-1)
4	9.99 (-1)	1.00 (+0)	9.99 (-1)	9.99 (-1)	9.99 (-1)	9.99 (-1)	9.99 (-1)

TABLE VI. AVERAGE FRACTION OF DEPOSITED DOSE WHICH DOES NOT PRODUCE IONIZATION

DOSE CROSS SECTIONS

Elastic scattering contribution	± 20 %
Inelastic scattering contribution	± 40 %
(n, p) and (n, α) reaction contributions	
B, N, O, F, S, Cl	± 30 %
C, Al, Si, Fe, Cu, Ge, Au	@ 2

(@ is used to denote "greater or less by the stated factor")

TRANSMUTATION CROSS SECTIONS

(n, f) fission reactions	± 20 %
(n, p) and (n, α) reactions	
B, N, O, F, S, Cl, Al	± 30 %
C, Si, Fe, Cu, Ge, Au	@ 2

ATOMIC DISPLACEMENT PRODUCTION

Error in $(1 - R_{av})$ when $R_{av} > 0.5$	± 40 %
Error in R when $R_{av} < 0.5$	@ 2

TABLE VII. ESTIMATE OF ERRORS

Boron and Nitrogen are included in the tabulations, but have (n, p) and (n, α) which are not negligible at energies below 1 kev. The additional contribution at lower energies can be calculated from the thermal flux (nv_0) by assuming a 1/v cross section at low energies with the following values at 2200 m sec^{-1}:

Nitrogen	1.68 (3) millibarns (n, p)
Boron	7.50 (5) millibarns (n, α)
	(a 0.48 mev gamma ray is emitted in 93 % of disintergrations)

ACKNOWLEDGMENT

We would like to express appreciation to Dr. Roy Reeves and to Miss Mery Gong of the Ohio State University Numerical Computation Laboratory for assistance and encouragement in the performing of the numerical computations.

REFERENCES

1. R. Aronson, J. Certain, H. Goldstein, and S. Presier; "Penetration of Neutrons from a Point Isotropic Fission Source in Water"; AEC Report NYO-6267, (NDA 15C-42) Superintendents of Documents, Sept., 1954

   J. Certain, H. Goldstein, M. Kalos, and P. Mittleman; "Penetration of Neutrons from a Point Fission Source through Carbon and Hydrocarbons"; (NDA 12-18), June, 1956

   also see: H. Goldstein; The Attenuation of Gamma Rays and Neutrons in Reactor Shields; Superintendent of Doc., 1957

2. W. R. Burrus, "Epi-thermal Dose and Atomic Displacement Production", Lockheed Aircraft Corp, Nuclear Report - 40, 1958

3. D. J. Hughes and R. S. Carter; "Neutron Cross Sections, Angular Distributions"; BNL-400, 1956

4. D. J. Hughes and J. A. Harvey; Neutron Cross Sections; BNL-325 and supplement, 1955-1957

5. A. Langsdorf, Jr. et alia; "Angular Distribution of Scattered Neutrons"; ANL-5567, 1956 (Also see Physical Review, Vol. 107, No. 4, pg. 1077, 1957)

6. D. J. Hughes, Pile Neutron Research, Addison-Westley Publishing Co., Cambridge, Mass., 1953, pg. 95

7. G. J. Dienes and G. H. Vineyard; Radiation Effects in Solids, Monographs in Physics and Astronomy, Vol. II, Interscience, 1957

8. A. H. Wapstra, "Isotopic Masses", Physica, Vol. 21, pg. 367-409, 1955

NUCLEAR RADIATION UNITS AND MEASUREMENTS

by

R.S. Caswell and S.W. Smith

National Bureau of Standards
Washington, D.C.

The basic principles underlying the establishment and use of units, standards and systems of measurement for nuclear radiations will be given, with specific reference to gamma rays, neutrons and mixed fields of gamma rays and neutrons, the latter being more commonly encountered in radiation effects problems. The measurement of the energy deposited by a radiation field in a sample of material may be approached through measurement of some characteristic of the field, i.e., exposure dose, flux, spectra, or through measurement of energy absorption directly, i.e., absorbed dose. The discussion will include the conditions for measurement of exposure dose and of absorbed dose, and current methods of dosimetry, instruments and techniques. Also included will be a brief discussion of the measurement of neutron flux and neutron spectra.

I. CONCEPTS

A. DESCRIPTIONS OF THE RADIATION FIELD

1. Energy spectrum and angular distribution. A complete description of the primary radiation field gives for each point in space, the number of particles of each kind (photons or neutrons), and their energy and direction of motion.

A description of this completeness may be desirable if the radiation effect under consideration has a significant dependence on energy (for example, an effect with a threshold energy for displacement such as electrical conductivity of germanium), or upon orientation (for example, in a thin crystal or a junction layer).

Frequently, however, we may not need to describe the field in such detail; we may wish to avoid the complexity of such a description; we may have no method at all to obtain this type of information; or our measurement methods may not be as refined as methods for obtaining simpler quantities. In these cases, we measure other quantities which describe the field in some way and give us the information needed for

evaluation of the problem we are studying. In these situations (which are most frequent) we may measure such quantities as intensity, number flux, exposure dose, or first collision dose.

2. Intensity (or energy flux density). Intensity of radiation at a given place is defined as the energy per unit time entering a small sphere of unit cross-sectional area centered at that place. The unit of intensity may be ergs per square centimeter second or watts per square centimeter. Intensity may be measured, for example, with a calorimeter. Intensity has often been measured for gamma rays, seldom for neutrons.

3. Number flux (density). Number flux is defined as the number of photons or neutrons which, per unit time, enter a sphere of unit cross-sectionsl area centered about the point of interest. This quantity is usually expressed in photons or neutrons per square centimeter second. It is commonly measured for neutrons, seldom for photons, by such techniques as foil activation, the "long counter," proton recoil counters, and counter telescopes. Note that there is some analogy between the number flux and the energy flux which are defined in similar ways, but in one case, energy is measured and in the other, one measures number of particles. The expression, "nvt", which has frequently been used in reporting radiation effect studies, is a time-integrated neutron flux. The accompanying gamma radiation is unspecified.

4. Exposure dose. Exposure dose (defined only for X- and gamma rays and not for neutrons) is a measure of the radiation based upon its ability to produce ionization. The unit of exposure dose is the roentgen, r. One roentgen is an exposure dose of gamma radiation such that the associated corpuscular emission per 0.001293 g of air produces, in air, ions carrying 1 electrostatic unit of quantity of electricity of either sign. The roentgen is a measure of the energy imparted to secondary particles at a given point in space, but not necessarily finally absorbed there. It may be expressed by a formula involving the cross-sections (of air) for interaction with the radiation:

$$R(E_\gamma) = \frac{k}{W} I(E_\gamma)\ \mu_{en}(E_\gamma) = \frac{k}{W} \sum_i n(E_\gamma)\ Ni\ \sigma_i(E_\gamma)\ \epsilon_i(E_\gamma) \qquad (1)$$

where $R(E_\gamma)$ = exposure dose in roentgens

E_γ = energy of the gamma-ray photons

k = constant that converts from ion pairs to roentgens

$I(E_\gamma)$ = intensity

$\mu_{en}(E_\gamma)$ = energy absorption coefficient for air in $\frac{cm^2}{gm}$

W = average energy required to produce an ion pair in air

$n(E_\gamma)$ = number flux of photons of energy E_γ

N_i = number of atoms per gram of the i^{th} kind in air

$\sigma_i(E_\gamma)$ = total cross section per atom

$\epsilon_i(E_\gamma)$ = average energy transferred to the electron from the photon of energy E_γ.

In equation (1) the product $I(E_\gamma)\mu_{en}(E_\gamma)$ is the rate at which energy is imparted to the medium by the radiation per gram of material. Similarly the summation in the term on the right in equation (1) represents the energy imparted to a gram of material. In both expressions, W converts from an energy unit to an ionization unit (the roentgen). For a radiation field with many photon energies present, it will be necessary to sum equation (1) over all energies to calculate the exposure dose in roentgens. If written out in detail, both μ_{en} and the expression $N_i \sigma_i \epsilon_i$ will contain the photoelectric, Compton, and pair production cross sections.

5. First collision dose. First collision dose is a measure of radiation at a certain place based on the energy imparted to secondary corpuscular radiation per gram of material. It may be expressed in ergs per gram. It also may be expressed by a formula:

$$D_f(E) = \sum_i \sum_j n(E) N_i \sigma_{ij}(E) \epsilon_{ij}(E) \qquad (2)$$

where N_i is the number of atoms per gram of type i in the material that can react with the primary radiation to produce charged particles, $\sigma_{ij}(E)$ is the cross section for the process of type j, and $\epsilon_{ij}(E)$ is the average kinetic energy imparted to charged particles from primary radiation of energy E.

It may be seen that there is considerable similarity between first collision dose (which is expressed in terms of energy) and exposure dose (which is expressed in terms of ionization). In figure 1 is sketched the typical behavior of the value exposure dose and/or first collision dose when a beam of radiation is incident upon a medium. Note the difference between the values of the first collision dose and of the absorbed dose (which we shall discuss next).

B. ENERGY ABSORPTION IN MATERIALS

1. Absorbed dose. Absorbed dose is the energy imparted to matter by (secondary or primary) ionizing particles per unit mass of irradiated material at the place of interest. It may be expressed in rads (1 rad = 100 ergs/g). In the case of secondary electrons produced by gamma-ray photons, the absorbed dose is the result of the electrons giving up energy along their paths to the medium, whereas the exposure dose and first collision dose occur in the process of the photons giving energy to the electrons. Absorbed dose carries the connotation "locally absorbed." In figure 1, the absorbed dose builds up in the surface layers of the medium because the number of secondary electrons is building up as more and more photons have made collisions. The exposure dose and first collision dose are falling, however, because there are fewer and fewer photons in the beam to impart energy to secondary electrons.

Where secondary particle ranges are short (for example, carbon recoils from neutrons in a graphite-wall chamber) the first collision dose and absorbed dose curves may be very similar. Where secondary particle ranges are long (for example, secondary electrons from 10-Mev gamma rays), the distributions may be quite different, since the electron may give up its energy to the medium far from where it was ejected or produced by the primary photon.

II. STANDARDS

A. GAMMA RAYS

1. Energies under 3 Mev

a. Roentgen standards. The standard for X-rays and gamma rays up to photon energies of about 3 Mev is essentially a technique of measurement. It is based on the ionization of air under the conditions specified in the definition of the roentgen.

(1) Free-air chambers. The free-air standard chamber is designed to meet these conditions as closely as possible either through design characteristics or by the application of the necessary corrections. Figure 2 shows the basic design and figure 3 shows an isometric view of the NBS free-air chamber for the measurement of X-rays generated at voltages up to about 250 kv.[1] This range of energies is of primary interest in biomedical fields and in other fields such as instrument design, where energy dependence effects are significant. Free-air chambers in this range have been developed to the stage that absolute measurements in orentgens are almost certainly within ± 1.1 percent, but probably within ± 0.5 percent. Intercomparison between the national standards of different countries shows an agreement of about ± 0.5 percent.[2]

Due to plate separation and electron equilibrium requirements, the size of the free-air chamber increases rapidly with photon energy and is no longer of practical dimensions above about 500 kv. Such a 500-kv chamber was developed at NBS, but its ponderous size and various complexities in its use make the 500-kv chamber unsuited for routine calibrations of instruments. By the use of air at pressures greater than atmospheric, it is possible to reduce the size of the chamber about in proportion to the pressure. Figure 4 shows a pressure chamber designed for photon energies up to about 1.5 Mev when operating at 10 atmospheres. New problems are introduced at these high pressures, however, in obtaining saturation conditions in which all of the ionization is measured. Such a pressure chamber is definitely a research tool, rather than a calibration facility.

(2) Cavity chambers. A cavity chamber of suitable design and under proper conditions of use, may be employed as an absolute device. Electron equilibrium must be established by surrounding the measuring volume with a layer of solid, ideally air-equivalent material, if air is the gas used. However, the surrounding material also produces secondary (scattered, characteristic, or annihilation) photons which may themselves produce high-speed electrons that con-

tribute to the ionization in the measuring volume. In addition, the surrounding material attenuates the photon beam. Thus, if the measuring instrument is used as an absolute device, corrections must be made for the secondary photon contributions and the attenuation.

On the other hand, a cavity chamber may be calibrated by comparison with an instrument of known sensitivity in a photon field of known energy or by calibration in a gamma-ray field which is fully known. This chamber may then be used as a secondary standard over the range of gamma-ray energies for which it has been calibrated and under other limitations imposed by the characteristics of the chamber.

(3) Calibrated fields. A gamma-ray field may likewise serve as a standard, if adequately calibrated or if its characteristics are known. A known weight of Ra^{226} encapsulated in 0.5-mm platinum-iridium and in equilibrium with its daughter products has been used as a standard gamma-ray field. Its long half life (1620 years) makes it attractive in spite of the rather complex gamma-ray spectrum. The gamma-ray emission from radium encapsulated as above has been carefully measured by a number of observers and is presently known to a sufficient degree of reliability (better than 1%) to be useful. A recent value for the emission constant, k(Ra) = 8.26 ± 0.05 r/mgh at 1 cm, was obtained by Attix.[3] This value of k(Ra) is lower than the widely accepted value, k = 8.4, in vogue until recently. On January 1, 1958, the National Research Council of Canada and NBS adopted the value of k = 8.25 as representing the best value at that time and are using it as the basis for the calibration of instruments in roentgens in the energy region from 0.5 to 3 Mev. Thus, the calibrations of instruments done prior to January 1958 require adjustment by about 1.8 percent to make them agree with present procedures.

The calibration of instruments is usually carried out by determining their response in calibrated Co^{60} or Cs^{137} gamma-ray fields which have been measured in roentgens with a cavity ionization chamber whose sensitivity has been determined either from the Bragg-Gray relation with a stopping power correction or from the calibration of the chamber with radium, together with a value for (k) the number of roentgens per hour at 1 cm from 1 mg of radium encapsulated in 0.5 mm of platinum. As the value for (k) is determined from cavity-chamber measurements, it is evident that all measurements in roentgens in the megavolt region actually depend upon a stopping-power correction at the present time. Measurements made at NRC and NBS of the ionization produced within cavity chambers having different wall materials are more nearly consistent with stopping power measurements of Bakker and Segre[4] than with earlier measurements.

The calibration basis (k = 8.25) adopted by NCR and NBS for megavolt radiation is based on the Bakker and Segre stopping-power values, an average excitation potential of 80.5 ev for air and the Sternheimer[5] density correction for ionization loss.

Figure 5 shows the gamma-ray facilities at NBS. Sources presently used for standard gamma-ray fields include Co^{60} with photon energies 1.17 and 1.33 Mev and resultant effective energy of 1.25 Mev, and half life of about 5.3 years; and Cs^{137} with effective photon energy 0.661 Mev and half life of about 33 years. Unfortunately, these gamma-ray fields must be continuously corrected for decay of the isotope and such corrections depend upon the accuracy with which half-life is known. This makes it desirable to remeasure the gamma-ray fields used as standards periodically.

2. Energies over 3 Mev (to 10 Mev)

a. 10-Mev limit. For the present discussion, only gamma-ray energies up to 10 Mev will be considered, as the gamma rays from nuclear reactions in mixed fields are almost entirely under 10 Mev. Above 3 Mev, measurement in roentgens becomes increasingly difficult due to the inability to establish electronic equilibrium. This is brought about by the increased range of the secondary electrons, so that the fraction of the photons which are transmitted through a thickness of air equal to the range of an electron having an energy equal to the photon, becomes small for high photon energies. Figure 6 shows this relationship.[6]

b. Standards.

(1) Calorimeter (Intensity). A logical approach to the measurement of the radiation is through the direct measurement of the incident radiation energy per unit area per second (intensity) by means of a calorimeter. The calorimeter measures the incident energy by recording the total energy absorbed. The unit of radiation for photon energies above 3 Mev would then be the watt-second per square centimeter instead of the roentgen. The calorimeter consists essentially of a lead cylinder placed in the beam of radiation and its temperature compared by means of thermocouples or thermisters to that of an identical cylinder that is shielded from the radiation. Results of such gamma-ray measurements are claimed to be accurate to 1 or 2 percent.

B. NEUTRONS

1. Standard sources. A convenient standard for some kinds of neutron measurements is a radioactive neutron source calibrated for neutron emission rate in neutrons/sec or for dose rate at a specified distance. All of these sources are rather weak, but they are very stable in time. International agreement in the calibration of national standard sources is of the order of ± 2 percent.[7,8] One of the best for a laboratory neutron standard is the plutonium-beryllium (α,n) source, which is obtainable from Mound laboratory. The AEC retains title to the plutonium which is lent to the user. These have a long half-life (24,400 years) and an average neutron energy of 4.5 Mev. If desired, they may be calibrated by NBS vs. a Ra-Be (γ,n) primary standard source to an accuracy of about 4 percent. (See figure 7.) The fast neutron flux at a distance r from a source of strength Q is $Q/4\pi r^2$ enutrons/cm^2 sec. In using the source in this way, one should be careful to check for possible anisotropy in the neutron emission.

2. Neutron flux. NBS also maintains a standard geometry which contains radioactive neutron sources (see figure 8) and supplies a uniform thermal neutron flux of about 4000 thermal neutrons/cm^2 sec for indirect calibration of unknown thermal neutron fluxes by irradiation of foils. Gold foils are usually used and are given 5-day irradiations.

A calibrated source may be used in a standard graphite pile to obtain a known thermal neutron flux. If done carefully, the uncertainty in the value of the flux will be chiefly that in the source strength of the radioactive neutron source.[9]

3. Dose. Highly developed standards do not exist for the measurement of fast neutron dose. A radioactive neutron source (such as Pu-Be) calibrated for dose rate at a known distance from the source, or the alpha-calibrated dosimeter of Hurst may be used.[10] However, nothing in the sense of a really convenient laboratory standard is available.

III. SYSTEMS OF MEASUREMENT

A. GAMMA RAYS

1. Gamma-ray spectra. Gamma-ray spectra may be measured directly, but other more easily obtained characteristics of the radiation are frequently found to be adequate.

a. Scintillation spectrometer. Where measurement of the gamma-ray spectrum is required, the scintillation spectrometer offers an effective means for a systematic survey of the spectrum. Data can be taken very quickly with multichannel analyzers; the scintillation crystals now available provide for a wide range of photon energies, and most of the corrections necessary can be made with reasonable accuracy. Although the resolution of the scintillation spectrometer is inherently low, in those cases where the spectrum is simple, the distortion of the measured distribution is small. This is particularly true for the gamma-ray spectra consisting of relatively few sharp lines.

b. Attenuation curves. Where the penetration of the radiation is the factor of interest, the information required may be obtainable from attenuation data.

(1) Half-value-layer. The H.V.L. is the thickness of attenuating material necessary to reduce the exposure dose rate produced at a point to one-half of its original value. If the radiation spectrum is composed of many wave lengths of various intensities, the H.V.L. will depend upon the amount of previous filtration. The concept of H.V.L. at high energies must be applied with caution, since the rate of change of dose rate with thickness or depth is not always a unique characteristic of the primary radiation which is being described.

(2) Effective energy. When the range of wavelengths in the spectrum is not too large (e.g., heavily filtered X-rays), an "effective energy" may be a useful index of radiation quality. This assumes that the penetration or the absorption of the radiation is closely similar to that of radiation having a single wavelength. If the absorption coefficient does not change appreciably over the range of wavelengths present in the spectrum, an average coefficient may be used corresponding to a single wavelength having a photon energy equivalent to the "effective energy." For example, in the case of cobalt-60 gamma rays, there are two gamma-ray lines of energies, 1.17 Mev and 1.33 Mev, which have an effective energy of about 1.25 Mev.

2. Exposure dose.

a. Cavity chambers. As was pointed out earlier, cavity chambers of suitable characteristics may be used to measure exposure dose in roentgens. Such a chamber is shown in Figure 9. This chamber was constructed for use as a transfer standard to permit the intercomparison of the primary free-air standards of different countries without the necessity of transporting them. The chamber has graphite walls and is air filled. It is used with a charge compensating air capacitor and an electrometer to measure ionization. As the graphite walls are not strictly air equivalent, the lack of homogeneity for wall material and gas causes energy dependence of a few percent mainly in the 50- to 250-kv X-ray region.

b. Carbon-dose chamber. Burrus[11] has proposed "carbon dose" as a means of describing the gamma-ray field to which materials are exposed. The "carbon dose" is defined as the energy per unit mass removed from an X- or gamma-ray field by a limitingly small mass of carbon placed at the point of interest. The definition implies that "carbon dose" can be measured with a graphite chamber having carbon dioxide filling gas in accord with the Bragg-Gray principle. A "carbon dose" is essentially a first collision dose in carbon but it is not a measure of exposure dose in roentgens.

c. Photographic methods. Photographic films have been used extensively for the measurement of radiation[12], although they do not have all of the desired characteristics for such measurements. Energy dependence of photographic emulsions is fairly large in the energy region up to about 0.3 Mev and then varies more slowly for higher energies. Filters to reduce energy dependence and plastic material to provide electronic equilibrium have been employed. Film sensitivity can be made to cover a rather wide range by the use of different emulsions and processing techniques. Although film dosimetry is inherently less accurate than some other systems of measurement, it has the advantage of being simple and inexpensive.

d. Solid state dosimeters. Measurements carried out with X- and gamma rays have indicated that semiconductors such as the p-n junction silicon solar photocells are suitable for dosimetry. These cells when irradiated produce a photovoltage causing an electric current to flow in an external circuit without an external source of power. The cells are simple to use, show practically no inertia of the photo effect and the photocurrent is temperature independent over a wide range when the external resistance is small. The photovoltage and photocurrent are proportional to exposure dose rates up to fairly high values, and are only slightly dependent on photon energy.

3. Absorbed dose of gamma rays.

a. Cavity chambers - Bragg-Gray principle. The most sensitive methods for determining absorbed dose involve ionization measurements in gases utilizing the Bragg-Gray principle. Radiation in passing through a solid imparts energy to charged particles which in turn impart their energy to the solid. The absorbed dose E_s, in a differential mass of the medium is due to the loss of kinetic energy of charged particles. If the differential mass of solid is replaced by gas, the energy imparted to a unit mass of the gas, Eg, obeys the relation

$$E_s = S \times Eg$$

where S is the ratio of the mass stopping power of the solid to that of the gas for the ionizing particles. If the average energy required to produce an ion pair in the gas is W,

$$E_s = SWJ$$

where J is the ionization per unit mass of gas. This equation is known as the Bragg-Gray relation[13,14] and is fundamental in the measurement of absorbed dose by ionization methods. However, its application requires that four conditions be met:

(1) Introduction of the cavity has a negligible effect on the distribution of the charged particles; hence, the linear dimensions of the cavity are small compared to the range of the particles in the cavity.

(2) The intensity of primary radiation must be substantially constant in the cavity and in the surrounding wall.

(3) Production of charge tertiary radiations (delta rays) must be small in the wall and gas cavity, or the cavity large compared with the range of gas-produced tertiaries[15].

(4) As S and, to some extent, W are functions of particle type and energy, their mean values must be found by the proper weighting of the spectrum of charged particles traversing the cavity.

Condition (1) is easily met for gamma rays, as the secondaries have a relatively long range. However, the heavy recoils produced by fast neutrons have a short range and would require reduced pressure to fulfill the condition set and this would result in weak

ionization currents. Condition (2) may be difficult to meet at transition layers between the surface and depth at which radiation equilibrium is established. Condition (3) is usually adequately met when the wall and gas are of approximately equal atomic number. The information for fulfilment of (4) is usually not known. However, if both wall and gas have the same atomic composition, $E_s = WJ^*$, where J^* is the ionization per unit mass of the wall equivalent gas. In this case, (1) is eliminated, (2) remains unchanged, (3) is fulfilled and (4) is easily met with respect to S, and W may be determined.

b. Calorimeter. The most fundamental physical method for the measurement of absorbed dose is through the temperature rise of the irradiated material. This rise is ordinarily exceedingly small for radiations of interest in biological studies, amounting to only about 2×10^{-6} degrees centigrade per rad in soft tissue. However, for radiation levels involved in radiation damage studies, the temperature rise is sufficient for accurate calorimetric measurements. A calorimeter measures the total dose absorbed by the material with no distinction between neutrons and gamma rays or radiation induced chemical reactions or atomic displacements. The latter two effects, however, are generally negligibly small.

A calorimeter recently developed at the National Bureau of Standards has been proposed as a possible standard for absorbed dose measurement. Figure 10 is a schematic diagram of the calorimeter. A sphere of graphite, A, 1 cm in diameter is supported on polystyrene pegs inside a graphite shell having inner and outer diameters of 1.4 cm and 2.2 cm. The rise in temperature of the central sphere permits an evaluation of the absorbed dose in graphite. Carbon was selected for the calorimetric element to approximate tissue in radiation absorption properties and to provide large enough thermal and electrical conductivities, so that the temperature and electrical power inputs can be accurately determined. As the specific heat of carbon is 0.7 joule per gram per degree centigrade, 10^5 rads will produce a temperature rise of 1.4 degrees centigrade, which can be easily measured.

B. NEUTRONS

1. Spectrum

a. Threshold detectors. Detectors sensitive to neutrons only above a given energy are called threshold detectors. Threshold reactions may be of the (n,p), (n,γ), (n,2n) or (n,fission) type leading to the production of a radioactive nuclide or fission particles. Some of the useful detectors are shown in Table 1. The method is characterized by very coarse energy resolution and low sensitivity, but has been useful for measuring radiation in nuclear reactors and radiation bursts from fission critical assemblies.

b. Photographic methods. A very large amount of neutron spectrum information has been obtained by photographic methods. Usually, in the case of a nuclear reactor, the emulsions are located outside the reactor. In this case, it is necessary to determine the spectrum in the core from measurements of the neutron spectrum which emerges from a duct. This problem has been considered by Eggler et al[16].

2. Neutron flux. Neutron flux may be measured in many ways, among them the long counter, foil activation, proton recoil counters and counter telescopes and associated particle counting. A review of the measurement of fast neutron flux has been given by Barschall, et al[17]. Extensive reviews will be available shortly in a book by Fowler and Marion, Fast Neutron Physics and in a forthcoming (1959) NBS Handbook, Measurement of Neutron Flux and Spectra.

3. First collison dose and absorbed dose. Since all neutron radiation fields contain gamma rays, we shall consider the problem of mixed radiation field dosimetry. The basic problem is to separate out the neutron dose and gamma-ray dose. There are several general approaches to this problem (which are to be discussed in more detail in an NBS Handbook on absorbed dose measurements, now in preparation).

a. Twin ionization chambers. In this method, which uses the Bragg-Gray principle, an hydrogenous chamber is used to measure the neutron + gamma dose and a non-hydrogenous chamber to measure the gamma ray dose. The neutron dose is obtained by subtraction. Examples of the hydrogenous chamber are polyethylene-ethylene, polystyrene-acetylene, and tissue equivalent plastic and gas chambers of Failla and Rossi[18]. Examples of the non-hydrogenous chamber are graphite-CO_2 and teflon-air chambers. This method is simple to use, but suffers from neutron sensitivity of the gamma-ray chamber (about 5 to 20 percent). It is useless for measurement of fast neutron dose in radiation fields in which the gamma rays predominate strongly.

b. Proportional counters with pulse-height discrimination between radiations. This method, suggested by Hurst[19], uses counters of atomic composition similar to that of the ionization chambers above, but has the advantage of much better discrimination between radiations. Large pulses are produced by heavy particle recoils from neutrons and small pulses by secondary electrons from gamma rays. In either case, pulse-height integration is used to evaluate the dose. Recent descriptions of a gamma-insensitive neutron dosimeter have been given by Wagner and Hurst[10], and of a neutron-insensitive gamma-ray dosimeter have been given by Caswell[20]. A neutron-insensitive gamma-ray dosimeter which accomplishes discrimination between the radiations without requiring pulse-height discrimination is the single-ion dosimeter of Auxier et al[21].

c. Photographic film. Photographic emulsions, particularly those of large grain size, are sensitive to gamma rays and discriminate strongly against neutron irradiation[22].

d. Chemical dosimeter. A neutron-insensitive gamma-ray chemical dosimeter has been reported by Sigoloff[23], which is based on the tetrachloroethylene system.

e. Threshold detectors. Use of threshold detectors to measure fast neutron dose has been reported by Hurst et al[24]. They used Pu^{239}, Np^{237}, U^{238}, and S^{32} as detectors.

TABLE I

THRESHOLD DETECTORS

Detector	Reaction	Product	$^{a}T^{1/2}$	$^{b}E_t$ (Mev)
Np^{237}	(n,f)	many	many	0.2
In^{115}	(n,n')	In^{115m}	4.5 hr	0.45
Ba^{137}	(n,n')	Ba^{137m}	2.6 min	0.60
U^{238}	(n,f)	many	many	0.7
S^{32}	(n,p)	P^{32}	14.3 days	1.7
P^{31}	(n,p)	Si^{31}	2.6 hr	1.8
Al^{27}	(n,p)	Mg^{27}	10 min	2.1
Fe^{56}	(n,p)	Mn^{56}	2.6 hr	5.0
Cu^{63}	(n,2n)	Cu^{62}	10 min	11.4
C^{12}	(n,2n)	C^{11}	20.5 min	20

a. $T^{1/2}$ = half life of product nucleus

b. E_t = approximate threshold neutron energy

REFERENCES

1. Wyckoff, H.O. and Attix, F.H., Design of Free-Air Ionization Chambers, NBS Handbook 64, (1957).

2. Report of the International Commission on Radiological Units and Measurements (ICRU) 1956, NBS Handbook 62, (1957).

3. Attix, F.H. and Ritz, V.H., A Determination of the Gamma-Ray Emission of Radium, NBS Journal of Research 59, 5, 293 Nov.(1957).

4. Bakker, C.J. and Segre, E., Phys. Rev. 81, 489 (1951).

5. Sternheimer, R.M., Phys. Rev. 88, 851 (1952).

6. Protection Against Betatron-Synchrotron Radiations Up to 100 Million Electron Volts, NBS Handbook 55, Feb. (1954).

7. Larsson, K.E., Present Status of Neutron Source Calibrations, J. Nuclear Energy 6, 322 (1958).

8. Caswell, R.S., Mosburg, E.R., Jr., and Chin, J. Standards for Neutron Flux Measurement and Neutron Dosimetry, Paper No. 522, Proceedings of the International Conference on the Peaceful Uses of Atomic Energy. United Nations (1958).

9. Hughes, D. J., Pile Neutron Research. Addison-Wesley, (1953).

10. Wagner and Hurst, G.S., Advances in the Standard Proportional Counter Method of Fast Neutron Dosimetry, Rev. Sci. Instr. 29, 153 (1958).

11. Burrus, W.R., Standard Instrumentation Techniques for Nuclear Environmental Testing. WADC Tech. Note 57-207; ASTIA No. AD-142179 (1957).

12. Ehrlich, M. and Fitch, S.H., Photographic X- and Gamma-Ray Dosimetry, Nucleonics 9, 5 (1951).

13. Gray, L.H., Ionization Method for the Absolute Measurement of Gamma-Ray Energy, Proc. Roy. Soc. (London), 156A, 578 (1936).

14. Gray, L. H., The Ionization Method of Measuring Neutron Energy, Proc. Camb. Soc. 40, 72, (1944).

15. Spencer, L.V. and Attix, F.H., A Theory of Cavity Ionization, Rad. Res. 3, 3 (1955).

16. Eggler, C., Huddleston, C.M., Krohn, V.E., and Ringo, G.R., Measurement of the Neutron Spectra of the Experimental Breeder Reactor, Nuclear Science and Engineering 1, 391 (1956).

17. Barschall, H.H., Rosen, L., Taschek, R.F., and Williams, J.H., Measurement of Fast Neutron Flux, Rev. Mod. Phys. 24, 1 (1952).

18. Rossi, H.H., and Failla, G., Tissue-Equivalent Ionization Chambers, Nucleonics 14, No. 2, 32 (1956).

19. Hurst, G.S., An Absolute Tissue Dosimeter for Fast Neutrons, Brit. J. Radiology 27, 353 (1954).

20. Caswell, R.S., Neutron-Insensitive Gamma-Ray Dosimeter, Radiology 68, 101 (1957).

21. Auxier, J.A., Hurst, G.S., and Zedler, R.E., A Single Ion Detector for Measurement of γ-Ray Ionization in Cavities, Health Physics 1, 21 (1958).

22. McLaughlin, W.L., and Ehrlich, M., Limitations in the Photographic Dosimetry of X- and γ-Rays, Radiation Research 9, No. 1 (1958).

23. Sigoloff, S.C., Fast Neutron Insensitive Chemical Gamma-Ray Dosimeter, Nucleonics 14, No. 10, 54 (1956).

24. Hurst, G.S., Harter, J.A., Hensley, P.N., Mills, W.A., Slater, M., and Reinhardt, P. W., Techniques of Measuring Neutron Spectra With Threshold Detectors--Tissue Dose Determinations, Rev. Sci. Instr. 27, 153 (1956).

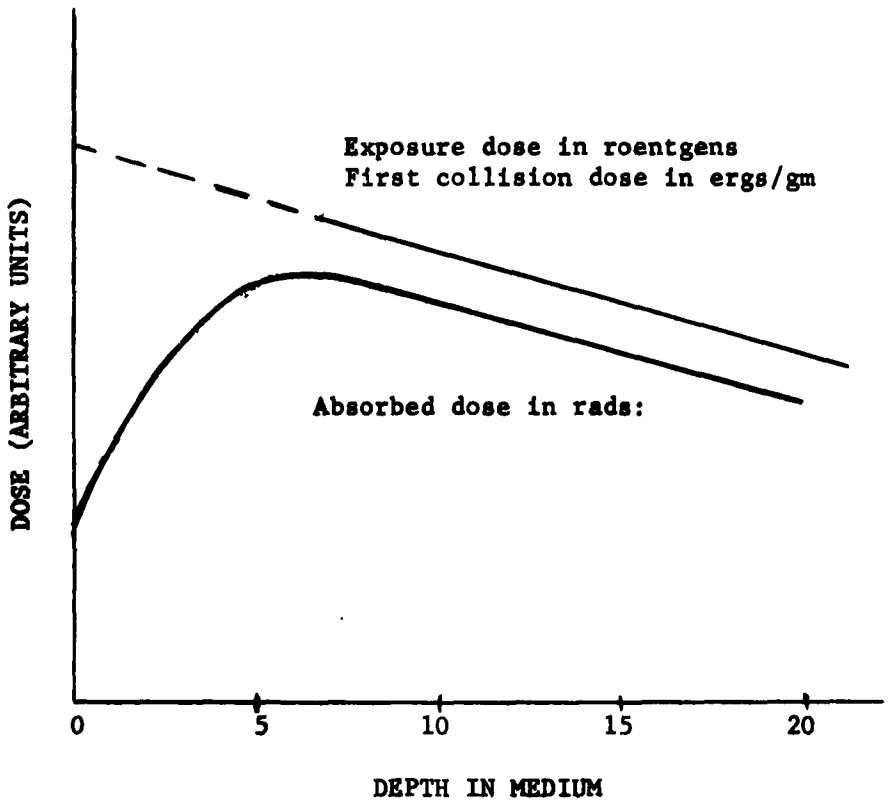

Figure 1. Difference between absorbed dose and either exposure dose or first collision dose in a medium.

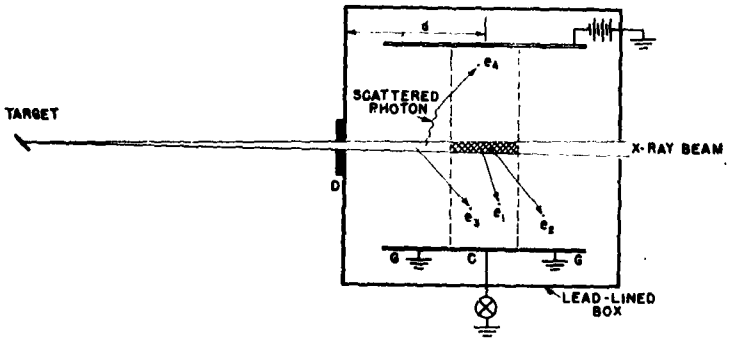

Figure 2. Schematic plan view of a parallel-plate ionization chamber.

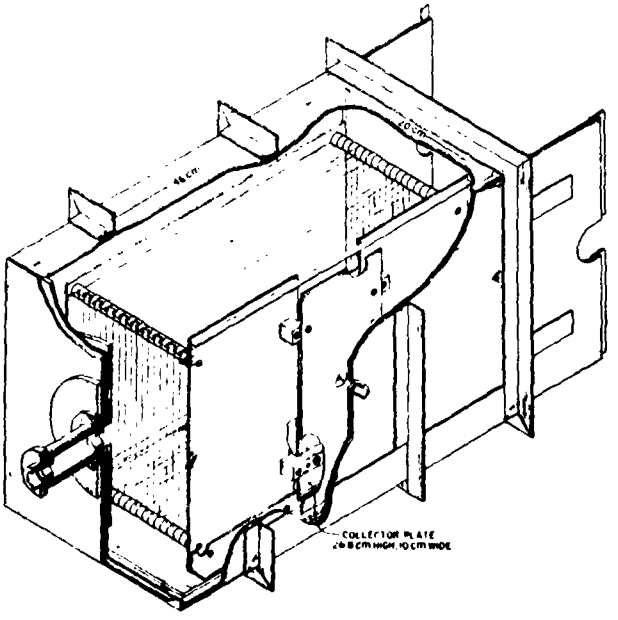

Figure 3. An isometric view of the NBS standard 250-kv free-air ionization chamber.

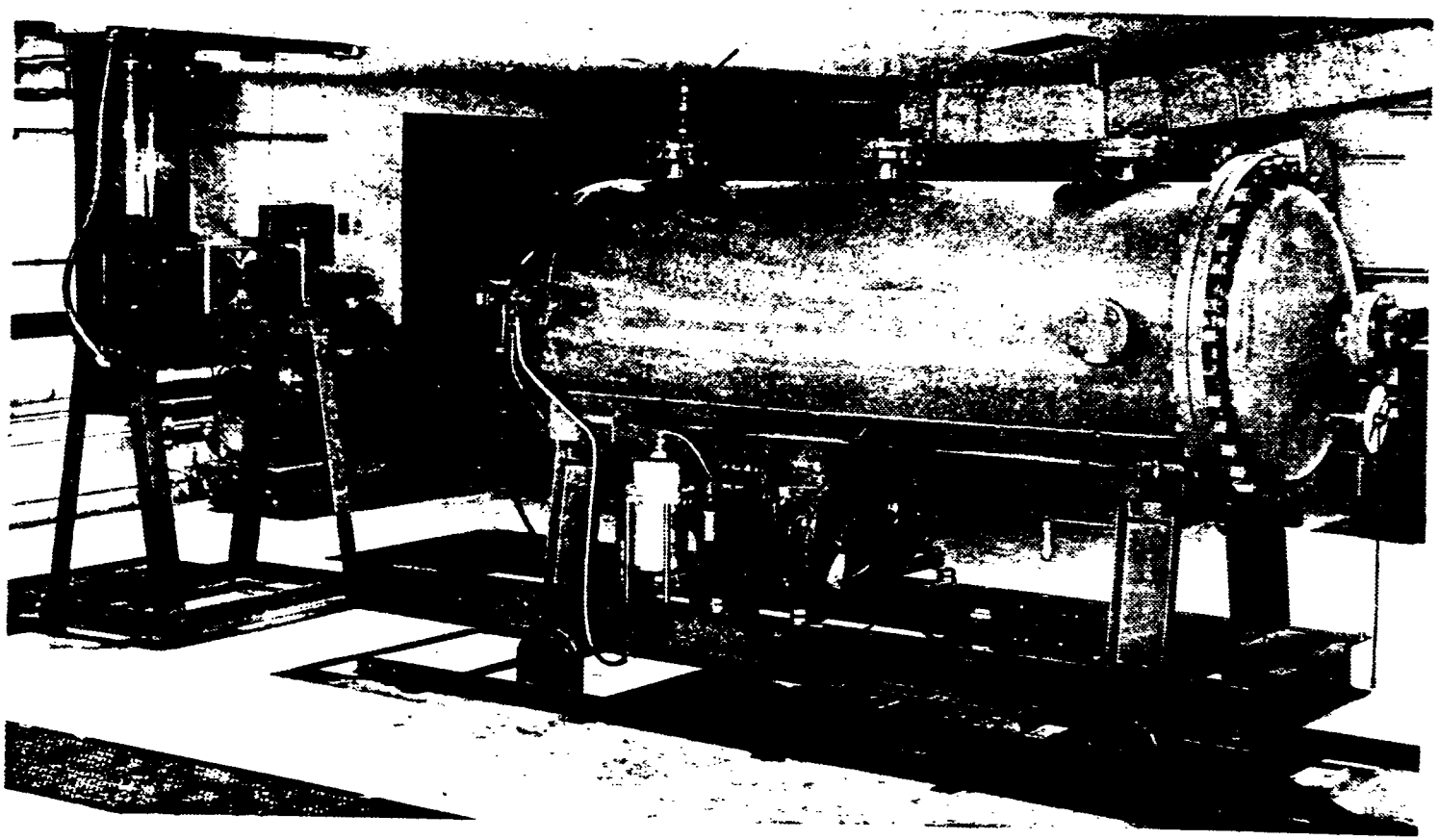

Figure 4. Pressure ionization chamber.

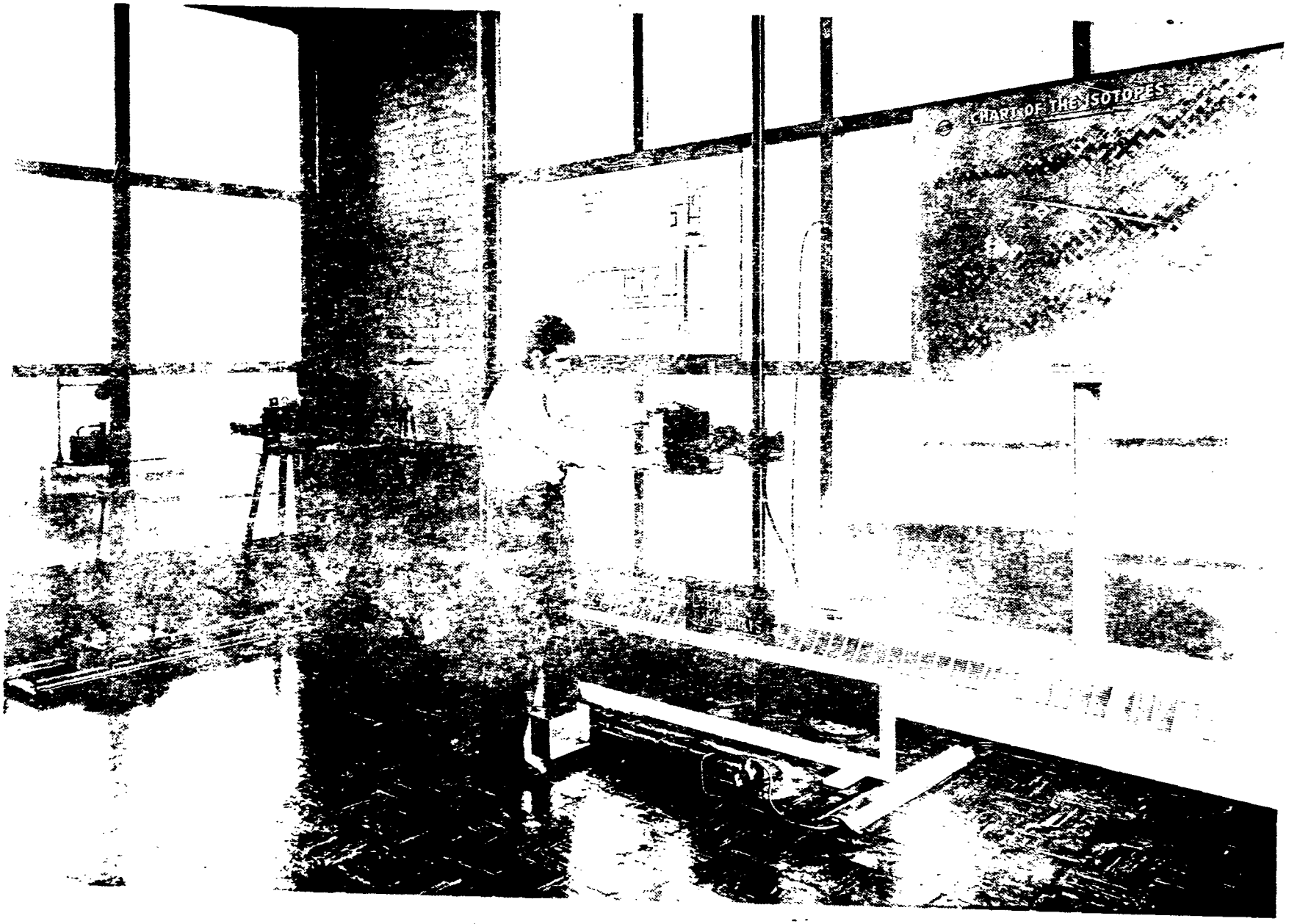

Figure 5. Gamma-ray facilities at NBS.

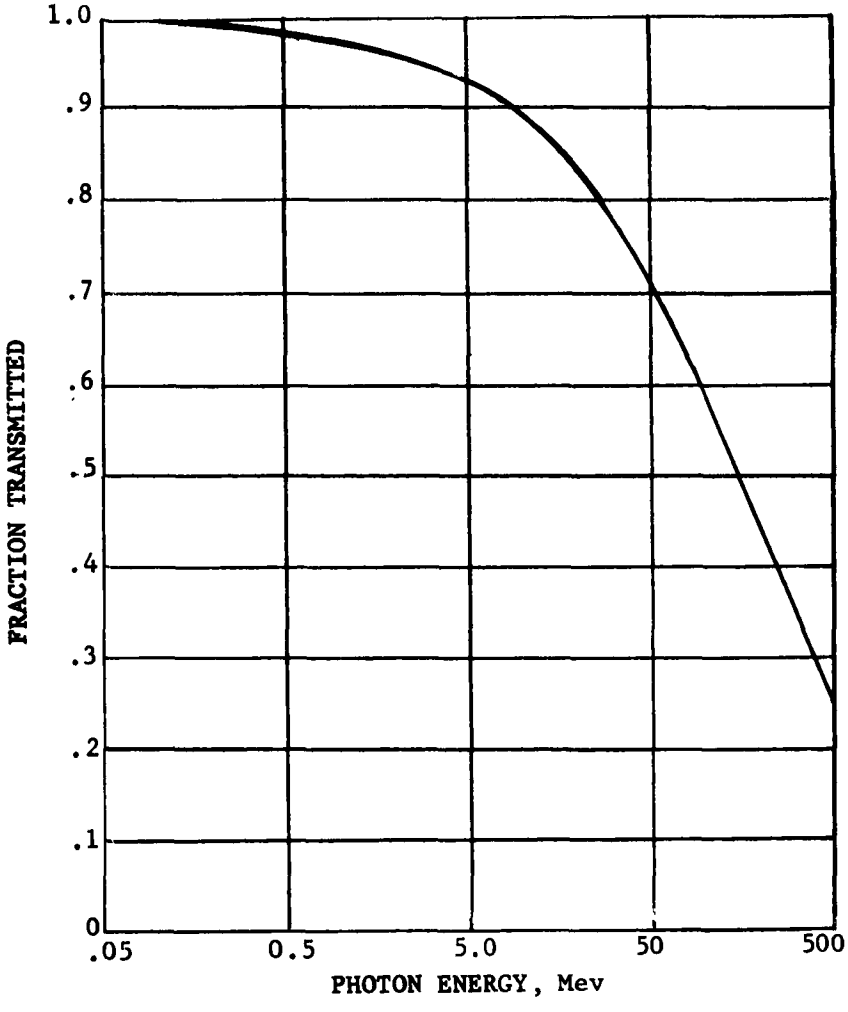

Figure 6. Fractional number of photons transmitted through an air wall thickness equal to the maximum range of the secondary electrons.

Figure 7. Primary standard Ra-Be photoneutron source surrounded by 4-cm diameter beryllium sphere.

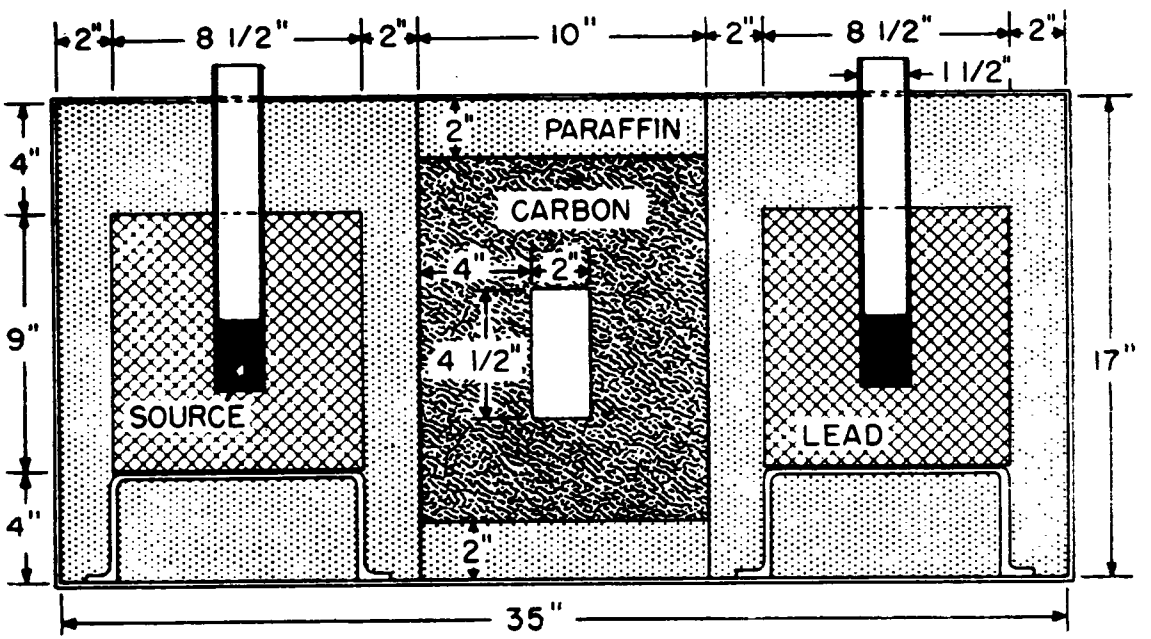

Figure 8. NBS standard thermal neutron flux geometry.

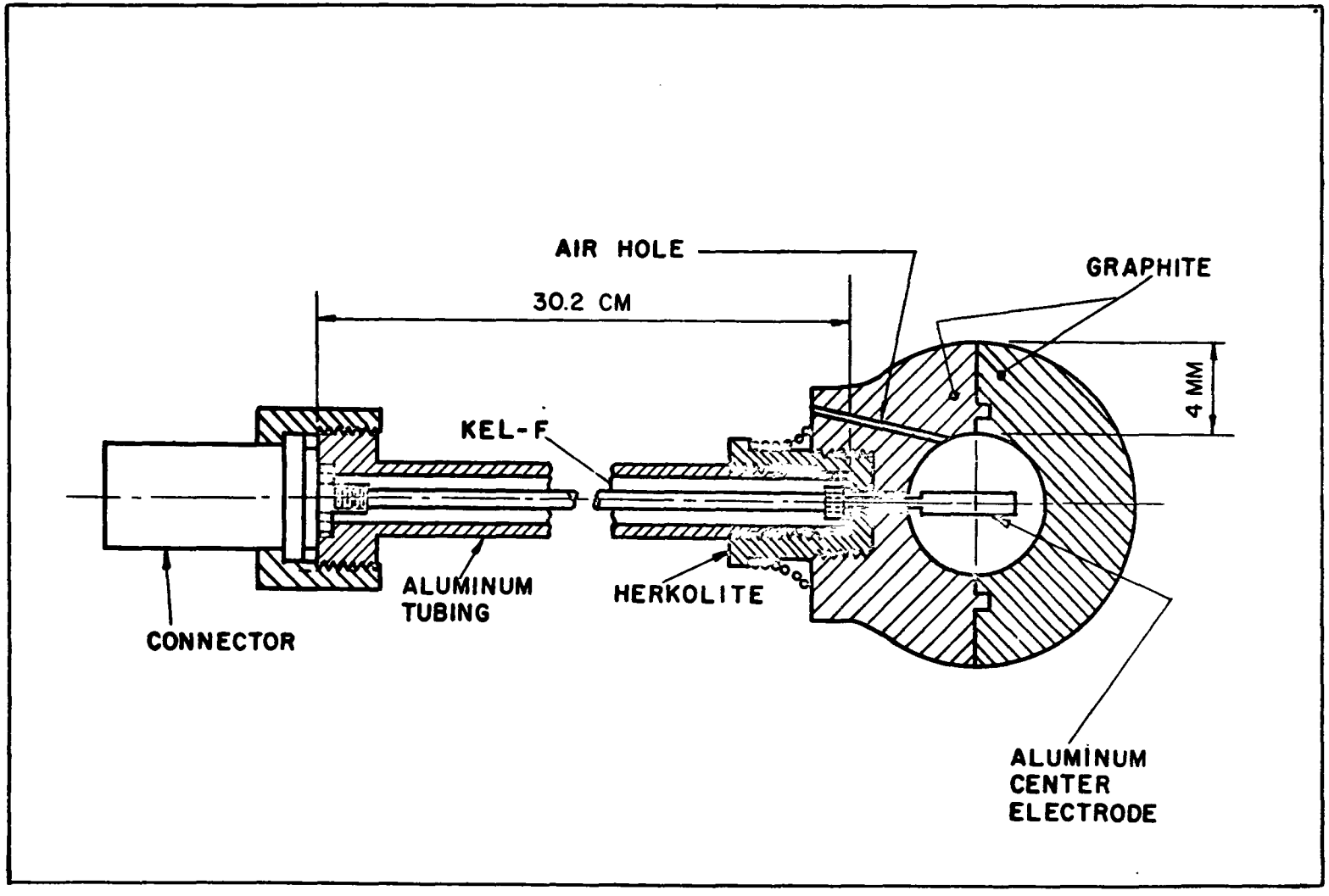

Figure 9. Graphite cavity chamber

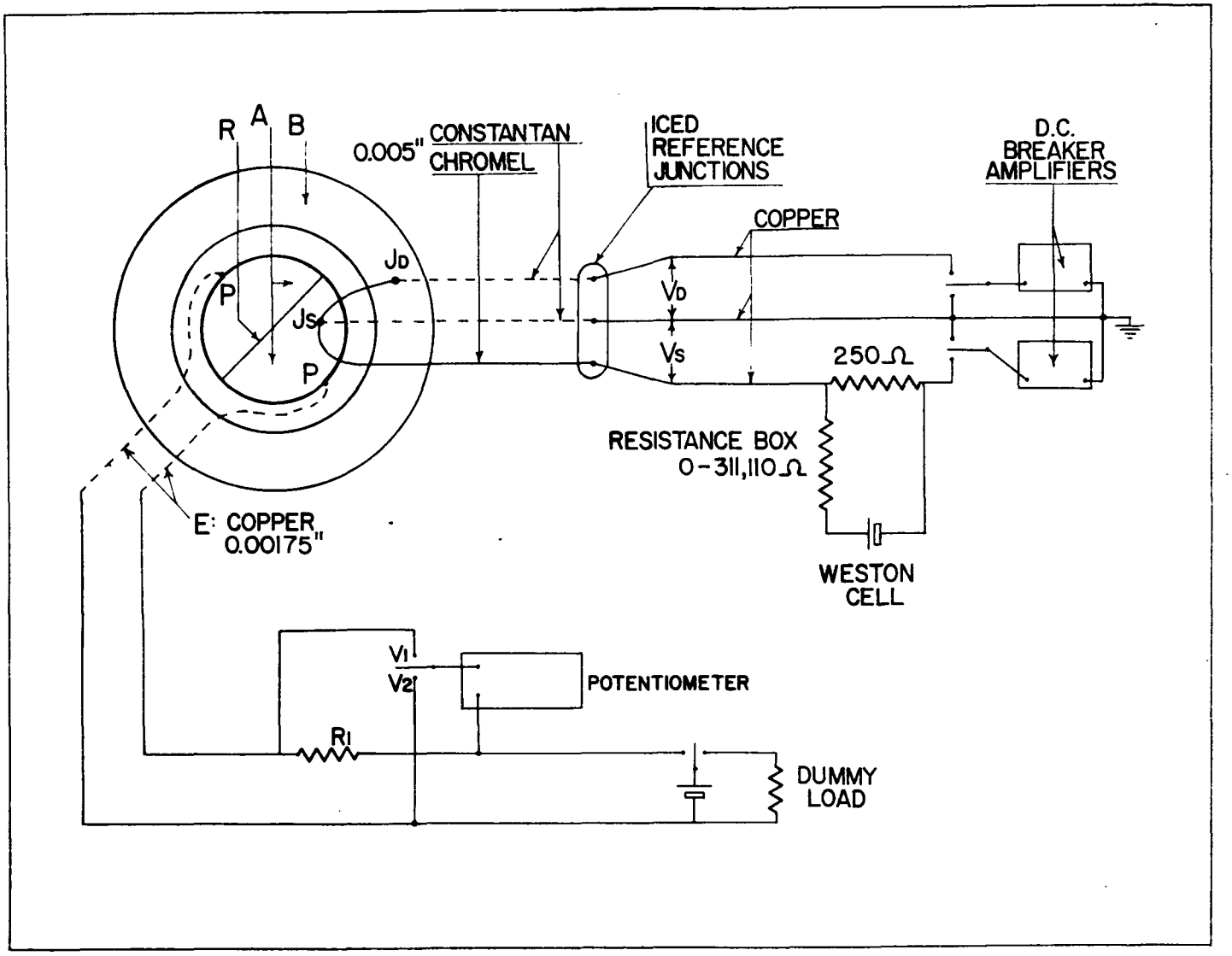

Figure 10. Schematic diagram of calorimeter proposed as possible standard for absorbed dose measurements.

COMPARISON OF RADIATION EFFECTS IN DIFFERENT FACILITIES

by

W.R. Burrus[a]
Physics Department
Ohio State University

and

W.T. Harper[b]
Missile Systems Division
Lockheed Aircraft Corporation

Regardless of any agreement reached on units and methods of measurement within the Nuclear Propelled Manned Aircraft Program, there still exists the problem of correlating the radiation-effects data reported by investigators in agencies that are not participating in the Program. To cope with this problem, a simplified method for consistent comparison of the data obtained in different facilities is presented. This is accomplished by expressing radiation environments in terms of "carbon-absorbed gamma dose" and "water-absorbed neutron dose." Although the method involves some simplifying assumptions and approximations, it is shown to be generally applicable to organic materials, which cause some of the most critical problems for the designer of nuclear-propelled aircraft. The sample calculations, tables, and curves presented may be used as a handbook for conversion of radiation dose data to common denominators. Such conversions permit comparison of data even when information on the spectral distribution of the radiation environment is lacking.

INTRODUCTION

Efforts to assimilate and correlate radiation-effects information for use in various studies have shown that the class of materials that presents the greatest number of problems is the organic class. Semiconductor devices, while very sensitive to radiation-induced changes, can be located by the aircraft designer at points sufficiently distant from the reactor to provide a relatively long expected lifetime. In many cases, such locations are not feasible for plastics, elastomers, and lubricants. Therefore, the aircraft designer must keep abreast of research leading to the development of more tolerant materials and the determination of the radiation tolerance of existing materials. This

[a] Formerly with Georgia Division of Lockheed Aircraft Corporation and with Wright Air Development Center.

[b] Formerly with Georgia Division of Lockheed Aircraft Corporation.

is not a simple matter, however; investigators report radiation environments in various units and sometimes do not report them at all. The problem would not be entirely eliminated by agreement on measuring and reporting methods within the Nuclear Propelled Manned Aircraft Program, since agencies that are not participating in the program have their own preferences and practices in reporting radiation-effects research.

This paper presents a method for systematic correlation of radiation-effects data, based on a method proposed by Burrus at the Second Semi-annual 125-A Radiation Effects Symposium.[1] The basis of the method, as modified here, is the expression of all radiation environments in terms of "carbon-absorbed gamma dose" (erg g^{-1}) and "water-absorbed neutron dose" (erg g^{-1}), either by making original measurements or by converting existing measurements.

GAMMA INTERACTION

Interactions between gamma radiation and matter are of three types:

(1) Photoelectric
(2) Compton scattering
(3) Pair production

The amount of energy deposited in a sample by any of these mechanisms depends upon the energy spectrum of the source, the material through which the gamma radiation has passed, and the composition of the sample.

The spectral dependence of the gamma interactions is evaluated by consideration of the following four spectra,[2] which are typical of those likely to be encountered:

I. A 1-mev source with no absorbing material between source and sample. This case is representative of most isotope sources where the samples are small and are not submerged in water.

II. A 1-mev point isotropic source attenuated by one mean free path (14.2 cm) of water. This case is representative of isotope sources that are surrounded by water or by other material having a low atomic number (e.g., spent fuel elements).

III. Approximate unattenuated fission gamma spectrum (with an assumed low-energy cutoff of 20 kev).

IV. Approximate point isotropic fission gamma spectrum attenuated by 100 cm of water. This case is representative of any fissionlike source that has penetrated a few mean free paths of material having a low-atomic number.

These four spectra are shown in Fig. 1. The area under this type of curve is not significant. Fig. 2 shows the dose per unit log E as a function of energy for spectrum IV; it indicates at what energies the various absorption processes are most important. The photoelectric cross section for gamma-ray interaction varies inversely as approximately the square of the energy. Therefore, most of the photoelectric contribution is due to radiation below 1 mev. The dose contributed by the pair-production process is seen to be negligible.

Let us now examine the manner in which the gamma-energy deposition processes depend upon the composition of the sample. Burrus shows that the following approximations are valid:

$$\sigma_t \propto Z^{4.5} \tag{1}$$

$$\sigma_c \propto Z \tag{2}$$

$$\sigma_p \propto Z^2 \tag{3}$$

where σ_t, σ_c, and σ_p represent the total interaction probability for the photoelectric, Compton, and pair-production interactions, respectively, and Z is the atomic number. Figure 3 shows the gamma dose relative to the Compton dose as a function of the effective atomic number for the spectra of interest. It can be seen that the pair-production contribution is negligible and the photoelectric contribution is small for materials having a low atomic number.

Next, let us examine the materials and compositions of interest to determine the value of the effective atomic numbers. In Table I, the average atomic number, the electron density, and the relative photoelectric contribution to dose are listed for various elements and materials. It will be noted that the values given for carbon are representative of the values for the plastics and elastomers. Therefore, the "carbon-absorbed gamma dose" is a good indicator of the energy deposited in the materials of low atomic number that are of interest here.

NEUTRON INTERACTION

The interaction of neutrons is more complicated than that of gamma radiation, since the "absorbed dose" for any material cannot be correlated with any one parameter.

Our interest is the calculation of absorbed energy in a sample that is subjected to neutron irradiation. The significant effects of neutron bombardment are ionization, dislocation, and the production of gamma radiation. The gamma radiation produced is important, but its effect is determined along with all the other gammas in an experiment. Ionization is more effective than displacement in causing physical and chemical changes in

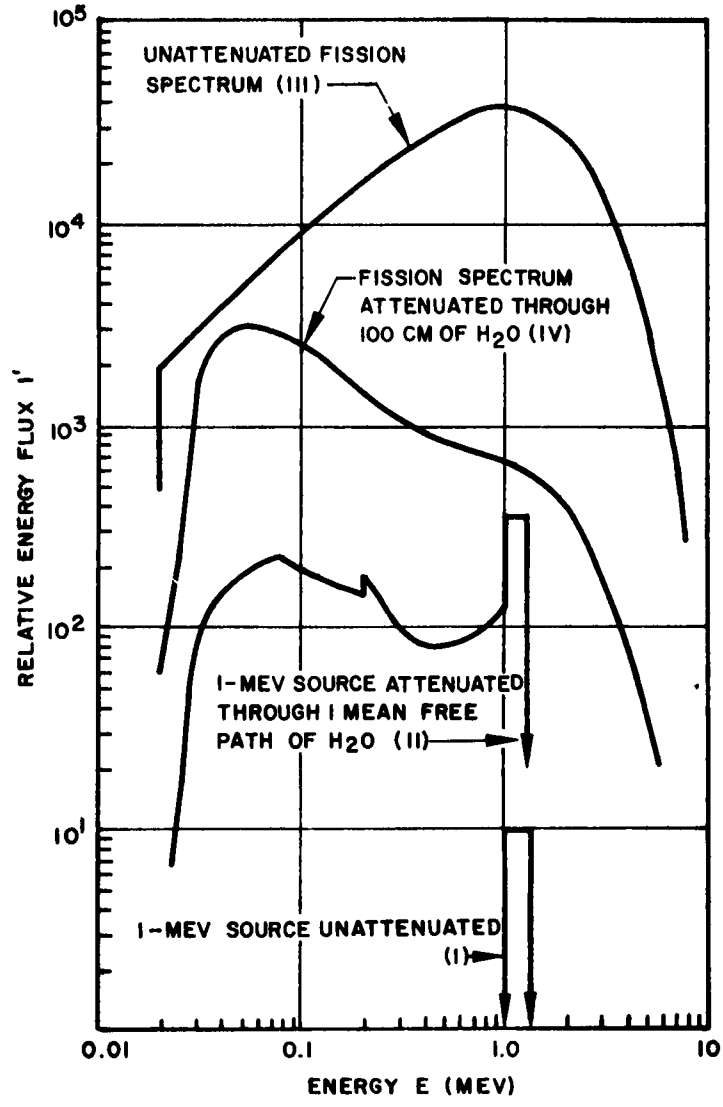

Fig. 1 Typical Gamma Spectra

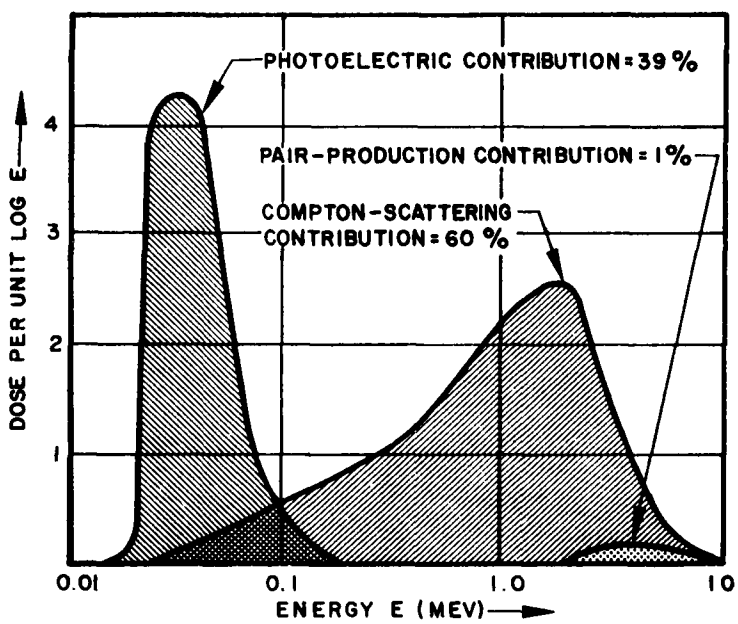

Fig. 2 Absorbed Dose Distribution, Spectrum IV

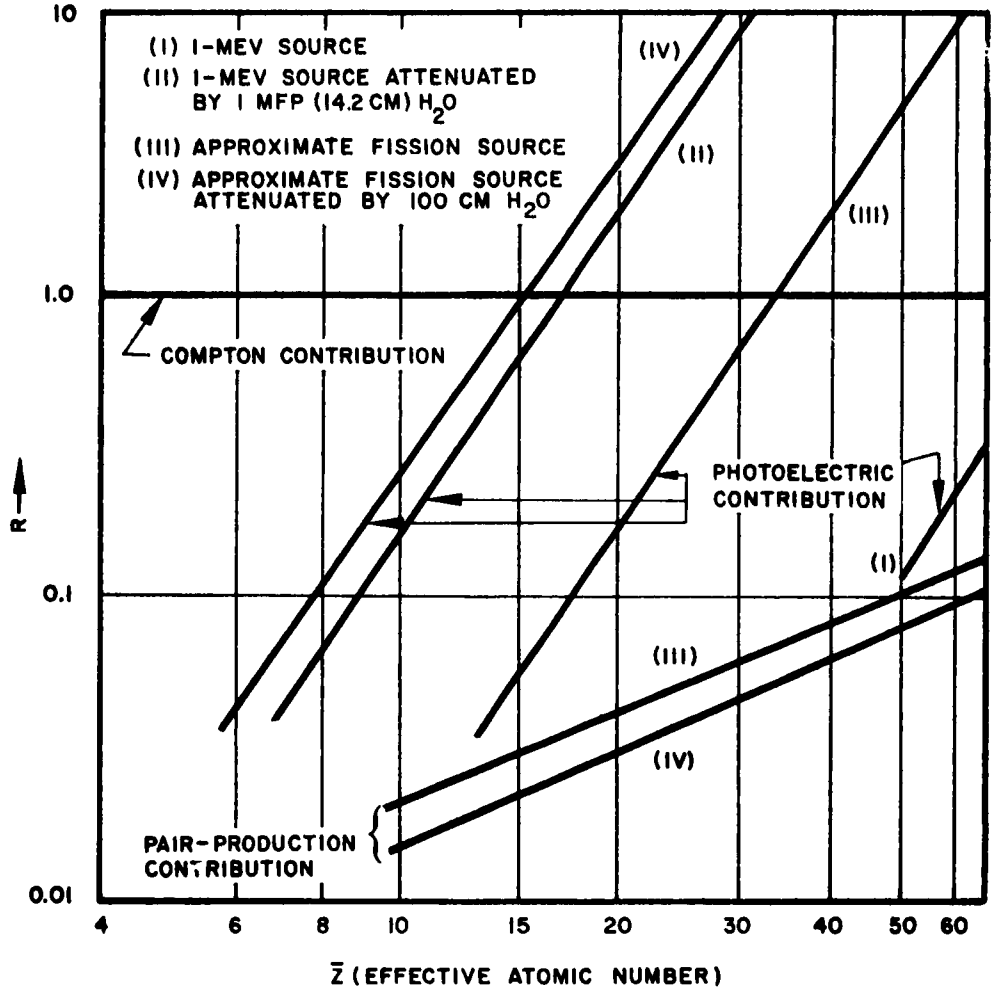

Fig. 3 Relative Gamma Dose per Electron

TABLE I

GAMMA ABSORPTION CONSTANTS

Material	Composition	$\bar{Z}$	N: Elec.g^{-1} ($\times 10^{-23}$)	P: Relative Photoelectric Contribution to Dose			
				I	II	III	IV
Hydrogen	H	1	5.97	0.000	0.000	0.000	0.000
Carbon	C	6	3.01	0.041	0.002	0.000	0.030
Nitrogen	N	7	3.01	0.071	0.004	0.000	0.051
Oxygen	O	8	3.01	0.115	0.007	0.000	0.083
Fluorine	F	9	2.86	0.165	0.009	0.000	0.125
Aluminum	Al	13	2.90	0.625	0.036	0.001	0.445
Sulfur	S	16	3.01	1.30	0.074	0.002	0.935
Chlorine	Cl	17	2.88	1.61	0.091	0.003	1.05
Argon	A	18	2.72	1.96	0.112	0.004	1.41
Copper	Cu	29	2.75	10.4	0.590	0.018	7.45
Polyethylene	$(CH_2)_n$	5.52	3.44	0.031	0.002	0.000	0.022
Nat. Rubber	$(C_5H_8)_n$	5.60	3.52	0.033	0.002	0.000	0.022
Polystyrene	$(CH)_n$	5.74	3.24	0.036	0.002	0.000	0.026
Nylon	$(C_6H_{11}ON)_n$	6.25	3.30	0.048	0.003	0.000	0.035
Water	H_2O	7.50	3.34	0.092	0.005	0.000	0.066
Tissue	$(C_5H_{40}O_{18}N)_n$	7.28	3.31	0.082	0.005	0.000	0.059
Lucite	$(C_5H_8O_2)_n$	6.55	3.25	0.057	0.003	0.000	0.041
Air	N_2 75.5% O_2 23.2% A 1.3%	7.77	3.01	0.105	0.006	0.000	0.075
Teflon	$(CF_2)_n$	8.48	2.89	0.139	0.008	0.000	0.097
Fluorothene	$(C_2Cl_3F)_n$	15.5	2.90	1.16	0.066	0.002	0.837
"Carbon-tet"	CCl_4	16.6	2.90	1.47	0.084	0.003	1.06
Trichloro-ethylene	C_2Cl_3H	16.0	2.93	1.28	0.073	0.002	0.923

noncrystalline materials. Displacement becomes significant in noncrystalline materials of high atomic weight, but our present interest is in hydrocarbons and materials having low atomic weight. The amount of ionization produced in hydrogenous materials is closely proportional to the absorbed dose; therefore, the comparison of the total absorbed dose resulting from neutrons in different irradiation facilities is significant.

The neutron energy absorption cross sections of interesting materials can be compared by considering the following three spectra, which represent the extremes expected to be encountered:

I. Graphite-moderated reactor neutron spectrum

II. Water-moderated reactor neutron spectrum

III. Unmoderated fission spectrum

The total energy absorption cross sections for several common elements and materials are given in Table II for the above neutron spectra.[3] It will be noted that the variation from spectrum to spectrum in the average energy absorption cross section for water is representative of the variation for hydrogenous materials. Therefore, "water-absorbed neutron dose" is a convenient unit for comparing neutron radiation effects in materials of interest here.

The cross sections in Table II can be used to compute absorbed neutron dose, provided the total energy flux is known. However, since the energy flux is not usually reported, it is necessary to convert the reported dosimetric units to energy flux. This is accomplished by use of the curves in Fig. 4 and the conversion factors in Table III.[3] Figure 4 is a plot of the integral flux for the three typical neutron spectra previously mentioned. It should be noted in Table III that the factor 2 mev per "fast" neutron is within 13 percent for all neutron spectra. Examples of the use of Fig. 4 and Table III in sample calculations will be presented later.

Summarizing to this point, it has been shown that "carbon-absorbed gamma dose" and "water-absorbed neutron dose" provide convenient common denominators for the correlation of radiation-effects data. It should be kept in mind that this method is limited to organic materials having a low atomic number.

SAMPLE CALCULATIONS

This section presents some sample calculations to show exactly how the foregoing concepts are applied. Gamma dose calculations are considered first.

TABLE II

TOTAL ENERGY ABSORPTION CROSS SECTIONS
(IN BARNS) FOR COMMON ELEMENTS AND MATERIALS

Material	Composition	Molecular Weight	Spectrum I Graphite Moderated	Spectrum II Water Moderated	Spectrum III Unmoderated
Hydrogen	H	1	2.3	1.7	1.3
Carbon	C	12	0.34	0.30	0.26
Nitrogen	N	14	0.31	0.28	0.26
Oxygen	O	16	0.28	0.25	0.21
Fluorine	F	19	0.26	0.25	0.26
Sulfur	S	32	0.22	0.27	0.31
Chlorine	Cl	35	0.11	0.13	0.14
Polyethylene	CH_2	14	4.8	3.7	2.9
Nat. Rubber	C_5H_8	68	20.	15.	12.
Polystyrene	CH	13	2.6	2.0	1.6
Nylon	$C_6H_{11}ON$	113	27.	21.	16.
Water	H_2O	18	4.8	3.7	2.8
Tissue	$C_5H_{40}O_{18}N$	402	98.	75.	58.
Lucite	$C_5H_8O_2$	100	20.	16.	12.
Teflon	CF_2	50	0.81	0.78	0.77
Fluorothene	C_2Cl_3F	168	1.2	1.2	1.2
"Carbon-Tet"	CCl_4	154	0.74	0.79	0.84
Trichloro-ethylene	C_2Cl_3H	130	3.2	2.7	2.3

TABLE III

CONVERSION FACTOR FOR "FAST FLUX" (INTEGRAL NUMBER FLUX) OVER 0.5 MEV TO TOTAL ENERGY FLUX

$\frac{\int_0^\infty E\,\phi'\,dE}{\int_{0.5\ mev}^\infty \phi'\,dE}$	Spectrum I: Graphite Moderated	Spectrum II: Water Moderated	Spectrum III: Unmoderated
	1.8 mev	2.3 mev	2.3 mev

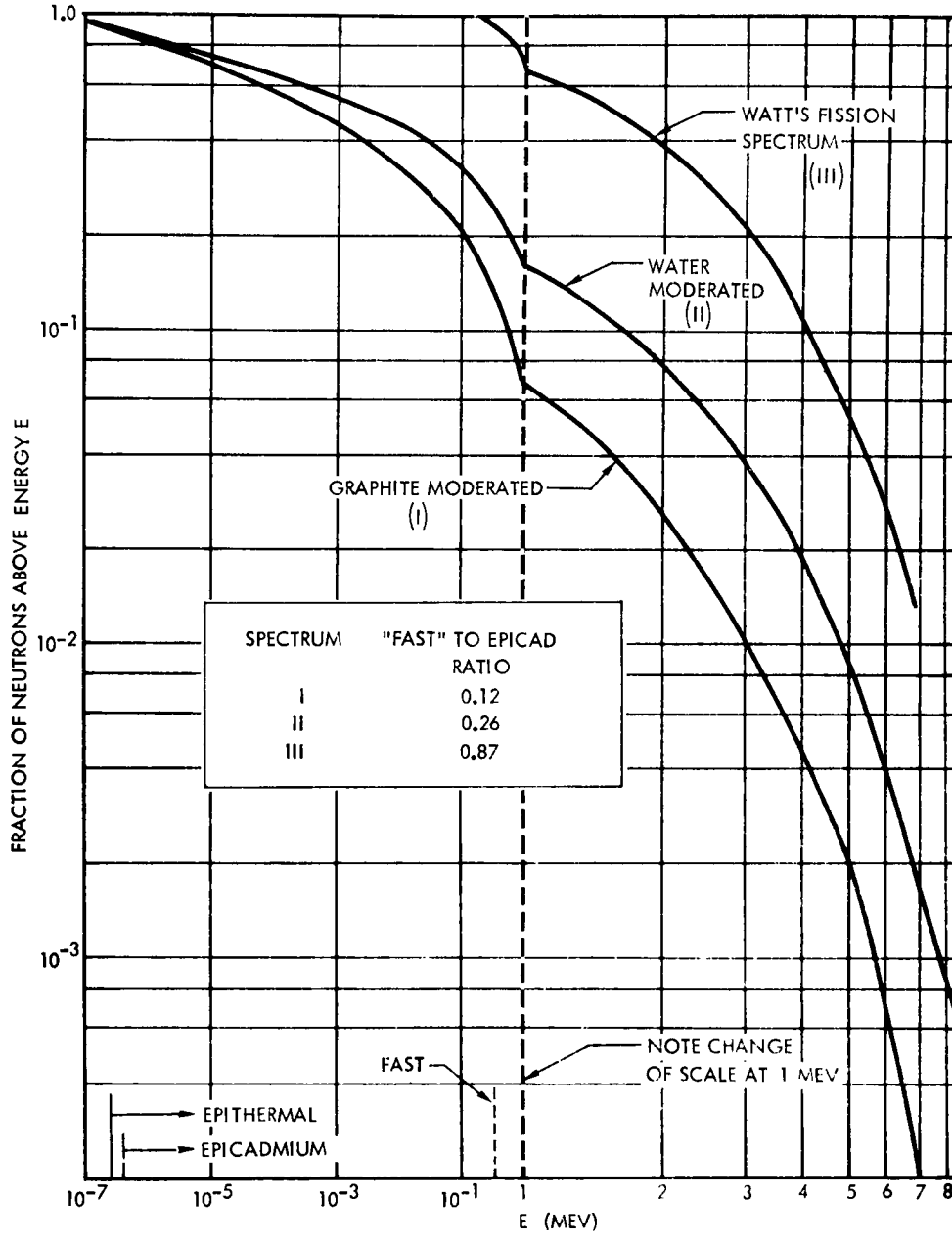

Fig. 4 Neutron Distributions of Various Sources

A. GAMMA DOSE CONVERSIONS

(1) When the exposure dose is given in roentgens (r):

Procedure: Find the "carbon dose," DC, in ergs per gram by use of the following relationship:

$$1\ r = 87.7\ erg\ g^{-1} \tag{4}$$

The choice of the value 87.7 used in Eq. (4) is discussed in the Appendix.

Example: Given a gamma exposure dose of 4.5×10^7 r, find the absorbed dose in carbon as follows:

$$4.5 \times 10^7\ r \times 87.7\ erg\ g^{-1}\ r^{-1} = 3.95 \times 10^9\ erg\ g^{-1} \tag{5}$$

(2) When the number flux is given (photons cm^{-2}):

Procedure: Find the gamma energy flux I by means of the following equation:

$$I = \bar{E}\,\phi \tag{6}$$

where I is the energy flux in mev cm^{-2}, $\bar{E}$ is the average photon energy in mev, and ϕ is the number flux in photons cm^{-2}. Table IV gives the average photon energy for various gamma spectra. Usually, Table IV will not be used, owing to the complications described below.

Because the number flux is never measured directly, an author reporting data in terms of number flux must have calculated the value from other measurements. In order to make the conversion to number flux, an average energy $\bar{E}$ must be known or assumed. The same value of $\bar{E}$ must be used in the calculations of interest here as was used in the original calculation if the results are to be meaningful and useful. Therefore, the average photon energy assumed by the person originally calculating number flux should be known before "carbon gamma dose" can be calculated. To date, the standard practice has been to assume a value of 1 mev for $\bar{E}$. This value should not be used here without first attempting to determine if it was the value used in the original calculation.

After the energy flux has been calculated, proceed to the next step, which gives the method for obtaining carbon dosage when the energy flux is known.

Example: Given a number flux Φ of 3.33×10^{17} photons cm^{-2} from a graphite-moderated reactor. First, find the average energy per photon $\bar{E}$ in Table IV for a graphite-moderated reactor. This value is seen to be 0.30 mev. Next, make the computation by substituting into Eq. (6) as follows:

$$I = (0.30 \text{ mev photon}^{-1}) \times (3.33 \times 10^{17} \text{ photons cm}^{-2})$$

$$I = 1 \times 10^{17} \text{ mev cm}^{-2} \qquad (7)$$

(3) When the gamma energy flux is given:

Procedure: The carbon dose DC is found by means of the following equation:

$$DC = NcK\bar{\sigma} I \qquad (8)$$

where Nc is the electron density of carbon ($Nc = 3.01 \times 10^{23}$ electrons per gram), K is a constant for converting from mev to erg ($K = 1.602 \times 10^{-6}$ erg mev^{-1}), $\bar{\sigma}$ is the average Compton energy absorption cross section per electron in cm^2, and I is the given energy flux in mev cm^{-2}. Table V gives the average Compton energy absorption cross section per electron for various gamma spectra.

Figure 5, taken from a National Bureau of Standards publication,[4] shows the absorption cross section of electrons for gamma radiation from 0.01 to 100 mev. This plot may be used to find $\bar{\sigma}$ for use in Eq. (8) for gamma spectra not given in Table V. The cross sections in Table V do not agree in all cases with the values that would be obtained from Fig. 5 by using the energy values listed in Table IV for the spectra of interest. This apparent discrepancy is attributed to the fact that some of the values of $\bar{\sigma}$ given in Table V are averaged over an energy spectrum and are not the cross sections at a single value of photon energy.

Example: Given an energy flux I of 1×10^{17} mev cm^{-2} from a graphite-moderated reactor. The carbon dose DC is calculated by substitution in Eq. (8). The electron density of carbon, Nc, is obtained from Table I. This value is seen to be 3.01×10^{23} electrons per gram. K is given above ($K = 1.602 \times 10^{-6}$ erg mev^{-1}). Table V gives $\bar{\sigma}$ for a graphite-moderated reactor as 0.082×10^{-24} cm^2 per electron. Substitution of these values in Eq. (8) gives

$$DC = (3.01 \times 10^{23} \text{ e g}^{-1}) (1.602 \times 10^{-6} \text{ erg mev}^{-1})$$
$$(0.082 \times 10^{-24} \text{cm}^2 \text{ e}^{-1}) (1 \times 10^{17} \text{ mev cm}^{-2}) \qquad (9)$$

TABLE IV

AVERAGE ENERGY, $\bar{E}$, OF VARIOUS GAMMA SPECTRA

Gamma Spectrum		Average Photon Energy $\bar{E}$ (mev)
I	Graphite- or Water-Moderated Reactor	0.3
II	Unattenuated Fission Source	1.0
III	Attenuated (14-in. Water) Isotope Source	0.35
IV	Unattenuated Isotope Source[a]	1.0
V	Unattenuated Cobalt – 60 Source	1.25

[a] E.g., spent fuel element.

TABLE V

AVERAGE COMPTON ENERGY ABSORPTION CROSS SECTION FOR VARIOUS GAMMA SPECTRA[a]

Gamma Spectrum		Cross Section Per Electron (barns)
I	Graphite- or Water-Moderated Reactor	0.078
II	Unattenuated Fission Source	0.079
III	Attenuated Isotope Source	0.091
IV	Unattenuated Isotope Source	0.093
V	Unattenuated Cobalt – 60 Source	0.089

[a] Revised from calculations by Burrus.

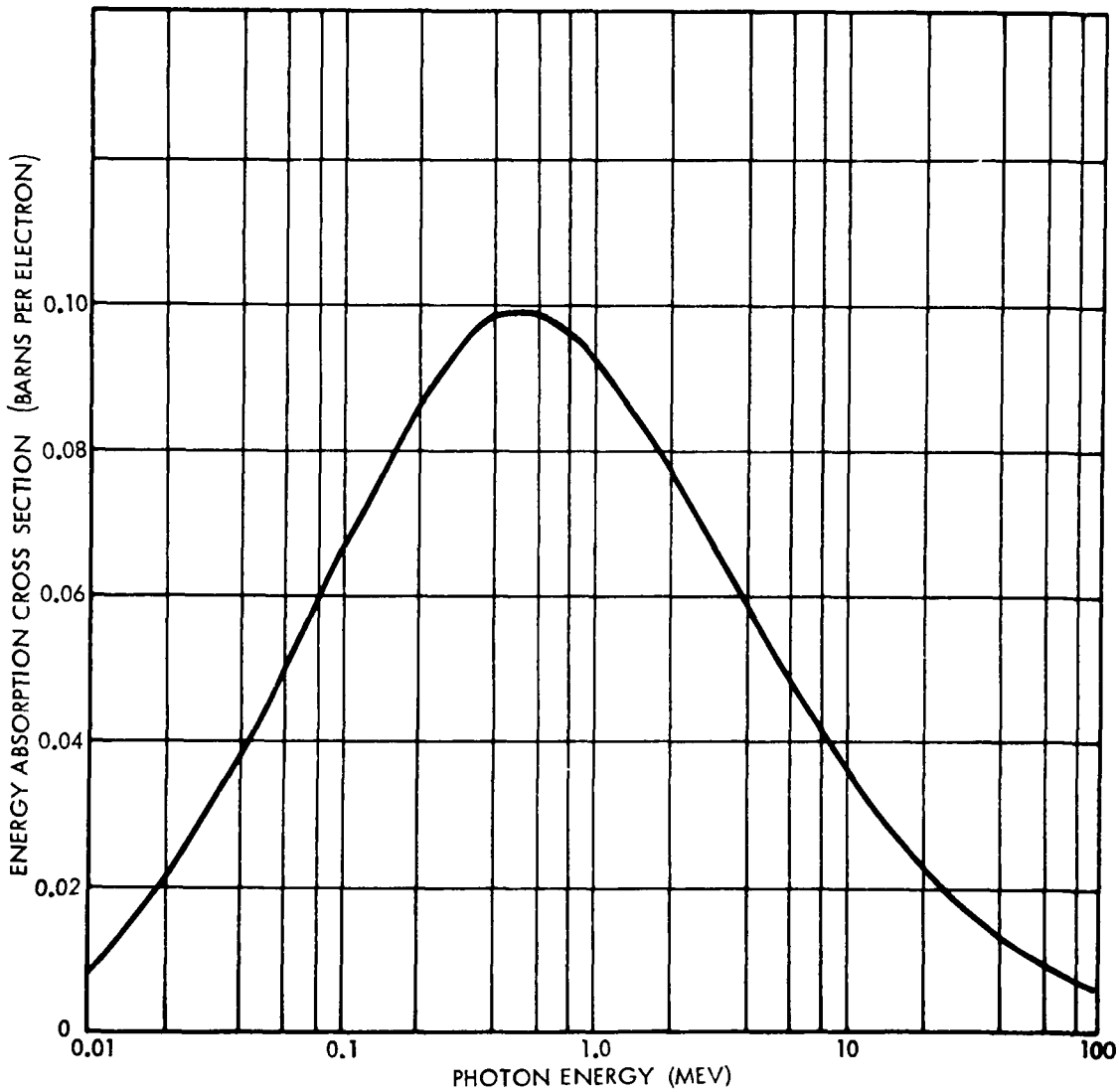

Fig. 5 Gamma Energy Absorption Cross Section for Free Electrons as Given by the Klein-Nishini Formula

Multiplication yields

$$DC = 3.95 \times 10^{9} \text{ erg } g^{-1}$$

(4) When absorbed gamma dose in some other material is given:

Procedure: In the event that the only information available describing a particular gamma environment is the absorbed dose (perhaps in rads) in a material other than carbon, and information is available as to the type of spectrum involved, it is relatively simple to calculate the carbon dosage. The following formula is used for this computation:

$$DC = Do \left(\frac{Nc}{No}\right)\left(\frac{1 + Pc}{1 + Po}\right) \qquad (10)$$

where

DC = absorbed dose in carbon (erg g^{-1})

Do = absorbed dose in reference material (erg g^{-1})

Nc = electron density of carbon (electron g^{-1})

No = electron density of reference material

Pc = photoelectric contribution to the dose relative to the Compton contribution in carbon (Table I)

Po = photoelectric contribution to the dose relative to the Compton contribution in the reference material (Table I)

For a number of elements and common materials, Table I lists the effective atomic number $\bar{Z}$, the electron density N, and values of P for the four different spectra. The value of P is selected from the applicable spectrum column.

Example: Given an absorbed gamma dose in polyethylene from a graphite-moderated reactor of 4.46×10^{7} rad, first convert from rad to erg g^{-1} by use of the following equation:

$$1 \text{ rad} = 100 \text{ erg } g^{-1} \text{ in the same material} \qquad (11)$$

Therefore,

$$Do = 4.46 \times 10^{7} \text{ rad} \times 100 \text{ erg } g^{-1} \text{ rad}^{-1}$$

$$Do = 4.46 \times 10^{9} \text{ erg } g^{-1} \text{ in polyethylene} \qquad (12)$$

Table I is now used to obtain the following values for the quantities in Eq. (10):

$$Nc = 3.01 \times 10^{23} \text{ electrons } g^{-1}$$
$$No = 3.44 \times 10^{23} \text{ electrons } g^{-1}$$
$$Pc = 0.041 \text{ (Spectrum I)}$$
$$Po = 0.031 \text{ (Spectrum I)}$$

Substituting the above values into Eq. (10) yields

$$DC = 4.46 \times 10^{9} \left(\frac{3.01 \times 10^{23}}{3.44 \times 10^{23}}\right)\left(\frac{1 + 0.041}{1 + 0.031}\right) \qquad (13)$$

and solving for DC gives

$$DC = 3.95 \times 10^{9} \text{ erg } g^{-1}$$

B. NEUTRON DOSE CONVERSIONS

(1) When an integral flux other than "fast" flux is given:

Procedure: Find "fast" flux and proceed to step (2). Figure 4 is a graph of the integral flux as a function of energy for various neutron sources. The "fast" flux may be determined by multiplying the given flux by the ratio of the "fast" flux to the given flux for the spectrum under consideration. Since epicadmium flux is frequently given, the ratio of the "fast" flux to the epicadmium flux for each spectrum is calculated and entered on the flux plot of Fig. 4. Other ratios may be determined from the plot as needed.

Example (a): Given an epicadmium integral flux of 1×10^{14} neutron cm^{-2} in a graphite-moderated reactor, find the "fast" integral flux. The ratio of "fast" to epicadmium flux for a graphite-moderated spectrum given in Fig. 4 is 0.12. Multiplying this ratio by the given flux,

$$\text{"Fast" integral flux} = (1 \times 10^{14} \text{ epicad neutrons}) \times (0.12) \qquad (14)$$

$$\text{"Fast" integral flux} = 1.2 \times 10^{13} \text{ "fast" neutrons } cm^{-2}$$

Proceed to step (2) for further conversion.

Example (b): Given an integral flux of 3.3×10^{15} neutrons cm^{-2} above 0.01 mev from a graphite-moderated reactor, find the "fast" integral flux. First, determine the ratio of "fast" neutrons to 0.01-mev neutrons from the plot in Fig. 4. The points of curve I lying on the energy values of interest are 0.067 at 0.5 mev ("fast"), and about 0.21 at 0.01 mev (energy of given flux). Then,

$$\frac{0.067}{0.21} = 3.2 \times 10^{-1} \text{ "fast" neutrons to 0.01 mev neutrons}$$

Multiplying this value by the given integral flux of 3.3×10^{15} neutrons cm^{-2} (0.01 mev),

$$\text{"Fast" integral flux} = (3.2 \times 10^{-1})(3.3 \times 10^{15} \text{ n cm}^{-2})$$

$$\text{"Fast" integral flux} = 1.05 \times 10^{15} \text{ neutrons cm}^{-2} \qquad (15)$$

Proceed to step (2) for further conversion.

A graphical method of finding the ratio of "fast" neutrons to the neutrons of any given energy may be used. The method consists of placing a sheet of semilogarithmic paper over the distribution plots on Fig. 4 so that 1.0 on the ordinate of the overlying graph intersects the curve at the energy value of the given neutron flux. Then the ratio of interest may be read directly from the overlying graph paper at the energy value of 0.5 mev for "fast" neutrons. Of course, the size of the cycles on the overlying sheet must be the same as those in Fig. 4.

(2) When "fast" flux is given:

Procedure: Convert to energy flux, then proceed to step (3). The given "fast" flux is multiplied by the conversion factor given in Table III.

Example: Given a "fast" integral flux of 7.5×10^{14} neutrons cm^{-2} from a graphite reactor.

Therefore,

$$I = 7.5 \times 10^{14} \text{ nvt (fast)} \times 1.8 \text{ mev n}^{-1}$$

$$I = 1.35 \times 10^{15} \text{ mev cm}^{-2} \qquad (16)$$

where I is the energy flux. Now proceed to the next step for final conversion to "water dose."

(3) When neutron energy flux is given:

Procedure: Calculate "water dose" D as follows

$$D = K (N_1 \bar{\sigma}_1 + N_2 \bar{\sigma}_2 \cdot \cdot \cdot + N_i \bar{\sigma}_i) I \qquad (17)$$

where

D = absorbed dose (erg g^{-1})

N_i = number of atoms of the i^{th} element per gram of the material of interest

$\bar{\sigma}_i$ = average energy absorption cross section of the i^{th} element (cm^2)

K = conversion from mev to erg ($K = 1.602 \times 10^{-6}$ erg mev^{-1}

I = energy flux (mev cm^{-2}) .

The values of N for the elements in various materials is given in Table VI, and $\bar{\sigma}$ may be found in Table II which gives the average energy absorption cross sections for several common elements.

Example: Given an energy flux I of 1.38×10^{15} mev cm^{-2} from a graphite-moderated reactor, find the "water neutron dose." From the preceding instructions, use Eq. (17), which takes the following form in the case of water:

$$DW = K (N_H \bar{\sigma}_H + N_O \bar{\sigma}_O) I \qquad (18)$$

where DW is the absorbed water dose, and the subscripts H and O are hydrogen and oxygen, respectively. The other symbols have the same meaning as in Eq. (17). The values for the symbols are as follows

$K = 1.602 \times 10^{-6}$ erg mev^{-1} (energy conversion)

$N_H = 6.7 \times 10^{22}$ atom g^{-1} (Table VI)

$\bar{\sigma}_H = 2.26 \times 10^{-24}$ cm^2 atom $^{-1}$ (Table II)

$N_O = 3.35 \times 10^{22}$ atom g^{-1} (Table VI)

$\bar{\sigma}_O = 0.28 \times 10^{-24}$ cm^2 atom $^{-1}$ (Table II)

$I = 1.38 \times 10^{15}$ mev cm^{-2} (given)

Substituting the above values into Eq. (18),

$$DW = 1.602 \times 10^{-6} \left[(6.7 \times 10^{22})(2.26 \times 10^{-24}) + (3.35 \times 10^{22}) (0.28 \times 10^{-24}) \right] 1.38 \times 10^{15}$$

$$DW = 3.56 \times 10^{8} \text{ erg } g^{-1}$$

TABLE VI

COMPOSITION OF MATERIALS: ATOMIC DENSITY IN ATOMS PER GRAM

(All densities have been multiplied by 10^{-22})

Material	Density of Element	Density of Compound						
		Hydrogen	Carbon	Oxygen	Nitrogen	Argon	Chlorine	Fluorine
Hydrogen	59.7							
Carbon	5							
Nitrogen	4.3							
Oxygen	3.76							
Fluorine	3.17							
Aluminum	2.23							
Sulfur	1.88							
Chlorine	1.7							
Argon	1.51							
Copper	0.95							
Polyethylene		8.6	4.3					
Natural Rubber		7.1	4.4					
Polystyrene		4.6	4.6					
Nylon		4.85	3.2	0.53	0.53			
Water		6.7		3.35				
Tissue		6	0.75	2.7	0.15			
Lucite		4.8	3.0	1.2				
Air				0.99	3.2	0.056		
Teflon			1.2					2.4
Fluorothene			0.81				1.2	
"Carbon-Tet"			0.73				2.9	
Trichloro-ethylene		0.46	0.92				1.38	

APPENDIX

THE CHOICE OF THE VALUE DC = 87.7 ERG G^{-1} PER ROENTGEN

The Air Force gives the absorbed dose in carbon as 87.7 erg g^{-1} per roentgen on the basis of Compton dose only.[5] The question arises as to what contribution the photoelectric effect makes toward absorbed dose. The International Commission on Radiological Units and Measurements (ICRU) has tabulated the values of the mass energy-absorption coefficients for a number of elements and substances for gamma radiation with photon energies of 0.010 mev to 10.0 mev.[6] The dose absorbed in air is given as 87.7 erg g^{-1} per roentgen based on the value of 34 ev recommended by the ICRU as the energy expended by the ionizing radiation per ion pair formed. The absorbed dose DC in carbon is calculated from Burrus' data[3] by the following relationship:

$$DC = Da \frac{(m \mu_{en})_{carbon}}{(m \mu_{en})_{air}} \qquad (19)$$

where Da is the absorbed dose in air, and $m \mu_{en}$ is the mass energy-absorption coefficient $cm^2 g^{-1}$.

Figure 6 shows a plot of the absorbed dose in carbon per roentgen as a function of photon energy as calculated with Eq. (19). (The value for W in the figure is from a National Bureau of Standards publication.[6]) The range of photon energies of interest in radiation-effects studies is from 0.3 mev to 3.0 mev. A statistical analysis of values calculated by Eq. (19) in this range gives 87.6 ± 0.15 erg g^{-1}. This value includes the photoelectric contribution to dose in addition to the Compton contribution. As long as the energy expended by ionizing radiation per ion pair formed in air is not defined more precisely than "probably between 33 and 35 ev," the use of 34 ev (as is currently recommended) introduces an uncertainty of ± 3%, which, when applied to 87.6, amounts to ± 2.6. It is seen that the standard deviation is insignificant by comparison.

The use of the same value of 87.7 erg g^{-1} r^{-1} for the energy absorbed in both carbon and air is convenient and is within the above calculated error. Therefore, in this report the value of 87.7 erg g^{-1} is used for the energy absorbed by carbon per roentgen of gamma radiation.

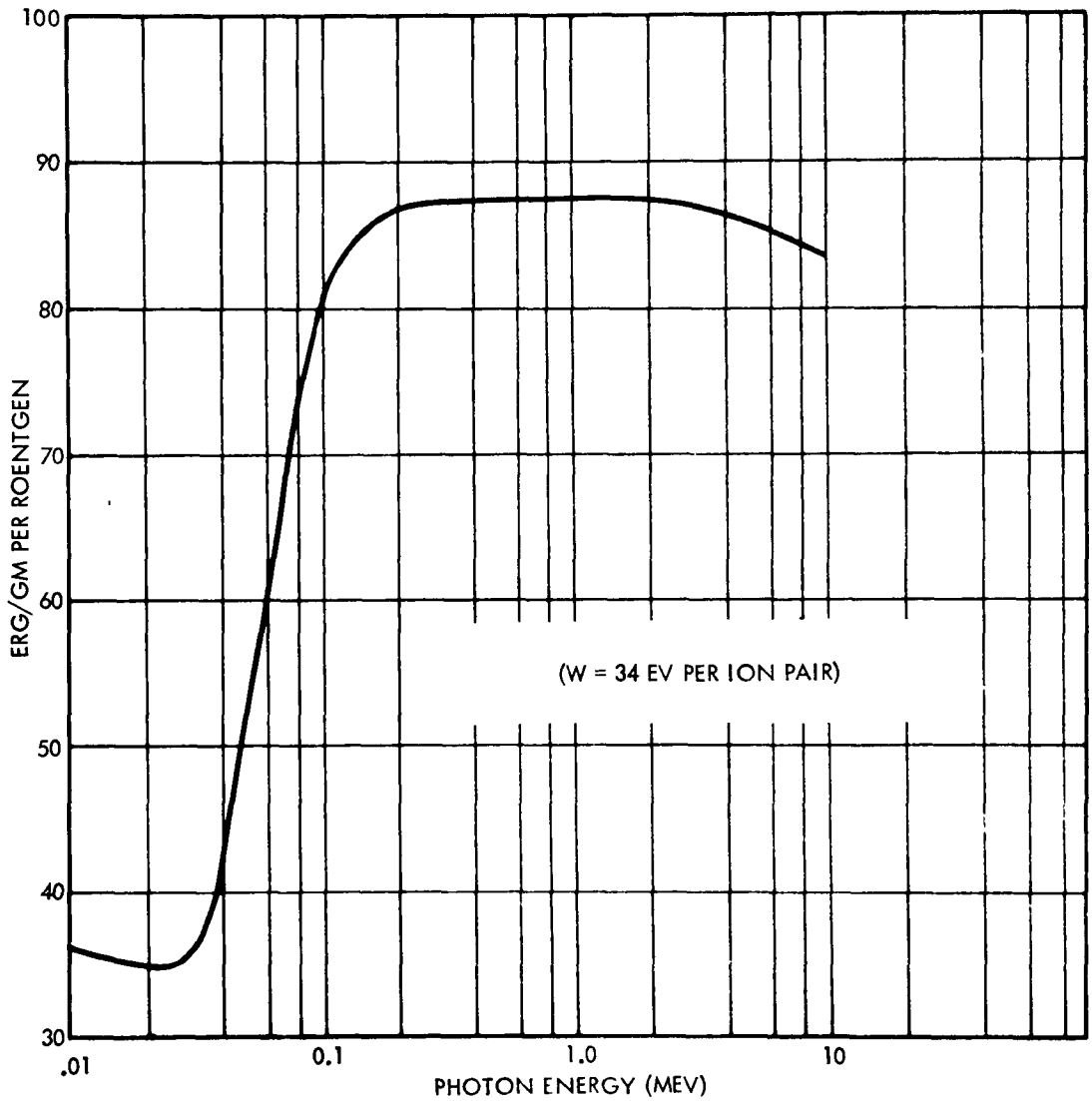

Fig. 6 Energy Absorption in Carbon

REFERENCES

1. Burrus, W.R., "How to Systematize the Correlation of Radiation Damage Data," presented at the Second Semiannual 125-A Radiation Effects Symposium, Battelle Memorial Institute, Columbus, O., October 22-23, 1957.

2. Lockheed Aircraft Corporation, Georgia Division, Gamma Removal Dose Calculations, by W.R. Burrus, NR-32, Marietta, Ga., July 1958.

3. Lockheed Aircraft Corporation, Georgia Division, Epi-Thermal Dose and Atomic Production Calculations, by W.R. Burrus, NR-40, Marietta, Ga., July 1958.

4. National Bureau of Standards, X-Ray Attenuation Coefficients From 10 Kev to 100 Mev, by Gladys White, NBS Report 1003, Washington, D.C., 1952 (unpublished).

5. Wright Air Development Center, Standard Instrumentation Techniques for Nuclear Environmental Testing, by W.R. Burrus, WADC Technical Note 57-207, ASTIA No. AD 142-179, Wright-Patterson Air Force Base, O., May 1957, p. 13.

6. National Bureau of Standards, Report of the International Commission on Radiological Units and Measurements (ICRU), 1956, NBS Handbook 62, Washington, D.C., April 10, 1957, p. 16.

THE DETERMINATION OF NUCLEAR PARAMETERS FOR EXPERIMENTAL RADIATION EFFECTS

by

G. A. Wheeler

Convair
A Division of General Dynamics Corporation
Fort Worth, Texas

Necessity for knowledge of radiation field is discussed. Current dosimetry techniques in use at Convair are presented together with the differences between present "state-of-the-art" and desired measurements. The magnitude of and difficulties encountered in Convair's mapping of the GTR field are detailed.

INTRODUCTION

In our field almost every plot made has some radiation parameter listed along one axis. Yet, frequently, much less thought is given to the determination of the radiation field than is given to the parameter on which the effects of radiation are being measured. One of the crosses we have to bear is that we must not only determine the effects of radiation but also develop methods for measuring the radiation field itself.

It is obviously important to obtain some measure of the total radiation to which a specimen is exposed. Just what this total measurement should be is not so obvious. Should it be the energy that would be absorbed from the field by air, tissue, carbon, or the material in question? Perhaps it should be the total number of particles or photons incident upon the specimen. It might be that only the particles or photons above a certain energy are important. Most likely it is all of these things at one time or another.

In any one particular radiation field it is not too important which of these measurements is used. When data from several sources are to be compiled, however, it is very important. What is taken for variation in material response may very well be variation in radiation parameters.

Until it is definitely ascertained which parameter is important for which property of which material, the best measurement is the number spectrum of both the gamma and

neutron fields. Present "state-of-the-art" in dosimetry does not provide this information.

CURRENT DOSIMETRY

Measurements of gamma fields at Convair are made with phosphate glass, chemical dosimeters, and ion chambers. Measurements of neutron fields are made with foils, tablets, solutions, BF_3 counters, and fast neutron dosimeters. The materials measure integrated field; the electronic detectors measure dose and neutron density.

Phosphate glass is used in pure gamma fields. This material is very sensitive to neutrons. Not only do the neutrons increase the darkening of the glass, they also produce a different glass color than do gammas.

The chemical dosimeters are the chlorinated hydrocarbon type developed by Taplin-Sigoloff[1] and modified by W. R. McIntosh of Convair. These dosimeters consist of 0.8 milliliters of carbon tetrachloride overlaid with 0.3 milliliters of water. They do not have a significant neutron sensitivity. This allows a direct determination of the gamma field. The dosimeters are wrapped with 0.010 inches of lead to reduce their low energy sensitivity. With this lead wrapping their response is very nearly that of tissue, and they have a useful range of 10^3 to 10^8R. They are irradiated in two-dosimeter packets which have a precision of $\pm$ 5 to 6% at the 95% confidence level. The values are accurate to $\pm$ 25% at the 95% confidence level. This accuracy will be considerably improved with primary Co^{60} standards and further calibration.

Two sizes of ion chambers are used to measure the gamma component of the reactor field: 50-cc, and 4-cc. The 50-cc ion chamber has a range of from 1 mr/hr to 5×10^4 R/hr. The 4-cc ion chamber has a range of from 10^3 R/hr to 5×10^5 R/hr. This chamber requires 7×10^8 N_f/cm^2-sec to give a 1% contribution to a 10^8 erg/gm(C)-hr gamma field.

Foils of gold, cobalt, indium, copper, aluminum, and nickle are used. These foils measure one centimeter square and are of various thicknesses from one-half to five mils. More than one nuclear reaction is measured by several of the foils.

Tablets of pure sulfur and a sulfur cream-of-tartar mixture are used to measure neutron fluxes greater than 2.9 Mev. The pure sulfur tablets were obtained from John Moteff of General Electric Company. These tablets have the advantages

of water insolubility and no interfering activity due to impurities. Their chief disadvantages are their brittleness and tendency to dust. A spray coating of acrylic resin reduces the disadvantages.

The sulfur cream-of-tartar tablets are a trade name patent medicine marketed by a local drug company. These tablets are about 18% sulfur. The remainder is potassium acid tartrate. The interfering half-lives disappear in two to four days leaving only 15-day phosphorus 32. There has been little dusting or chipping. These tablets however are water soluble and will deteriorate in a high humidity atmosphere.

Solution detectors are prepared from known concentrations of chemically pure salts. Generally, chlorides, nitrates, and sulfates are used.

The BF_3's and FND's are of conventional design.

Present technology does not enable a complete analysis of the reactor field. Neutron and gamma spectra cannot be measured directly with the reactor at any practical power. Gamma spectra can be recorded with either scintillation or magnetic spectrometers. However, they cannot be used in the high reactor flux field because so much shielding is required. The gamma spectrum above 0.5 Mev has been calculated by the moments method[2]. The dose rate computed from this spectrum agrees well with the measured dose rates. This is the best gamma information that can be obtained at present.

Neutron measurements are in considerably better shape. Activation of various isotopes allow measurement of the neutron flux at several energies in the spectrum[3]. Threshold detectors are used in the fast region, ie., greater than 1 Mev; resonance detectors are used in the 1/E region; and 1/V detectors are used in the thermal region. The shape of the neutron spectrum can also be calculated[4]. When this shape is normalized to the experimental values a fairly reliable picture of the neutron field is obtained. This procedure is cumbersome to use and makes changes in the neutron field with location, shielding, specimen placement, etc., difficult to investigate.

MAPPING THE GTR FIELD

Irradiations previous to September 1957 were performed at ambient temperature in boral-covered boxes. These boxes were hung from the reactor frame with the face of the box against the frame. From September 1957 thru August 1958, irradiations were performed in boxes placed on movable platforms

near the reactor. The thickness of water between the reactor frame and the face of the boxes could be varied from 0 to 12 inches. The ambient boxes and new boral-covered, temperature- controlled boxes were used on these platforms. Since August 1958, a dry-pool shuttle system has been used. This system is discussed in another paper at this meeting.

It was desirable to determine the field within these irradiation volumes for several reasons. This knowledge would allow the experimenters to predict the fluxes to which their materials would be exposed. By placing samples on isodose lines each of a series of samples would receive the same exposure. Also, few measurements of the field would be required during each irradiation since most samples only slightly perturb the field. It is always important, however, to make some measurements during each run to insure against errors in placement and reactor power level.

The fast neutron and hard gamma fluxes were calculated at 288 points in the wet pool system and 60 points in the dry pool system. These computations were reduced to isodose maps and used until experimentally determined flux information was available.

Wet Pool Chambers

The irradiation chambers were mapped in each of their positions with sulfur tablets, gold foils, and a combination of phosphate glass and chemical dosimeters. All gamma measurements previous to this mapping were made with phosphate glass. A cross calibration between phosphate glass and chemical dosimeters was attempted so that past measurements could be correlated with the maps. Close to reactor the field drops off rapidly. Therefore, it is essential to know the flux map at the front, center, and back of the box. Each box was mapped in its position closest to and farthest from the reactor as well as midway between these two positions. It was decided that the flux should be measured at a minimum of seventeen points on each rack.

More extensive investigations of the neutron spectrum were carried out in separate runs. Packets containing foils and/or solutions of eleven elements were irradiated on the centerline of the middle racks of each box.

The above program required 35 runs of 2 hours each at a reactor power of 100 kw. These runs were spaced over a 6-week period to reduce the load on tne counting room facilities. For the neutron mapping portion, a total of 1224 sulfur tablets and 1224 gold foils were activated. The gamma mapping required 840 chemical dosimeter packets and 448 pieces of phosphate glass. The neutron spectrum work required 12 packets containing 6 solutions and 12 foils each.

To obtain proper statistics, about 10 minutes counting time was required for each activated detector. Repeat counts were made on the foils after each half-life until three counts agreed within 5%. On the average four separate counts were required per detector. The total counting time was about 2000 counter hours. The detectors were counted on end-window, 2π, or 4π counters, depending upon their activity and form.

The measured neutron field agreed within 30% with the calculated field. The measured gamma field agreed within 20% with the calculated field. These results lend considerable credence to the calculation method.

Phosphate glass proved to be highly unsatisfactory as a gamma detector in the reactor field. The percent light transmittance at various wavelengths is used to read out the glass. It was found that there was a color change in the glass. This resulted in a different dose reading at each wavelength. In fact the dose read with 500 mμ-light was frequently a factor of two higher than the dose read with 650 mμ-light. The average of the dose read at 5 wavelengths was used as the "true" value. This value differed from the dose measured by chemical dosimeters. The difference was dependent upon the water distance from the reactor. At 4 inches from the reactor face, the phosphate glass read high by a factor of 2.3. At 18 inches from the reactor, it was high by a factor of 1.1. The n/γ ratio in the former case was 2.1×10^{-2} and in the latter case was 1.5×10^{-3} on a particle basis. These effects can perhaps be calibrated but this seems unnecessary at present. We have discontinued the use of phosphate glass in the reactor fields.

Shuttle System

The mapping of the shuttle system was somewhat simpler than the boxes. The reactor had a constant shield configuration. Only the flux field variation in air had to be determined. The fact that the reactor now had 3-Mev capability did raise some new problems, however. One of these problems was that in extended runs the detectors would become excessively activated. Cobalt was used to determine the thermal and epithermal fluxes rather than gold. This lowered the detector activity and extended the time which could be allowed between irradiation and the counting of the foils.

The second problem of the new reactor was that rod shadowing might change the flux distribution. The reactivity of the GTR decreases 3% during a 20-hour run at 3 Mw. This necessitates the removal of three of the four shim rods. Different rod positions result in flux profile changes in the test volumes. This change was in the order of 8% for the 500 kw GTR. It is anticipated it will be higher for the 3 Mw GTR.

The volume above each of the three shuttles was mapped. Three planes parallel to the reactor face were mapped on each shuttle. Again, the field at 17 points in each plane was measured with a packet of detectors. This packet contained a pair of chemical dosimeters, a sulfur tablet, cadmium covered gold, bare gold, a cadmium covered cobalt foil, and a bare cobalt foil. The detectors were separated the minimum distance which would prevent interactions. Three hundred and six packets were exposed in six reactor runs. The runs were for 3 hours at 500 kw.

Three runs were made with the core reactivity normal. These runs were replicates and were necessary to give proper statistical confidence in the results. For the other three runs the reactor core was uniformly poisoned. These runs were also replicates. It was necessary to remove three shim rods in order to operate the poisoned core. The radiation field information obtained from these runs will allow us to assess the effect of rod shadowing on the flux profile.

In addition to mapping the volumes, the absolute neutron spectrum was investigated, and the use of wire for neutron measurements was explored. Sulfur, cobalt, silver, manganese phosphorous, aluminum, and magnesium were used in the spectrum work. These detectors give information in several neutron energy ranges. The mapping and spectrum work required 2844 detectors. This required about 1750 hours of counter time.

To map more thoroughly and to develop more efficient methods of mapping, several lengths of wire were activated. The wire was a cobalt-aluminum alloy consisting of 1% cobalt and 99% aluminum. It was exposed in the planes parallel to the reactor on which the detector packets were located. It was also exposed in planes perpendicular to the reactor face. It was hoped that at least relative neutron fluxes could be obtained from the wire. Perhaps absolute values can be obtained by relating the wire activity to the activity of the packet detectors. A counter was designed and built for scanning the wire. This consists of a shielded sodium iodide crystal with a hole drilled radially through its center. Wire is fed through the crystal and shield by two pairs of rubber-rimmed wheels. The multiplier phototube and electronics are of conventional design.

To simplify the reduction of detector data a computer program has been developed. The foil identification and its location during exposure are punched on tape. After exposure, the run number, the time at start and end of irradiation, and the reactor power level are punched on another tape with the foil identification. As the foils are counted, the time at which the count was started, the duration of the counting

time, and the total number of counts accumulated during that time are punched on a third tape along with the foil identification. The background for each counter is determined regularly. This number is also automatically punched for each count. The efficiency of each counter for each type of detector is recorded on magnetic tape for use in the computer. The foil identification includes a number which will call the proper efficiency out of the machine memory.

The three punched tapes form the input data to the computer program. The output is the saturated activity of the foil, the saturated activity per watt of power level, and the particular flux or fluxes which can be computed from the detectors used. Cadmium ratios are computed and the thermal flux determined. For elements with two radioactive isotopes, the saturated activity of each is computed. The average machine time required for these computations is one second per detector. The results are printed out in any desired order by location number. Very little sorting of the final results is required.

Various attempts have been made to use electronic detectors to measure the GTR field in the irradiation volumes. With a few notable exceptions, these attempts have not been successful. Most of the instruments are sensitive to radiation of a type other than the type they are intended to measure. They generally measure a much lower field than that used in radiation effects work.

The neutron and gamma fields in the boral-covered boxes were measured with BF_3 counters, FND's and ion chambers. To avoid saturating these instruments a power level less than 5 watts must be used. A new core was used so that the gamma background would not interfere with the measurements. Data were obtained but when extrapolated to 100 kw they did not agree with the values measured with the nonelectronic detectors.

The 3-Mw GTR cannot be operated satisfactorily below a power of 20 watts. This prohibits the use of many of the electronic detectors since the field is too high to measure, or the interfering types of radiation are too high. The field on the shuttles was measured with a thermopile, a 50-cc ion chamber, and a 4-cc ion chamber. A traversing mechanism which allowed vertical and longitudinal movement of the detectors was built.

Readings were taken at 5 power levels between 25 watts and 100 kw by fixed detectors on two sides of the reactor and by the traversing detectors on the third side. From these data any changes in the reactor field with power level can be detected.

CONCLUSION

The investigations discussed are considered only the first step in determining the reactor field. It may be that changes in rod position, power level, core age, fission product buildup, etc., will cause changes in the field. Both the flux profile and the energy distribution of the field could be affected. Until these investigations are completed several detectors will be irradiated in each run in order to relate the actual exposure of the samples to the more extensive field determinations.

REFERENCES

1. S. J. Sigoloff, "Fast Neutron Insensitive Chemical Gamma Ray Dosimeter," Nucleonics Vol. 14 (1956).

2. R. L. French, Reactor Shield Penetrations, Convair-Fort Worth Report FZM-913 (13 May 1957).

3. W. E. Dungan, Neutron Spectrum Measurements With Radioactivants, Convair-Fort Worth Report MR-N-177, NARF-57-57T (30 December 1957).

4. J. Romanko, The Neutron Spectrum of the GTR, Convair-Fort Worth Report MR-N-148, NARF-57-2T (30 January 1957).

CALORIMETRIC DOSIMETRY PROGRAM AT LOCKHEED*

by

Roger L. Gamble
Lockheed Nuclear Products
Lockheed Aircraft Corporation
Georgia Division, Marietta, Georgia

To measure energy deposition in organic materials, low cost calorimetric radmeters of both the adiabatic and steady state types have been designed. The ranges of these instruments are from 5×10^4 rads per hour to 10^7 rads per hour.

Consideration of the nature of the aircraft subsystems irradiation tests to be conducted at Air Force Plant No. 67 indicated that placement of organic radmeters throughout the irradiation volume would yield significant information for dose-damage correlation. Since radiation damage can perhaps be compared more practically on the basis of rads in a standard organic material than on the basis of rads in the materials in question, it was decided that all organic radmeters would be made of the same organic material.

Calorimetric radmeters are desirable in this application because they are essentially absolute. The decision was made to make these radmeters of polystyrene for the following reasons:

1. Polystyrene has high radiation resistance.

2. It has a low cross-section for endothermic chemical reactions. (More than 95% of the energy absorbed goes into heating the material.)

3. Foamed polystyrene is available commercially.

4. The thermal properties of the material are known.

As a first step in studying a type of calorimetric radmeter, the simple configuration shown in Figure 1 was tested. This configuration consisted of a right circular cylinder of solid polystyrene two inches in diameter and one inch thick, placed inside a 10-inch cube of styrofoam. The temperature of the cylinder was measured with a General Electric D-204 thermistor in a bridge circuit with a galvanometer. Radiation heating was simulated by passing electric currents through resistance-wire heaters in the cylinder and in

* Protection on certain features discussed herein is being sought through appropriate patent applications.

the cube, and the currents were calculated to give equal temperature rise rates in the cylinder and in the cube. A major advantage in this arrangement was that radiation could pass through the styrofoam with practically no attenuation and heat the cylinder inside. Actually, the object of this test was to see how long the heated styrofoam would effectively insulate the cylinder and maintain a linear heating curve for the cylinder. As shown in Figure 2, the linearity of heating lasted approximately as long as the "time constant" of a solid cube of styrofoam. This time constant is the reciprocal of the constant in the exponent of e in the first Fourier term in the solution of the temperature equation.

The second step in this investigation was to surround the cube of styrofoam with a so-called adiabatic wall to eliminate heat leakage. This wall consisted of six rectangles of thin styrofoam with heating grids a half-inch from their outer surfaces. Calculations of grid current necessary to eliminate heat leakage were performed in advance and adjusted every quarter-hour for nine hours. Currents in the cube and in the cylinder were held constant at values calculated to produce a temperature rise of 3° per hour. The resulting heat curve was linear for the 9-hour test.

As a third step, the grid heaters in the adiabatic wall were replaced by a continuous aluminum foil wall 0.0005 inch thick and 1-1/8 inch wide backed with waxed paper to provide electrical insulation and mechanical strength. On each face of the adiabatic wall were seven foil windings, and a spacing of 1/32 inch was maintained between the windings with numerous small patches of Scotch Tape. The entire wall was surrounded by a cubical shell of styrofoam two inches thick. The temperature of the adiabatic wall could be kept equal to that of the cylinder at all times to eliminate heat leakage. A resistance thermometer in a simple Wheatstone bridge was used to measure the temperature of the cylinder. The difference between the temperature of the cylinder and that of the adiabatic wall was detected by means of a second resistance thermometer cemented to the wall and included in the same Wheatstone bridge with the first thermometer.

One-half of the polystyrene cylinder was milled slightly to accommodate the thermometer, and the two halves were cemented together with polystyrene coil dope. The foil was folded and bent back at the end of each turn in such a manner that the area of the foil was equal to the surface of the cube, except for the 1/32-inch spacing between the turns. Furthermore, this manner of folding made use of the electrical insulating quality of the waxed paper backing so that no part of the foil was short-circuited. This calorimeter is shown in Figure 3. Current for the adiabatic wall was supplied by an ordinary 6.3-volt filament transformer, and the primary voltage of the filament transformer was adjusted by means of a Powerstat. The bridge circuits are shown in Figure 4. The cylinder bridge was calibrated to read temperature directly with a scale factor of 0.1° C per Helipot division. The temperature difference detector bridge had a sensitivity of 0.006° C per millimeter on the galvanometer scale. The dose D in rads is given in terms of the temperature rise (ΔT)° C, as follows:

$$D = 4.18\ C\ (\Delta T) \times 10^5 \text{ rads.} \qquad (1)$$

C = 0.32 cal/gm/deg C is the specific heat of polystyrene.

This radmeter performed satisfactorily in a cobalt-60 gamma-ray field of 4.86×10^4 rads per hour, in which ΔT was 4° C in 11 hours. During the irradiation, the temperature rise was linear in time; after the cobalt-60 source was removed, the temperature remained stationary.

The adiabatic radmeter would require either constant manual adjustment or elaborate automatic control of the wall temperature. In the systems test to be performed at Air Force Plant No. 67, it would not be practical to operate a large number of radmeters of this type. Instead, a steady state radmeter has been designed to fulfill requirements at this plant. The construction of this simple instrument is shown in Figure 5. The two resistance thermometers are in a bridge circuit, as shown in Figure 6. The recorded voltage is proportional to the temperature difference between these thermometers. Because of symmetry, no heat flows across the interface between the two halves of the 8-inch cube.

THEORY OF THE STEADY-STATE RADMETER

It can be shown that if the parallelepiped of Figure 7 has a constant uniform heat source density G and a constant uniform thermal conductivity K and if the surface temperature is kept at 0° of temperature, then the steady-state temperature T_∞ along the line through the center of the parallelepiped parallel to the x-axis is given by

$$T_\infty = F \sum_{q=0}^{\infty} \sum_{p=0}^{\infty} \frac{(-1)^q \left[\sinh \frac{A_{qp}c}{2}\right]\left[\cosh \frac{A_{qp}c}{2} - 1\right]\left[\sin \frac{(2p+1)\pi x}{a}\right]}{(A_{qp})^2\ (2p+1)(2q+1) \sinh\ (A_{qp}c)} \qquad (2)$$

$$\text{where } F = \frac{32\, a^2 b^2\, G}{\pi^2 K} \qquad (3)$$

$$\text{and } A = \frac{\pi}{ab}\left[(2q+1)^2 a^2 + (2p+1)^2 b^2\right]^{1/2} \qquad (4)$$

It is interesting to compare this with the temperature T_s in a sphere of radius R under the same conditions. T_s at radius r is given by

$$T_s(r) = \frac{G}{6K}\left(R^2 - r^2\right) \qquad (5)$$

For comparison, let the parallelepiped be the 8-inch cube of Figure 5; but, for simplicity, let 8 inches be the unit of length. Then a = b = c = 1. The volume of the cube is also 1 unit ^{3}. Now compare a sphere of equal volume. Its radius is

$$R = \left[\frac{3}{4\pi}\right]^{1/3} \tag{6}$$

Let T_{oo} be the term in equation (2) with q = p = o.

$$T_{oo} = \frac{32G}{\pi^2 K} \frac{\sinh (A_{oo}/2 \sin (\pi x) \left[\cosh (A_{oo}/2)-1\right]}{A_{oo}^2 \sinh A_{oo}} \tag{7}$$

$$\text{where } A_{oo} = \pi\sqrt{2}. \tag{8}$$

ΔT_{oo}, the first term in the temperature difference of the resistance thermometers in Figure 5 is given by

$$\Delta T_{oo} = T_{oo} (1/2) - T_{oo} (1/8) \tag{9}$$

$$\Delta T_{oo} = 0.0398 \quad G/K. \tag{10}$$

Δ Ts, the temperature difference between the center of the sphere of unit volume and points 1/8 unit from the surface is

$$\Delta Ts = Ts (o) - Ts (R-1/8) \tag{11}$$

$$\Delta Ts = 0.0408 \quad G/K . \tag{12}$$

Practically, the T_{oo} term is about all that is needed; so for design purposes, the temperature difference between the thermometers can be calculated as if they were inside a sphere of a volume equal to that of the cube and the outer thermometer at the same depth as in the cube. Of course, a spherical radmeter could be used; but cutting spherical sectors presents some difficulties. Spherical sectors would have to be used to keep heat flow parallel to the interfaces.

The following factors can prevent the steady state radmeter from reaching a true steady state in operation:

1. Fluctuations in reactor power

2. Buildup of fission products and environmental radioactivity

3. Fluctuations in ambient temperature

To evaluate power fluctuations, consider a square-wave reactor power cycle; that is, one in which the power is a constant P_c during a time interval Δt and zero at all other times. Figure 8 shows how the calculated temperature difference ΔT between the thermometers in the radmeter of Figure 5 behaves in time, with the surface temperature constant. ΔT_∞ is the steady state value of ΔT corresponding to P_c, with $\Delta t = \infty$. The dose rate R in rads per second at P_c is given by

$$R = 4.18 \times 10^5 \quad G/\rho \quad \text{rads/sec.} \tag{13}$$

where G is in calories per unit^3 per second, and ρ is the density of styrofoam in grams per unit^3.

The dose D in rads absorbed during Δt seconds is

$$D = 4.18 \times 10^5 \quad G \ \Delta t/\rho \text{ rads.} \tag{14}$$

From equation (2)

$$G = B \ \Delta T_\infty \tag{15}$$

Where B is a complicated constant. Therefore

$$D = 4.18 \times 10^5 \ B\Delta T_\infty \Delta t/\rho \, . \tag{16}$$

It can be shown that

$$\Delta T_\infty \Delta t = \int_o^\infty \Delta T dt \tag{17}$$

where ΔT is the temperature difference between the inside and outside thermometers at any time. Physically, this means that the rectangular area $\Delta T_\infty \Delta t$, which appears in equation (16), is equal to the area under the solid curve in Figure 8. In the case of an arbitrarily varying power cycle, the cycle can be considered as a superposition of an infinite number of square wave power cycles. Then, because of the linearity of the system, it can be seen that

$$D = 4.18 \times 10^5 \quad \frac{B}{\rho} \int_o^\infty \Delta T \ dt \quad \text{rads} \tag{18}$$

This result should be expected on the basis of the conservation of energy. ΔT can be recorded on a strip recorder, and the integral of equation (18) can be evaluated numerically to find the dose absorbed during an arbitrarily varying power cycle. When many such radmeters are operating simultaneously, it is not necessary to record ΔT continuously for each one. It is necessary to record ΔT in only one of them and to normalize the others by measuring ΔT at the same time on the recorded radmeter and on an unrecorded one.

Normally, the ambient temperature will fluctuate during a test. This fluctuation will affect the value of the integral in equation (18); so a correction must be made. The evaluation of this correction can be approached in two ways: a long, formal way and a short, intuitive way. In the formal approach the contribution to the integral in equation (18) from a step function in the ambient temperature is calculated by integrating the transient solution of the temperature equation. Then the correction is evaluated by considering the changing ambient temperature as an infinite superposition of infinitesimal step function. It was found by experiment that the transient temperature following a step in ambient temperature agreed within 5% of the calculated values. It was also shown by experiment that the integral of ΔT for superimposed steps was the sum of the integrals of the individual steps. So much for the formal approach.

The short, intuitive approach is as follows: An increase in ambient temperature causes heat to flow into the radmeter. This effect is opposite to radiation heating, which causes heat to flow out of the radmeter. This means that when the ambient temperature θ_f at the end of a test is greater than that θ_i at the start of the test, equation (18) needs a positive correction added to it to give the real dose. The amount of heat involved per gram when the temperature difference is $(\theta_f - \theta_i)$ is $C\ (\theta_f - \theta_i)$; where C is the specific heat. Therefore the corrected formula for dose is

$$D = 4.18 \times 10^5 \left[\frac{B}{\rho} \int_0^\infty \Delta T \, dt + C\ (\theta_f - \theta_i) \right] \text{ rads.} \qquad (19)$$

An extreme example of the application of this formula is to the adiabatic radmeter. There $\Delta T = 0$; so equation (19) reduces to equation (1). It can be shown that the two approaches to the ambient temperature correction are equivalent. For example, consider a one-dimensional radmeter of length π and unit cross-section.

By the long, formal approach, the correction per degree is

$$4.18 \times 10^5 \ \frac{32K}{\pi^3 \rho} \int_0^\infty \sum_{p=0}^{\infty} \frac{(-1)^p}{2p+1} \ e^{-(2p+1)^2 \frac{K}{\rho C} t} \ dt \text{ rads} \qquad (20)$$

By the short, intuitive approach, it is

$$4.18 \times 10^5 \ C \text{ rads.} \qquad (21)$$

And carrying out the integration shows that (20) and (21) are equal.

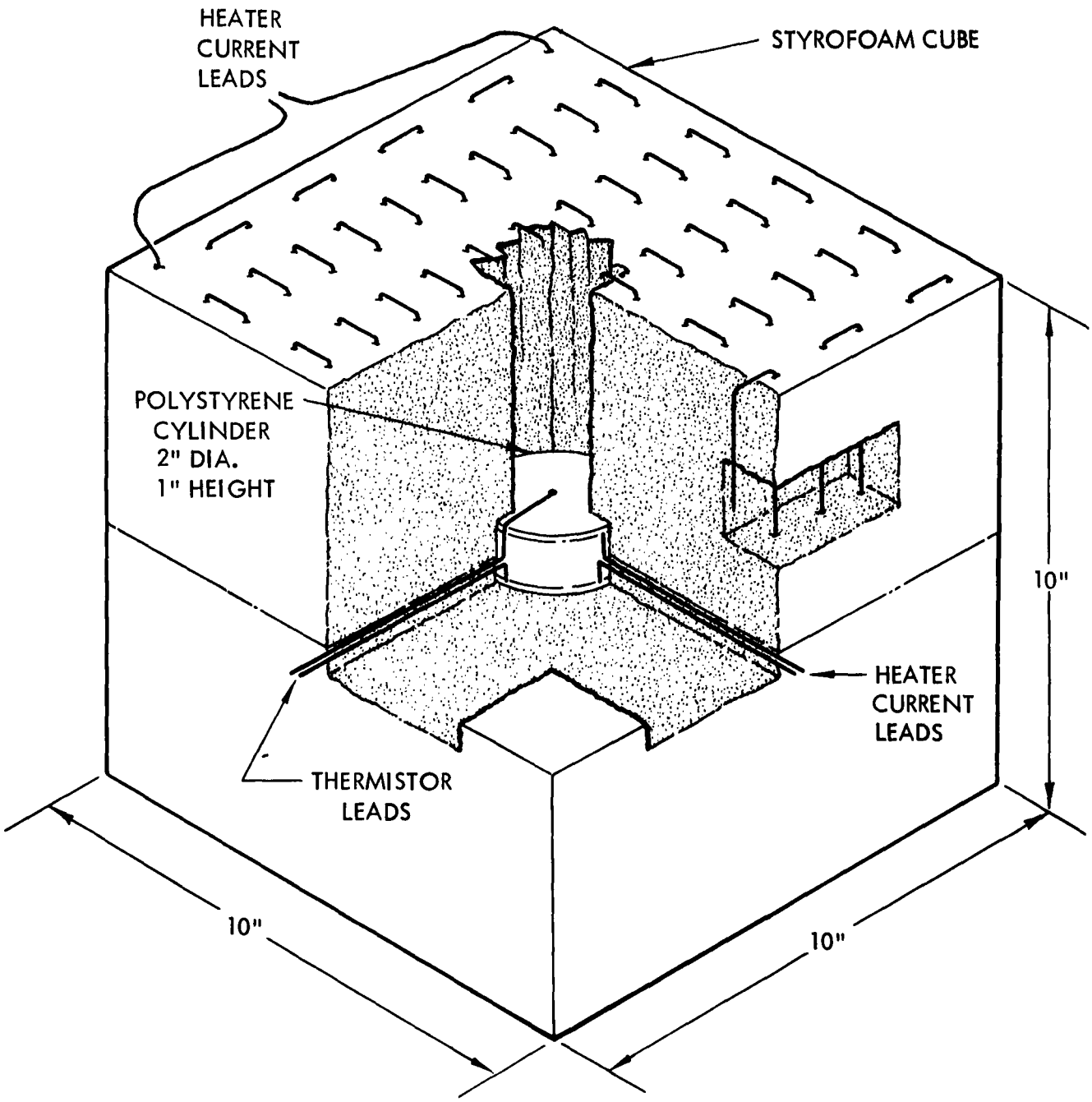

FIGURE 1. CALORIMETER WITHOUT COMPENSATION FOR HEAT LEAKAGE.

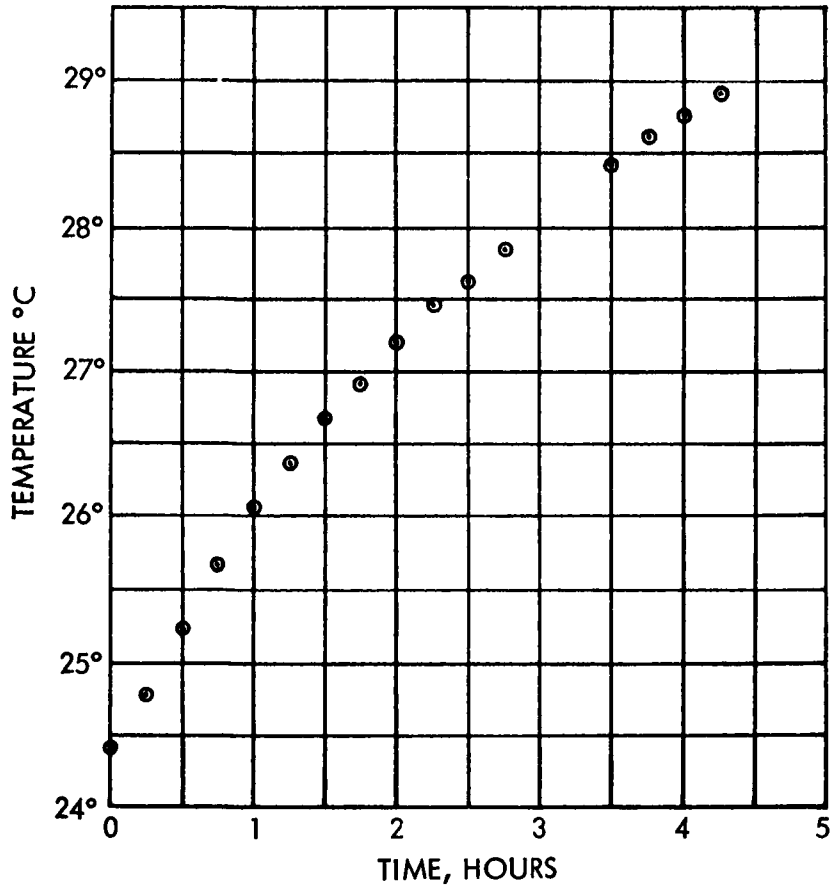

FIGURE 2. TEMPERATURE RISE OF ELECTRICALLY HEATED CALORIMETER WITHOUT COMPENSATION FOR HEAT LEAKAGE.

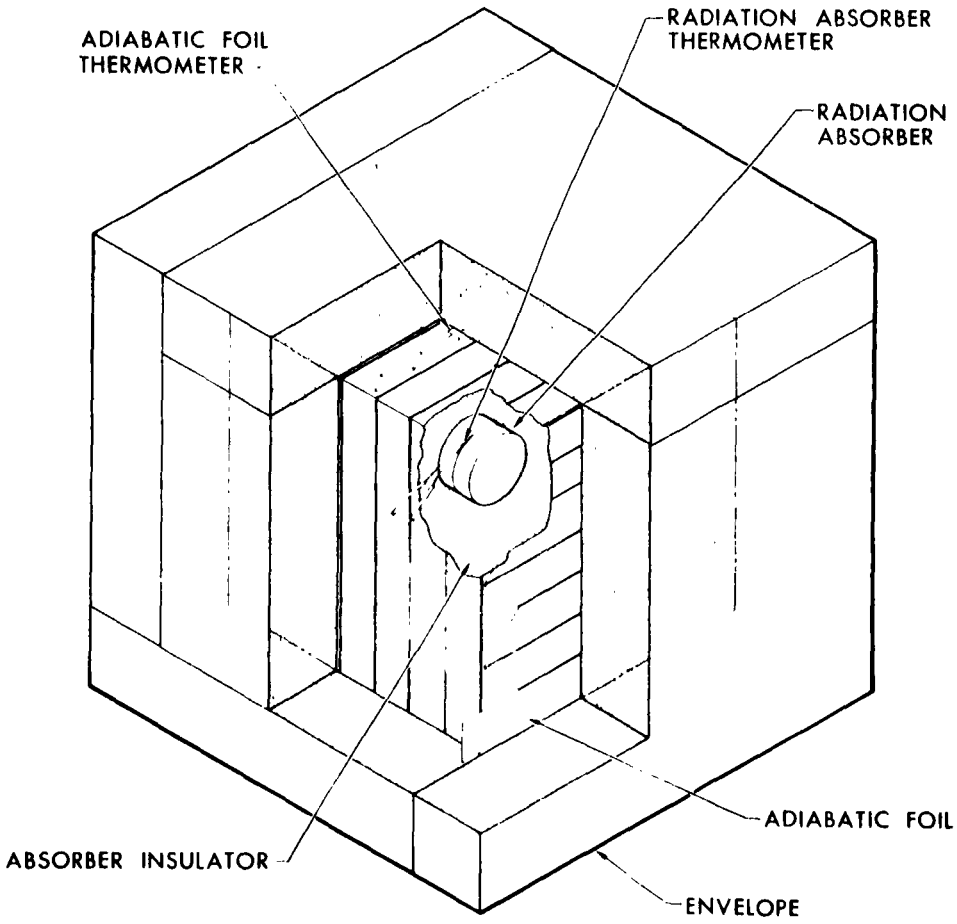

FIGURE 3. ADIABATIC CALORIMETER.

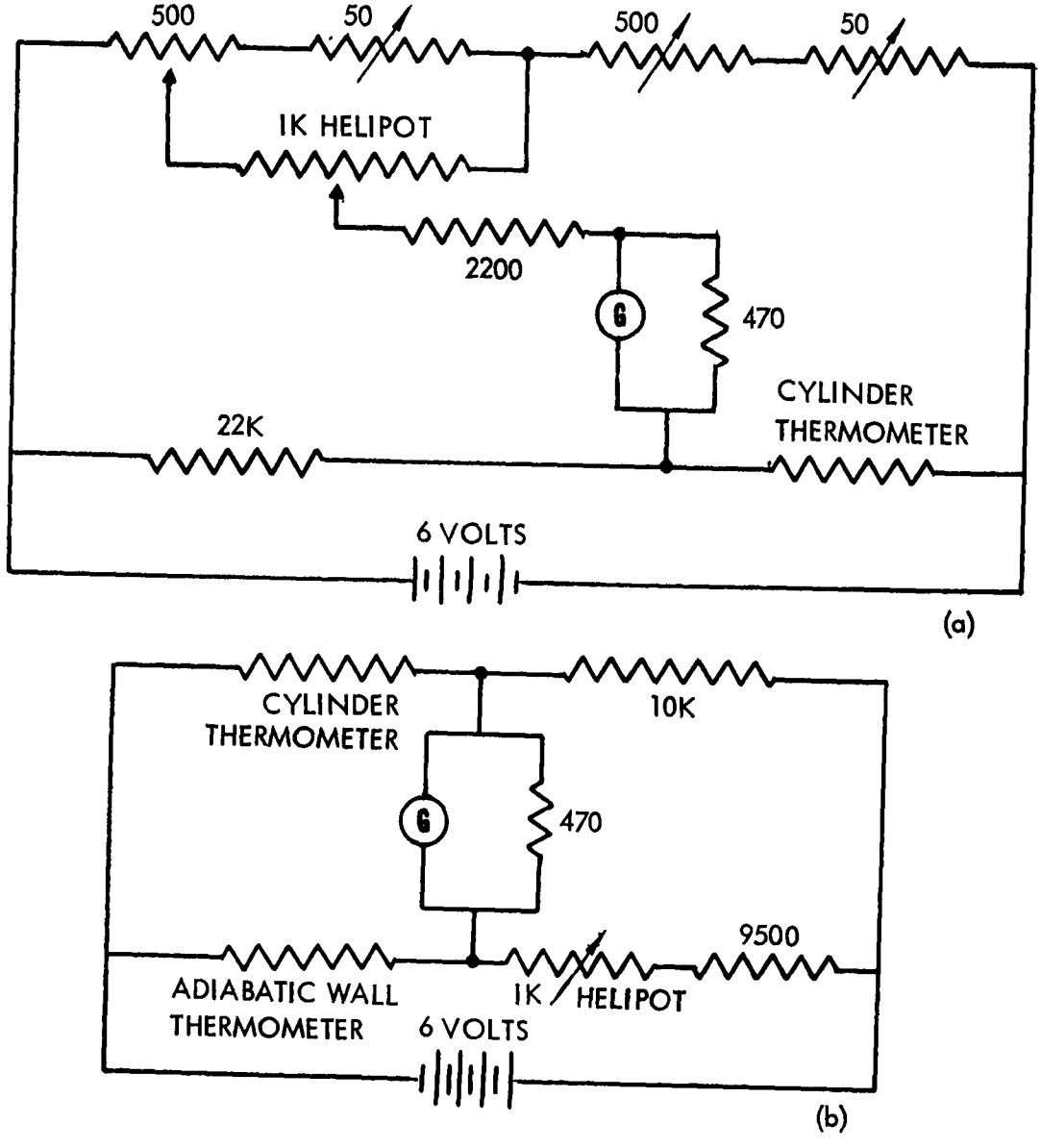

FIGURE 4. (a) BRIDGE FOR TEMPERATURE MEASUREMENT.
(b) BRIDGE FOR TEMPERATURE DIFFERENCE DETECTION.

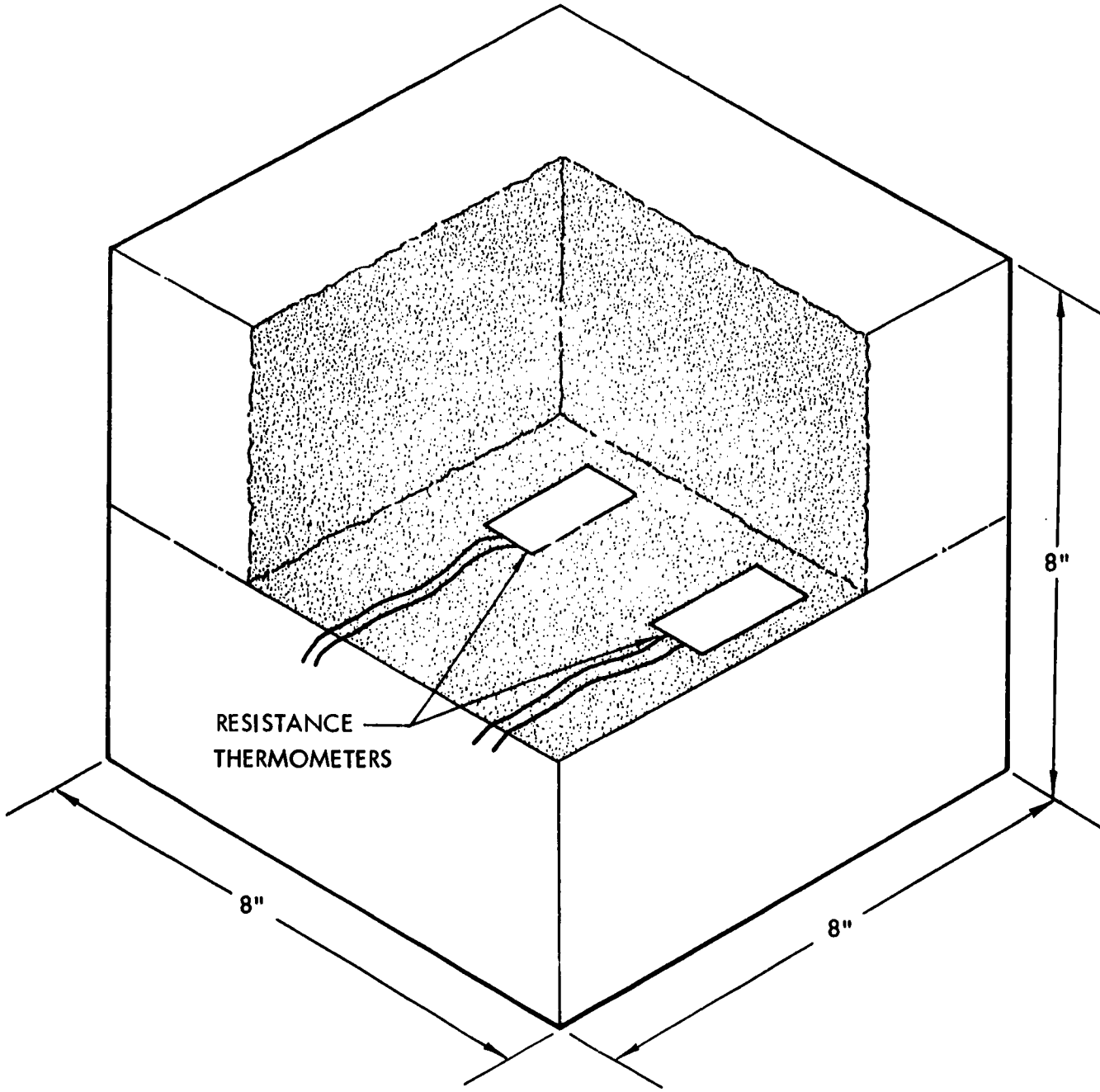

FIGURE 5. STEADY-STATE CALORIMETER

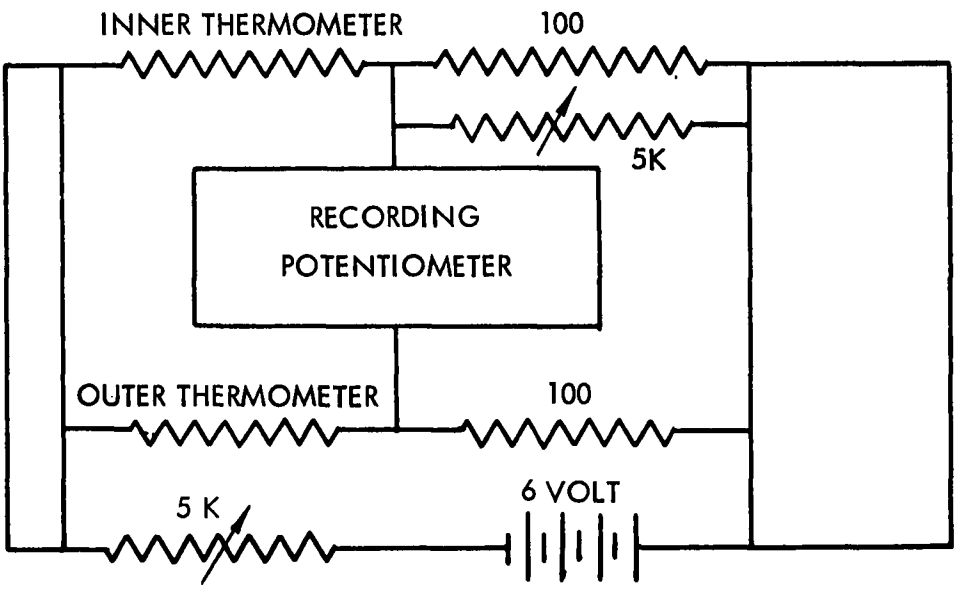

FIGURE 6. BRIDGE CIRCUIT FOR STEADY STATE CALORIMETER.

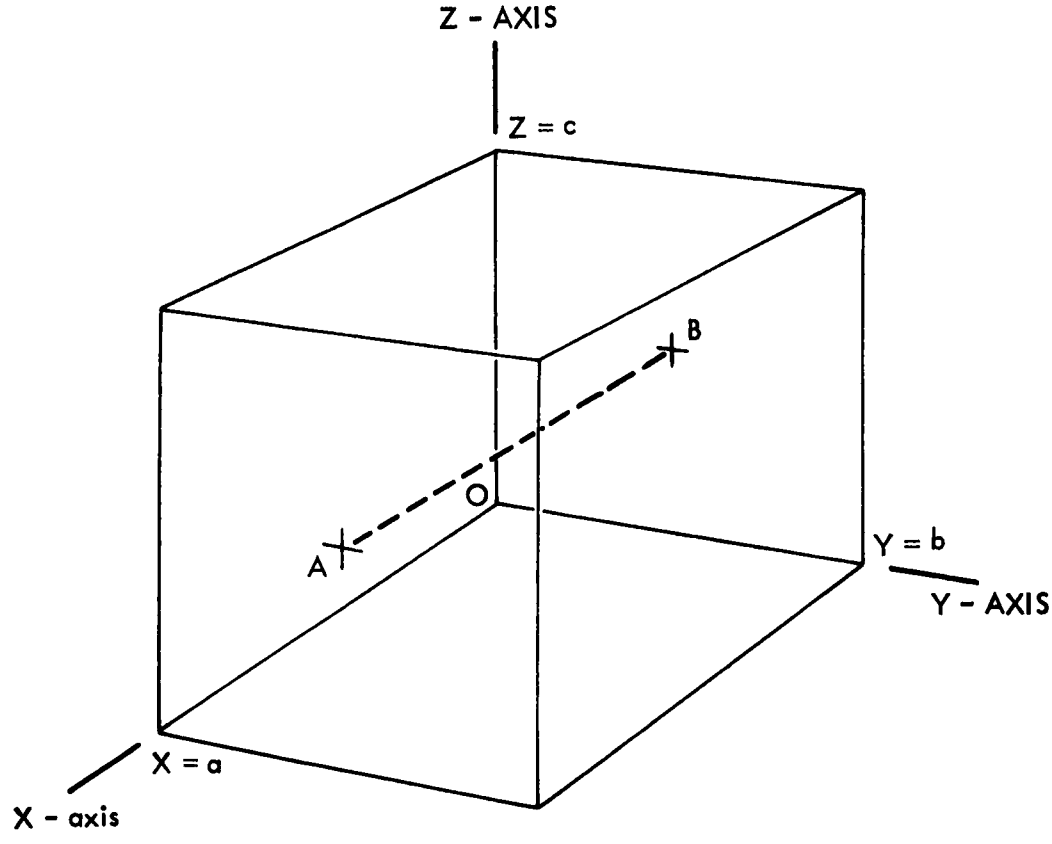

FIGURE 7. RIGHT PARALLELEPIPED WITH HEAT SOURCE DENSITY G AND ZERO SURFACE TEMPERATURE. STEADY STATE TEMPERATURE ON LINE AB IS GIVEN BY EQUATION (2).

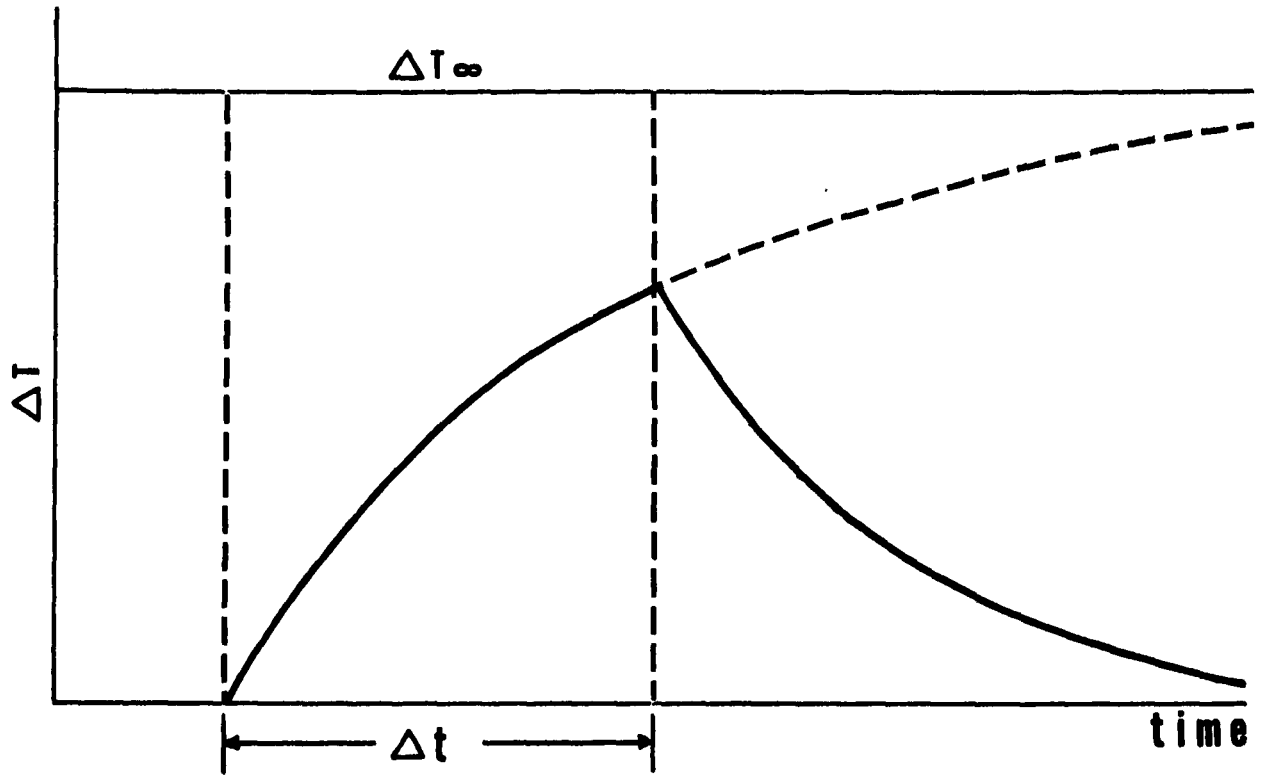

FIGURE 8. VARIATION OF TEMPERATURE DIFFERENCE BETWEEN THERMOMETERS RESULTING FROM CONSTANT HEAT SOURCE DURING Δ t

DOSIMETRY AND ENERGY DISTRIBUTION OF FAST NEUTRONS USING LI I

by

F. D. SCHUPP and S. L. RUBY

Radiation & Nucleonics Laboratory
Materials Engineering Department
Westinghouse Electric Corporation
East Pittsburgh, Pennsylvania

The use of Li^6I(Eu activated) scintillation crystals for neutron spectroscopy in the energy range above one Mev has been investigated. The scintillation spectrometer has moderate resolution, high efficiency, and is useable in an isotropic flux; it presents the absolute number of neutrons as well as spectral distribution. A technique of subtracting gamma-ray background by use of a matched Li^7I(Eu) crystal is given. Pulse height spectra with monoenergetic neutrons from 1.6 to 18 Mev are reported. A preliminary study of the energy spectrum of the fast neutron distribution obtained from a partially unshielded pressurized water type reactor core will be presented.

This paper was not available for publication.

NEUTRON FLUX ENERGY DISTRIBUTION OF THE BNL REACTOR SHIELDING FACILITY[a]

by

Miss M. M. Donnelly and
M. M. Weiss

Bell Telephone Laboratories, Incorporated,
Whippany, New Jersey

A study has been made to determine the neutron flux energy distribution of the BNL reactor shielding facility employed in the semiconductor radiation damage studies by Bell Telephone Laboratories. This facility offers an opportunity for a critical comparison between the mathematical methods available to compute the fast flux and the experimental methods using foil activation techniques. The methods and equipment used and the results obtained are described. The major effort of flux distribution measurement was in the energy range from 0.1 to 10 Mev.

INTRODUCTION

To make effective use of the available nuclear data for semiconductor radiation damage studies an accurate knowledge of the high energy neutron spectrum at places of interest in the radiation facility is necessary. The radiation damage experiments performed by BTL to date were conducted in the tank shielding facility of the Brookhaven reactor. This is a water tank above the northeast section of the reactor. A natural uranium converter plate is located approximately 24" below the water tank to provide a high energy neutron flux. The source plate is covered on top and sides with a 1/4" boral sheet. A removable boral sheet is located at a distance approximately 12" below the

[a]This work has been supported by the Air Force through Wright Field Air Development Center, Contract AF33(600)-32662

natural uranium plate. This essentially cuts the supply of thermal neutrons to the source plate and, when desired, the thermal and epi thermal neutrons from the source plate to the water tank (fig. 1). The 3 inch layer of lead and bismuth shown in fig. 1 reduces the gamma flux emitted from the reactor. The water tank is an aluminum structure 48" square at the bottom and in four steps (each one foot apart) becomes a 62" square. The total height is 12 ft.

CALCULATION OF FLUX DISTRIBUTION

To calculate the fast flux it was desired to take into account the unique features that make hydrogen a good moderator, namely:

(1) A neutron can loose all or an appreciable fraction of its energy in a single collision with a proton, and

(2) the neutron cross section for hydrogen increases strongly with decreasing energy from 10 Mev to 0.1 Mev.

The energy change in a single collision is so great that each succeeding mean free path is in general shorter than the previous one. The distribution of neutrons in water is dominated by the more energetic ones which travel without collision and are distributed more or less exponentially and by those neutrons which are slowing down in a relatively short distance beyond the point of their initial collision.

The Corn Pone multigroup code, written and perfected at Oak Ridge National Laboratory is a method for dealing with hydrogen which takes into consideration the slowing down kernel and the strong correlation between angle of scattering and energy loss of neutrons at each collision.(1) This ingenious solution correlates the P_1 approximation to the Boltzmann transport equation and the Goertzel-Grueling non-age theory for hydrogen. This method is essentially exact for hydrogen within our present knowledge of neutron cross sections. The rapid change in the hydrogen cross section over the fission spectrum has been included by using a large number of high energy groups. Table 1 shows the energy group division from 10 Mev to 1 Mev.

Table 1

Group	Lethargy Limits	Energy Limits - ev
1	0 - .25	10^7 - 7.78801 x 10^6
2	.25 - .5	7.78801 x 10^6 - 6.06531 x 10^6
3	.5 - .75	6.06531 x 10^6 - 4.72367 x 10^6
4	.75 - 1.00	4.72367 x 10^6 - 3.67879 x 10^6
5	1.00 - 1.25	3.67879 x 10^6 - 2.86505 x 10^6
6	1.25 - 1.50	2.86505 x 10^6 - 2.23130 x 10^6
7	1.50 - 1.75	2.23130 x 10^6 - 1.73774 x 10^6
8	1.75 - 2.00	1.73774 x 10^6 - 1.35335 x 10^6
9	2.00 - 2.25	1.35335 x 10^6 - 1.05399 x 10^6
10	2.25 - 2.50	1.05399 x 10^6 - 0.82085 x 10^6

The following assumptions were made in the calculation of the fast flux along the center line in the shielding facility.

1. The geometry is a slab.

2. The fission spectrum is that of U^{235} as measured by Cranberg et al[2]. No known fission spectrum for natural uranium is available.

3. Inelastic scattering effects for elements other than uranium were neglected.

4. Angular distribution of neutrons scattered by oxygen were neglected.

5. The neutron flux spectrum obtained was calculated for 1 neutron per cm^2 per sec per watt. To compare the calculated and experimental values the flux spectrum was normalized to the experimental $Mg(n,p)$ measurement at 6.6 Mev obtained while the BNL reactor was operating at 14 megawatts. At the present time it is impractical to determine the thermal flux striking the source plate per unit reactor operating power since the fuel loading of the reactor is periodically being changed. Therefore an absolute value for the flux cannot be obtained by means other than normalization.

6. Changes in the cross section of U^{238} due to production of large quantities of fission products, the build up of plutonium and the destruction of U^{235} were neglected.

The energy spectrum of neutrons calculated at the bottom of the water tank and 1, 2, 3, 5 and 7 inches from the bottom is shown in figure 2. These values are normalized to the fission density value of 1.94×10^9 neutrons per cm^3 per sec obtained when the BNL reactor was operating at 20 megawatts and loaded with natural uranium fuel elements.(6) It can be noted that within 1 cm at 1 Mev the neutron flux is reduced by a factor of 2 from 5.65×10^8 to 2.65×10^8. Fig. 3 shows the spatial distribution of the neutron flux summed over the energy region from 10 Mev to 1 Mev. along the center line of the reactor.

The validity of the results depends on uncertainities in the fission spectrum, and inaccuracies in the cross sections due to a limited knowledge of anisotropic scattering and inelastic scattering of neutrons.

EXPERIMENTAL MEASUREMENT OF THE NEUTRON FLUX DISTRIBUTION

The computed spectra for the space points of interest in the shielding facility described above are being checked and normalized experimentally by the standard method of activation of thin foils of appropriate isotopes.

This method was chosen over others used by workers in this field because of its relative simplicity, its adaptability in the absence of elaborate instrumentation, and a minimum disturbance to the neutron flux being measured. In principle, this technique is readily adaptable for use as a routine monitor of the integrated flux during the radiation damage experiments.

For these measurements the spectrum was considered in three groups; the fast flux region from 0.1 to 10 Mev, the resonance region from 0.4 ev to 0.1 Mev, and the thermal region up to 0.4 ev (the Cadmium cut-off). Since the fast flux region is of primary significance for the radiation damage studies in semi-conductors, this region was examined more closely. A number of threshold (n,p) and (n,α) reactions given in table 2 are being used to measure the flux in this region.

Table 2

Reaction	Reaction Threshold in Mev	Effective Threshold Eeff in Mev	Cross Section in barns	Half-Life of Product Nucleii
$P^{31}(n,p)Si^{31}$	.19	2.9	.075	2.65 hrs.
$S^{32}(n,p)P^{32}$	.42	3.3	.300	14.3 days
$Al^{27}(n,p)Mg^{27}$	1.34	3.7	.039	9.45 min.
$Mg^{24}(n,p)Na^{24}$	4.4	6.6	.048	15.0 hrs.
$Al^{27}(n,\alpha)Na^{24}$	2.2	7.8	.111	15.0 hrs.

The effective threshold energies were computed for a point along the center line of the shielding facility 2 cm from the bottom of the water tank.

These threshold reactions produce a radioactive species different from that formed by thermal-neutron capture, thus making it possible to identify the fast neutron interaction. These reactions do not have a sharply defined threshold energy and the capture cross section above the threshold is not a simple function of the energy. For this study the method described in Appendix I is used. An effective threshold energy is calculated from the computed spectrum and the penetration function for the charged particle emitted during the reaction. This value of the energy is then used to calculate the effective cross section for the reaction.

These computations have been programmed for the BTL Leprechaun computer to facilitate the examination of the variations in the effective thresholds and the effective cross sections as a function of the neutron spectrum at different space points of interest.

The techniques developed to make these measurements were designed to avoid absolute counting wherever possible. The sigma pile at BNL (a known source of thermal neutrons) was used as the standard to calibrate the radiation counters used to determine the activation obtained for each reaction listed above.

For each measurement in the shielding facility the procedure described in Appendix II was employed. Another

aspect of these measurements involved the cross-normalization of fission rate in the converter plate to the power level of the reactor for each measurement. During the period when these measurements were made, the BNL Reactor was being reloaded and the core configuration was changed after almost every shut-down. This upset any nominal power vs neutron flux data previously available. Thermocouples located in the vicinity of the uranium plate were used to monitor the thermal neutron flux incident on the converter plate and the average value of the thermocouple readings during each measurement were used to normalize successive measurements.

RESULTS

Measurements, as described above, are now in process. Preliminary results have been obtained for the following reaction as shown in table 3.

Table 3

Total Fast Flux Above the Effective Threshold Energies

Reaction	E_{eff} Mev	Φ_{eff} (measured) n/cm^2-sec	Normalization Constant	Φ_{eff} (normalized) n/cm^2-sec
$Mg^{24}(n,p)Na^{24}$	6.6	2.33×10^8	4.21	5.53×10^7
$Al^{27}(n,\alpha)Na^{24}$	7.8	8.55×10^7	4.21	2.03×10^7

Fig. 4 shows the computed fast Φ_{eff} above energy E as a function of E where Φ_{eff} is the total neutron flux with energies above E_{eff}.

REFERENCES

1. Blizard, E. P. and Simon, A., "Applied Nuclear Physics Division Annual Report for Period Ending Sept. 10, 1956" Oak Ridge National Laboratory, ORNL 2081.

2. Cranberg, L., Frye, G., Nereson, N., and Rosen, L., "Fission Neutron Spectrum of U^{235}" Phys. Rev. Ser II, 103, 1956, pp. 662-702.

3. Hughes, D. J., "Pile Neutron Research," Addison-Wesley (1953).

4. Wapstra, A. H., Physica, 21(1955).

5. Bethe, H. A., Rev. Mod. Phys. 9, 69, 163(1937)

6. Kouts, H. and Pratt, W., "Calibration of the Brookhaven Shielding Studies Fission Source", BNL-2796, 11/29/51.

APPENDIX I

The method described by Hughes[3] was used to recompute the effective thresholds. The value of the incident neutron kinetic energy at which the probability for these reactions occurring (E_t) exceeds zero was recalculated from the isotopic mass data compiled by Wapstra[4]. The probability for the penetration of the coulomb field by the emitted charged particle was then computed for these values of E_t from the equation derived by Bethe[5].

$$P(E) = \exp\left[- \frac{4zZe^2}{(vh/2\pi)} \text{ arc cos } (x^{1/2}) - x^{1/2}(1-x)^{1/2} \right], \quad (1)$$

where z = 1 for protrons and 2 for α particles,

Z = nuclear charge of product nucleus,

e = electronic charge

v = particle velocity = $(^{2E'}/_{m})^{1/2}$,

$x = E'/B$, where $E = E - E_T$ and B is the coulomb barrier height = zZe^2/r ergs or $\frac{0.96\ zZ}{A^{1/3}}$ Mev,

E = incident neutron energy,

E_t = threshold for the reaction,

r = radius of product nucleus and,

A = atomic weight of product nucleus,

L = Planck's constant.

It is assumed that the cross-section for this reaction as a function of energy, $\sigma(E)$, is proportional to this probability function. An effective threshold for this reaction is then computed which substitutes a step function for $\sigma(E)$ by solving the following equation.

$$\int_0^\infty P(E)\, N(E)\, dE = \int_{E_{eff}}^\infty N(E)\, dE, \qquad (2)$$

where $P(E)$ is defined by equation (1), $N(E)$ is the computed neutron flux distribution as a function of energy, and E_{eff} is the effective threshold.

Equation (2) is equivalent to the expression

$$\int_0^\infty \sigma(E)\, N(E)\, dE = \sigma_o \int_{E_{eff}}^\infty N(E)\, dE, \qquad (3)$$

where $\sigma(E)$, the cross-section function approaches σ_o at saturation just as $P(E)$ approaches unity.

APPENDIX II

PROCEDURE FOR THE CALIBRATION OF THE RADIATION COUNTERS

The purpose of this method, as mentioned in the text, is to avoid the necessity for absolute counting. Since a known source of thermal neutron flux (BNL sigma pile) is available, it is employed as a primary standard to which all measurements are compared. Unfortunately, some of the thermal neutron activations required to yield the same product nucleii as that from the threshold reactions have small activation cross sections and short half-lives. This coupled with the low value of the thermal flux in the sigma pile (of the order of 10^4 n/cm^2-sec) requires as an intermediate step, the use of the pneumatic tubes thermal neutron irradiation facilities of the BNL reactor where the flux is of the order of 10^{12} to 10^{13} n/cm^2-sec. Since this flux is not known with any degree of accuracy and since it is presently subject to change, the sigma pile is used to determine the flux in the pneumatic tube.

This cross calibration procedure was accomplished by the use of gold foil for which the thermal neutron activation cross section is well known. The following analysis summarizes the computation procedure employed.

The counting rate obtained from a gold foil irradiated in the sigma pile is

$$C_{Au}^{s} = E_{Au}\, \sigma_{Au}^{th}\, \Phi^{s}\, (1-e^{-\lambda_1 t})\, (e^{-\lambda_1 \theta}), \qquad (4)$$

where

E_{Au} is the radiation counter efficiency for activated gold,

σ_{Au}^{th} is the thermal neutron activation cross section,

Φ^{s} is the flux in the sigma pile,

λ_1 is the decay constant for gold^{198}

$(1-e^{-\lambda t})$ is the correction for decay during the irradiation time t,

and $e^{-\lambda\theta}$ is the correction for decay after the sample is removed from the pile until the time of count θ.

now

$$C_{Au}^{P} = E_{Au}\ \sigma_{Au}^{th}\ \Phi^{P}\ (1-e^{-\lambda_1 t})\ (e^{-\lambda_1 \theta}), \qquad (5)$$

where C_{Au}^{P} is the counting rate from a gold foil irradiated in the thermal flux in the pneumatic tube

Φ^{P} is the unknown flux in the pneumatic tube.

From equations (4) and (5) Φ^{P} can be determined.

Then for each threshold reaction studied a thermal neutron activation in the pneumatic tubes producing the same product nucleus is made for which the counting rate is given by

$$C_{x}^{P} = E_{x}\ \sigma_{x}^{th}\ \Phi^{P}\ (1-e^{-\lambda_x t})\ (e^{-\lambda_x \theta}), \qquad (6)$$

where E_x is the counter efficiency for the radioactive product nucleus σ_x^{th} is the thermal neutron activation cross section for the reaction in question, and

λ_x is the decay constant for the product nucleus.

Since Φ^{P} has been determined from the gold measurements, E_x can now be calculated. Finally, the counting rate obtained from the threshold reaction is

$$C_{y}^{f} = E_{x}\ \sigma_{y}^{f}\ \Phi_{eff}^{f}\ (1-e^{-\lambda_x t})\ (e^{-\lambda_x \theta}) \qquad (7)$$

where σ_y^f is the effective cross section for the threshold reaction,

Φ_{eff}^{f} is the total neutron flux with energies about E_{eff}.

From equation (7), knowing σ_y^f and using E_x obtained from equation (6), Φ_{eff}^{f} is obtained.

For some reactions, it may be possible to eliminate the intermediate pneumatic tube step if the cross sections for the required reactions are sufficiently large.

SECTION OF MOBILE PLATES
UNDER SQUARE WATER TANK

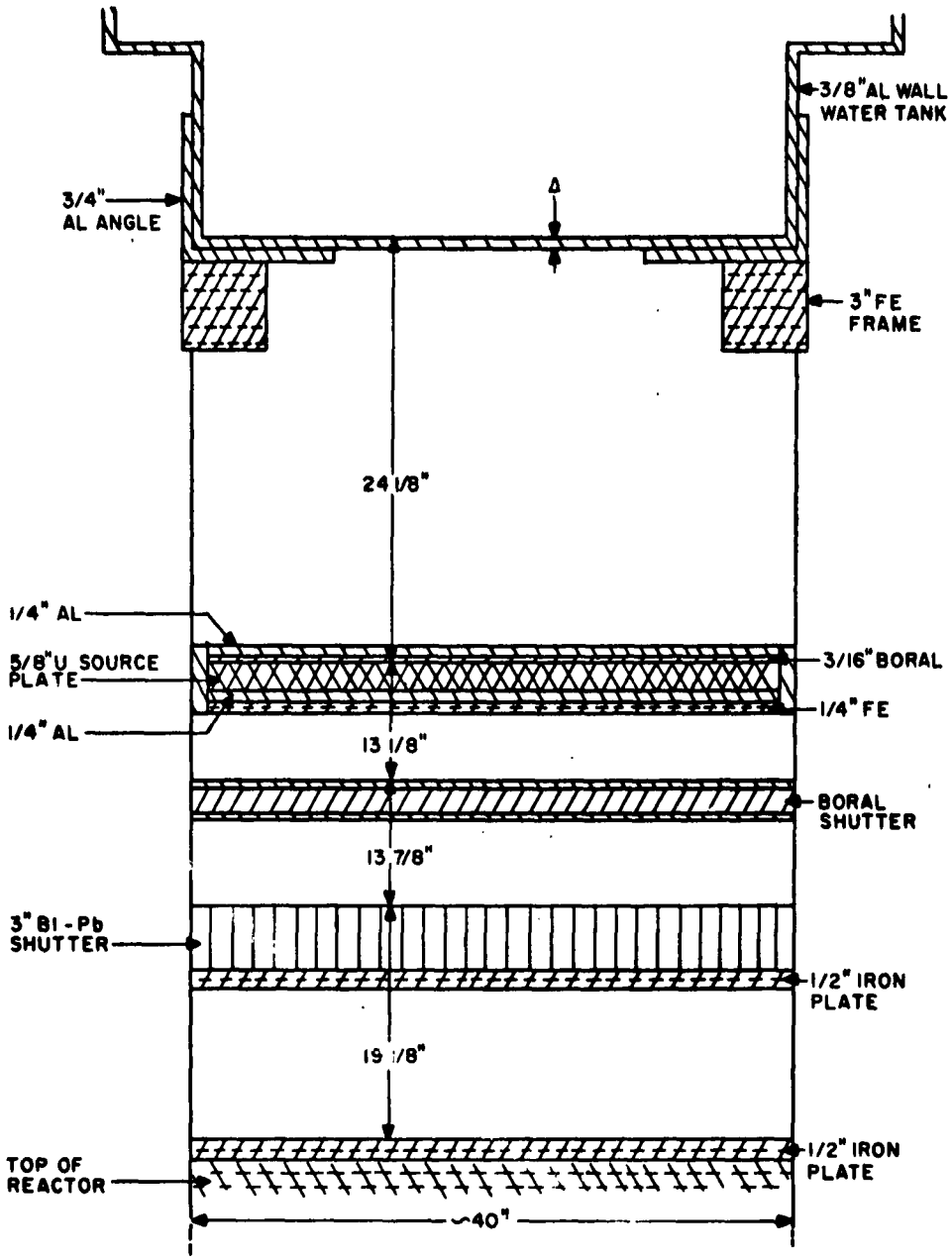

Δ = TANK BOTTOM DEFLECTION APPROXIMATELY 1/2"

ALUMINUM
IRON
BORAL
URANIUM
BISMUTH
GRAPHITE

NOT TO SCALE

FIG-1

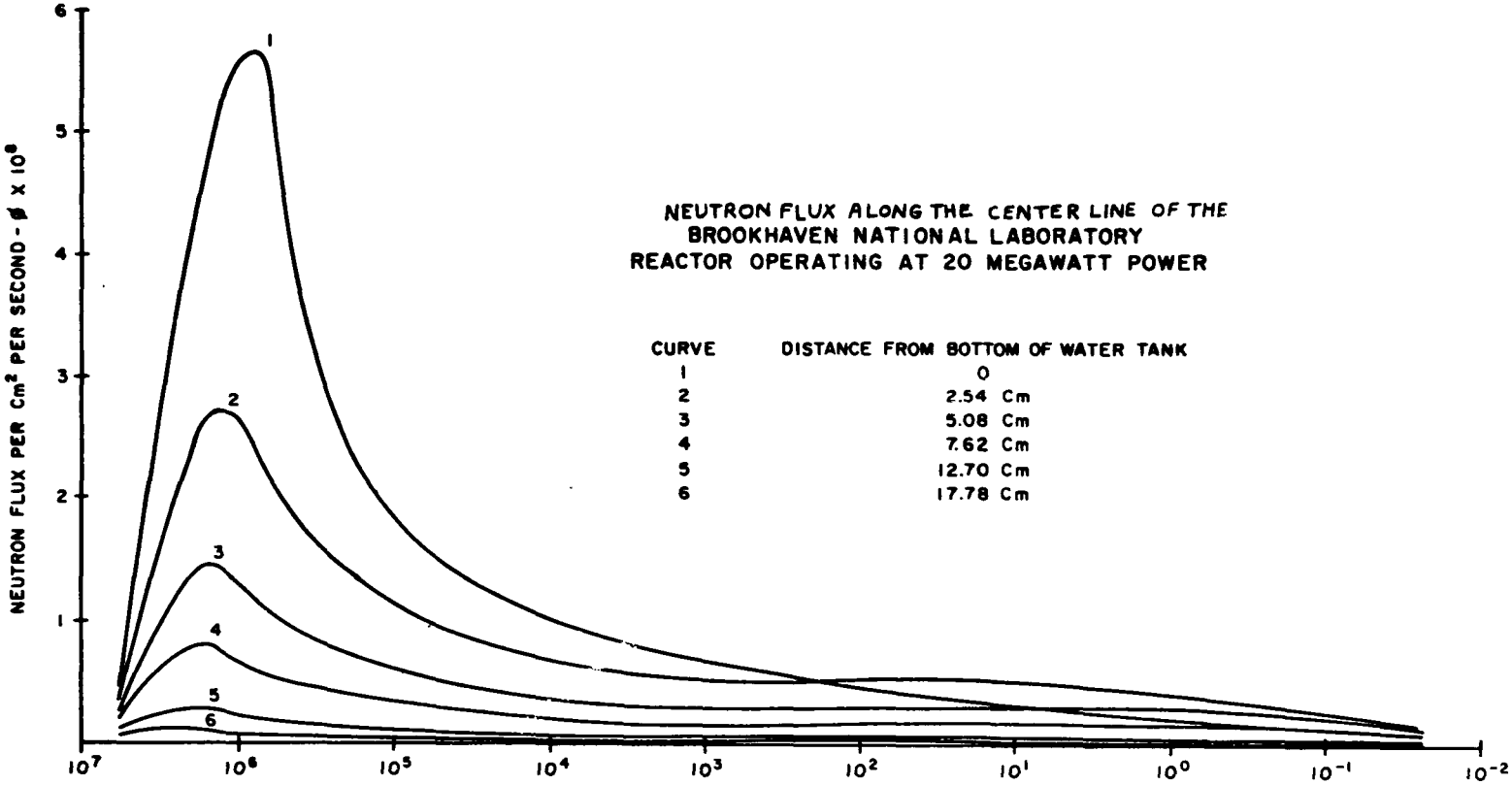
NEUTRON FLUX ALONG THE CENTER LINE OF THE
BROOKHAVEN NATIONAL LABORATORY
REACTOR OPERATING AT 20 MEGAWATT POWER
CURVE
DISTANCE FROM BOTTOM OF WATER TANK
1
0
2
2.54 Cm
3
5.08 Cm
4
7.62 Cm
5
12.70 Cm
6
17.78 Cm
NEUTRON FLUX PER Cm² PER SECOND - ϕ X 10⁸
ENERGY - eV
6
5
4
3
2
1
10⁷
10⁶
10⁵
10⁴
10³
10²
10¹
10⁰
10⁻¹
10⁻²

FIG-2

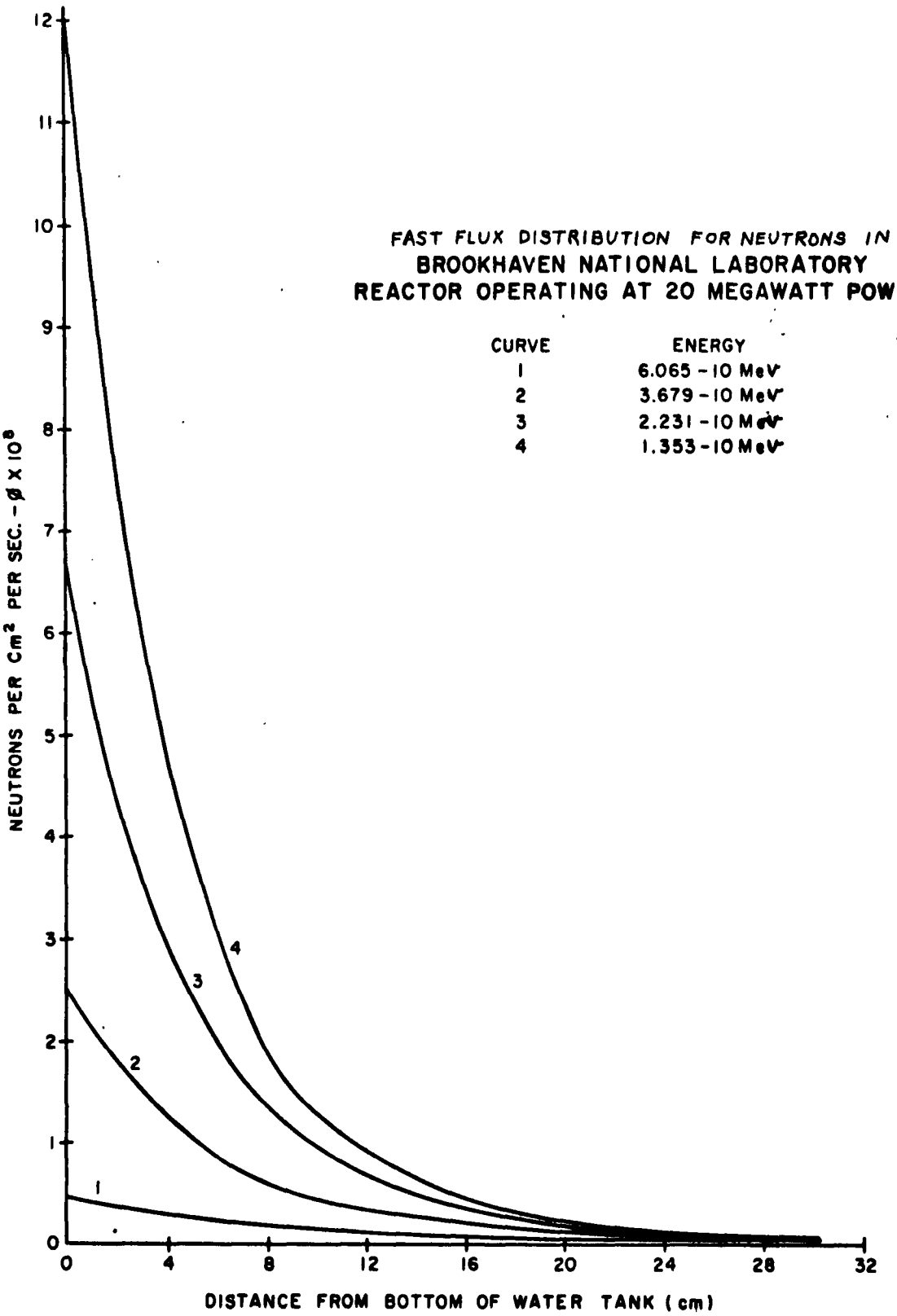
FAST FLUX DISTRIBUTION FOR NEUTRONS IN WATER
BROOKHAVEN NATIONAL LABORATORY
REACTOR OPERATING AT 20 MEGAWATT POWER
CURVE ENERGY
1 6.065 - 10 MeV
2 3.679 - 10 MeV
3 2.231 - 10 MeV
4 1.353 - 10 MeV
NEUTRONS PER Cm² PER SEC. - ø X 10⁸
DISTANCE FROM BOTTOM OF WATER TANK (cm)
0
1
2
3
4
5
6
7
8
9
10
11
12
0
4
8
12
16
20
24
28
32

FIG-3

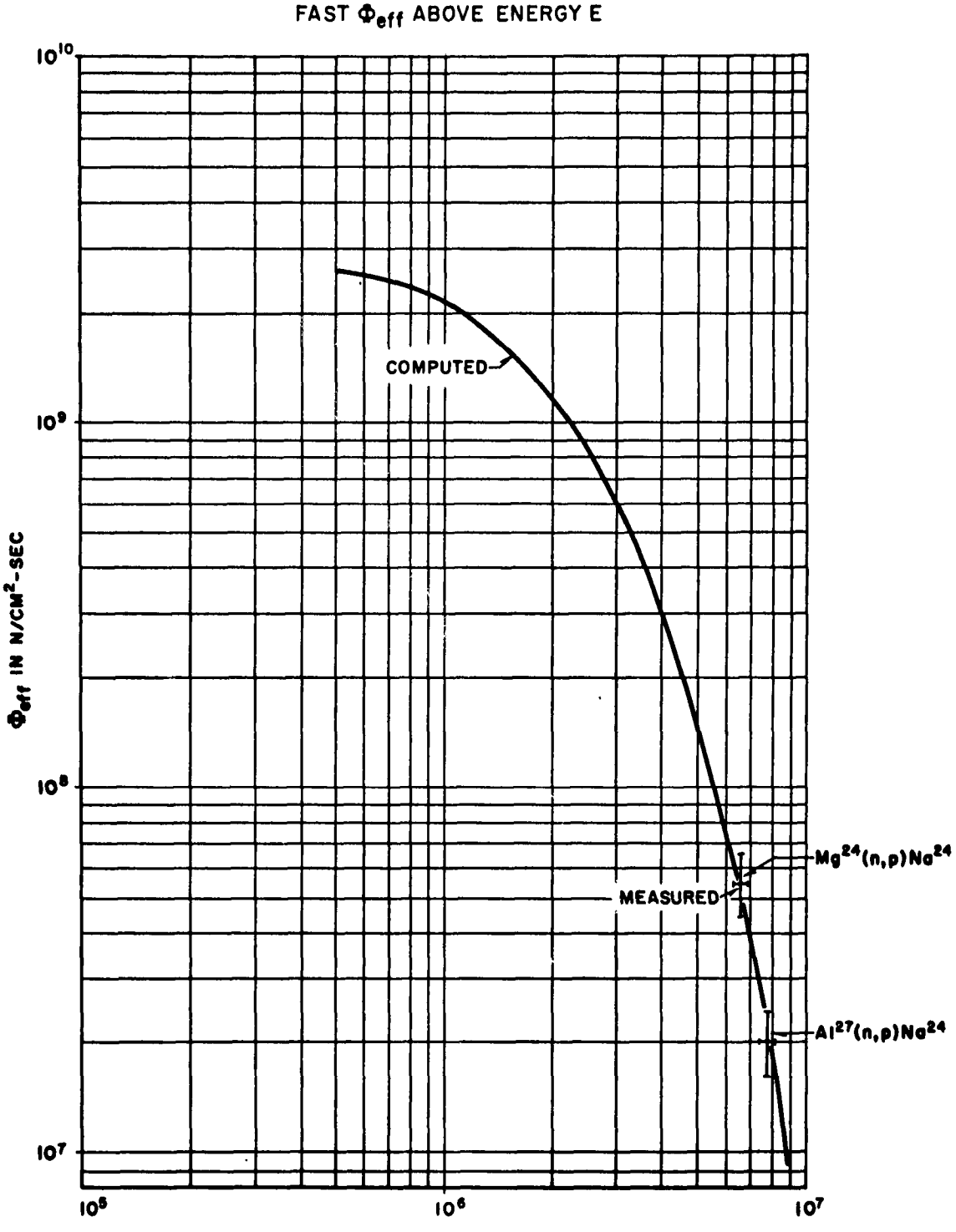
FAST Φ_{eff} ABOVE ENERGY E
10^{10}
10^{9}
10^{8}
10^{7}
Φ_{eff} IN N/CM^2-SEC
COMPUTED
MEASURED
$Mg^{24}(n,p)Na^{24}$
$Al^{27}(n,p)Na^{24}$
10^{5}
10^{6}
10^{7}
E IN Ev

FIG 4

THE EFFECTS OF NUCLEAR RADIATION ON SPARK GAPS

by

G. I. Duncan

General Electric Company
Specialty Transformer Department
Fort Wayne, Indiana

and

J. C. Fraser
B. Valachovic

General Electric Company
General Engineering Laboratory
Schenectady, New York

ABSTRACT

The General Electric Company has completed a program covering the testing of spark gaps in the Brookhaven National Laboratory's graphite reactor. It consisted of a two-week in-pile exposure designed to investigate the voltage breakdown strength of air at various pressures in the presence of the following radiation levels:

Fast Flux : 1×10^{11} fast neutrons/cm^2 sec

Thermal Flux : 2×10^{12} thermal neutrons/cm^2 sec

Gamma Flux : 1×10^{12} gamma photons/cm^2 sec.

This paper describes the components tested, the test equipment and circuitry, the dynamic pressure system used, and discusses the data obtained. Curves are presented showing the effects noted, and the results of the tests are summarized. This paper covers work performed under Contract AF-33(616)-5579.

INTRODUCTION

With the emphasis today upon extended environmental conditions for electronic equipment used in military aircraft and guided missiles, there is a pressing need for the simultaneous testing of such equipment under two or more of these extreme environments. This paper describes a program completed by the General Electric Company covering the testing of spark gaps in the Brookhaven National Laboratory's graphite reactor. It consisted of a two-week in-pile exposure (hole E-52) designed to investigate the voltage breakdown strength of air at various pressures in the presence of intense nuclear radiation of the following approximate levels:

Fast Flux : 1×10^{11} fast neutrons/cm^2 sec

Thermal Flux : 2×10^{12} thermal neutrons/cm^2 sec

Gamma Flux : 1×10^{12} gamma photons/cm^2 sec

The work described in this paper was part of Air Force Contract No. AF-33(616)-5579 for developing temperature and radiation tolerant electronic power transformers.

Present environmental goals as established by the Air Force for electronic power transformers are 100,000 feet altitude, 500°C ambient temperature, and intense nuclear radiation, approximating the levels previously mentioned. Since terminal spacings have previously been designed for air dielectric strengths to approximately 50,000 feet and temperatures up to 125°C, additional information was required on breakdown voltages under these new conditions.

Previous work on determining the voltage spacing characteristics as a function of air density up to altitudes of 150,000 feet has not included high temperature or radiation. A search of the literature revealed little or no information on the subject. Consequently, an experiment was designed and conducted to obtain this information.

DESCRIPTION

Test Variables and Levels

The dielectric breakdown strength of air is dependent upon: density, electrode spacing, electrode material, electrode configuration, frequency of voltage, and rate of increase of voltage.

To get the maximum amount of information, it was decided to obtain data for three levels of gap spacing and three levels of air pressure, with and without radiation. The gap spacings selected were 1/16 inch, 1/8 inch and 1/4 inch. Rod electrodes were selected for the gaps as it was felt that they would more closely approach the non-uniform fields normally encountered with terminals than would other types of gaps.

Air pressure was selected as a variable instead of air density because in free space the air pressure is not affected by changes in temperature, whereas temperature does affect air density. Air pressure can be directly related to altitude independent of temperature. The air pressures originally selected were 760, 76 and 7.6 millimeters of mercury which correspond roughly to sea level, 50,000 feet, and 100,000 ft. altitude respectively.

Voltage breakdown and d-c conductivity measurements were made on the spark gaps in a simulated reactor mock-up for the no-radiation condition, and in the E-52 hole at Brookhaven for radiation conditions.

Because of random variations in breakdown voltage, a spark gap can be expected to give only approximate values. To obtain reasonably correct values of breakdown voltage, the average of a number of measurements was taken.

Test Specimens

Two independent, identical test specimens were built and used to insure test reliability. They are shown in Figures 1 through 4. Each specimen consisted of an electrode holder having three gaps in a hermetically sealed stainless steel cylinder. The gap electrodes were made from 1/8 inch diameter nickel spark plug electrodes, the faces of which were machined flat to eliminate rounded edges. They were held in place by sheets of 1/8 inch thick aluminum phosphate bonded muscovite mica separated by 1/4 inch thick aluminum spacers. All electrodes on one side of the assembly, and the aluminum spacers, were connected to a stainless steel

FIGURE 1 ELECTRODE ASSEMBLY.

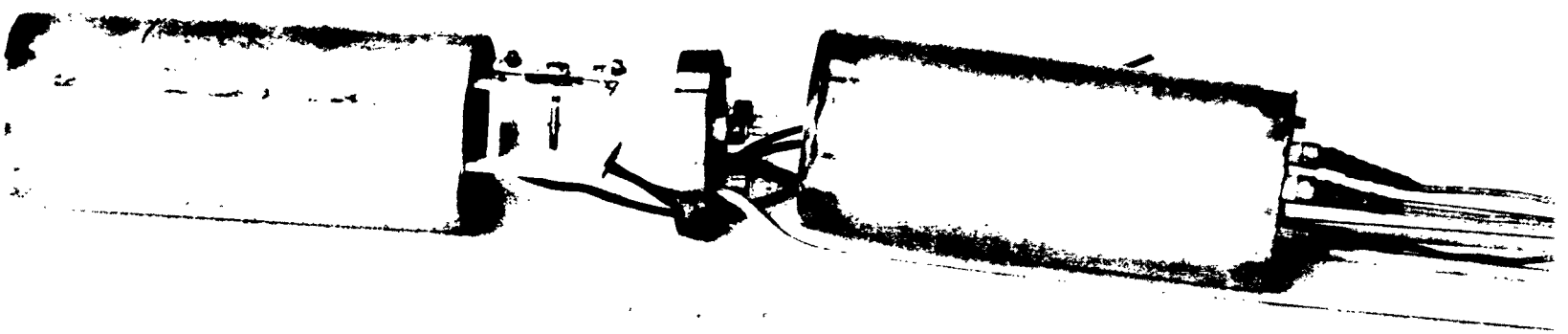

FIGURE 2 SPARK GAP ASSEMBLY.

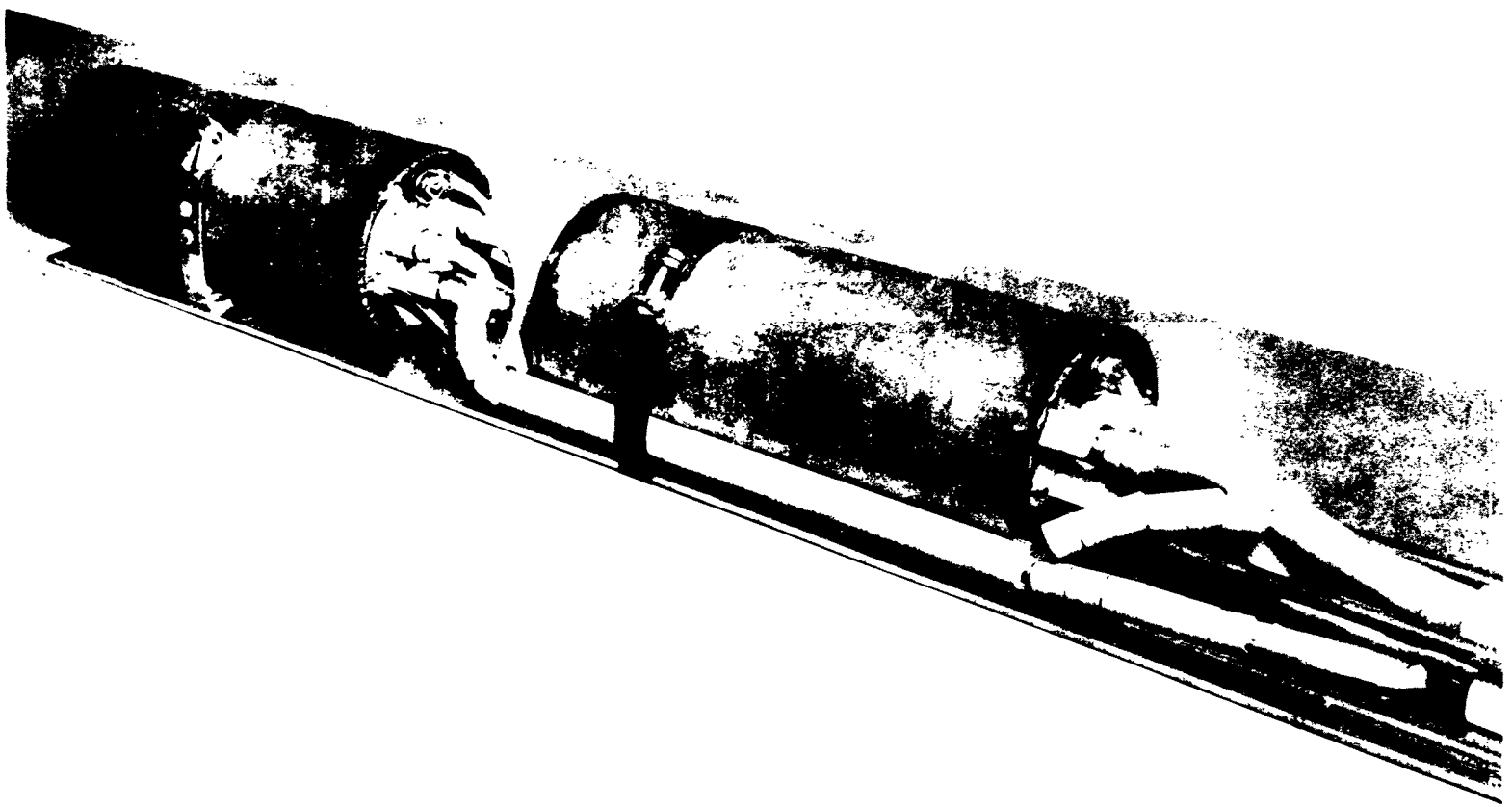

FIGURE 3 SPARK GAP TEST SPECIMENS AND TRAY.

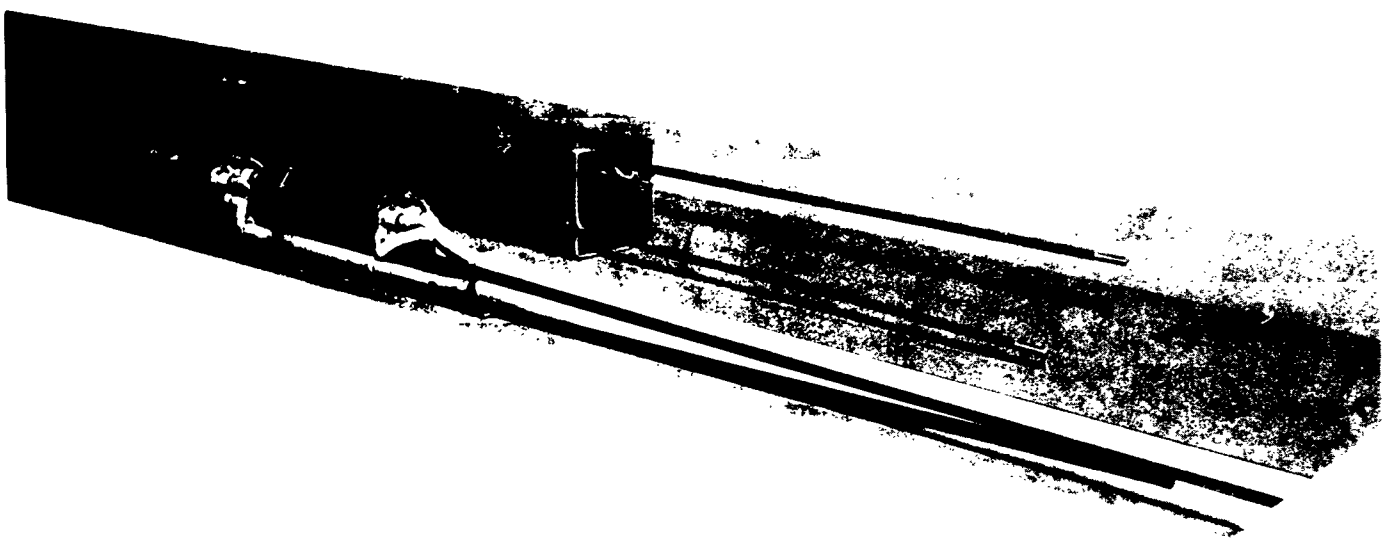

FIGURE 4 SPARK GAP TEST SPECIMENS AND CONTAINER.

steel ground strap, which was resistance welded to the front end of the test cylinder. The mica sheet on the high voltage side of the assembly was threaded for ease in adjusting the gaps; gauge blocks were used to set the gaps.

The test cylinder for each assembly consisted of a 3 inch O.D., .065 inch thick, 7 inch long stainless steel cylinder, with a stainless steel cap welded into each end. Two 1/4 inch O.D., .035 inch thick wall tubes for the dynamic pressure system were arc welded into the front end cap. Three alumina ceramic hermetic terminals were brazed into the front cap using a 5 percent silver, 95 percent cadmium brazing alloy. The high voltage leads for the gaps were brought out of the cylinder through these terminals. A small stainless steel screw was projection welded to the front cap for use as a ground terminal. Both caps were arc welded into the ends of the stainless steel cylinder.

Electrical connections between the high voltage electrodes and the hermetic terminals were made with 1/32 inch silicone rubber insulated AWG No. 18 solid copper conductor, using mechanical connectors at the electrodes, and silver brazing to the terminals. The high voltage leads from the terminals to the outside wall of the reactor consisted of a short length of the above copper wire brazed to 1/16 inch aluminum conductors insulated with a 3/64 inch wall of silicone rubber.

Instrumentation

Because of the inaccessibility of the spark gap cylinders in the reactor, remote instrumentation was required. A conventional potential transformer of the instrument type was used in reverse to supply the high potential. The normal transformer secondary was used as the input in this application and a G. E. Type P3 voltmeter was used to measure this input voltage. In the output side of this potential transformer, which is normally the primary side, there was a limiting resistor to prevent excessive load on the transformer when the spark gap broke down.

A cathode ray oscilloscope was used to indicate breakdown through the change in spark gap voltage wave shape. The voltage control on the input side of the transformer consisted of two autotransformers connected to give coarse and fine control.

The d-c conductivity measurements were made using a Keithley d-c vacuum tube voltmeter of the electrometer type as the basic measuring element. This is a battery-operated

unit which measures d-c voltage directly; it measures current in conjunction with a decade shunt. These measurements were made at approximately 90 volts d-c.

Temperature measurements were made using a chromel-alumel thermocouple located in the test container midway between the two test cylinders. Because of the gamma heating effect upon cylinder materials, particularly the stainless steel, test cylinder temperatures increased at a gradual rate throughout the test up to 153°C. Temperature measurements made in the E-52 hole previous to the start of this test showed a hole temperature of approximately 70°C.

Dynamic Pressure System

A dynamic measuring system, with continuous air flow was used to obtain air pressure control within the spark gap test cylinders. Calibrated restrictions on the inlet and outlet sides of the cylinders were used for each pressure required below atmospheric. For atmospheric measurements in the cylinders, the outlet valves were closed, and an inlet by-pass valve opened, so that the vacuum system could continue "pump-down" while atmospheric measurements were being taken.

The two test cylinders were connected in parallel during pump-down. The arrangement of pressure valves permitted selection of either cylinder for measurements, as desired. A thermocouple type pressure measuring instrument, a mechanical rough pump, and an air-cooled diffusion pump were connected on the outlet side of the test cylinders. A mercury barometer was connected in the inlet side of the test cylinders. The desired settings were thus obtained quickly and maintained indefinitely.

TESTS

Systems Tests

To check the test container and cylinders thoroughly before placing them in operation at the reactor site, a full scale mock-up of the reactor hole was constructed so that, except for radiation, all operating conditions could be duplicated as nearly as possible. It consisted of an aluminum inner duct 1/4 inch thick, 4 inches by 4 inches inside dimensions, and 18 feet long, to simulate the 4 inch square test hole in the Brookhaven reactor. By means of strip heaters surrounding the duct, it could be heated to temperatures as high as 200°C, so that reactor hole ambient temperatures could be duplicated.

Systems tests were performed to measure the breakdown voltage, a-c rms, the d-c conductivity of the spark gaps, and the operation of all instrumentation under simulated reactor operating conditions, except for radiation. Tests were performed with the spark gap tray and cylinder assembly inserted into the test container and placed in the reactor mock-up. The samples were exposed to the following approximate temperatures as determined by a thermocouple located in the test container: 26°C, 75°C, 129°C, 169°C. Three different pressures were recorded for the spark gap tests. They were, approximately: 760, 76, and 7.6 millimeters of mercury. Spark gap breakdown voltages and d-c conductivity measurements between gap electrodes were taken.

Radiation Tests

The radiation testing was carried on at Brookhaven National Laboratory in the E-52 hole. The test container was inserted into the reactor on Friday, June 13, 1958. After several low level runs to check the "poisoning" effect of the test container on reactor operation, the reactor was brought to 11 megawatts on June 14. Except for a brief emergency shutdown on June 17, it was operated for the balance of the test period at 13 megawatts. The test specimens were in the reactor for a total elapsed time of approximately 330 hours, and were removed from the reactor on June 28, 1958. During this test, manual measurements of breakdown voltage and d-c insulation were made periodically.

Test Results

A representative sampling of curves was plotted from the test data obtained and is presented in Figures 5 through 9. Figure 5 shows the spark gap breakdown voltage under conditions of no-radiation as a function of test cylinder pressure for the 1/16 inch gap in cylinder no. 2, with a family of curves showing various temperatures at which breakdown measurements were made. Figure 6 shows corresponding information for the radiation condition. These two figures clearly demonstrate the increase in breakdown voltage with increasing pressure (for the pressure range considered) and a decrease in breakdown voltage with increasing temperature.

Figures 7, 8, and 9 show a comparison of breakdown voltages under no-radiation conditions with those under radiation conditions for three representative temperatures. A comparison of these three curves shows a definite correlation between decrease in breakdown voltage and the presence of a radiation environment. At atmospheric pressure and 100°C there is an approximate spread of 600 volts; at 130°C, 700 volts; at 160°C, 500 volts.

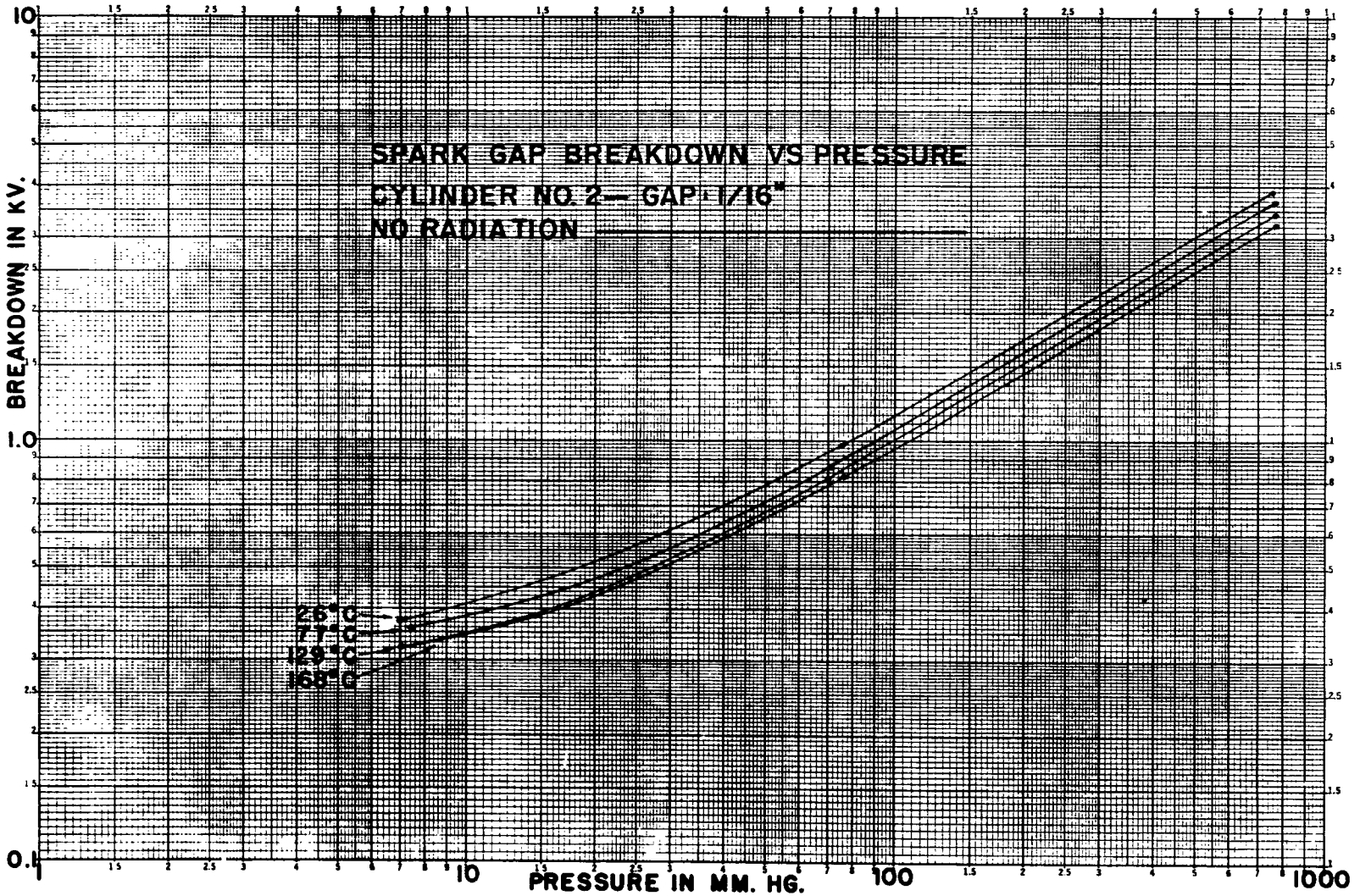
SPARK GAP BREAKDOWN VS PRESSURE
CYLINDER NO. 2— GAP 1/16"
NO RADIATION
26°C
77°C
129°C
168°C
BREAKDOWN IN KV.
PRESSURE IN MM. HG.
10
1.0
0.1
100
1000

Figure 5

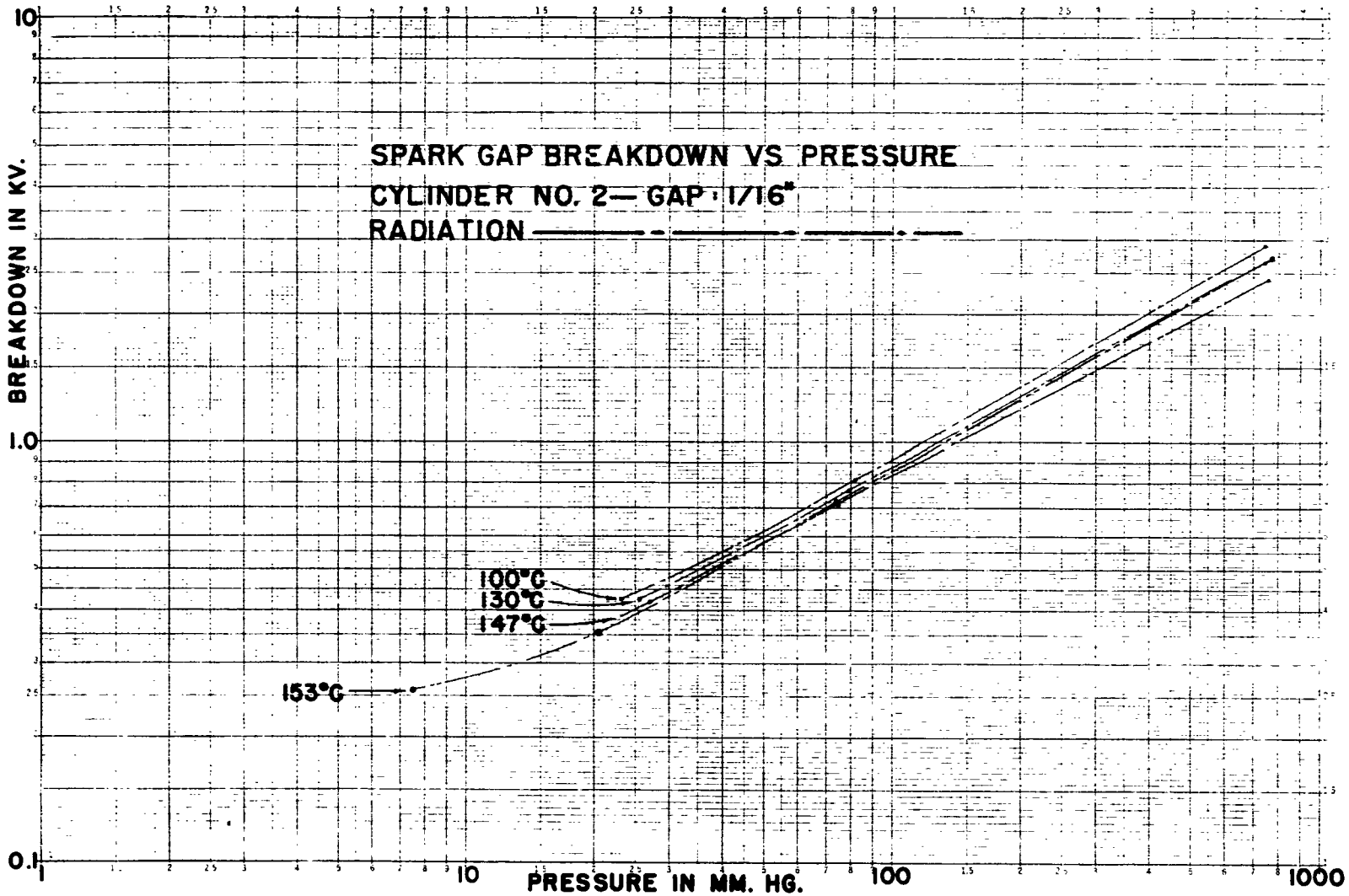
SPARK GAP BREAKDOWN VS PRESSURE
CYLINDER NO. 2— GAP : 1/16"
RADIATION
BREAKDOWN IN KV.
10
1.0
0.1
100°C
130°C
147°C
153°C
10
100
1000
PRESSURE IN MM. HG.

Figure 6

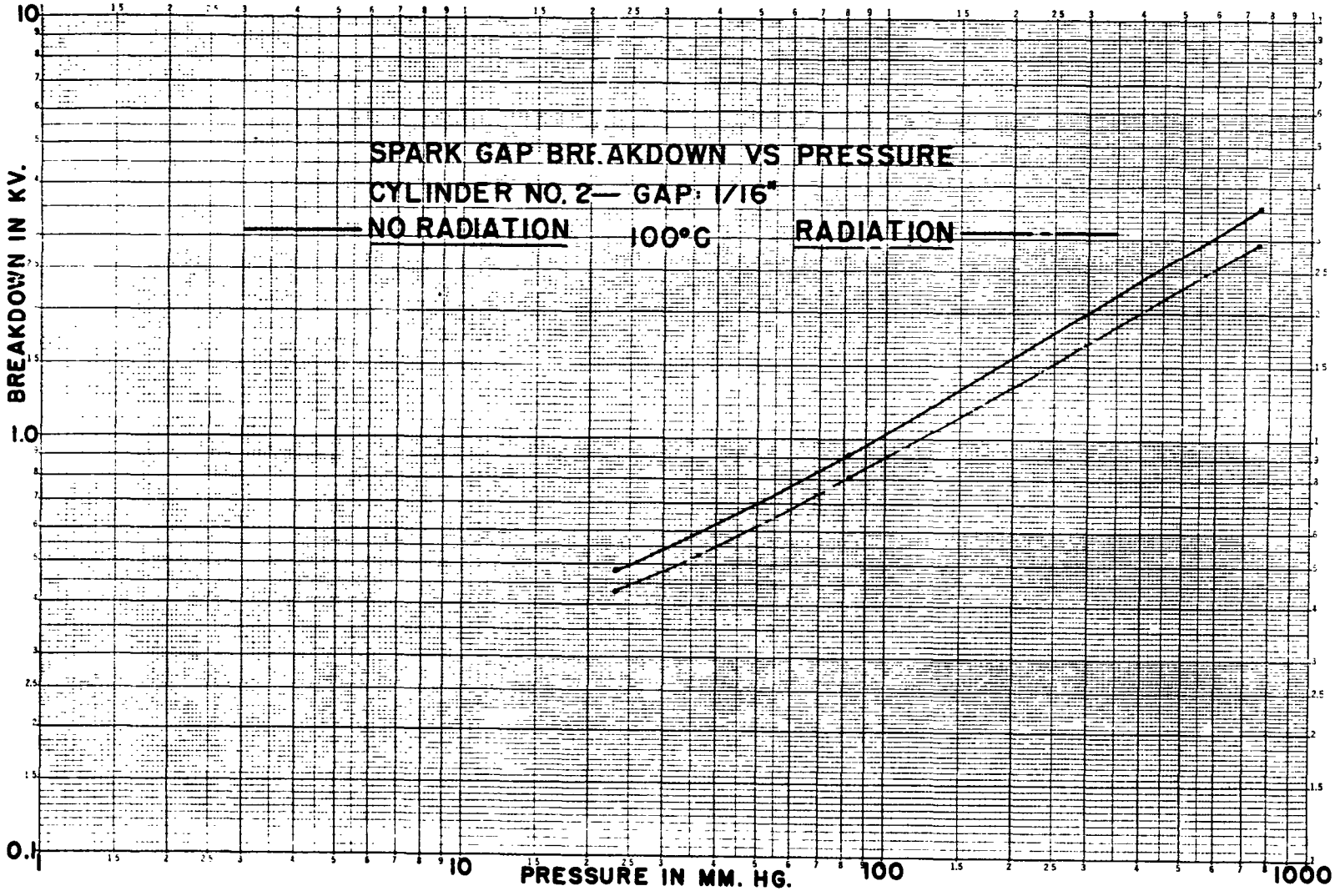
SPARK GAP BREAKDOWN VS PRESSURE
CYLINDER NO. 2— GAP: 1/16"
NO RADIATION
100°C
RADIATION
BREAKDOWN IN KV.
10
1.0
0.1
10
100
1000
PRESSURE IN MM. HG.

Figure 7

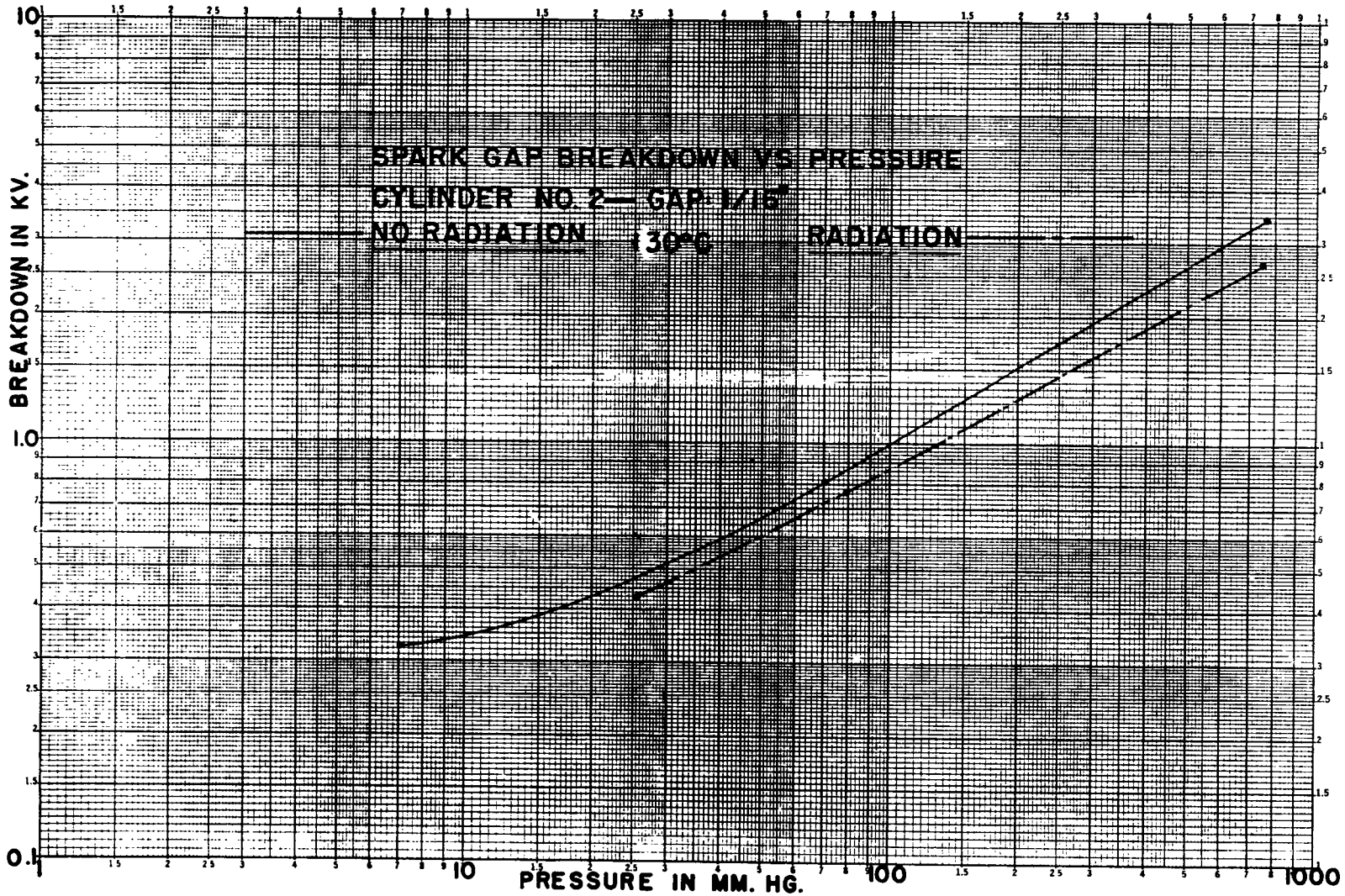
SPARK GAP BREAKDOWN VS PRESSURE
CYLINDER NO. 2— GAP 1/16"
NO RADIATION
130°C
RADIATION
BREAKDOWN IN KV.
PRESSURE IN MM. HG.
10
1.0
0.1
10
100
1000

Figure 8

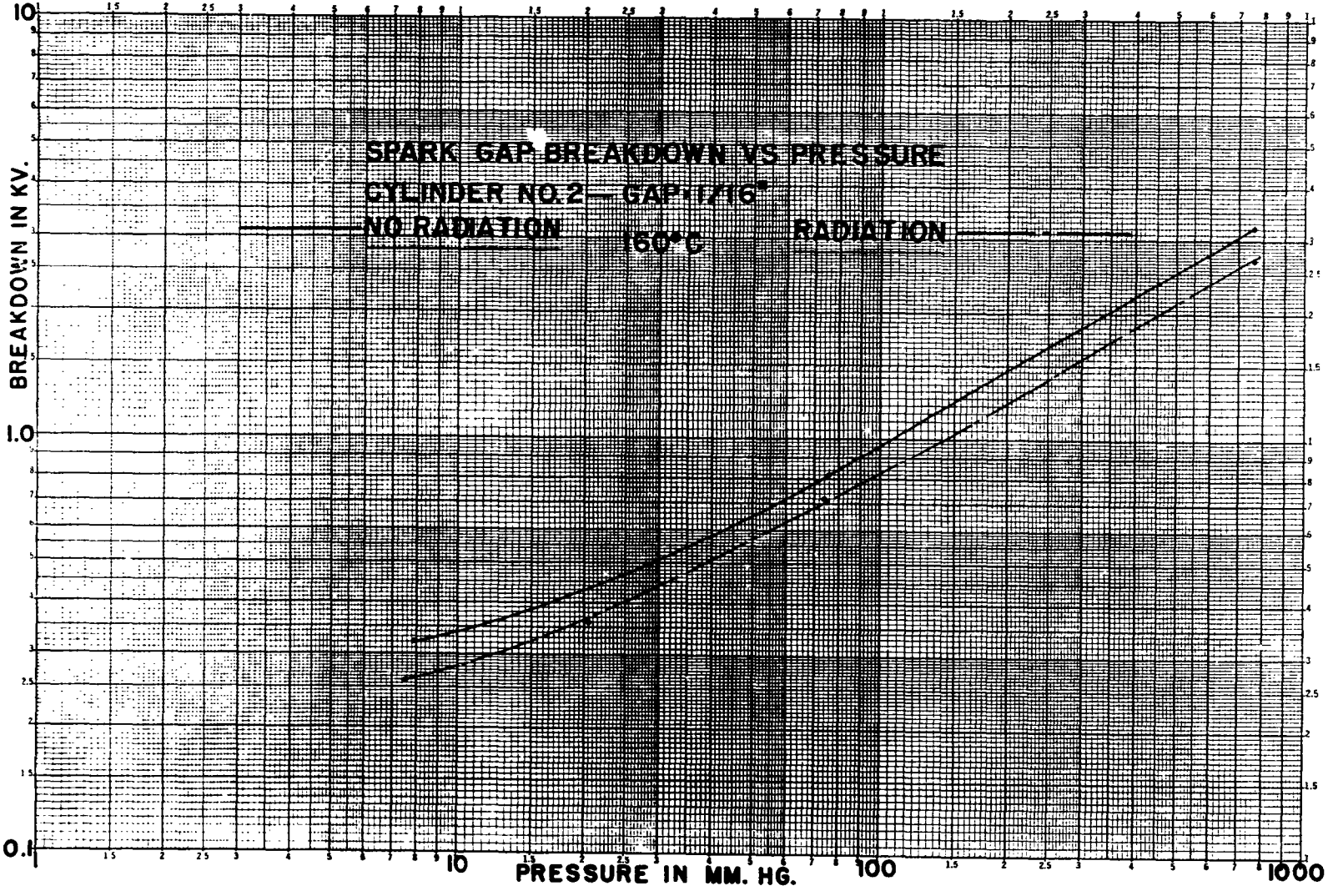
SPARK GAP BREAKDOWN VS PRESSURE
CYLINDER NO. 2 — GAP .1416"
NO RADIATION
150°C
RADIATION
BREAKDOWN IN KV.
10
1.0
0.1
10
100
1000
PRESSURE IN MM. HG.

Figure 9

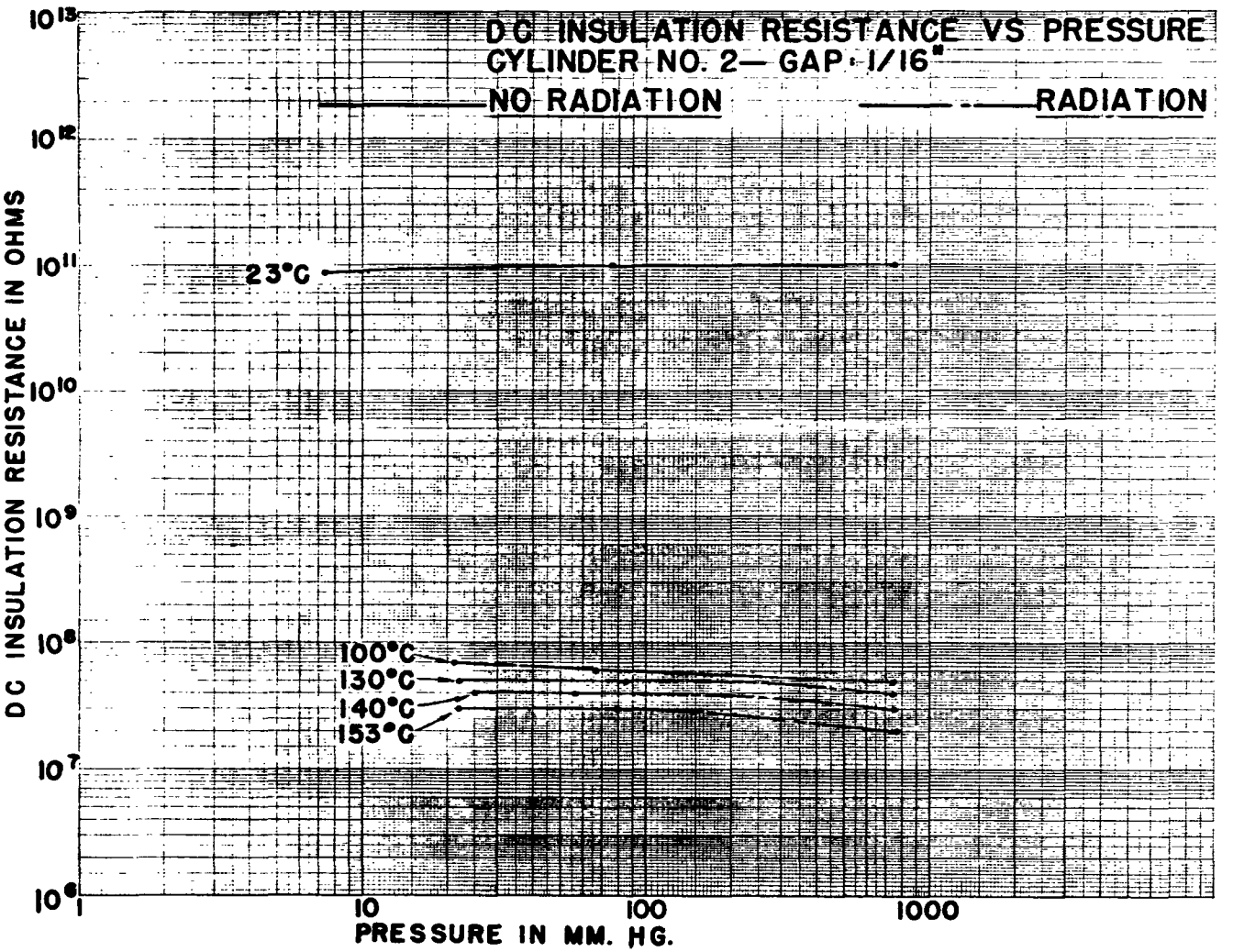
DC INSULATION RESISTANCE VS PRESSURE
CYLINDER NO. 2— GAP 1/16"
NO RADIATION
RADIATION
DC INSULATION RESISTANCE IN OHMS
10^{13}
10^{12}
10^{11}
10^{10}
10^{9}
10^{8}
10^{7}
10^{6}
23°C
100°C
130°C
140°C
153°C
1
10
100
1000
PRESSURE IN MM. HG.

Figure 10

Figure 10 shows the gap d-c insulation resistance as a function of test cylinder pressure for the 1/16 inch gap in cylinder no. 2 for both the no-radiation and radiation conditions. The no-radiation measurements were made at 23°C. Radiation measurements were made at four temperatures ranging from 100°C to 153°C.

Radiation accounted for at least a three decade lowering in gap d-c insulation resistance. Changes in d-c insulation resistance, under radiation conditions, as a result of varying temperatures, were less than half a decade.

CONCLUSIONS

The spark gap irradiation tests were successfully completed at Brookhaven in June, 1958. The data obtained in this test, and the curves plotted from those data indicate that nuclear radiation had a noticeable effect on spark gap breakdown voltage.

Test results indicate that under conditions of intense nuclear radiation, spark gap breakdown occurs at lower voltage values. The photoelectric effect of nuclear radiation makes available a large number of electrons in the gap at all times to start ionization, resulting in increased conductivity, and breakdown at lower voltage values.

Earlier investigators of spark gap breakdown found that accuracy could be increased by irradiating the gaps with ultraviolet light, with a resulting reduction in the average value of breakdown voltage by several percent. It is to be expected that nuclear radiation would have an appreciably greater effect. Since radiation is a form of energy, the probability of photoionization is proportional to the radiation density.

These tests confirm results obtained in a similar program involving reactor irradiation of electronic transformers. Even though radiation has some measurable effect upon operating characteristics, it can be safely assumed that equipment which is suitable for operation in extreme environmental conditions of temperature and pressure is equally suitable for operation in radiation environments of the type considered here.

Knowledge in the field of radiation effects is still in the early stages of development. The amount of general information on components under radiation is particularly limited. It is hoped that the experimental data obtained in these

tests will serve to shed some light upon the theories advanced, and will be helpful in evaluating and conducting subsequent tests on all types of electronic components. These tests will serve as the basis for a designer to establish safe voltage breakdown distances between terminals, and between terminals and ground, for transformer applications under extreme altitude and radiation conditions.

ACKNOWLEDGMENT

We are deeply indebted to the staff members of the Brookhaven National Laboratory Reactor Department, and in particular Messrs. J. J. Floyd, G. C. Kinne, R. W. Powell, and F. P. Reeve, for their cooperation and assistance in the performance of our radiation testing program.

RADIATION TESTING AND PROPERTIES OF A BORON NITRIDE DIELECTRIC CAPACITOR

by

G. R. Van Houten, T. C. O'Nan & J. T. Hood

P. R. Mallory & Co., Inc.
Indianapolis, Indiana

Tests to date include:

1) Study of boron nitride powders and compacts in a reactor environment.

2) Fabrication and testing of capacitor bodies from reactor irradiated boron nitride.

3) Operational testing of boron nitride capacitors in a high gamma environment.

Results to date indicate:

1) Good experimental verification of theoretical calculations.

2) Boron Nitride is definitely a preferred material for high temperature dielectric applications.

3) Boron nitride dielectric capacitors which are constructed to be self (neutron) shielding retain normal physical properties during and after irradiation.

4) Instantaneously gamma induced current leakage, as expected, varies as the square root of the gamma photon density. Such leakage can be appreciable at high voltage gradients.

5) Gamma scattering and capture causes local heating in proportion to the gamma photon density and energy. This gamma heating may increase the dielectric temperature enough to cause appreciably increased current leakage.

6) As a result of direct and indirect gamma induced leakage, limited gamma shielding may be necessary for high voltage units or for very large uncooled units. Similar problems with other dielectrics would generally be of even greater magnitude.

A. INTRODUCTION

P. R. Mallory & Co., Inc. is developing, under Air Force Contract No. AF 33(600)-34121, a Jet Engine Ignition Capacitor for operation at an ambient temperature of 500°C. Development of any type of capacitor for operation at 500°C is a real challenge, but the requirements for a Jet Engine Ignition capacitor are even more severe, inasmuch as the unit must operate under an extremely high applied voltage. Specified design parameters are:

Capacitance rating:	3 microfarads
Voltage rating:	3000 volts for pulsed service (5 cycles/second)
Energy storage capacity:	12 joules
Temperature requirements:	Capable of continuous operation at ambient temperatures from -65°C to + 500°C.
Radiation requirements:	Capable of meeting design specifications while being subjected to high intensity neutron and gamma radiation (gamma flux 10^{13} photons per square centimeter/second having average energy 1MEV. Neutron flux 10^{11} neutrons per square centimeter per second, having an average energy of 1MEV).
Capacitance tolerance:	±10%
Insulation resistance:	5 megohms/microfarad minimum at 500°C.
Dielectric strength:	150% rated voltage for 1 minute at 500°C.
Moisture resistance:	As specified in Method 106 of MIL STD-202.
Vibration:	From 10 to 3000 cycles per second, with

	an amplitude of .03" from 10 to 70 cycles per second and a vector acceleration of 15G from 70 to 3000 cycles per second.
Shock:	Equal to 50G for 11 milli-seconds duration.
Acceleration:	Equal to 30G constant acceleration.

It is theoretically possible to develop a high insulation resistance material with a zero temperature coefficient of electrical resistance over a wide temperature range, but as yet no such material is known. For the typical insulator, insulation resistance drops as the temperature rises; as the resistance drops, the electrical leakage at a given voltage increases. This leakage is considerable at higher applied voltages, and heats the capacitor by the I^2R loss. This raises the temperature further and in turn causes further heating. This can and does lead to run-away failure, much in the fashion of a nuclear reactor having a positive temperature coefficient of reactivity.

A thorough review and evaluation of all known insulation materials incated that only a few might be suitable for use as a capacitor dielectric at 500°C. While new capacitor dielectrics suitable for use at 500°C could theoretically be developed, this would require an extended theoretical study of such properties as electron and ion mobilities, recombination coefficients and the effect of basic dielectric structure and impurity concentrations on changes in these properties.

The problem is somewhat analogous to the synthesis of a suitable oxidation resistant tungsten base alloy. The latter has already received many man years of effort and should require many more man years of effort before solution. The same will be true for synthesizing new high temperature capacitor dielectric materials. Therefore, P. R. Mallory & Co. proceeded with the evaluation of known materials which might lead to a suitable high temperature capacitor at a reasonably early date. Promising materials included magnesium oxide, aluminum oxide and boron nitride. Of these, only boron nitride samples possessed the insulation resistance necessary to fabricate a high voltage high temperature electrostatic capacitor. Unfortunately for the attainment of small sizes, no dielectric material with high K and high dielectric strength also has sufficiently high insulation resistance above 350°C.

P. R. Mallory & Co. is developing several new capacitor dielectric materials for the 350 to 450°C temperature range. Capacitors employing these dielectrics will be much more compact than those employing boron nitride as a dielectric, however only boron nitride offers the possibility of high insulation resistance and excellent performance characteristic at temperatures of 500°C and higher.

This discussion of reasons for the selection of boron nitride as a dielectric material has heretofore ignored the effects of radiation on the dielectric material. Reasons why boron nitride is also a superior dielectric material in both gamma and neutron radiation fields will be found in

the body of the report.

B. PROCEDURE

After deciding that boron nitride represented the best high temperature dielectric material available, it then became necessary to prove whether or not boron nitride would perform suitably in a high radiation environment. According to contract specifications, thermal neutrons were to be screened out by a 1/8" boron equivalent shield. Primary problems, therefore, were to be fast neutrons and gamma rays. Two types of effects were to be considered, permanent and transient.

1. Gamma Radiation

A recent General Electric report describes a series of preliminary calculations which were verified by the results of in pile irradiation testing of the General Electric ceramic vacuum triode. This work, by J. R. Crittenden[1], has been employed as a basis for comparison in estimating transient effects of gamma radiation on boron nitride dielectric material.

Gamma photons may affect electronic component operation in several ways, but the interaction with orbital electrons is of greatest significance. The gamma ray is essentially an ionizing radiation, displacing electrons which in turn can cause further ionization. A comparison of P. R. Mallory & Co. calculations for boron nitride with General Electric calculations for aluminum oxide will be found in the Appendix. The total number of electrons displaced is actually proportional to the energy absorption coefficient rather than the mass absorption coefficient which is employed in the Appendix. Mass absorption coefficients rather than energy absorption coefficients are used only to permit ready comparison with Crittenden's figures. Whether using mass or energy absorption coefficients, boron nitride is theoretically (and actually) superior to alumina.

2. Neutron Radiation

Although thermal neutrons are supposedly all filtered out, it is possible that some of the faster neutrons can be degraded to thermal and accordingly it seems desirable to mention the effect of thermal neutrons on boron. Specifically, boron is a $\frac{1}{V}$ absorber, the reaction product being lithium and helium ions. It is therefore apparent that a thermal neutron-boron interaction would yield an appreciable amount of permanent damage to the structure and, through the introduction of the lattice defects, would probably result in significant reduction in the insulating properties of the dielectric.

Fast and epithermal neutrons are much more likely to undergo a scattering interaction with boron rather than an absorption interaction. When a scattering interaction occurs, some or all of the energy of the incident neutron is transferred to the struck nucleus, causing it to

recoil and leave some or all of its electrons behind. The struck nucleus may assume either a regular lattice site or an interstitial position (commonly called a Frenkel defect) and may therefore constitute permanent damage and consequent impairment of the insulation resistance of the material. Therefore, it was decided to irradiate boron nitride powder and bodies in the Brookhaven reactor for a period of six weeks in order to determine the magnitude of any permanent effects.

It is apparent from the data in the Appendix that, if the capacitor body is adequately surrounded by additional boron nitride, the permanent damage done either by fast neutrons or by thermal neutrons will be negligible.

Mallory was then ready for the second step in its radiation testing. From the preliminary calculations (see Appendix) it seemed likely that gamma radiation would have by far the greatest transient effect. Therefore, small capacitors were fabricated for testing in gamma fluxes of various intensities. The capacitors were tested in a Cobalt 60 unit at the Cook Inland Laboratories. As the data in the Appendix show, the leakage current varies as the square root of the gamma flux, as expected. There was good agreement between theoretically predicted and actually measured leakages. The test further verified the superiority of boron nitride over alumina.

The next step in the Mallory program, possibly to be completed prior to this radiation effects symposium meeting, is the gamma irradiation of samples at various elevated temperatures. This experiment should permit the determination of electron-mobilities and recombination coefficients as a function of temperature. Inasmuch as boron nitride is a good thermal insulator, gamma heating can generate appreciable thermal gradients. Future testing will employ the use of thermocouples to determine these temperature gradients so that the overall equation for the effect of gamma radiation may include the appropriate coefficient for internal heat generation effects.

Reactor testing will not be undertaken again until final prototype capacitors have been prepared. Some of the finished units will be encased in tungsten base alloy. Just as surrounding the electrodes with an extra thick layer of boron nitride will take care of any thermal neutrons, placing the capacitor in a tungsten metal container, such as Mallory-1000 which can also serve as a gamma shield, will reduce both gamma heating effects and transient gamma induced leakage effects. The final thickness of the gamma shield container will depend upon the minimum reduction in inherent capacitor leakage absolutely essential for acceptable black box performance. It would be preferable to have no gamma shield at all, but figures in the appendix imply that even with further improvement in dielectric purity (or impurity), contract specifications cannot be met without some shielding.

P. R. Mallory & Co. is already acquainted with the problems of electrical performance testing of electronic components in a reactor irradiation field, having made in pile measurements on its film resistor

in the Brookhaven reactor under Air Force Contract No. AF 33(616)-3643. Shielding of leads for a 4500v applied voltage, however, will greatly complicate the operation. Although this high voltage will add greatly to the cost and difficulty of making in pile electrical measurements, procedures for making these measurements are within the range of possibility.

C. CONCLUSIONS

The data given in the Appendix show:

1) Good agreement between theoretical predictions and experimental data for transient gamma effects occuring at room temperature.

2) The general superiority of boron nitride as a dielectric as compared with other materials such as alumina.

3) The excellent prospects of success for a high temperature boron nitride dielectric capacitor.

D. ACKNOWLEDGEMENT

The authors gratefully wish to acknowledge the efforts and advice of Mr. Al Speak and Clifford Winston, Electronic Components Laboratory, Wright Air Development Center, under whose cognizance this work was performed.

E. APPENDIX

This appendix consists of excerpts from Progress Reports No. 3, 4 and 6, Air Force Contract No. AF 33(600)-34121.

1. Calculation of Gamma Interaction Effects

a. Equation for Gamma Absorption

$I = I_0 e^{-\mu x}$ where: I = gamma photons leaving (cm^2-sec.)
I_0 = incident gamma photon intensity (cm^2-sec.)
e = natural number
μ = linear absorption coefficient (cm^{-1})
x = thickness of material (cm.)

b. Calculation for 1cc of Al_2O_3

$\mu = 4 \times 0.067 = 0.268 \ cm^{-1}$
(density of Al_2O_3 = 4)

μ of water = 0.067 for 1 MEV photons (mass absorption coeff.)

Note: We believe this value is slightly high for the mass absorption coefficient and about 2-1/2 times higher than the value obtained using the energy absorption coefficient.

$$\frac{I}{I_o} = e^{-\mu x} = e^{-(0.268)}\ (1) = 0.765\ (0.77)$$ (mass absorption coefficient basis)

Therefore 1cc of Al_2O_3 attenuates 23.5% of the incident 1MEV gamma radiation.

c. Calculation for 1cc. of BN

Assume that the average density of BN is about 1.80 gr./cm³ as compared to the theoretical density of 2.25 gr/cm³, or 80% of theoretical density.

$$B \tilde{=} \frac{10.8}{24.8} \tilde{=} 43.6\% \times 1.80\ gr./cm.^3 = 0.785\ gr./cm^3$$

$$N \tilde{=} \frac{14.8}{24.8} \tilde{=} 56.4\% \times 1.80\ gr./cm.^3 = 1.015\ gr./cm.^3$$

μ BN = $\rho_B x_{\mu B} + \rho_N x_{\mu N}$

= density of boron x absorption coefficient of B + density of nitrogen x absorption coefficient of N

= 0.785 x 0.0587 + 1.015 x 0.0636

= 0.1105 (mass absorption coefficient)

$$\frac{I}{I_o} = e^{-\mu x} = e^{-(0.1105)}\ (1) = 0.896$$ (mass absorption coefficient basis)

Therefore 1cc of BN at density of 1.8 gr/cm.³ absorbs or scatters out 10.4% of 1MEV gamma energy.

2. Tabulation of Comparative Information on BN and Al_2O_3

Factor	BN	Al_2O_3
Ratio fast to thermal electrons	10^3	10^3
Attenuation of 1MEV gamma energy particles	10.4%	23.5% (23%)
Electron mobility (cm./sec per volt/cm.)	(10^{-4} 10^{-3} with enough lattice defects)	10^{-3}

Factor	BN	Al_2O_3
Recombination coefficient (cm^3/sec)	(10^{-8} 10^{-7} with enough lattice defects)	7×10^{-10}

BN compares well or is superior to Al_2O_3 in all factors tabulated here.

3. Calculations of Gamma Induced Currents in BN and Al_2O_3 Materials

Calculation of Free Electrons per $cm.^3$

$$N_o = \left[\frac{(Q)}{(a)}\right]^{1/2}$$

where: N_o = free electrons per cm^3 per sec.
Q = rate of electron release per cm^3 per sec.
a = coefficient of recombination $cm.^3$/sec.

Use a gamma radiation intensity as specified, i.e., 10^{13} gamma photons per cm^2 per sec. at 1MEV energy level.

$$n_o = \left[\frac{\begin{pmatrix}\text{1MEV gamma mass} \\ \text{absorption coeff}\end{pmatrix} \times \begin{Bmatrix}\text{gamma photon} \\ \text{radiation intensity}\end{Bmatrix} \times \begin{Bmatrix}\text{ratio of fast to} \\ \text{thermal electrons}\end{Bmatrix}}{(\text{Coefficient of recombination})}\right]^{1/2}$$

$$= \left[\frac{(0.N) \times (\text{photons/cm}^2 \text{ per sec.}) \times (\text{thermal electron released per fast particle})}{(\text{recombinations per cm}^3 \text{ per sec. at 1MEV ratio})}\right]^{1/2}$$

FOR BN

$$\text{BN } n_o = \left[\frac{(0.104)\ (10^{13})\ (10^3)}{1 \times 10^{-8}}\right]^{1/2}$$

$= 3.23 \times 10^{11}$ electrons per cm^3 per sec. released by 10^{13} gamma photons per cm^2 per sec. at 1MEV

FOR Al_2O_3

$$Al_2O_3\ n_o = \left[\frac{(0.235)\ (10^{13})\ (10^3)}{7 \times 10^{-10}}\right]^{1/2}$$

$$= (3.35 \times 10^{24})^{1/2}$$

$= 1.83 \times 10^{12}$ electrons per cm^3 per sec. released by 10^{13} gamma photons per cm^2 per sec. at 1MEV.

BN appears $\frac{1.83 \times 10^{12}}{3.23 \times 10^{11}} = 5.66$ times as good as Al_2O_3 in this respect.

a. Calculations of Gamma Induced Current Level per cm^3

$\dot{i} = \frac{AV}{L} e u n_0$ where: A = area of electrodes in cm^2
V = applied voltage in volts.
L = thickness of dielectric in cm.
e = electronic charge in coulombs.
u = electronic mobility in cm^3/volt - sec.
n_0 = electrons per cm^2 per sec. induced by 10^{13} gamma photons per cm^2/sec. at 1MEV.

FOR BN

Set v = 100 volts

$$\dot{i}_{BN} = \left(\frac{1cm^2 \times 100v}{1\ cm}\right) \times \left(1.602 \times 10^{-19}\ \text{coulombs}\right) \times \left(10^{-4}\ cm^2\ \text{per v./sec.}\right) \times \left(3.23 \times 10^{11}\ \text{electrons per } cm^3 \text{ per sec.}\right)$$

$= 5.16 \times 10^{-10}$ amperes per cm^3 induced by 10^{13} gamma photons per cm^2 per sec.

$\dot{i}_{BN} = 5.16 \times 10^{-4}\mu a$ at voltage stress of 100v per cm., a very low value compared to our requirement.

FOR Al_2O_3

Set v = 100 volts (for direct comparison to Crittenden's[2] data)

$$\dot{i}_{Al_2O_3} = \left(\frac{1cm^2 \times 100v}{1\ cm}\right) \times \left(1.602 \times 10^{-19}\ \text{coulombs}\right) \times \left(10^{-3}\ cm^2\ \text{per v per sec.}\right) \times \left(1.83 \times 10^{12}\ \text{electrons per } cm^3 \text{ per sec.}\right)$$

$= 2.93 \times 10^{8}$ amperes per cm^3 induced by 10^{13} gamma photons per cm^2 per sec.

$\dot{\iota}_{Al_2O_3} = 2.9 \times 10^{-2}$ a at voltage stress of 100v per cm., a very low value compared to our requirement

BN appears $\frac{2.93 \times 10^{-2}}{5.16 \times 10^{-4}} = \underline{56.6 \text{ times as good as } Al_2O_3}$ in this respect.

c. Calculation of Gamma Induced Current Level in Conventional Mallory Laboratory Test Body Size at Voltage Stress Level of 4500v.

A = 0.52 in^2 = 3.36 cm^2/ L = 0.020 in = .051 cm./ V = 4500v

$$\dot{\iota}_{BN} = \left(\frac{3.36\text{cm}^2 \times 4500\text{v}}{.051 \text{ cm}}\right) \times \left(\frac{1.602 \times 10^{-19}}{\text{coulombs}}\right) \times \left(\frac{10^{-4} \text{ cm}^2 \text{ per v}}{\text{per sec.}}\right) \times \left(\frac{3.23 \times 10^{11} \text{ electrons per}}{\text{cm}^3 \text{ per sec.}}\right)$$

= 1.53×10^{-6} amperes induced by 10^{13} gamma photons per cm^2 per sec.

$\dot{\iota}_{BN}$ = 1.53μa at voltage stress of 4500v on 0.020 in. electrode spacing

$$R_{BN} = \frac{V}{I} = \frac{4.5 \times 10^3 \text{v}}{1.53 \times 10^{-6} \text{a}}$$

= 2.95×10^9 ohms

$$\text{Vol } R_{BN} = \frac{R \times 2 \times (\text{in. dia.})^2}{\text{in. tk.}}$$

$$= \frac{2.95 \times 10^9 \times 2\ (.81)^2}{.020}$$

= 1.95×10^{11} ohm. cm.

$$\dot{\iota}_{Al_2O_3} = \left(\frac{3.36\text{cm}^2 \times 4500\text{v}}{.051 \text{ cm}}\right) \times \left(\frac{1.602 \times 10^{-19}}{\text{coulombs}}\right) \times \left(\frac{10^{-3} \text{ cm}^2 \text{ per v}}{\text{per sec.}}\right) \times \left(\frac{1.83 \times 10^{12} \text{ electrons}}{\text{per cm}^3 \text{ per sec.}}\right)$$

= 8.68×10^{-5} amperes induced by 10^{13} gamma photons per cm^2 per sec.

$I_{Al_2O_3}$ = 86.8 μa at voltage stress of 4500v on .0.020 in. electrode spacing.

$$R_{Al_2O_3} = \frac{V}{I} = \frac{4.5 \times 10^3 v}{86.8 \times 10^{-6} a}$$
$$= 5.2 \times 10^7 \text{ ohms}$$

$$\text{Vol } R_{Al_2O_3} = \frac{R \times 2 \times (\text{in. dia.})^2}{\text{in. tk.}}$$
$$= \frac{5.2 \times 10^7 \times 2(.81)^2}{.020}$$
$$= 3.4 \times 10^9 \text{ ohm. cm.}$$

BN appears $\frac{1.95 \times 10^{11}}{3.4 \times 10^9}$ = 57 times as good as Al_2O_3, but below the required volume resistance level (over 1×10^{13} ohm cm.) by about a decade.

For the anticipated worst possible case, if one would assume that there are enough lattice defects in BN to change the characteristics to the alternate estimated values proposed by Dr. Middleton, calculations on BN would proceed as follows:

Change: (1) Electron mobility (cm/sec. per volt/cm) from 10^{-4} to 10^{-3}

(2) Recombination coefficient (cm^3/sec) from 10^{-8} to 10^{-7}

$$N_o \text{ BN} = \left[\frac{(Q)}{(a)}\right] 1/2 = \left[\frac{(0.104)\ (10^{13})\ (10^3)}{1 \times 10^{-7}}\right] 1/2 = (1.04 \times 10^{22})^{1/2}$$
$$= 1.02 \times 10^{11}$$

electrons per cm^3 per sec. released by 10^{13} gamma photons per sec. at 1 MEV. With the higher recombination coefficient, this value is reduced from the previously calculated 3.23 x 10^{11} at a 1×10^{-8} cm^3/sec. recombination coefficient

$$I \text{ BN (std. test body, etc)} = \frac{AV}{L} \text{eun}_o = \left[\frac{(3.36 cm^2 \times 4.5v \times 10^3)}{(\quad 5.1 \times 10^{-2} \text{ cm} \quad)}\right] \times$$
$$\left[\frac{(1.602 \times 10^{-19})}{(\quad \text{coulombs} \quad)}\right] \times$$

$$\left[\begin{matrix}(10^{-3}\ \text{cm}^2/\text{volt}) \\ (\text{per second}\quad)\end{matrix}\right] \times \left[\begin{matrix}(1.02 \times 10^{11}\ \text{electrons}) \\ (\text{per cm}^3\ \text{per second}\quad)\end{matrix}\right]$$

$$= 4.8 \times 10^{-6}\ \text{amperes induced by } 10^{13}\ \text{gamma photons per cm}^2\ \text{per sec.}$$

BN = 0.48 μa at voltage stress of 4500v on 0.020 in. electrode spacing, assuming structure with enough lattice defects for use of these alternative values.

BN then appears $\frac{8.68}{0.48}$ = 18.1 times as good as Al_2O_3 in this respect.

$$BN_R = \frac{E}{I} = \frac{4.5 \times 10^3 v}{4.8 \times 10^{-6} a} = 9.4 \times 10^{+8}\ \text{ohms}$$

$$BN\ \text{Vol}\ R = \frac{R \times 2\ (\text{in. dia.})^2}{\text{in. tk.}} = \frac{9.4 \times 10^8 \times 2\ (.81)^2}{.020} = 6.2 \times 10^{10}\ \text{ohm. cm.}$$

, well below the required volume resistance level of over 1 x 10^{13} ohm. cm.

BN then appears only $\frac{6.2 \times 10^{10}}{3.4 \times 10^9}$ or still 18.3 times as good as Al_2O_3 in this respect.

3. Calculation of probable fast neutron effect.

The microscopic absorption cross section of boron for neutrons varies as an inverse function of particle velocity. Accordingly, total cross section values for fast neutrons are of the magnitude of 3-4 barns, as compared to a value of about 755 barns in the thermal energy range. A figure of 3.5 barns will be employed as a basis for subsequent calculations. The reaction cross section for nitrogen does not follow any simple functional relationship. Numerous maxima and minima (resonance peaks) are found in the fast neutron energy range. An approximate average value of 3.5 barns will be assumed as a basis for subsequent calculations.

Fast neutron reactions should principally be of the scattering type. Practically speaking, only those neutrons which have been slowed to thermal energies within the heart of the BN dielectric would be absorbed there. The number of internal slow down absorptions should be small. Therefore, the principal deleterious effects to be expected from fast neutron reactions would be ionization and introduction of lattice defects since there would be little transmutation. The fast neutron reaction characteristics of boron nitride dielectric material are shown by the following equation.

$$I_x = I_0 e^{-(\sum_{i=1}^{N} Ni\sigma i)(x)}$$

As previously defined.

$$I_x = I_0 e^{-(4.34 \times 10^{22} \text{ B or N nuclei per cm}^3)(\sigma B + \sigma N)(x \text{ cm. thickness})}$$

$$\frac{I_x}{I_0} = e^{-(4.34 \times 10^{22})(3.5 + 3.5)(10^{-24})x} = e^{-.304x}$$

If we set

$$\frac{I_x}{I_0} = 0.01 = e^{-0.304x}$$

then $e^{-0.304x} = 100$

$$x = \frac{4.6}{0.304} = 15.1\text{cm.}$$

Thus, it can be seen that the Boron Nitride must be more than 15cm. thick if 99% of the incident fast neutron radiation is to suffer at least one collision.

The scattering properties of various nuclei are clearly delineated in current literature[5]. A useful quantity in the study of the slowing down of neutrons is the average logarithmic energy decrement per collision (ξ). This value is functionally related to the mass number of the atoms or nuclei involved, according to the following equation.

$$\xi = 1 + \frac{(A-1)^2}{2A} \ln \frac{A-1}{A+1}$$

where: ξ = average logarithmic energy decrement per collision

A = mass number, i.e., atomic weight.

In collisions with specific scattered nuclei, a neutron always loses, on the average, the same fraction of the energy it had before collision. This fraction decreases with increasing mass of the nucleus.[5] The average number of collisions to reduce the energy of a fast neutron from an initial level (E_1) to a lower level (E_2) is then obtained by the following equation.

$$\text{Average number of collisions required} = \frac{\ln \frac{E_1}{E^2}}{\xi}$$

where: E_1 = initial neutron velocity in e.v.

E^2 = final neutron velocity in e.v.

ξ = average logarithmic energy decrement per collision of nuclei

Typical scattering properties of various nuclei representing ξ and the average number of collisions required to reduce velocity from 2 M.E.V. to a .025 e.v. thermal level have been tabulated in the literature.[5] Some of these values are presented in the following table.

Table IV

Neutron Scattering Properties of Nuclei[5]

Element	Mass No.	ξ	Collisions to thermalize
Hydrogen	1	1.000	18
Deuterium	2	0.725	25
Helium	4	0.425	43
Lithium	7	0.268	67
Beryllium	9	0.209	86
Carbon	12	0.158	114
Oxygen	16	0.120	150
Uranium	238	0.00838	2172

Accordingly, ξ is inversely proportional to the number of scattering collisions required to slow down a fast neutron to the thermal energy range. The product $\xi \Sigma_s$, Σ_s = macroscopic cross section for scattering, is called the macroscopic slowing down power. It represents the slowing down capacity of all the nuclei in one cubic centimeter of material.

$$\Sigma_s = \sum_{i=1}^{N} N_i \sigma_i = \frac{N_o \rho_{BN} \sigma_{BN}}{M_{BN}}$$

where: N_o = Avogadro's number of 6.02×10^{23}

ρ_{BN} = density in gr./cm^3. - 1.80 (80%)

$\sigma_{BN} = \sigma_B + \sigma_N$ = microscopic (scattering) cross section for fast neutrons in barns x 10^{-24}

M_{BN} = molecular wt. = 24.83

For boron nitride, this macroscopic cross section for scattering fast neutrons (Σ_s (BN)) is calculated as follows:

$$\Sigma_{s(BN)} = \frac{(6.02 \times 10^{23})\ (1.80\ \text{gr./cm}^3)\ (\sigma_B + \sigma_N)}{24.83}$$

$$= (4.36 \times 10^{22})\ (3.5 + 3.5)\ (10^{-24})$$

$= 0.307\ cm^{-1}$

The mean value for the average logarithmic energy decrement per collision ($\overline{\xi}$) for neutrons slowing down in a system of several nuclear species, i.e. boron nitride, consisting of boron nuclei and nitrogen nuclei, is defined by:

$$\overline{\xi} = \frac{\sum_{i=1}^{N} (\Sigma_{si}\, \xi_i)}{\Sigma_s}$$

where: i represents each of the different nuclei involved

Σ_s = macroscopic cross section for scattering for boron nitride as previously calculated

$\sum_{i=1}^{N} \Sigma_{si}\, \xi_i$ = Summation of products of $\Sigma_{si}\, \xi_i$ values for each of the i different types of nuclei involved

The following procedure is accordingly employed to calculate $\overline{\xi}$ for the BN molecule.

a.) Calculation of Σ_s value for boron.

$$\Sigma_{s(B)} = N_B \sigma_B = (4.34 \times 10^{22})\ (3.5 \times 10^{-24})$$

b.) Calculation of ξ value for boron.

$$\xi_{(B)} = 1 + \frac{(10.82-1)^2}{2 \times 10.82} \ln\left[\frac{(10.82-1)}{(10.82+1)}\right]$$

$$= 1 + 102.5\ (\log 9.82 - \log 11.82)$$

$$= 1 - 0.828$$

$$= 0.172$$

c.) Calculation of Σ_s value for nitrogen

$$\Sigma_{s(N)} = N_N \sigma_N = (4.34 \times 10^{22})\ (3.5 \times 10^{-24})$$

$$= .152\ cm^{-1}$$

d.) Calculation of ξ value for nitrogen

$$\xi_{(N)} = 1 + \frac{(14.01-1)^2}{2 \times 14.01} \ln\left[\frac{(14.01-1)}{(14.01+1)}\right]$$

$$= 1 + 13.9 (\log 13.01 - \log 15.01)$$

$$= 1 - 0.863$$

$$= 0.137$$

e.) Calculation of $(\Sigma_{s(B)} \xi_{(B)} + \Sigma_{s(N)} \xi_{(N)})$

$$= 0.152 \times 0.172 + 0.152 \times 0.137$$

$$= .0262 + .0208 = .0470 = \bar{\xi}\Sigma_s$$

f.) Calculation of $\bar{\xi}$ for BN

$$\bar{\xi}_{BN} = \frac{0.047}{0.307}$$

$$= 0.153$$

Using these values, the macroscopic slowing down power for boron nitride is then calculated as follows:

$$\bar{\xi}_{BN} \Sigma_{s(BN)} = (0.153) \times (0.307 \text{ cm}^{-1})$$

$$= 0.047$$

As was shown previously, the quantity I_x/I_o essentially represents the fraction of neutrons which have escaped scattering in passing through x cm thickness of material. Actually, the number of neutrons passing through in the x direction is somewhat greater than I_x, since many neutrons will have scattered in this direction. The scattering mean freepath (λ_o), which is the average distance a neutron travels before being involved in a scattering collision, can be determined for BN material using the following equation.

$$\lambda_o = \frac{1}{\Sigma_{s(BN)}}$$

$$= \frac{1}{0.307 \text{ cm}^{-1}}$$

$$= 3.26 \text{ cm.}$$

For purposes of comparison, the macroscopic slowing down power will be calculated for aluminum oxide, one of the more promising dielectric materials investigated in other laboratories.[3,4]

a.) Calculation of Σ_s value for aluminum.

$$\Sigma_{s(Al)} = N_{Al}\sigma_{Al}$$

$$= N_{Al_2O_3} \times 2 \times \sigma_{Al}$$

$$= (2.32 \times 10^{22})(2)(4 \times 10^{-24})$$

$$= 0.186 \text{ cm}^{-1}$$

where: $N_{Al_2O_3} = 2.32 \times 10^{22}$, ref. Crittenden's work.[2]

$Al = 4$ barns $\times 10^{-24}$, ref. Crittenden's work.[2]

b.) Calculation of ξ value for aluminum

$$\xi_{(Al)} = 1 + \frac{(27-1)^2}{2 \times 27} \ln\left[\frac{(27-1)}{(27+1)}\right]$$

$$= 1 + 28.8 (\log 26 - \log 28)$$

$$= 1 - 0.924$$

$$= 0.076$$

c.) Calculation of Σ_s value for oxygen.

$$\Sigma_{s(O)} = N_O\sigma_O$$

where: $\sigma_O = 4$ barns $\times 10^{-24}$

$$= N_{Al_2O_3} \times 3 \times \sigma_O$$

$$= (2.32 \times 10^{22})(3)(4 \times 10^{-24})$$

$$= 0.278 \text{ cm}^{-1}$$

d.) Calculation of ξ value for oxygen

$$\xi_{(O)} = 1 + \frac{(16-1)^2}{2 \times 16} \ln\left[\frac{(16-1)}{(16+1)}\right]$$

$$= 1 + 16.2 (\log 15 - \log 17)$$

$$= 1 - 0.88$$

$$= 0.120$$

e.) Calculation of $(\Sigma_{s(Al)} \xi_{Al} + \Sigma_{s(O)} \xi_{O})$

$$= 0.186 \times 0.076 + 0.278 \times 0.120$$

$$= .0141 + .0334 = .0475 = \bar{\xi}\Sigma_s$$

f.) Calculation of Σ_{is} for Al_2O_3

$$\Sigma_{s(Al_2O_3)} = N_{Al_2O_3} (2 \times \sigma_{Al} + 3 \times \sigma_{O})$$

$$= (2.32 \times 10^{22}) (2 \times 4 + 3 \times 4) (10^{-24})$$

$$= .464 \text{ cm}^{-1}$$

The scattering mean free path for Al_2O_3 is the reciprocal of this value.

$$\lambda_o = \frac{1}{0\ 464}$$

$$= 2.26 \text{ cm}$$

g.) Calculation of $\bar{\xi}_{Al_2O_3}$

$$\bar{\xi}_{Al_2O_3} = \frac{0.0475}{0.464}$$

$$= 0.1025$$

Using these values, the macroscopic slowing down power for aluminum oxide is then computed as follows:

$$\bar{\xi}_{Al_2O_3} \Sigma_{Al_2O_3} = (0.1025) (0.464 \text{ cm}^{-1})$$

$$= 0.0475$$

The collision probability-energy decrement product for aluminum oxide has been proven experimentally to be satisfactorily small. Since these calculations indicate that this macroscopic slowing down powers of Al_2O_3 and BN are approximately equivalent, there should be no problem with BN.

At the specified 10^{11} fast neutrons/cm²-sec. level, a calculation of the number of collision (essentially scattering) reactions which would occur in each cubic centimeter of BN dielectric would proceed as follows:

Σ nv = rate of neutron reactions per second.

where: Σ = macroscopic cross section (cm^{-1})

nv = fast neutron flux (N_f cm/cm³-sec.)

$$\Sigma \text{ nv} = \Sigma_{s(BN)} \text{nv}$$

$$= (0.307 \text{ cm}^{-1}) (10^{11} N_f \text{ cm/cm}^3\text{-sec.})$$

$$= 3.1 \times 10^{10} \text{ neutron reactions per cm}^3\text{-sec.}$$

With the required 1000 hours operation (3.6×10^6 seconds) a total of $3.1 \times 10^{10} \times 3.6 \times 10^6$ or 1.12×10^{17} interactions would occur between fast neutrons and B or N nuclei in each cubic centimeter of material. With 4.24×10^{22} B or N target nuclei per cubic centimeter, this would correspond to epithermal neutron collisions with 1.12×10^{17} or 2.64×10^{-6} (about .0003%) of the B or N nuclei present.

The energy spectrum for epithermal neutrons will vary with the type of reactor being employed and the nature and distribution of materials placed between the neutron source and the electrical component which is being considered. With thermal neutron effects being substantially cancelled (either by a natural boron shield or other methods proposed previously), the principal danger of transmutation effects from the epi-thermal neutron spectrum (fast and intermediate types) should be from the lower energy portion of this spectrum which would require only a few collisions to slow to thermal energy levels where chances for absorption are markedly greater. In view of the uncertainty of the fast neutron energy level distribution involved a theoretical analysis of this situation is quite difficult. A tabulation of the number of collisions required in boron nitride to reduce source neutrons of various energy levels to I.e.v. (maximum energy for thermal neutrons) is helpful in visualizing the situation.

Table V

Tabulation of Number of Collisions required in BN to slow Epithermal Neutrons from indicated energy levels to Thermal Neutrons at one e.v.

Initial epithermal neutron energy level in e.v. (E_1)	Neutron Classification	Number of collisions required to slow to one e.v. (E_2) i.e. $\ln \left[\frac{E_1}{E_2}\right] \Big/ \xi_{(BN)}$

Initial epithermal neutron energy level in e.v. (E_1)	Neutron Classification	Number of collisions required to slow to one e.v. (E_2) i.e. $\ln \left[\frac{E_1}{E_2}\right] \div \xi(BN)$
2 M.e.v.	Fast	95
1 M.e.v.	"	90
100 K.e.v.	"	75
10 K.e.v.	"	60
1 K.e.v.	Intermediate	45
100 e.v.	"	30
10 e.v.	"	15

The epi-thermal neutron energy spectrum should only contain a small percentage of neutrons with energies as low as 10 e.v. With a mean free path (λ_o) of 3.26 cm and 15 collision required to slow to thermal energy of 1 e.v., a given neutron should travel 48.7 cm total distance in order to slow within this energy span. Accordingly, it is quite probable, the probability increasing with higher energy levels, that a significant percentage of neutrons would escape from rather than be absorbed in the capacitor structure.

With only about .0003% of the target B or N nuclei being involved in collisions with fast neutrons (as previously calculated) and with only some small (but undetermined) fraction of these being slowed sufficiently to make absorption likely, transmutation effects from fast neutrons would appear relatively negligible when compared to transient ionization effects and the introduction of lattice defects resulting from the neutron scattering reactions.

When considered in conjunction with the previously calculated ionization effects for gamma radiation at the indicated flux density, it would appear that it may not be possible to maintain specified insulation resistance levels even with boron nitride, and certainly not with any other currently known dielectric materials, during the period of exposure to the gamma and neutron radiation environment which has been stipulated. The majority of this effect, however, would be only transient. Any permanent damage, resulting from fast neutron scattering, "knockons" and "thermal spikes" and to a somewhat lesser degree from transmutations after ultimate slow down, would not appear to be of sufficient magnitude to impair dielectric characteristics significantly. This belief, of course, must be substantiated by actual post irradiation testing which will be initiated later.

FIRST NUCLEAR IRRADIATION TESTS ON BORON NITRIDE DIELECTRIC MATERIAL

a. Sample Preparation

During the third quarterly period, preliminary calculations were made to indicate the probable order of magnitude of effects which the stipulated nuclear radiation environment should have upon the boron nitride dielectric material. It appeared that the transient ionization induced by the gamma and fast neutron radiations would probably be too great to maintain the required insulation resistance levels during the period of exposure. Any permanent damage, however, which might result from fast neutron scattering phenomena, was not anticipated to be of sufficient magnitude to impair post irradiation dielectric characteristics significantly. Accordingly, static in pile irradiation testing of boron nitride dielectric material was scheduled to check the validity of this belief.

All samples for this study were compacted from the first lot of boron nitride supplied by the Fielding Chemical Co. (the purest material available in sufficient quantity at that particular time). Samples were tested in both the "green" (as pressed) condition and after sintering for 5 hours at 1300°C in ammonia. No electroding was applied prior to irradiation in order to prevent any detrimental effects or radioactivity which the radiation might cause in the conductive silver paint, frit, etc.

Control data were obtained for fired and unfired discs selected at random from their respective lots. These results are included in Table III (Ref. samples 1084-311 to 321 for fired material and samples 1084-363-364 on unfired material).

In order to prevent breakage of the thin, rather fragile boron nitride discs, they were inserted in loosely conforming cavities which had been machined in locating discs of 99.9% aluminum sheet. Some of these enclosed samples were then wrapped in high purity (99.99%) aluminum foil. Others were placed individually in aluminum cans which were evacuated, flushed with helium, and then hermetically sealed. This closure was intended to prevent access to air, which might conceivably lead to thermal decomposition of BN to B_2O_3 under the conditions of testing. This latter arrangement is shown in Figure I, Illustration B, except that only one BN disc was placed in each can instead of several as pictured (and initially planned). Both of these sets of samples were unshielded against any potentially detrimental thermal neutron activity.

The other set of samples was stacked in a similar, hermetically sealed aluminum can with an isolated layer of compacted BN powder (from the same source of supply) completely surrounding the portion containing the discs which were being tested. This latter arrangement is shown in Figure I, Illustration A. This "self shielding" corresponded to a minimum of 1/8 in. thick material with an approximate density of 1.8 gr./cm^3) in the directions perpendicular to the axis of the can and approximately 7/16 in. thick material (with an approximate density of 1 gr./cm^3) about the circumferance. The "minimum shielding" so obtained was distinctly less than that

which is now permitted by the currently approved 1/8 in. thickness of natural boron material. (In the third quarterly report, it was calculated that 1/8 in. BN of density 1.8 gr/cm^3 would shield out all but 2.7×10^{-5}% of the incident thermal neutrons while 1/8 in. of natural boron would shield out all but 2×10^{-12}%.)

b. Irradiation Conditions

On October 26, 1957, eighteen discs of boron nitride were placed in the Brookhaven National Laboratory natural uranium, graphite moderated, air cooled reactor for static irradiation at "in pile" temperature. Details of previous sample history are summarized in the following table.

Table VI

Pre-Irradiation History of Boron Nitride Sample Discs for Static Irradiation Test

Code Number	Sample Number	Sintering History	Foil Wrapped	Hermetically Sealed in Al Can (w.He)	BN Self Shielding
56	1084-396	Unfired	----------	Together	Yes
F-22	1084-395	Fired	----------	"	"
F-16	--------	Fired	----------	"	"
57	1084-389	Unfired	----------	"	"
F-40	1084-386	Fired	----------	"	"
F-44	--------	Fired	----------	"	"
60	1084-399	Unfired	----------	"	"
F-32	1084-388	Fired	----------	"	"
F-36	1084-394	Fired	----------	"	"
54	1084-397	Unfired	Yes	No	No
68	1084-398	Unfired	----------	Alone	"
F-41	--------	Fired	----------	"	"
F-31	1084-392	Fired	----------	"	"
F-23	1084-393	Fired	Yes	No	"
53	1084-391	Unfired	----------	Alone	"
59	1084-390	Unfired	Yes	No	"
F-30	1084-387	Fired	"	No	"
F-39	1084-385	Fired	----------	Alone	"

The samples were loaded into three aluminum cans prior to placing them in the reactor. The first can (A) contained the discs which were "self shielded" by BN powder and enclosed in a single hermetically sealed aluminum container. This included codes F36, F32, 60, F44, 57, F16, F22, and 56 in sequence, the last named being closest to the center of the pile. This hermetically sealed container was placed about one quarter length from the end of the outer can (A) which was farthest from the center of the pile.

The remainder of space within the outer can (A) was filled with aluminum foil and air.

The second can (B) contained the following codes - 54, 68, F-41, F-31, and F-23 - arranged in sequence, the last named being closest to the center of the pile. Again, the remainder of the space around these rather uniformly spaced samples was filled with aluminum foil and air. In this case, the two end discs were foil wrapped and the three intervening samples were hermetically sealed in individual aluminum containers.

The third can (C) contained the following codes - 53, 59, F-30, and F-39 - arranged in sequence, the last named (again) being closest to the center of the pile. As in the other two cans, the remainder of the space around the rather uniformly spaced samples was filled with aluminum foil and air. In this instance, the two discs were hermetically sealed in individual aluminum cans and the two intervening discs were foil wrapped. All three outer cans (A, B, and C) were hermetically sealed by soldering, according to the standard practice at Brookhaven.

These three containers were inserted in hole E-26 of the reactor during shutdown on October 26, 1957, at about 11:00 A.M. This hole is 7 ft., 6 in. from the center of the pile on one plane and 4 ft., 4 in. from the center along the second plane. Within this hole, the containers were the following respective distances from the center of the pile along the third plane -- (C) 5 ft., 8 in., (B) 6 ft., 4 in. and (A) 7 ft., 6 in.

The reactor was started up during the night of October 26th, and attained running power sometime early the next morning. The samples were then irradiated for one reactor cycle, corresponding to a total of 285 hours (at a neutron flux of $2.3 \times 10^{12} n/cm^2$-sec., based upon the old fuel loading). Since they have put in a number of fuel elements using enriched uranium, the flux pattern has changed somewhat and the new pattern has not yet been measured. Accordingly, Mr. Floyd (of Brookhaven) had put some cadmium coated aluminum-cobalt foils in among our samples in order to check the epithermal neutron flux. These foils showed the epithermal neutron fluxes in the various cans were as follows ------ (A) $1.5 \times 10^{11} n/cm^2$-sec., (B) $1.05 \times 10^{11} n/cm^2$-sec., and (C) $1.9 \times 10^{11} n/cm^2$-sec. Mr. Floyd felt that we could assume a neutron flux density of at least 10^{11} fast neutrons $/cm^2$-sec., with the new loading, based upon calculations at the old loading.

During irradiation, the operating power level was about 16 MW with in pile temperatures of approximately 75° to 125°C. The reactor was shut down at midnight on November 7, 1957, and the samples were removed from the pile on November 9, 1957, and stored in a lead pig until November 14, 1957, when they were removed from their containers by one of our engineers, Mr. W. O. Cook. (The individual cans checked approximately 20 mr at 3 inches before opening.)

c. Preliminary Evaluation of Irradiated Samples

After removal from their containers at the Brookhaven National

Laboratories, the approximate residual radioactivity levels on the individual samples were as follows.

Table VII

Residual Radioactivity Levels on Irradiated Boron Nitride Specimens Measured at Brookhaven November 14, 1957

Code No.	BN Self Shielding	Color	Activity
56	Yes	Light Pink	Approximately 2 mr. at contact
F-22	"	Greyish	" 1 " " "
F-16	"	"	" 1 " " "
57	"	Light Pink	" 2 " " "
F-40	"	Greyish	" 1 " " "
F-44	"	"	" 1 " " " (Cracked in two)
60	"	Light Pink	" 2 " " "
F-32	"	Greyish	" 1 " " "
F-36	"	"	" 1 " " "
54	No	Choc. Brown	" 12 " " "
68	"	" "	" 14 " " "
F-41	"	" "	Broken during opening
F-36	"	" "	Approximately 6 mr. at one inch
F-23	"	" "	" 3 " " " "
53	"	" "	" 12 " " " "
59	"	" "	" 10 " " " "
F-30	"	" "	" 5 " " " "
F-39	"	" "	" 30 " " " "

All the samples changed from their initial white color during irradiation. The unshielded discs (whether sintered or not) turned a chocolate brown color. The shielded discs, however, showed differences in colors according to whether they had been sintered or not - the former turning greyish and the latter a light pink. The resisual radioactivity levels were also much higher on the unshielded samples. When the can containing the boron nitride powder shielding material was opened a color change was also evident in this powder. There was a color gradient from the chocolate brown color at the outside of the can to the light pink shade nearest the inside.

After these initial observations were completed, the individual discs were placed in compartments in a bakelite holder and were brought back to our laboratory in Indianapolis. The boron nitride powder which had been used for shielding was placed in a plastic jar and was also brought back at the same time. (The initial activity outside these containers was about 2 mr. at contact.)

Upon receipt in our Indianapolis laboratory, the irradiated boron nitride samples were reweighed to establish the order of magnitude of change in physical characteristics which had resulted from the static irradiation process. These data are summarized in the following table.

Table VIII

Change in Weight on Irradiated Boron Nitride Discs

Code No.	Initial Weight	Final Wt.	Change	%Change	Had Been Sintered	Had Been Shielded
F-39	0.5916 gr.	0.5933 gr.	.0017	+0.29	Yes	No
F-31	0.5667	0.5684	.0017	+0.30	"	"
F-30	0.5260	0.5348	.0088	+1.76*	"	"
F-23	0.4440	0.4511	.0071	+1.60*	"	"
53	0.6934	0.6954	.0020	+0.29	No	"
68	0.6322	0.6330	.0008	+0.13	"	"
59	0.6318	0.6413	.0095	+1.50*	"	"
54	0.6362	0.6438	.0096	+1.51*	"	"
F-22	0.4296	0.4293	.0003	-0.07	Yes	Yes
F-16	0.4621	0.4620	.0001	-0.02	"	"
F-40	0.5520	0.5522	.0002	+0.04	"	"
F-44	0.5750	0.5576	.0174	-3.0**	"	"
F-32	0.5766	0.5768	.0002	+0.03	"	"
F-36	0.5246	0.5251	.0005	+0.10	"	"
56	0.6582	0.6573	.0009	-0.14	No	"
57	0.5970	0.5959	.0011	-0.18	"	"
60	0.6274	0.6266	.0008	-0.13	"	"

*These samples had been wrapped in aluminum foil; the others had been hermetically sealed in a helium atmosphere.

**This sample had cracked in two, which could readily have led to the significant weight loss encountered (through powder shredding).

The pattern of these data was fairly consistent. The four samples which were foil wrapped instead of hermetically sealed showed weight gains ranging from 1.5 to 1.8%. The greatest weight gains would be expected on these discs, since limited access to air was permitted and some conversion of BN to B_2O_3 under thermal neutron bombardment could occur. The remaining unshielded samples, which had been hermetically sealed, showed much smaller weight gains ranging from 0.1 to 0.3%. The samples which had been protected from major thermal neutron effects by a boron nitride shield showed small weight changes ranging from a gain of 0.1% to a loss of 0.2%; all of these samples had been hermetically sealed.

After the discs had been weighed, some measurements of the current residual radioactivity were again made using a Geiger-Muller tube as a counter in combination with a Scaler manufactured by the Nuclear Instruments and Chemicals Corporation of Chicago, Illinois. Readings were taken both with and without absorbers in the counting chamber. This procedure was repeated after certain elapsed periods of time. Typical data (obtained when absorbers were omitted from the system) are summarized in the following table; this includes counts per minute initially and after various periods of time and the calculated values for radioactivity decay constant (λ).

Table IX

Radioactivity Counts on Irradiated Boron Nitride Discs

Code No.	Had Been Sintered	Had Been Shielded	First Reading			Third Reading		
			Date	Elapsed Hours	Count	Elapsed Hours	Count	Decay Constant
F-23	Yes	No	11/18	0	7091	336	3990	.00173
F-30	"	"	"	"	7690	---	---	---
F-31	"	"	"	"	9218	45	7656	.0041
F-39	"	"	"	"	54,316	407	5189	.0058
53	No	"	"	"	18,159	336	8389	.0023
54	"	"	"	"	22,627	360	11,350	.00192
59	"	"	"	"	16,676	429	7,768	.00178
68	"	"	"	"	24,827	172	14,034	.0033
F-16	Yes	Yes	11/15	"	1844	91	1064	.00602
F-22	"	"	11/18	"	672	360	366	.00169
F-32	"	"	11/15	"	896	162	508	.00396
F-36	"	"	"	"	963	115.5	576	.00446
F-40	"	"	"	"	1240	358	671	.00172
F-44*	"	"	11/18	"	1102	---	---	---
56	No	"	11/18	"	2628	360	1198	.00218
57	"	"	11/15	"	3302	91.5	1984	.00555
60	"	"	11/15	"	3635	117.5	2012	.00502

*This sample was broken, so no further measurements were made.

The radioactive decay constants in the preceding table were calculated by means of the following equation.[9]

$$\lambda = \frac{2.303 \log \frac{N_o}{N_t}}{t}$$

where: N_o = initial activity (count)
N_t = activity (count) at time t
t = elapsed hours when recheck was made.

The marked variations of decay constant (λ) with time on a given sample, as well as the variations between samples, clearly demonstrated that several nuclides with different decay rates were present. Readings with different shields in the counting chamber indicated that more than two nuclides with different energy levels were involved. However, no identification of these materials has been possible at the present time.

There was no completely consistent pattern of difference in residual radioactivity levels between fired and unfired discs which had not been shielded from thermal neutron effects. The samples which had been shielded with boron nitride were less radioactive than the unshielded samples. In this case, the fired samples were consistently less active than the unfired ones. A possible clue to a source of some of these differences was presented by comparative spectrographic analyses of the boron nitride material in the unfired condition, the fired condition, and the fired condition after irradiation. These data are presented in the following table.

Table X

Spectrographic Analyses Comparing Irradiated and Non Irradiated Boron Nitride

Constituent	Unfired Fielding Lot 1	Fired Fielding Lot 1	Fired and Irradiated Fielding Lot 1 (Unshielded, Code F-41)
Boron (B)	Major constituent	ibid	ibid
Iron (Fe)	0.04%	0.031%	0.023%
Silicon (Si)	trace	trace	heavier trace
Magnesium (Mg)	trace	smaller trace	smaller trace
Aluminum (Al)	trace	very light trace	very light trace
Calcium (Ca)	trace	very light trace	very light trace
Copper (Cu)	trace	very light trace	very light trace
Silver (Ag)	very light trace	None	None

It can be seen that firing the boron nitride in ammonia in the conventional manner reduced the overall level of impurities. (Irradiation after firing appeared to lower the iron content and raise the silicon content). When shielded during irradiation, some of the materials which became radioactive must have been of the type which was partially or

completely removed during this furnacing step. This could explain the lower level of residual radioactivity on the fired samples under these conditions. This same factor may have been involved in the case of the unshielded samples, since all the fired discs were distinctly less active than the unfired ones, except for the case of code F-39.

After obtaining these measurements of residual radioactivity, the irradiated specimens were electroded with silver paint in the customary manner and electrical characteristics were then determined. These data are included in Table III (Ref. samples No. 1084-385 to 399). Dielectric parameters of the samples which had been shielded from thermal neutron activity were markedly different from equivalent data on samples which had not been shielded, as is shown in the following table.

Table XI

Dielectric Parameters on Irradiated Boron Nitride Discs

Code No.	Sample No.	Had Been Sintered	Had Been Shielded	Room T. K	500°C K	Vol. R. at 500°C (in ohm. cm.)
F-23	1084-393	Yes	No	3.87	9.82	4.5×10^{9}
F-30	" -387	"	"	4.08	9.62	5.9×10^{9}
F-31	" -392	"	"	3.82	8.19	2.7×10^{9}
F-39	" -385	"	"	3.70	6.62	4.6×10^{9}
53	" -391	No	"	4.16	8.60	5.5×10^{9}
54	" -397	"	"	4.02	8.00	8.2×10^{9}
59	" -390	"	"	4.15	8.75	1.9×10^{10}
68	" -398	"	"	4.12	8.70	4.5×10^{9}
F-22	" -395	Yes	Yes	3.66	4.07	1.7×10^{13}
F-32	" -388	"	"	3.68	4.08	2.3×10^{13}
F-36	" -394	"	"	3.68	4.07	2.0×10^{13}
F-40	" -386	"	"	4.03	4.36	2.1×10^{13}
56	" -396	No	"	3.86	4.35	6.6×10^{13}
57	" -389	"	"	3.94	4.35	8.0×10^{13}
60	" -399	"	"	3.79	4.32	3.0×10^{13}

Characteristics of the irradiated, shielded discs were at least as good as for the control samples which had not been irradiated (Ref. Table III, Samples 1084-311 to 321 and 364-365.) All of these irradiated specimens exceeded the 5 megohm-microfarads requirement. These findings were in excellent agreement with our preliminary calculations which had

predicted that any permanent damage, which would result from fast neutron or gamma activity, would not be of sufficient magnitude to impair post irradiation dielectric characteristics significantly. Accordingly, it can be concluded that boron nitride dielectric material (either sintered or unfired) does not suffer any permanent damage from irradiation, so long as adequate shielding against thermal neutron damage is supplied. The 1/8 in. thick natural boron shielding, which is now permitted by the modified contractual requirements, should be more than adequate in this respect, since the 1/8 in. thick boron nitride powder shield gave sufficient protection through 285 hours of in pile irradiation.

Significant, and presumably permanent, impairment in dielectric properties was evident on all the irradiated specimens which had not been shielded against thermal neutron effects. The 500°C insulation resistance dropped at least three orders of magnitude on both fired and unfired discs, and 500°C K values were abnormally high. To date, there has been no significant improvement in insulation resistance on these samples with decreasing residual radioactivity levels. At the present decay rates, however, it will be sometime before counts have decreased to the levels initially encountered on the shielded, irradiated specimens. Also, any possible improvements which might be obtained from the action of thermal energy - annealing for extended periods of time at high temperatures - are yet to be determined. However, it would appear fairly likely that this impairment indielectric characteristics from thermal neutron reactions is permanent. Fortunately, this is not an important consideration because of the protective boron shielding which is now stipulated.

The next phase of radiation testing of boron nitride dielectric material will involve initial study of the magnitude of transient, ionizing effects to be encountered during the period of actual exposure to radiation. This will probably consist of operational testing of specimens in the presence of strong gamma radiation from a Cobalt 60 source. In this manner, we should obtain a good indication of the accuracy of our previous calculations which predicted that the ionization induced by gamma and fast neutron radiation activity would probably be too great to maintain required insulation resistance levels during the period of actual irradiation.

TRANSIENT EFFECTS OF GAMMA RADIATION ON BN

The Co^{60} gamma radiation facilities of the Inland Testing Laboratory at Morton Grove, Illinois, were employed to measure the transient induced conductivity in BN. The facility is ideal for this type measurement in view of the infinitely and rapidly variable flux rate except that the maximum usable flux was 2×10^{11} gamma photons per cm^2 per sec. which is only 2% of the 10^{13} flux density specified for this development.

Four multi-electrode capacitor sections were selected for measurement. Measurements at room temperature before the test were as follows.

1084-593

Made of unpurified Fisher BN

Capacity ($\mu\mu$f)	Insulation Res. (Ohms)	Ohms/Mfd.
524	1.9×10^{11}	1×10^{8}

1084-594

Made of unpurified Fisher BN

Capacity ($\mu\mu$f)	Insulation Res. (Ohms)	Ohms/Mfd.
754	2.8×10^{11}	2.1×10^{8}

1084-592

Made of unpurified Fisher BN

Capacity ($\mu\mu$f)	Insulation Res. (Ohms)	Ohms/Mfd.
449	5×10^{11}	2.5×10^{8}

1084-529

Made of purified Fisher BN

Capacity ($\mu\mu$f)	Insulation Res. (Ohms)	Ohms/Mfd.
150	7×10^{11}	1.05×10^{8}

Measurements were all made at room temperature and at only one potential, 175 volts, obtained from a battery source. Polyethylene insulated co-axial leads approximately 20 ft long were employed. A leakage measurement was made on the open circuit leads at radiation densities between 0 and 2×10^{11} photons/cm^2/sec. This value ranged between 5.3×10^{11} ohms at 0 radiation to 6×10^{10} at 2×10^{11} photons/cm^2/sec. It was deduced that this variation was probably due to ionization pick-up on the open termination. Therefore, a measurement was made with the leads terminated with a glass encased carbon film resistor at 0 and 2×10^{11} photons/cm^2/sec.

Gamma Intensity	Ohms.
0	1.11×10^{8}
2×10^{11}	1.17×10^{8}

The variation is within error of measurement. This test was interpreted to indicate that the leads, when terminated with any impedance commensurate with those being measured, represented a fixed value of approximately

5.3×10^{11} ohms without regard to radiation level. This value has been considered as a parallel path with the unknown and the values presented here are so corrected. These values have been plotted for the four individual samples and are shown on Fig's. #6, 7, 8 and 9. These measurements are valid for these measuring conditions only, that is, at 175 volts and room temperature.

The induced conduction in an inorganic insulating material is inversely proportional to the square root of the recombination coefficient and is directly proportional to the electron mobility. The variation of these factors with temperature is affected by the impurities and other lattice defects within any compound. It seems, therefore, that the variation of induced conduction with temperature can best be determined by measurements at various temperatures on a specific material. These measurements have not as yet been made on the material being employed, which is known not to be of a high order of purity.

Now that some experimental data illustrating the actual effects of gamma irradiation at various intensities upon the electrical resistivity of boron nitride have been acquired, a comparison can be made between predicted behavior and actual performance. Observed values for experimental parallel plate structures will be compared to those calculated for various levels of measured radiation intensities (using parameters corresponding to the preceding "worst possible case"). Since the electrode spacings and alignments of the different capacitor bodies varied somewhat, a representative average configuration will be assumed as the basis for calculations. The specified parameters will then be:

Electrode area (A) - 1.5 cm^2 x 6 plates = 9 cm^2

Dielectric thickness (L) - .04 cm.

Applied test voltage (V) - 175 volts.

For each measured gamma radiation intensity, the first step involves calculation of free electrons released per cubic centimeter per second.

$$N_o = \left[\frac{(Q)}{(a)}\right]^{1/2}$$

where: N_o = free electrons per cm^3 per sec.

Q = rate of electron release per cm^3 per sec.

a = coefficient of recombination per cm^3 per sec.

$$BNno = \left[\frac{(\text{1MEV gamma mass absorption coeff.}) \times (\text{gamma photon radiation intensity}) \times (\text{ratio of fast to thermal electrons})}{(\text{Coefficient of recombination})}\right]^{1/2}$$

$$BNno = \left[\frac{(0.104)\ (\text{gamma photon radiation intensity } (10^3))}{(1 \times 10^{-8})}\right]^{1/2}$$

$$= \left[(1.04 \times 10^{10})\right]^{1/2} \times \left[\frac{(\text{gamma photons})}{(\text{cm}^2\ \text{sec.})}\right]^{1/2}$$

$$= 1.02 \times 10^5 \times \left[\left(\phi\ \frac{\text{gamma photons}}{\text{cm}^2\ \text{sec.}}\right)\right]^{1/2} = \frac{\text{electrons}}{\text{cm}^3 - \text{sec.}}$$

This value for each measured radiation intensity is then employed to calculate the respective level of gamma radiation induced current, using the previously employed equation.

$$\text{L BN} = \frac{AV}{L}\ \text{euno}$$

$$= \left[\frac{(9\ \text{cm}^2)\ (175\text{v})\ (1.602 \times 10^{-19}\ \text{coulombs})\ (10^{-3}\ \text{cm}^3/\text{volt-cm})}{(.04\ \text{cm})}\right]$$

$$\times (1.02 \times 10^5) \left[\frac{\text{gamma photons}}{\text{cm}^2\text{-sec.}}\right]^{1/2}$$

$$= 6.4 \times 10^{-13} \times \left[\frac{\text{gamma photons}}{\text{cm}^2\text{-sec.}}\right]^{1/2} = \frac{\text{amps}}{\text{cm}^3\text{-sec.}}$$

The measured resistance on a capacitor should then be equivalent to the following expression.

$$\text{Measured R} = \frac{\text{Open circuit lead R x R due to irradiation}}{\text{Open circuit lead R + R due to irradiation}}$$

$$\text{R due to irradiation} = \frac{\text{Applied test voltage (V)}}{\text{Gamma radiation induced current (L BN)}}$$

$$= \frac{175\text{v}}{6.4 \times 10^{-13}\left[\left(\frac{\text{gamma photons}}{\text{cm}^2 - \text{sec.}}\right)\right]^{1/2}}$$

$$= \frac{2.74 \times 10^{14}}{\left[\left(\frac{\text{gamma photons}}{\text{cm}^2 - \text{sec.}}\right)\right]^{1/2}} = \text{R (Ohms)}$$

For the highest measured gamma radiation intensity which was employed for testing - (2×10^{11} gamma photons per cm^2 per sec.) - the expected resistivity level would then be calculated as follows.

$$R \text{ due to irradiation} = \frac{2.74 \times 10^{14}}{(2 \times 10^{11} \text{ photons per cm}^2 \text{ per sec}) \; 1/2}$$

$$= \frac{2.74 \times 10^{14}}{4.48 \times 10^{5}}$$

$$= 6.1 \times 10^{8} \text{ ohms}$$

$$\text{Expected capacitor resistance} = \frac{\text{Lead resistance} \times R \text{ due to irradiation}}{\text{Lead resistance} + R \text{ due to irradiation}}$$

$$= \frac{(5.3 \times 10^{11} \text{ ohms lead R}) \times 6.1 \times 10^{8} \text{ ohms}}{5.3 \times 10^{11} + 6.1 \times 10^{8}}$$

$$= \frac{3.24 \times 10^{20}}{5.306 \times 10^{11}}$$

$$= 6.1 \times 10^{8} \text{ ohms}$$

Measured (corrected) resistance values for this highest gamma radiation intensity were as follows on three capacitor units tested.

1084-529 - 4.1×10^{9} ohms

1084-593 - 3×10^{9} ohms

1084-594 - 1.8×10^{9} ohms

These figures were all within less than an order of magnitude from the predicted values. In view of the assumptions made concerning average electrode configurations and spacings for the capacitor bodies and the probable order of precision of measurements, the compared values would be judged to be in generally good agreement. Accordingly, the parameters for calculation for "the worst possible case" appear to be reasonably representative of the lower level of performance of boron nitride dielectric material.

The estimated maximum gamma induced current in a 3 mfd capacitor with BN dielectric based on the objective dielectric thickness of .005" would be:

$$\left[\frac{(10^{5} \text{ cm}^2) \; (4.5 \times 10^{3} \text{V}) \; (1.602 \times 10^{-19} \text{ coulombs}) \; (10^{-3})}{1.27 \times 10^{-2}} \right] \times$$

$(1.02 \times 10^5)\ (10^{13}\ \text{gamma photons})^{1/2} = 1.82$ amps

A maximum leakage current of this magnitude could exist due to gamma radiation alone without regard to that contributed by fast neutrons and/or temperature effects at 500°C.

Apparently the proposed capacitor would not be of any practical utility without gamma shielding under the conditions of the exhibit.

BIBLIOGRAPHY

1. Glosstone, S., Principles of Nuclear Reactor Engineering

2. Crittenden, J. R., The Effect of In-Pile Radiation on the G. E. Ceramic Triode, General Electric Co., Aircraft Nuclear Propulsion Department, Cincinnati, Ohio.

3. Ultrathermic 500°C Capacitor, American Machine and Foundry Co., Scientific Reports No. 1, 2, 3 - Contract AF 33(616)-3605.

4. Ultrathermic 500°C Capacitors, Servomechanisms, Inc. - Scientific Report No. 1 - Contract No. AF 33(616)-3611.

5. Glosstone, S. and Edlund, N. C., The Elements of Nuclear Reactor Theory

Closure Drawing

FIG. I

Illustration "A" (17.4 Grams-Boron)
Total Weight Of BN = Approx 39.6 Grams
Total Weight Of Aluminum = Approx 56 Grams

Illustration "B" (2.0 Grams-Boron)
Total Weight Of BN = Approx 4.5 Grams
Total Weight Of Aluminum Approx 40 Grams

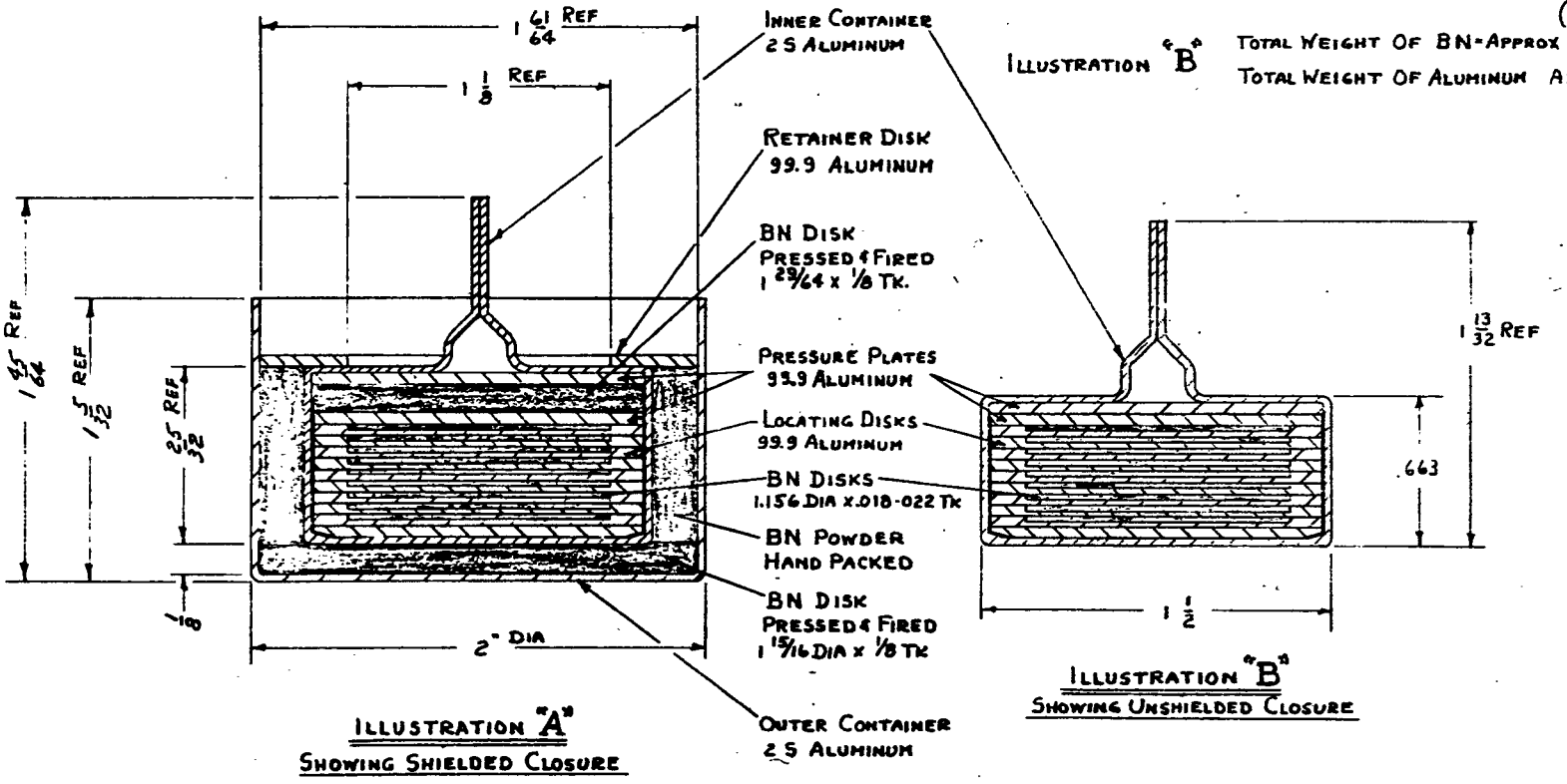

Illustration "A"
Showing Shielded Closure

Illustration "B"
Showing Unshielded Closure

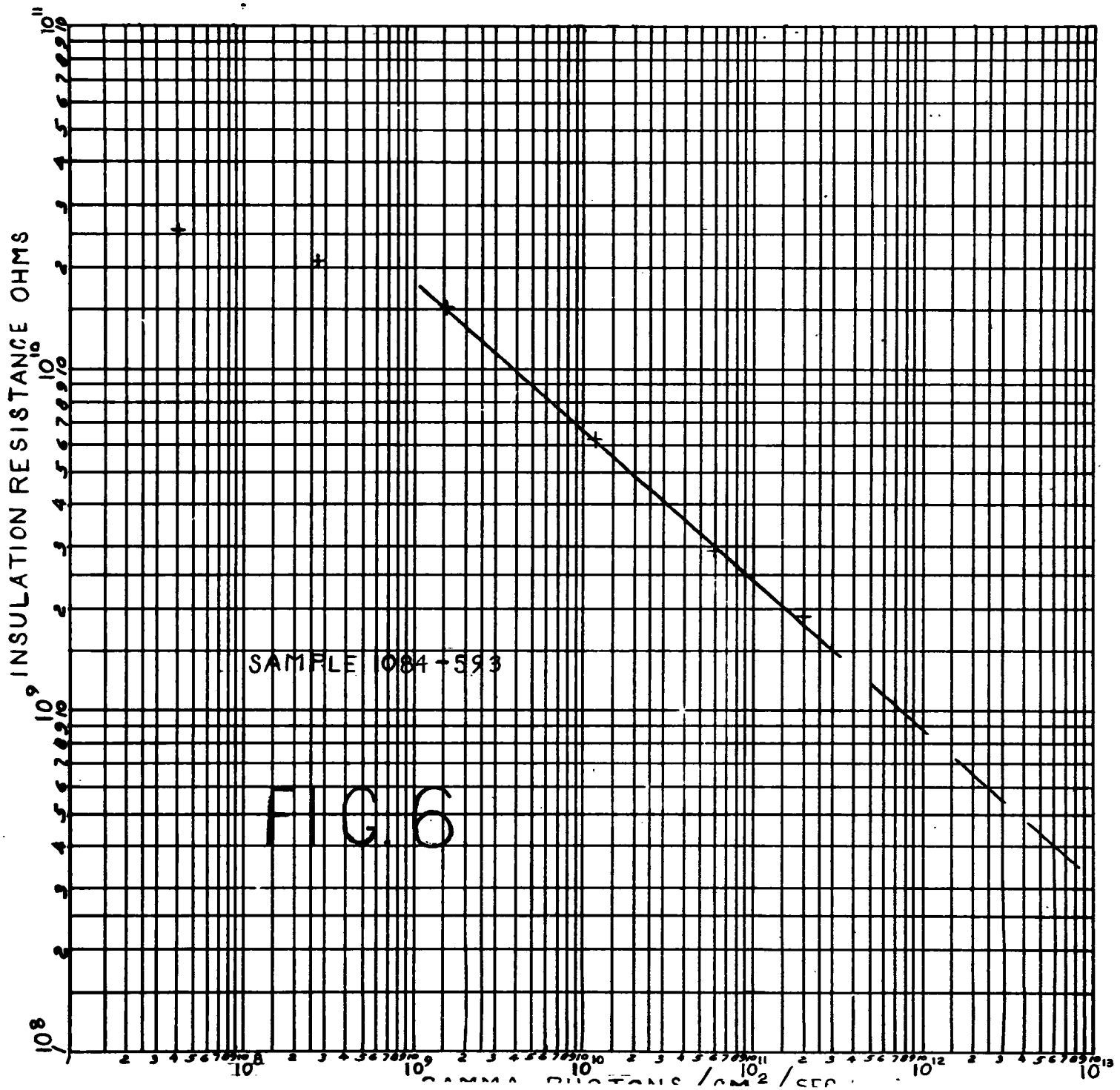
INSULATION RESISTANCE OHMS
SAMPLE 1084-593
GAMMA PHOTONS / CM2 / SEC

FIG. 6

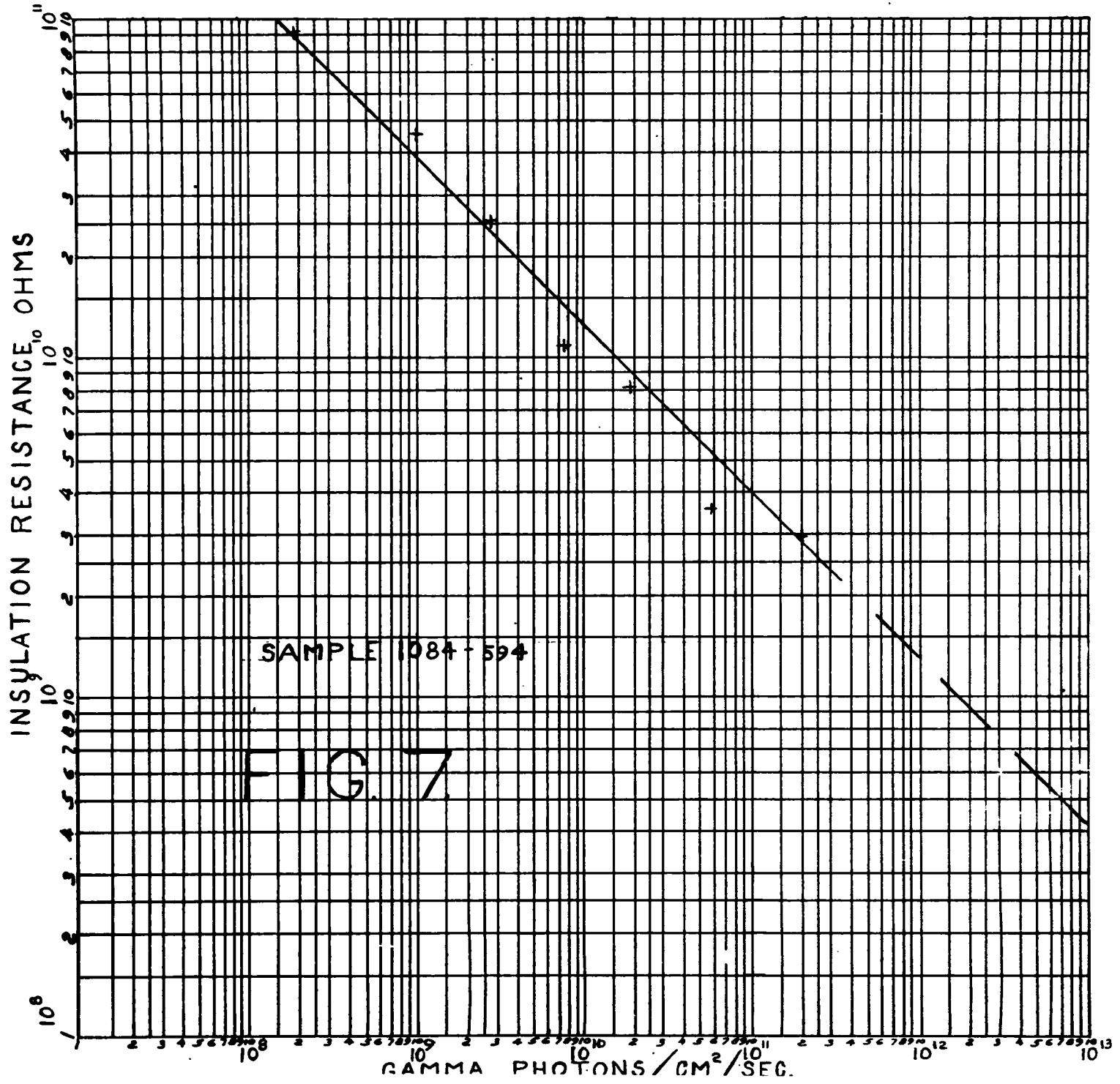
INSULATION RESISTANCE, OHMS
GAMMA PHOTONS / CM² / SEC.
SAMPLE 1084-594

FIG. 7.

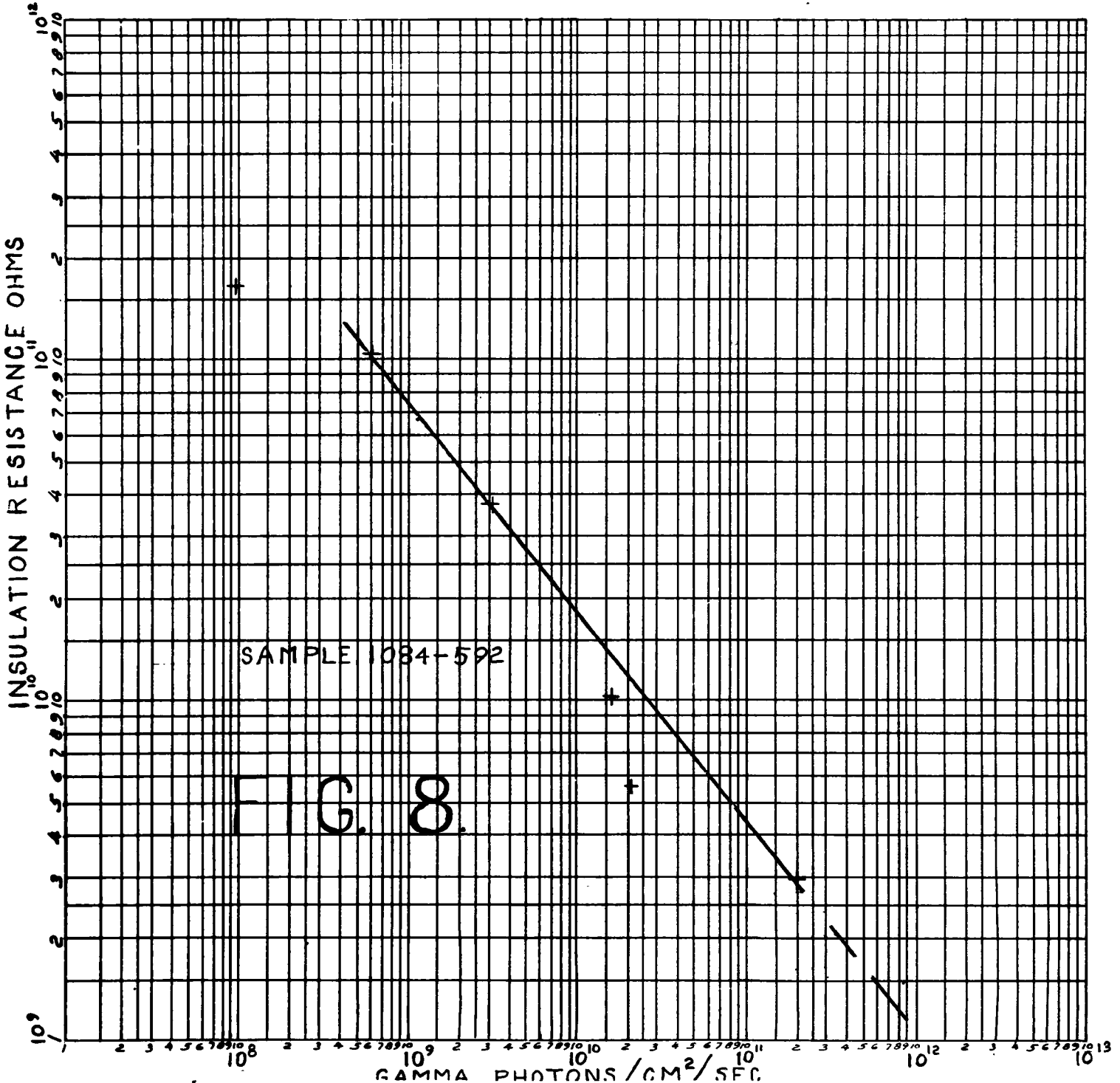
INSULATION RESISTANCE OHMS
SAMPLE 1084-592
GAMMA PHOTONS/CM²/SEC

FIG. 8.

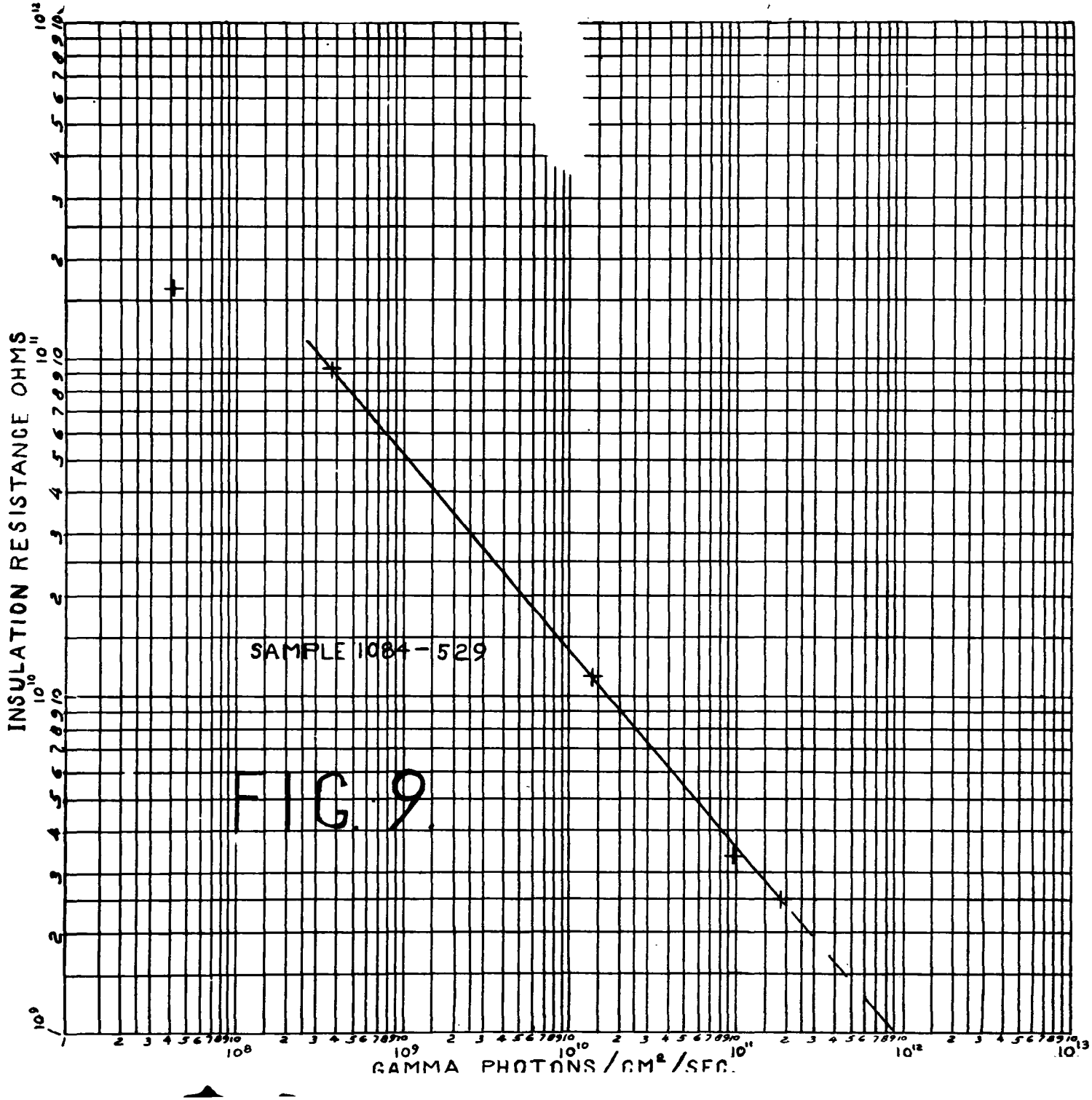
INSULATION RESISTANCE OHMS
SAMPLE 1084-529
GAMMA PHOTONS/CM²/SEC.

FIG. 9.